JOURNAL OF
APPLIED CHEMISTRY

OF THE USSR

(ZHURNAL PRIKLADNOI KHIMY)

IN ENGLISH TRANSLATION

		Domestic	Foreign
Printed in the United States	Annual Subscription..............	$60.00	$65.00
	Annual Subscription for libraries of non-profit academic institutes	20.00	
	Single Issues	7.50	

SIGNIFICANCE OF ABBREVIATIONS MOST FREQUENTLY
ENCOUNTERED IN SOVIET PERIODICALS

FIAN	Phys. Inst. Acad. Sci. USSR.
GDI	Water Power Inst.
GITI	State Sci.-Tech. Press
GITTL	State Tech. and Theor. Lit. Press
GONTI	State United Sci.-Tech. Press
Gosenergoizdat	State Power Press
Goskhimizdat	State Chem. Press
GOST	All-Union State Standard
GTTI	State Tech. and Theor. Lit. Press
IL	Foreign Lit. Press
ISN (Izd. Sov. Nauk)	Soviet Science Press
Izd. AN SSSR	Acad. Sci. USSR Press
Izd. MGU	Moscow State Univ. Press
LEIIZhT	Leningrad Power Inst. of Railroad Engineering
LET	Leningrad Elec. Engr. School
LETI	Leningrad Electrotechnical Inst.
LETIIZhT	Leningrad Electrical Engineering Research Inst. of Railroad Engr.
Mashgiz	State Sci.-Tech. Press for Machine Construction Lit.
MEP	Ministry of Electrical Industry
MES	Ministry of Electrical Power Plants
MESEP	Ministry of Electrical Power Plants and the Electrical Industry
MGU	Moscow State Univ.
MKhTI	Moscow Inst. Chem. Tech.
MOPI	Moscow Regional Pedagogical Inst.
MSP	Ministry of Industrial Construction
NII ZVUKSZAPIOI	Scientific Research Inst. of Sound Recording
NIKFI	Sci. Inst. of Modern Motion Picture Photography
ONTI	United Sci.-Tech. Press
OTI	Division of Technical Information
OTN	Div. Tech. Sci.
Stroiizdat	Construction Press
TOE	Association of Power Engineers
TsKTI	Central Research Inst. for Boilers and Turbines
TsNIEL	Central Scientific Research Elec. Engr. Lab.
TsNIEL-MES	Central Scientific Research Elec. Engr. Lab.—Ministry of Electric Power Plants
TsVTI	Central Office of Economic Information
UF	Ural Branch
VIESKh	All-Union Inst. of Rural Elec. Power Stations
VNIIM	All-Union Scientific Research Inst. of Meteorology
VNIIZhDT	All-Union Scientific Research Inst. of Railroad Engineering
VTI	All-Union Thermotech. Inst.
VZEI	All-Union Power Correspondence Inst.

N o t e : Abbreviations not on this list and not explained in the translation have been transliterated, no further information about their significance being available to us. — Publisher.

TABLE OF CONTENTS

40 YEARS OF SOVIET SCIENCE IN THE FIELD OF SILICATE CHEMISTRY AND TECHNOLOGY

P. P. Budnikov

The Great October Socialist Revolution opened wide possibilities for the development of science, which had to find fundamentally new routes for the development of technology, industry, and culture, in close association with practice, experience, and the creative activity of the people.

The new tasks which confronted science necessitated new forms of its organization. Large scientific research institutes were established in the most important branches of industry. As long ago as 1918 an Institute of Silicates was established in Moscow; this provided the basis for the subsequent establishment of Institute of Cement, Glass, Refractories, Construction Ceramics, Electrical Ceramics, Building Materials, Asbestos, etc. The Institute of Ceramics and then the Institute of Silicate Chemistry, Academy of Sciences USSR, were founded in Leningrad.

The work of these institutes and of the university laboratories has made a large contribution to socialist industry.

There is now no field of silicate science which is not being studied in the Soviet Union.

Silicate science is the basis of the complex production of building materials, refractories, and other products of the silicate industry. Investigations of, and searches for new silicate materials involve the use of modern physical, chemical, and radiochemical methods — microscopy, electron microscopy, viscosimetry, thermochemistry, x-ray analysis, etc. An important role in the development of the science of silicates and building materials has been played by mineralogy, petrography, crystal chemistry, crystallography, and crystal optics.

Among the scientists who have made important contributions to Soviet silicate science, mention must be made of Academicians N. S. Kurnakov (1860-1941), F. Yu. Levinson-Lessing (1861-1939), V. I. Vernadsky (1863-1945), A. E. Fersman (1883-1945), D. S. Belyankin (1876-1953), A. A. Baikov (1870-1946), K. K. Gedroits (1872-1932), I. V. Grebenshchikov (1887-1953) and others who participated in considerable development of crystallography, mineralogy, petrography, geochemistry, soil science, and the physical chemistry of silicates, and assisted in the solution of a number of most important practical problems set by the party and the government.

In illustration, we need only refer to the work of N. S. Kurnakov and his school on the development of methods of physicochemical analysis, and in particular of thermal analysis.

N. S. Kurnakov, who developed the concepts of singular points and phases of variable composition (daltonides and bertollides), belonged to the generation of our national chemists, the immediate followers of the scientific ideas and traditions of the great Russian chemists D. I. Mendeleev, A. M. Butlerov, and N. N. Beketov.

F. Yu. Levinson-Lessing laid the foundations of our national systematic experimental research in the field of high-temperature physicochemical equilibria in silicate systems.

V. I. Vernadsky worked on such diverse problems as the chemistry of minerals, meteorites, radioactive processes, the biosphere, the geochemical classification of chemical elements, etc.

In his investigations, V. I. Vernadsky raised some very important scientific problems, which are of great significance both in theory and in practice. These include the problems of widely disseminated and rare

elements, the role of organisms in geochemical processes, the determination of the ages of rocks, and the structure of silicates.

He correlated his researches in the field of aluminosilicate structure with some questions relating to the structure of aluminosilicate products of the silicate industry. In this respect his work on the intramolecular changes in kaolinite during high-temperature firing, and on the structure of porcelain (separation of mullite) is of great interest to specialists in the field of silicate chemistry.

V. I. Vernadsky and his pupil A. E. Fersman, simultaneously with V. M. Goldschmidt, formulated the fundamental laws and investigated the most important aspects of a new scientific discipline — geochemistry. Their geochemical researches were carried out in parallel with mineralogical studies of the sites of useful minerals in the territory of the USSR. As a result, 42 new minerals were discovered, and new special forms of mineral materials, such as apatite, nepheline, etc., were studied.

The extensive scientific results obtained by V. I. Vernadsky and A. E. Fersman are summarized in articles on the geochemistry of individual elements, in a number of fundamental reviews of mineralogy, and in the theoretical works: V. I. Vernadsky's "Essays on Geochemistry" and A. E. Fersman's "Geochemistry."

The development of silicate science, physical chemistry, crystal chemistry, and the demands of industry for more and more improved products for the needs of modern, rapidly growing technology, required detailed investigations of the phase composition and structure of the products of the silicate industry (the so-called "technical stones,") Native stones and rocks had already been studied for a long time by petrographers.

One of our most eminent petrographers, D. S. Belyankin, worked on the mineralogy and structure of artificial stones. Being a distinguished scientist in the field of regional and general petrography, D. S. Belyankin devoted much of his labors to systematic studies of artificial stones, mainly the products of the silicate industry, and laid the foundations of a new branch of petrography — technical petrography.

On his initiative a special section of technical petrography, which was under his charge to the last day of his life, was established in 1932 in the former Petrographic Institute of the Academy of Sciences USSR. V. V. Lapin and B. V. Ivanov were his closest talented pupils and assistants in this section.

D. S. Belyankin, who always strove for the closest approach between scientific research and the problems of the silicate industry, trained a whole galaxy of young Soviet scientists. Among the work carried out by himself and his pupils (V. V. Lapin, B. V. Ivanov, N. A. Toropov, and others) on the most important products of the silicate industry, mention must be made of studies of the microstructure of various refractories, cement, glass, porcelain, and metallurgical and fuel slags. This work of the Belyankin school is the foundation of the physical chemistry of silicates, and its results are widely used in the solution of numerous applied problems in the silicate industry. The work on technical petrography assisted the adoption of petrographic techniques in research practice, and such investigations are now widely performed in all the leading industrial institutes. Technical petrography is also being adopted on a fairly large scale in testing of raw materials and finished products at numerous factories of the cement, refractory, ceramic, glass, metallurgical, and other industries.

In view of the continuous growth and development of industry, further prospects for the extension of this new branch of petrographic science are very extensive.

It would be unjust not to mention the role played by eminent foreign scientists; honorary member of the Academy of Sciences USSR, Academician H. Le Chatelier, and G. Tamman who guided the work of a number of young Soviet scientists abroad; these later became eminent exponents of Soviet silicate science (A. A. Baikov, D. Kh. Zavriev, I. F. Ponomarev, and others).

The work of N. V. Belov and his school is of fundamental significance in relation to silicate structure and the nature of the action of mineralizers. On the basis of this work, which extends the profound prognostications of a remarkable Russian scientist, E. S. Fedorov, the founder of crystallography, the chemistry and technology of silicates are becoming increasingly closer to mineralogy, and crystallochemical analysis is becoming a necessary part of every serious investigation in the field of silicate technology.

The work of Ya. I. Frenkel on the general theory of the liquid state, and of A. A. Lebedev and I. V. Grebenshchikov on the glassy state, has played an important part in investigations of silicate melts. This work confirmed the structural relationship between a solid silicate and its liquid melt. In the development of this

research, O. A. Esin and his school created an elaborate theory of the structure of silicate slag melts, and thereby rendered much help to silicate technologists in studies of the kinetics of many processes involving silicate melts.

K. K. Gedroits was an outstanding specialist in the fields of soil sciences and agricultural chemistry, the founder of the science of soil colloids and of their role in the formation and fertility of the soil. As the result of his researches, K. K. Gedroits developed the concept of the soil sorption complex, which is the combination of the organic and mineral substances in the soil, with colloidal properties, and which is the most active part of the soil in the physicochemical sense. The role of colloids in the earth's crust was further investigated by F. V. Chukhrov, I. I. Ginzburg, I. D. Sedletsky, N. I. Gorbunov, and others.

Colloidochemical concepts have been widely used in silicate chemistry and technology in the USSR owing to the work of P. A. Rebinder and his school. P. A. Rebinder guided numerous investigations of the influence of surface layers on the properties of suspensions, emulsions, foams, colloidal systems, and deformable solids.

These researches gave rise to a number of new methods and technological processes: modifications of rock-drilling processes and of beneficiation of useful minerals by flotation, improvements of the quality of disperse and colloidal materials, various fillers, pigments, building materials, and lubricants.

The development of the silicate industry in the USSR was aided by the work of our scientific research institutes and universities, where our specialists worked under the guidance of leading Soviet scientists. The cooperation of Soviet scientists undoubtedly assisted the fulfillment of the great tasks set by the five-year plans for the development of the national economy of the USSR. By their researches Soviet scientists enriched the science of refractories, produced a series of new refractories, and improved the properties of existing materials.

V. E. Grum-Grzhimailo was the first to put forward a theory of the firing of Dinas refractories.

He considered that the lime added to quartz or quartzite forms about 8-10% of a liquid phase during firing; this liquid phase wets the quartz grains and thereby cements them together. At high temperatures the quartz grains crack and dissolve in the glass phase. With correct firing, this cracking of the quartz grains occurs in the glass melt which wets the grains; the grains therefore have high mobility. Because of this mobility, the cracking process does not go beyond the limits of microscopic displacements. The glass fills the cracks and occupies the pores in the Dinas brick, and the whole growth of grain volume occurs without affecting the external outline of the brick. Here the glass serves, on the one hand, as a spring which mitigates the action of the forces in the metamorphism of quartz, and on the other, as a cement which fills the cracks and keeps the brick intact; it also acts as a solvent. The high stability of Dinas bricks in furnaces is mainly determined by the degree of conversion of the silica present in the bricks into tridymite during firing.

We developed the work of V. E. Grum-Grzhimailo on the influence of the mineralizing properties of various ferruginous slags, waste products from metallurgical processes. Scale and hearth cinders, being the richest in ferrous oxide, proved to be the most effective mineralizers. The investigations of I. S. Smeliansky showed that manganous oxide has an analogous effect. The advantage of manganese compounds is that they are inert to carbon monoxide, and therefore they are valuable mineralizers, especially for Dinas bricks used in coke ovens.

I. S. Kainarsky and L. I. Karyakin compared the ionic radii of the cations of various mineralizers and showed that additions of iron and manganese oxides to Dinas batches increase the wetting power of the silicate melts to a greater extent than calcium oxide, and that the action of iron oxide differs little from that of manganese oxide. These authors also studied different varieties of cristobalite and the conditons of their formation.

According to I. S. Kainarsky, the action of a mineralizer in the conversion of quartz to cristobalite (which occurs before formation of the liquid phase) depends on incorporation of the cations in the voids of the quartz lattice; as a result, the lattice is deformed and the activation energy of the transformation process is lowered.

S. M. Mamykin showed that the action of mineralizers directly depends on the temperature of formation of supersaturated melts, and the greater the crystallization power of the melt formed, the more effective is any given complex mineralizer.

N. N. Sinelnikov studied the kinetics of polymorphic transitions of silica in the presence of mineralizers. Crystallochemical analysis of the structural relationships between the principal modifications — quartz, tridymite and cristobalite — provided deeper insight into the mechanism of the interconversions of the principal forms of silica.

N. N. Sinelnikov used an adiabatic vacuum calorimeter in the development of a comparative method for the measurement of small heat effects by means of thermal analysis in vacuum, the temperatures being measured by means of a differential thermocouple to an accuracy of $0.002°$. By this method it was possible to determine within 2-3% the tridymite contents of fired quartz specimens, from the heat effect of the $\gamma - \beta$ transition of tridymite.

The work of I. S. Kainarsky on the technology of Dinas, based on the use of crystalline quartzites in bodies of small particle size, is well known.

This work has appreciably improved the quality of Dinas, increased producitivity, and led to the development of the production of a new type of high-density, high-silica Dinas for crowns of Martin furnaces. With the use of such Dinas steel smelting is accelerated, and furnace standstills during repairs and the consumption of Dinas are decreased.

The problem of multiple utilization of the salt wealth of the Sivash Sea is being successfully solved by the close cooperation of Russian (N. S. Kurnakov, N. S. Spiro, P. T. Danilchenko, A. M. Ponizovsky, and others) and Ukrainian (A. A. Alentiev, A. S. Berezhnoi, E. S. Burkser, P. P. Budnikov and others) scientists. Much work has been done on the technology of magnesium oxide production from Sivash brine, and of refractories from magnesium oxide; this is of great importance for metallurgy in the South.

A. S. Berezhnoi carried out numerous investigations on the formation of magnesian and other silicates, spinelides, and titanates in the solid phase.

As the result of these investigations the course of formation of forsterite, monticellite, merwinite, spinel, magnesiochromite, magnesioferrite, various titanates, and magnesium stannate was determined. A. S. Berezhnoi jointly with L. I. Karyakin, studied the conditions for the formation of cordierite. These investigations are not only of great theoretical significance, but are of interest from the technical aspect.

A. S. Berezhnoi studied the thermal transitions of magnesium silicates containing isomorphous additions of ferrous oxide. As a result, he prepared new refractories from olivinites, dunites, serpentinites, and other magnesium silicates. He studied the collective recrystallization of silicates, spinelides, and oxides, and obtained results which provided a scientific basis for the technology of highly refractory materials.

A. S. Berezhnoi investigated the structure of four-component systems containing periclase. He applied to silicate systems the method developed by A. A. Bochvar for the construction of phase diagrams for multicomponent systems, and drew a number of significant conclusions concerning the physicochemical processes of refractory corrosion in steel-smelting furnaces. A. S. Berezhnoi carried out research on the condensation coarsely disperse systems under pressure and on heating (sintering).

The work of G. V. Kukolev covers a wide range of problems associated with the physicochemical principles of silicate technology. He developed the fundamentals of the theory and methods of acceleration of the sintering of refractories, especially by regulation of the properties of the solid and liquid phases, the structure of the crystal lattice, and of the melt.

On the basis of the fundamental work of O. A. Esin and his school on the structure of silicate melts, G. V. Kukolev demonstrated the possibility of wide utilization of phase equilibria and phase diagrams in the production of dolomite and Dinas refractories and for variation and explanation of their properties. He developed the physicochemical and technological aspects of the production of high quality water-resistant dolomite bricks and of metallurgical dolomite with a high content of free lime. He also wrote a sound text book on the physical chemistry of silicates.

Our investigations of the influence of chromium oxide on the degree of binding of calcium oxide in dolomite led to the production of a new type of chrome—dolomite refractory. Chromite is used as stabilizer. The chromium oxide in the clinker is combined with lime in the form of chromoalite. The chrome—dolomite refractory is a substitute for chrome—magnesite bricks. It has hydraulic properties and may also be used for production of refractory concrete.

G. V. Kukolev, jointly with the author of this review, proposed the use of colloidochemical methods of liquefaction and of decreasing the moisture contents of slurries in the production of Portland cement, and a method for accelerating grinding of the raw mix with addition of electrolytes.

The use of oxygen in metallurgy, in particular in the Martin process, enabled Soviet metallurgists to develop a new technology of steel production, with wide prospects of further increases in the productivity of Martin furnaces. An urgent problem in this connection was the increase of the resistance of Martin furnaces by improvement of existing and development of new types of refractories. Whereas formerly the Dinas crown of the Martin furnace was adequate for normal operating conditions, now, when the refractory is under very severe conditions owing to the intensification of steel production, more stable materials are required.

As the result of studies of the specific properties of chrome—magnesite refractories (research by A. S. Frenkel, A. P. Panarin, V. V. Goncharov, and others) A. S. Frenkel developed an original design for a suspension—brace chrome—magnesite crown, adopted with great success in Martin furnaces.

With the use of these crowns the productivity of Martin furnaces has been considerably increased, the specific fuel consumption has been reduced, high-alloy steels can be smelted, and the durability of the furnaces has been more than doubled. These investigations also solved the problem of increasing the stability of other parts of the Martin furnace by the use of new refractories (including those based on forsterite) for regenerators.

Ya. V. Klyucharov investigated the physicochemical processes which occur in the service of various refractories in cement rotary kilns, and which cause wear of the furnace lining.

The phase composition and technical properties of refractories before and after service in industrial kilns were compared; this revealed the nature of the reactions between Portland cement clinker and chrome—magnesite, talc, and fireclay refractories under various service conditions: in thick and thin layers, with and without water cooling of the kilns, by the action of clinkers differing in mineralogical composition, etc. As a result of these investigations the most stable types of refractory linings have been recommended to the cement industry and adopted in practice; this has greatly reduced the consumption of refractories and increased kiln productivity.

Clays, the primary raw materials of the refractory and ceramic industries, have been studied in detail by Soviet scientists. F. D. Ovcharenko investigated the hydrophilic properties of clay materials by their heats of wetting.

In Ovcharenko's investigations the heat of wetting was used as a quantitative measure of the transition of free water into the bound state, and for calculation of the effective specific surface of clays. As the result of these researches Ovcharenko found that the active centers (the more highly electronegative atoms) in the surface of the clay particles bind water molecules by means of hydrogen bonds; the surface becomes covered with a monomolecular layer and liberates heat. The amount of bound water calculated from the heat of wetting corresponds to the amounts determined by the indicator and the hygroscopic methods. The hydrophily coefficients determined by Rebinder's method show that all clays are highly hydrophilic ($\beta = 2$-3). However, there is no definite correlation between the value of β and the mineral composition of a clay; this is probably because the interaction of the disperse phase with the dispersion medium depends not only on the polarity of the latter, but also on the structure of the clay material. Exchange ions influence the hydrophilic properties of clays. The following series of cations represents their influence on the amount of bound water and the heats of wetting of clays: $Ca^{++} > H^+ > Na^+ > K^+$.

In the course of experimental and theoretical studies of vacuumized clays and ceramic bodies we established, jointly with. D. Alperovich, that the physicochemical effects found to occur during the evacuation process may be explained with the aid of the modern physicochemical theory of surface phenomena, which forms the basis of the science of disperse systems. An important role in this respect was played by the work of P. A. Rebinder and his school on the hydrophilic and hydrophobic properties of mineral colloidal systems, by the work of A. M. Frumkin on the kinetics of adhesion of small bubbles to mineral particles, and by the work of B. V. Deryagin on the physicochemical properties of very thin liquid films at microbubble—particle boundaries. These theroretical investigations have provided a reliable scientific basis for the correct understanding of the physicochemical processes accompanying the vacuum treatment of ceramic bodies.

A. I. Avgustinik studied the spontaneous thixotropic reinforcement of clays and ceramic bodies in the pasty state; this effect is now taken into account and studied in soils and ceramic raw minerals.

In the first complete Soviet text book on the physical chemistry of silicates the describes research on the kinetics of silicate formation, presents new equations, develops calculation methods, and presents the principles of thermodynamics in relation to silicates.

A. I. Avgustinik developed the fundamental principles of industrial "micronization" of silicate raw materials (porcelain and special bodies, dolomite refractories, cement slurry) whereby the firing temperatures may be lowered, and devised a technique for the artificial drying of ceramic ware by means of high-frequency current for rapid drying of massive high-voltage insulators.

O. P. Mchedlov-Petrosyan studied the crystallochemical and thermochemical relationships in the changes in clays on heating, and put forward a new interpretation of the causes of the first exothermic reaction.

This question was the subject of a prolonged discussion. D. S. Belyankin and his pupils considered that the evolution of heat was the consequence of mullite formation, and others held the same opinion. E. K. Keler and his associates believe that formation of γ-alumina is the cause of the exothermic effect. O. P. Mchedlov-Petrosyan showed that the exothermic process is caused by reconstruction of the lattice, which precedes mineral formation and coincides with it only in the ideal case. If breakdown of the kaolinite crystals occurs, γ-alumina may separate out, while the presence of certain impurities or peculiarities in the original kaolinite crystals may suppress the exothermic effect.

Considerable attention has been devoted to the phase diagram for the system $Al_2O_3-SiO_2$, which is of great technical importance. N. L. Bowen and J. W. Greig (1924) established the composition of the binary compound $3Al_2O_3 \cdot 2SiO_2$ — mullite — in this system. The first reference to this phase appeared as long ago as 1890 in V. I. Vernadsky's papers. According to Bowen and Greig's phase diagram, mullite melts at 1810° with decomposition into corundum + liquid. However, N. A. Toropov and F. Ya. Galakhov showed in their investigations, with the aid of a vacuum microfurnace with a tungsten heater, that mullite melts without decomposition.

Recently these authors established the existence of solid solutions of mullite and alumina. These investigations are of great significance for ceramic technology. By means of high-temperature thermal analysis we, jointly with S. G. Tresviatsky, and V. N. Kushoskovsky, confirmed Toropov and Galakhov's findings of the congruent fusion of mullite.

V. V. Goncharov, G. V. Kukolev, D. N. Poluboyarinov, M. F. Nazarenko, and others have carried out a number of investigations of the influence of various mineralizers and of the temperature on the mullitization of clays and kaolins.

R. L. Pevzner used the principle of the thermite process (N. N. Beketov's aluminothermy, 1859) to produce a high-alumina fused refractory, "thermitomullite," which contains 78.5% mullite, 13.5% corundum, and 8% iron spinel.

A. S. Ginzburg, M. V. Osipov, A. A. Litvakovsky, and N. M. Neshchadimova carried out a series of investigations which led to the development of a technological process for the production of mullite refractories by the electrofusion and casting process. N. V. Solomin developed the physicochemical principles of the production of fused refractories.

A. A. Litvakovsky, demonstrated the favorable effects of the introduction of ZrO_2 into fused mullite refractories and developed the principles of the technological production of a mullite—corundum—baddeleyite refractory. He also, jointly with the present author, studied the high-alumina region of the ternary system $Al_2O_3-SiO_2-ZrO_2$.

To accelerate the recrystallization of γ-alumina and to facilitate sintering, it is recommended introducing small amounts of various additives (Fe_2O_3, MgO, ZnO, MnO, B_2O_3, cryolite, etc.), in the form of chlorides or oxides, into finely divided alumina. It is important that the grain size in the ware should not exceed $3-4\,\mu$, and that no acicular crystallization should occur. Otherwise the corundum ware will be of poor quality, especially, with regard to thermal stability and mechanical properties (see papers by I. I. Kitaigorodsky, N. M. Pavlushkin, N. E. Filonenko, D. N. Poluboyarinov, G. N. Duderov, V. A. Bron, V. K. Karklit, N. P. Stepichev, the present author, and others). These researches led to the production of high-quality aviation sparkplugs, cutting tools, dies, and other articles.

Our investigations, jointly with Kh. O. Gevorkyan, of the system kaolin—quartz-feldspar demonstrated the role of glass of the formation of porcelain structure during firing, and the influence of glass as a structure-forming constituent on the properties of porcelain.

We carried out a critical review of the generally accepted views on the firing of fine ceramics, provided an explanation of the mechanism of the contact interaction of feldspar melts with high-melting phases, and studied the kinetics of the firing of ceramic bodies. It was found that in the formation of porcelain the feldspar melt is not only a cementing material for the high-melting crystalline particles and a solvent for the high-melting components, but also a medium for complex diffusion processes which lead to the formation of high-quality porcelain ware.

V. P. Barzakovsky studied the influence of the composition of glazes for high-voltage porcelain insulators on their microstructure and crystallizing power.

A. E. Fradkin carried out basically new research on residual stresses in porcelain insulators.

The problem of residual stresses in porcelain arose in connection with the production, in the USSR, of large insulators for 400 kv voltage. The research on residual stresses included: study of the mechanism of their formation, development of methods of determination, experimental measurements of residual stresses, and development of heat treatment conditions during the cooling process for regulation of the magnitude of the residual stresses.

It was found that for large insulators the best treatment is cooling of the annealing type in the range 500-800°, which ensures the minimum stresses on the insulator surface.

During recent years extensive research has been carried out under the guidance of V. G. Avetikov on magnesia insulator ceramics.

The influence of talcs of different origins and compositions on the properties of high frequency steatite insulators has been studied. The influence of individual components of steatite and cordierite bodies on the dielectric loss of steatite at radio frequencies, on the heat resistance of the ceramic materials, and other properties was elucidated. The phase composition and structure of magnesia ceramics were studied, and the correlation between certain characteristics and the composition and contents of the glass phase in the steatite was demonstrated. These researches led to the development and industrial production of steatite materials based on Onotsk and Shabrovsk talcs, which are suitable for the production, by various technological processes, of strong high-frequency and high-voltage insulators and electrical equipment.

G. N. Voronkov developed a method of combined thermal analysis with simultaneous synchronous objective recording of heating curves (direct and differential) together with curves for changes of the linear dimensions, weight, and electrical resistance of the material.

Apparatus for studying materials by this method at temperatures up to 1450° has been disigned and constructed. The simultaneous synchronous and objective recording of several parameters provides much more detailed information on the nature of the processes in the material, based on the interrelationships between the individual values. E. K. Keler has carried out investigations of the same type.

Several of our scientists have studied the theory of reactions in mixtures of solids, and especially the mechanism and kinetics of these reactions. The initial stages of this research are presented in the monograph by A. S. Berezhnoi and myself.

Later, O. P. Mchedlov—Petrosyan carried out thermodynamic investigations of solid-phase reactions in silicate system ($CaO-SiO_2$; $MgO-Al_2O_3$); the primary formation of orthosilicates in alkaline-earth metal oxide-silica systems was explained, and it was shown that mullite is formed primarily when kaolinite or the mixed oxides are heated. This work demonstrated the value of thermodynamic studies of solid-phase silicate systems.

A. M. Ginstling carried out theoretical and experimental studies of the "elementary" processes which constitute reactions in solids, and demonstrated the important role of the gaseous and liquid phases in many reactions of this type.

By his studies of reaction kinetics in mixtures of crystalline solids, A. M. Ginstling was able to determine the causes of the apparent contradictions in published papers on this problem. They are essentially the consequence of a tendency to extend, without justification, the laws governing the course of some particular stage of a reaction under particular conditions, to the whole reaction, to reactions similar to it, and even to all so-called solid-phase processes.

A. M. Ginstling derived equations for the kinetics of reactions in mixtures of crystalline reactants under different conditions. His systematic investigations led to certain new principles relating to the selection and regulation of the practical conditions of such reactions.

The research of Soviet scientists on the chemistry and technology of cements covered studies of processes which occur in cement production, the mineral composition of cements, hardening, and the influence of various factors on these processes. A series of investigations deals with the formation of Portland cement clinker during burning; the influence of mineralizers; evaluation of the most important properties of cement from its mineral composition; the synthesis of individual minerals constituting Portland cement clinker; and the hydration of clinker minerals.

At the same time searches were made for new kinds of cements, with high strength in massive concrete constructions after short hardening times; colored cements; expanding cements; cements based on local raw materials and industrial wastes (blast-furnace and other metallurgical slags, nepheline slurry, wastes from the winning of asbestos, etc.). Much work has been done on the corrosion of cement. The corrosion of concrete was studied in relation to a number of factors which influence the stability of concrete in corrosive media.

A. A. Baikov created our generally accepted theory of the hardening of cements. The essential feature of Baikov's theory is that every hardening substance (cement) must pass through a colloidal stage, even though at the end of the hardening process the cement mass consists of crystalline formations with appreciable solubility in water. Solubility of the products of hardening is an important condition of hardening itself, as insoluble substances could not be visibly crystalline, although it is because of their presence that the crystalline state, which converts the whole cement mass into a monolithic entity, is formed. The solubility of a substance does not hinder its separation in the colloidal state in presence of a solvent; it merely determines the instability of the colloidal system (gel) which is formed. The sequence of all the changes in cement under the action of water is represented by the following simple scheme: a discontinuous aggregation of grains (cement paste), weakly bound gel (set cement), mechanically strong crystalline concretion (hardened cement); a necessary condition for these transformations is the presence of a liquid phase, such as water, in which the processes of solution, colloid formation, and crystallization take place.

Thus, the formation of supersaturated solutions of lime immediately after immersion of Portland cement in water is a necessary consequence of the separation of lime in the colloidal state, which is inevitable under such conditions, and the aqueous solution of lime, saturated with respect to colloidal particles of calcium hydroxide, must be supersaturated with respect to larger crystalline formations of calcium hydroxide; this is found to be the case.

P. A. Rebinder and his associates have done extensive research on the theory of setting and hardening of cements, based on physicochemical investigations of the mechanism of structure formation in suspensions under specific conditions of chemical interaction between a solid disperse phase and a liquid dispersion medium, and of crystallization of the hydrated phase.

These investigations showed that the setting and hardening of cements constitute a developing complex process involving hydration, spontaneous dispersion of the mineral particles of the cement clinker, formation of coagulational thixotropic structures, and the development of a crystallization structure of newly formed hydrates from the latter by crystallization from supersaturated aqueous solutions.

O. P. Mchedlov-Petrosyan reached similar conclusions concerning the crystallochemical dispersion of cement grains, his model being serpentinite cement.

He examined the crystallochemical processes accompanying hydration and advanced the idea that disturbance of coordination is the principal cause of the cementing properties in monomineral cements; he pointed out the role of the alkaline medium in hydration, to which attention had also been drawn by A. V. Volzhenskii and G. N. Sivertsev.

V. A. Kind and V. F. Zhuravlev attempted to correlate cementing properties with Mendeleev's periodic system. V. F. Zhuravlev correlated the effective radius of the alkaline-earth metal ion forming a compound of the type of calcium silicate, aluminate, or ferrite, with the presence or absence of cementing properties in the compound.

N. A. Toropov studied the phase composition of Portland cement clinker, regarded as consisting of phases of variable chemical composition formed predominantly by solid solutions.

He investigated the constitution of alite, belite, and tetracalcium aluminoferrite. As the result of analysis of his experimental data he concluded that the liquid phase of cement clinker contains much less lime than the clinker as a whole; one consequence of this is crystallization of $5CaO \cdot 3Al_2O_3$.

As the result of thermal and x-ray investigations of the system $5CaO \cdot 3Al_2O_3 - 4CaO \cdot Al_2O_3 \cdot Fe_2O_3$ Toropov concluded that crystals of $4CaO \cdot Al_2O_3 \cdot Fe_2O_3$ dissolve $5CaO \cdot 3Al_2O_3$ with a small excess of calcium oxide, up to the composition $8CaO \cdot 3Al_2O_3 \cdot Fe_2O_3$ N. A. Toropov's investigations are not only of theoretical interest, but are of great practical significance, as they aid in the solution of the problem of improving the quality of Portland cement.

The production of new types of Portland cement in the USSR was aided by the work of S. D. Okorokov, Yu. M. Butt, and S. L. Volfson on the synthesis of pure cement minerals and investigations of their properties during hardening in isolated form and in mixtures with each other. S. D. Okorokov also proposed a method for formulation of the composition of raw mixes according to the chemical and mineralogical characteristics of the cement clinkers.

M. I. Strelkov proved theoretically and experimentally that aluminate clinker is the most suitable for slag Portland cements; this is now generally accepted and applied in practice at the Russian cement works.

The new concept of aluminate saturation coefficient has been introduced, and used to determine the influence of magnesium on the maximum lime content of Portland cement; a method for calculation of the actual mineral composition of clinker has been developed.

New graphical and analytical methods for calculation of composition of raw mixes for given standardized mineral compositions of the clinker have been proposed. These methods have been used to work out schemes for the blending of raw mixes to give clinkers of predetermined composition, with an original procedure for the production of slurry without the use of correction tanks, directly in the raw feed cycle. This is particularly important in automatic cement factories. M. I. Strelkov also developed the theoretical principles of the production of "800" grade high strength rapid-hardening Portland cement.

The hydrotechnical construction developed in our country demands high-quality cements with definite setting times, with low exothermic effects during setting and hardening, with minimum shrinkage, and, with high resistance to frost, corrosion, abrasion, and cavitation under the action of flowing water.

One of the most urgent tasks set scientists by the builders was the selection of cements for durable concrete and ferroconcrete constructions. This problem is additionally important because concrete construction is carried out under very severe climatic conditions in the North and South, with frequent variations of the temperature and humidity conditions, and with water of high mineral contents in hot dry climates.

As the result of many years of research by our scientists it was found that pozzolana cements have great advantages in many cases over Portland cement for hydrotechnical construction. Important work was done by S. I. Druzhinin, who is one of the pioneers in the discovery and studies of the properties of hydraulic admixtures. The pozzolanization of Portland cement is the subject of a special work compiled by a commission on the use of admixtures, with the participation of A. A. Baikov, V. A. Kind, V. N. Yung, S. M. Royak, G. M. Rushchuk, and others.

The technical specifications for cement have been developed and recommended as the result of further research by our scientists and an extensive discussion on problems of the selection of cements and the required properties for use in concrete in hydrotechnical constructions. This extensive investigation was carried out with the participation of V. N. Yung, B. G. Skramtaev, S. V. Shestoperov, P. P. Budnikov, V. V. Stolnikov, Yu. M. Butt, S. M. Royak, B. A. Kuvykin, L. A. Kaiser, S. A. Mironov, Yu. A. Nilender, B. V. Zalesski, and others.

The execution of the great construction program also set our scientists the task of finding ways of increasing the durability of constructions — the stability of concrete and ferroconcrete under the influence of chemical and physical factors. Numerous investigations of the corrosion of concrete were carried out by our scientists: A. A. Baikov, V. A. and V. V. Kind, B. G. Skramtaev, S. M. Royak, V. M. Moskvin, Yu. M. Butt, S. D. Okorokov, and others. These investigations were concerned with the causes of corrosion and means of combating it.

These researches laid the foundations of a theory of concrete corrosion, which can be used for development of measures for the protection of concrete and ferroconcrete against corrosion and for ensuring the durability of constructions in corrosive media. The effects of the nature of the mineralized aqueous medium on the hardening of concrete have been determined. The problem of sulfate-resistant Portland cement has been solved.

Our researches showed that calcium hydrosulfoaluminate may be a structurally useful compound in cement under appropriate physicochemical conditions.

The addition of calcium sulfate to high-alumina Portland cement, in quantities greater than prescribed by the standard, increases the resistance of the hardened cement to aqueous solutions of sodium, magnesium, and calcium sulfates. The more tricalcium aluminate in the cement combines with calcium sulfate during the first stages of hardening (up to 28 days), according to L. A. Gudovich), the higher the sulfate resistance of the cement will be.

Investigations carried out by the author jointly with I. G. Goldenberg and G. S. Valberg showed that calcium sulfate in aluminate cement in presence of a liquid phase forms hydrosulfoaluminate, which has a favorable influence on the properties of this cement; the strength increases rapidly, the cement expands on hardening, and the strength increases considerably on hardening at the elevated temperatures resulting from the heat effect of the process or from external heating. As the result of these investigations we produced, jointly with B. G. Skramtaev and I. V. Kravchenko, an expanding gypsum—alumina cement, which has acquired great practical importance.

As the result of studies of the chemistry of processes in the system blast-furnace slag-calcium sulfate—$Ca(OH)_2$ or $Mg(OH)_2$, P. P. Budnikov and his associates (L. G. Gulinova, V. K. Gusev, and V. M. Lezhoev) developed new types of cements — clinkerless sulfate—slag and low-clinker slag cements. The author's theory of the hardening of slag cements was confirmed in practice and forms the basis of the technological production of various sulfatized cements.

The formation of calcium hydrosulfoaluminate in clinkerless or low-clinker slag cements has a favorable effect on their properties. Hydrosulfoaluminate is the cause of the early cement strength, and by its formation it assists the separation of other new substances — calcium hydroaluminates and hydrosilicates — which increase further the strength of the cement.

It was found that certain surface-active organic substances (sulfite alcohol liquor, lignosulfonates, resin soaps, etc.) may be vary effective in relation to the economical use of cement, workability of the concrete mix, control of the setting time, decrease of heat evolution during the initial setting period, and improvement of the mechanical properties, water impermeability, and frost resistance of the concrete. The physicochemical principles of the action of surface-active additives on cement pastes and concrete were developed by P. A. Rebinder.

Many problems relating to the plastification of cement and concrete were solved as the result of extensive research on the influence of surface-active substances on the properties of cements and concrete; the results of this research are widely applied in the cement industry and construction practice. A team of scientists took part in this work: P. A. Rebinder, S. V. Shestoperov, V. V. Stolnikov, A. V. Satalkin, B. G. Skramtaev, F. M. Ivanov, S. M. Royak, V. I. Soroker, B. D. Trinker, Yu. M. Butt, S. A. Mironov, V. M. Medvedev, N. A. Moshchansky, L. Ya. Reznik, G. I. Logginov, and others.

S. V. Shestoperov showed that the addition of sulfite waste liquor to cement makes it possible to increase the gypsum content of the cement. This makes the cement and concretes based on it more resistant to various physical and corrosive chemical external influences, and increases their strength.

V. V. Stolnikov's investigations showed that abietates (resin soaps), sodium naphthenates, cottonseed oil, etc., have considerable surface activity at the liquid—air interface in cement pastes. When introduced with the mixing water, these additives cause the formation of a fairly fine emulsion of air in the system and increase the volume of air stably dispersed in the concrete mixture.

Although 0.08% additions of these air-entraining additives (such as sodium abietate) decrease the strength of the concrete somewhat, they reduce considerably the water—cement ratio of concrete mixes. Air-entraining additives considerably reduce the friction of concrete mixes against pipe walls.

M. I. Khigerovich and B. G. Skramtaev ground cement clinker with sodium naphthenates to obtain a hydrophobic cement with a number of technically valuable properties. This cement does not lose its activity during prolonged storage. When the concrete is mixed, the hydrophobic adsorbed films become partly detached as the result of stirring, and the cement becomes capable of hydration.

It was shown by the work of A. V. Voizhensky, Yu. M. Butt, P. I. Bazhenov, I. A. Khint, and others that the hardening of ordinary lime—sand blocks under hydrothermal treatment occurs by the reaction between silica and calcium hydroxide to form calcium hydrosilicate, which serves as the binding material.

In the production of silicate building materials, the presence of clay in the lime—sand mass was considered harmful and its content was limited to 8%. However, the results of our researches, and later of the work of the Russian Institute of Local Constructional Materials, refuted the existing view and demonstrated the very favorable effects of clay in raising the strength of the product formed by hydrothermal treatment. The work of the author of this review showed that hydrothermal treatment weakens the bonds in the crystal lattice in clay, and alumina and silica became capable of reacting chemically with calcium hydroxide to form tetracalcium hydroaluminate and calcium hydrosilicate respectively; these are the binding substances in clay—lime building materials under conditions of hydrothermal treatment.

In the development of the science of glass in the USSR, an important part was played by our scientific research institutes and the laboratories of technical colleges and universities.

During the past three or four decades the science of glass has been provided with an elaborate theoretical basis. The study of phase equilibria was applied to investigations of a number of new types of glasses, of great practical importance; new types of glass with predetermined characteristics and conforming to various require- ments have developed as the results of studies of the structure of glass and of its physical and chemical proper- ties.

The State Optical Institute provided the scientific basis for the production of optical instruments and optical glass in the USSR. Much credit in this respect is due to S. I. Vavilov, D. S. Rozhdestvensky, I. V. Gre- benshchikov, A. A. Lebedev, A. N. Terenin, V. P. Linnik, N. N. Kachalov, A. I. Tudorovsky, K. S. Evstropev, V. V. Vargin, K. G. Kunanin, and others.

I. V. Grebenshchikov and his team developed the theory and practice of the clarification of optical glass.

The problem of the production of glass with a low coefficient of reflection is of exceptional practical importance for the optical instrument industry. Reflection in optical instruments was formerly reduced by de- crease of the number of optical parts, the use of glass of low refractive index, and by cementing of glass sur- faces with transparent resins with refractive indices similar to that of glass.

At the present time the amount of light reflected from glass surfaces is reduced by formation of ultrathin films (about 1375 A thick) on the surface of optical glass, the refractive index of the film being much less than that of the glass. Such a film on the glass surface lowers the coefficient of reflection, and "clarifies the surface" as the result of interference effects between the light reflected from the film surface and the glass surface under the film.

No less important is the problem of conferring the maximum coefficient of reflection to a glass surface. This is achieved by application of a film of definite thickness and with the maximum possible refractive index; this makes the glass capable of reflecting linearly polarized light.

Soviet scientists have made important contributions to the science of the glassy state. As long ago as 1921, A. A. Lebedev published the results of his researches on the annealing of optical glasses and put forward the theory of the crystallite state of glass. A. A. Lebedev's crystallite hypothesis caused our scientists to reject the concept of glass as an undercooled liquid.

A discussion of the status and future development of the theory of glass structure showed that the develop- ment of the crystallite hypothesis and the hypothesis of short-range order led to a unified view on the nature of spatial order in the atomic arrangement in glass, indicative of the presence of chemical bonds.

Extensive research, which provided valuable material for the formulation of the theory of glass structure, was carried out by our scientists V. V. Tarasov, V. V. Vargin, O. K. Botvinkin, A. A. Appen, I. I. Kitaigorodsky, K. S. Evstropev, M. V. Okhotin, I. F. Ponomarev, E. A. Porai-Koshits, K. G. Kumanin, O. A. Esin, M. P. Volaro- vich, N. N. Kachalov, E. F. Gross, V. A. Florinskaya, and others.

N. N. Kachalov investigated questions of the grinding and polishing of glass. He found that the viscosity of the liquid used has a great influence on the rate of grinding. Tests of various surface-active substances (valeric, lactic, and caproic acids, sodium oleate, etc.) showed that they had an accelerating effect when added to aqueous liquids.

I. I. Kitaigorodsky's researches on the crystallizability and crystallization rates of glasses in the five-component system $SiO_2-Al_2O-CaO-MgO-Na_2O$ led to the development of industrial alumina—magnesia glass compositions adopted in mechanized window-glass works of the USSR.

These researches provided the material and technical basis for intensified mechanized production of glass. Studies of the kinetics of the glass-formation process led to the development of the principles of glass melting in thin layers, and to the practical execution of the process. I. I. Kitaigorodsky developed leadless glasses for electric lamps, carried out extensive work on coloration and opacification of glasses, and introduced the results into production. He and his associates produced foam glass, and assisted in starting up the first foam-glass factories.

I. F. Ponomarev devoted much attention to the physical chemistry of silicates. He developed a method of forced crystallization of glass, which made it possible to study the crystallization properties of substances which crystallize with difficulty. The method is simple and suitable for use in works conditions. Different variations of this method, proposed by T. N. Keshishian, are extensively used in Russian and foreign research laboratories.

M. A. Matveev carried out theoretical and experimental research on the synthesis and analysis of alkali silicates; he studied the physicochemical properties and structure of these silicates in various forms of aggregation. The conditions for the formation of crystalline sodium trisilicate, its microstructure, and its thermodynamic and other properties were determined as the result of these investigations.

M. A. Matveev also studied aqueous and vapor-phase hydration and solution of glassy alkali silicates, and developed an industrial process for the production of alkali hydrosilicates and articles made from them.

The work of M. A. Bezborodov laid the foundation of quartz-glass production in the USSR. He studied the rate of crystallization of quartz glass in relation to the gaseous medium (hydrogen, carbon monoxide, hydrogen sulfide, carbon dioxide, air, etc.).

Bezborodov explained the effects observed in the process, and correlated them with the surface tension of glass and with the chemical processes which occur in glass when it is heated in a gaseous medium. He laid the foundation of systematic research on the physicochemical processes of silicate formation during glass melting. M. A. Bezborodov studied sodium and potassium borosilicates used in electrovacuum technology, sodium and potassium aluminoborosilcates used for high-temperature thermometers, medium flint-glass batches used for optical purposes, and others, and developed a combined method for studying silicate and glass formation, which has been applied in other investigations.

The physical chemistry of silicates has been advanced considerably by the work of O. K. Botvinkin and his associates.

Botvinkin's work on the applicability of Raoult's law to silicate melts showed that when various meta-silicates are added to sodium disilicate the melting point decreases in direct proportion to the molecular concentration of the melt. In his work on the electrical conductivity of silicate melts Botvinkin showed that the law of Rasch and Hinrichsen is applicable only above and below the anomalous region. Walden's law was found to apply to glasses. In his studies of beryl glasses transparent to x-rays, Botvinkin obtained Lindeman glass on the assumption that the coefficient of absorption is an additive function of the absorption coefficients of the individual elements, and a function of the atomic number. The only glass-forming elements of low atomic number can be lithium, beryllium, and boron.

Additional information on the achievements of Soviet scientists in the field of silicate chemistry and techology can be found in the literature sources cited below [1-9].

LITERATURE CITED

[1] P. P. Budnikov, Ukrain. Chem. J. 12, 11-12, 472-476 (1937).

[2] P. P. Budnikov, J. Appl. Chem. 22, 11, 1097-1124 (1947).

[3] P. P. Budnikov, Achievements of Soviet Science in the Silicate Field in 30 Years (Bureau of Technical Information, Ministry of Building Materials RSFSR Press, Moscow, 1949).*

[4] P. P. Budnikov, Ceramic Coll. 2, 15-20 (1939).

[5] P. P. Budnikov, The Silicate Industry in the Five-Year Plans (Acad. Sci. Ukrainian SSR Press, Kiev, 1940) pp. 541-556. *

[6] V. V. Yurganov, Ten Years of GEIS (Office and Science and Technology, VSNR USSR Press, Moscow, 1928).*

[7] I. F. Ponomarev, "The Siberian Silicate Industry" Bull. Siberian Engineers 7 (1927); Review of the Activities of the Institute of Glass (Moscow, 1932); Essays on the History of the Academy of Sciences USSR, Chemical Sciences (Izd. AN SSSR, Moscow, 1945).*

[8] A. A. Balandin, B. M. Berkengeim, and A. N. Nesmeyanov, Progr. Chem. 16, 5, 513 (1947).

[9] A. A. Grinberg, Progr. Chem. 12, 3, 165 (1943).

*In Russian.

THE NITROGEN INDUSTRY OF THE USSR

E. Ya. Melnikov

Tsarist Russia did not really have a nitrogen industry; there were only a few units for the production of nitric acid from Chile saltpeter, which produced 49,180 tons of acid in 1916; a factory with an output of about 10,000 tons of ammonium nitrate per year was completed in Yuzovka (Stalino) in 1917 [1], based on original research and the project of Engineer I. I. Andreev. Although this factory was among the most advanced undertakings for those times, it did not produce synthetic ammonia, but converted ammonia liquors from coke-oven by-products into weak nitric acid and ammonium nitrate.

The creation and development of the nitrogen industry presented very great difficulties. This branch of industry differs fom all other chemical industries in requiring very complex equipment of high energy consumption, which operates at high pressures and both at high and very low temperatures, is subject to the action of corrosive media, and which requires considerable know-how for its construction and utilization.

In 1928 the M. I. Kalinin works were built in Dzerzhinsk; this was really the prototype of the modern nitrogen industry, as it was the first in the Soviet Union to achieve the complete nitrogen cycle — the production of synthetic ammonia, nitric acid and nitrogenous fertilizers.

The years of the first five-year plans were years of rapid development of the nitrogen industry. In 1930 the Dzerzhinsk works were considerably extended, and in 1932-1933 the Berezniki, Stalinogorsk, and Gorlovka nitrogen fertilizer combines were brought into operation.

With the start of the intensive development of the chemical industry, "Khimstroi" was organized in 1926, and the "Khimproekt" planning institute in 1928. The "Giprokhim" and "Giproazot" institutes were later organized developments of the latter. In 1931 the Scientific Research Institute for Nitrogen (GIA) was established. Thus, from the very start of the development of the nitrogen industry steps were taken to establish and train numerous groups of qualified research, planning, design, construction, and operating workers, capable of fulfilling the task of creating a powerful nitrogen industry based on advanced technology, without resort to foreign help.

By the middle of the 1930's our machine-building industry mastered the production of complex equipment for the nitrogen industry. Therefore in the latter part of the 1930's all the undertakings which were being built, modernized, or expanded were equipped with Russian machinery, equipment, and apparatus, based on Russian research, planning and design.

The diverse raw-material and economic conditions and the great distances in the USSR uregently necessitated the development of a number of new and promising methods for the production of gas for ammonia synthesis, in addition to the gasification of coke, which had already been achieved, and the separation of coke-oven gas at low temperatures.

This problem was successfully solved in the latter half of the 1930's when, as the result of extensive research, the continuous gasification of brown coal in the GIAP (State Institute of the Nitrogen Industry) gas producer, tube and shaft catalytic vapor—oxygen—air conversion of methane-containing gases, and the electrolysis of water could be brought into industrial operation [2-4].

Apart from methods adopted for the production of dilite nitric acid with and without the use of high pressures, a Russian combined method for the production of dilute nitric acid was brought into operation — by the

oxidation of ammonia without the use of pressure, with absorption of nitrogen oxides at a pressure of 7 atmo - spheres. The first units for the production of synthetic urea, based on the results of Russian research, were built and brought into successful operation.

Ammonia nitrate, the principle nitrogenous fertilizer, was also produced by a process developed by Soviet specialists — neutralization in the "ITN" apparatus with utilization of the heat of neutralization of nitric acid by ammonia, evaporation in high-speed evaporators, and granulation of the product in a granulating tower.

In 1940 the nitrogen industry of the USSR occupied third place in world production of synthetic ammonia.

However, the war started by Fascist Germany did great damage to a number of nitrogen factories. Never- theless, during the years of the Great Patriotic War the nitrogen industry of the USSR fully supplied the defense requirements of strong nitric acid and ammonium nitrate. The twelve post-war years were years of rehabilita- tion and further development of the industry. The nitrogen industry has now become a mighty branch of the chemical industry; it supplies nitrogenous fertilizers for the needs of agriculture and chemical products for the rapidly growing industrial demands.

Figures illustrating the growth of nitrogenous fertilizer production during the period 1933-1955 are given below. The output of nitrogenous fertilizers is calculated as ammonium sulfate, including the products of the coke-oven industry [5].

	1933	1935	1940	1945	1950	1955
Nitrogenous fertilizers (in 1000 tons)	110.9	374.5	972	744.7	1908.3	2984

During the Sixth Five-Year Plan the nitrogen industry will continue its rapid development, with a corres- ponding increase in the output of nitrogenous fertilizers, which will reach about 1,200,000 tons, calculated as pure nitrogen, in 1960 [6], or about 5,900,000 tons calculated as ammonium sulfate (including coke-oven by- products).

To ensure this large increase in the output of nitrogenous fertilizers it is intended to build new factories and to extend and reconstruct existing works.

The characteristic features of the factories being built or extended are: a) the use of cheaper raw materi- als, including natural gas from oil wells, coke-oven gas, and gases from petroleum processing; b) extensive coordination of the nitrogen industry with the production of heavy organic synthesis — alcohols, aldehydes, amines, synthetic resins for artificial fibers and plastics, and intermediates for synthetic rubber. During recent years petroleum chemistry has been coordinated with the nitrogen industry; other features are: c) extension of the range of mineral fertilizers, especially in concentrated form; d) construction of nitrogen works of high power, based on advanced technological processes. Large works are provided with large and highly productive units and machines, the output per individual unit generally being 50,000-75,000 tons of ammonia per year; 6) multiple automation.

In some factories, where considerably expansion is difficult, obsolete equipment is being replaced by more efficient and productive equipment, and additional automation is being introduced.

In this way it will be possible to effect considerable decreases in capital costs, to decrease the numbers of operational and maintenance personnel, and to reduce production costs.

Production of synthetic ammonia. The most important sources of raw material for the production of syn- thetic ammonia have up to now been coke, coke-oven gas, and brown coal.

Both intermittent and continuous gasification are widely used for production of nitrogen-hydrogen mixture from coke. In continuous gasification, steam—oxygen—air blow is used in the producers. Brown coals are gasi- fied in GIAP producers, with steam—oxygen—air blast. A characteristic feature of GIAP producers is their continuous operation and the possibility of the construction of very powerful gas-producer units.

Coke-oven gas is converted into nitrogen-hydrogen mixture for ammonia synthesis, both by low-tempera- ture separation with the utilization of unsaturated hydrocarbons for organic synthesis, and by catalytic or high- temperature steam—oxygen—air conversion. Thus, oxygen is now being used fairly extensively in the nitrogen industry.

As the result of research work, planning, and trials it is possible to obtain gas for ammonia synthesis by several methods from a number of other sources, including natural gas and oil-well gas, gas from petrochemical works, and peat. The production of nitrogen-hydrogen mixtures from liquid fuels will soon be achieved.

Factories which use coke-oven gas for conversion into synthetic ammonia have the lowest production costs. The production of a nitrogen-hydrogen mixture from coke-oven gas also involves lower capital investment and labor costs.

Below are given data on the production costs of ammonia, capital investment, and labor costs per ton, the data for coke-oven gas being taken as 100%.

Raw material	Production cost (%)	Capital investment (%)	Labor costs (%)
Coke-oven gas, low-temperature separation	100	100	100
Coke	120-150	110	125
Brown coal	140-175	125	130

Because of the discovery of large sources of natural gas in the northern Caucasus, in the regions of the middle Volga and beyond the Volga, in the northern Urals, and a number of other regions, and because of the rapid construction of gas pipelines in the country, natural gas will become a most important raw material for the nitrogen industry in the near future. Natural gas is close to coke-oven gas as a raw material for ammonia synthesis in respect of production costs, capital investment, and labor costs per unit of production. Therefore, in order to decrease production costs, several nitrogen fertilizer combines are already being converted from the use of coke to natural gas. Calculations have shown that the additional capital outlay involved in conversion to natural gas is recovered in a little more than 1 year. This shows that the conversion of these factories to the use of natural gas is very advantageous economically. Whereas at the present time most ammonia is made by gasification of coke, with coke-oven gas occupying the second place as a source of raw materials, in the very near future most ammonia will be made from the cheapest raw materials — coke-oven and natural gases.

The changes in the structure of the raw material supplies for the nitrogen industry of the country [7] are shown below.

Raw material	Amounts (%) in the years	
	1956	1960
Coke	40	16
Coal	5	8
Coke-oven gas	34	34
Natural gas	–	29
Other sources	21	13
Total	100	100

In the near future factories designed for the use of oil-well gas as raw material will also be built; the gas will be subjected to low-temperature oxidation by oxygen with the production of aldehydes and methanol in addition to nitrogen-hydrogen mixture.

During the Sixth Five-Year Plan the production of ammonia will be combined with the production of acetylene from methane-containing gases by thermal oxidation with the use of oxygen. After separation of acetylene and other admixtures, the gas will be used for conversion into ammonia-synthesis gas; this should lower considerably the cost of ammonia. The experimental work required for solution of this problem is being actively pursued.

When ammonia is made from coke-oven gas, gases made by the gasification of coke and brown coal, or gases made from liquid fuel, these gases must be freed from hydrogen sulfide. Both wet and dry methods of purification are used in the nitrogen industry; in particular, by means of bog iron ore, active carbon, sodium arsenite solution, and amines. Each of these methods has its fields of application. However, in view of the

necessity to lower capital investment and production costs work is necessary on uses of more effective and easily regenerated absorbents with the production of sulfur or sulfuric acid.

The extensive use of oxygen in the conversion of methane-containing gases, brown coal, coke, and liquid fuels justifies the use, in new factories, of the liquid nitrogen obtained from air for washing the converted gas in order to remove carbon monoxide, methane, and argon. This is a more economical method than the former process for removal of carbon monoxide in cuprammonium solution at pressures of 120 or 320 atm. The cost of ammonia can be reduced by about 5% and capital investment by up to 8% with this method (Fig. 1).

To increase the profitability of synthetic ammonia production, the present ammonia synthesis units with outputs of 60-100 tons per day are being replaced in the new large works by units producing up to 200 tons/day, with average outputs of 40 tons and more per day per 1 m^3 of catalyst contained in the reaction chambers. It is interesting to note that during the past 25 years the productivity of the catalyst has been at least trebled. During the same period, owing to improved design and construction of the high-pressure vessels produced by the machine-building factories, the weight of metal per 1 m^3 of equipment volume has been more than halved.

Turbine pumps are being installed for circulation of the synthesis gas in order to simplify the synthesis of ammonia and to decrease the contamination of the gas with oil vapor, with a consequent increase of catalyst productivity. To make the process more economic, at some works a considerable proportion of the heat of the synthesis reaction is utilized for such purposes as preheating the condensate used as feed water for the power station boilers. More universal methods of utilizing this heat are now being developed.

It is interesting to note that during the past 15 years ways have been found of using equipment designed for ammonia synthesis, for the production of methanol; this provides for greater flexibility in the use of such equipment.

Trials of multiple automation of the principal sections of the ammonia industry are being carried out in order to maintain the technological conditions at the optimum level and to increase labor productivity.

Production of dilute nitric acid. The units for the production of dilute nitric acid, built during the past five-year periods, operate according to different schemes. In addition to units in which the ammonia is oxidized and the oxides absorbed without the use of pressure, there are a number of units in which the oxidation and absorption are carried out under pressures of 5-8 atmospheres, and also combined units with oxidation without pressure and absorption at 3.5-7 atmospheres.

In recent years intensive work has been done on improvement of the existing methods for the production of dilute nitric acid. The improved combined process which is being adopted involves the use of 3.5-4 atm. pressures for absorption, with fairly complete absorption of nitrogen oxides in water without additional absorption in aqueous soda solutions (Fig. 2). The process requires relatively little power consumption (about 220 kw-hr per ton of monohydrate), and has an efficient absorption system owing to the existence of a foam regime in the absorption tower. At the same time, the design of the plates is such that they are simple to make. With the use of this process, capital investment can be reduced by 25% relative to the widely used process operated at atmospheric pressure. The process adopted for oxidation and absorption makes automation fairly simple.

In view of the fact that in large-tonnage units the ammonia conversion section is very cumbersome, and the use of turbocompressors for the oxidized gas is rather complicated, work on improvements of the combined process is now accompanied by work on radical improvements of the process for oxidation and absorption under pressure. This work is being carried on in two directions — toward a decrease of the specific consumption of platinum to reach the levels attained in processes with low-pressure oxidation, and toward a decrease of power consumption by increase of energy recovery in gas turbines.

To decrease platinum consumption, one existing low-pressure ammonia oxidation unit has for several years been using a two-stage catalyst, platinum being used only in one stage. In another works a large industrial unit operates with a nonplatinum catalyst. It is very likely that in the future nitric acid units will operate without the use of platinum [8].

In recent projects, as the result of the use of large and highly productive equipment, combined process schemes, and extensive automation, labor productivity has been trebled in comparison with the labor productivity in leading units of the existing undertakings of the Main Administration of the Nitrogen Industry.

Fig. 1. Flow sheet for the production of ammonia from natural gas. 1) Saturation tower; 2) heat exchanger; 3) methane converter; 4) humidifier; 5) carbon monoxide converter; 6) boiler; 7) heat exchanger for water heating; 8) water-heating and condensation tower; 9) absorber; 10) alkali scrubber; 11) compressor ($P_{KOH} = 320$ atm.); 12) filter; 13) condensation tower; 14) ammonia condenser; 15) turbine circulation pump; 16) ammonia synthesis column; 17) water condenser; 18) separator for liquid ammonia.

Production of nitrogenous fertilizers—More than 20 years have passed since the time when ammonium nitrate, which is a concentrated nitrogenous fertilizer containing 34% nitrogen, became the main fertilizer produced by the Soviet nitrogen industry. The Soviet Union pioneered the extensive agricultural use of ammonium nitrate in the pure state. Since 1942 the United States, using USSR experience, also began to make extensive use of pure ammonium nitrate in agriculture.

Work carried out by the institutes and the factories of the nitrogen industry on reduction of caking of ammonium nitrate during storage, by the use of inorganic additives, has been successfully completed. Several types of granulated ammonium nitrate, practically noncaking, are now being produced in the USSR (Fig. 3).

Experience of the agricultural use of ammonium nitrate containing inorganic additives, over a number of years, has shown that it is partially free from caking not only when stored under good conditions, but also if stored under less favorable conditions on site. It is easily disseminated, both immediately after supply and when applied to the soil. Recrystallization and breakdown of the granules during storage is very rare and insignificant.

Because of the low production costs of ammonium nitrate, it high content of combined nitrogen, its good fertilizer properties, and its noncaking characteristics, it continues to occupy the leading place among the nitrogenous fertilizers.

Automation was successfully introduced during 1956-1957 at the main sections of the ammonium nitrate unit of the Lisichansk Chemical Combine; this will raise productivity and reduce costs.

Sodium and calcium nitrates are produced in several factories. Sodium nitrate is made only by conversion of nitrite + nitrate liquors from alkali absorption of nitrogen oxides remaining after acid absorption. Calcium nitrate is made by conversion of nitrite + nitrate liquors from the alkaline absorption of nitrogen oxides. A certain amount is produced during the production of fertilizers by the nitric acid decomposition of phosphates.

Calcium nitrate is not made specially in our country by neutralization of nitric acid, owing to the high cost of nitrogen in the product. Therefore sodium and potassium nitrate play a relatively small role among the nitrogenous fertilizers.

The extensive use of synthetic urea, not only in industry but also and primarily in agriculture, has been recently hindered by the high cost of nitrogen in this product. Therefore intensive research and planning work has recently been carried out in order to improve the technological processes and raise the degree of utilization of ammonia and carbon dioxide, and to introduce larger and more productive equipment into the synthetic-urea units. As a result of this work, the cost of nitrogen in the form of urea, produced by the large units, is close to the cost of nitrogen in the cheapest nitrogenous fertilizer, ammonium nitrate (allowing for the cost of transport to the consumer). This provides technical justification for development of this process and for the use of urea as a highly concentrated nitrogenous fertilizer, containing 46% nitrogen, and for fodder.

With the aim of lowering further the costs of nitrogen in fertilizers and to decrease the specific capital investment in the construction of undertakings of the nitrogen industry, successful large-scale field trials were carried out in 1956 in the Ukraine and Uzbekistan with the direct use of ammoniacal liquors and liquid ammonia as liquid fertilizers.

The use of liquid fertilizers in agriculture rose sharply in 1957. There are serious grounds for believeing that liquid fertilizers will be used extensively in the state and collective farms in the near future.

It must be noted, however, that the successful adoption of liquid fertilizers requires the creation of economical and easily maintained stores in the consuming regions, and improvement in the design of the equipment used for application of the fertilizers.

The nitrogen industry of the Soviet Union also produces mixed fertilizers, containing nitrogen, phosphorus, and potassium, made by decomposition of aptite by nitric acid followed by ammonia treatment and addition of potassium chloride. The present output of mixed fertilizers is relatively small, but intensive experimental work is in progress, with the aim of simplifying the technological processes for their production and lowering the specific costs of the nutrients. Therefore the relative proportion of mixed fertilizers will increase very appreciably in the near future.
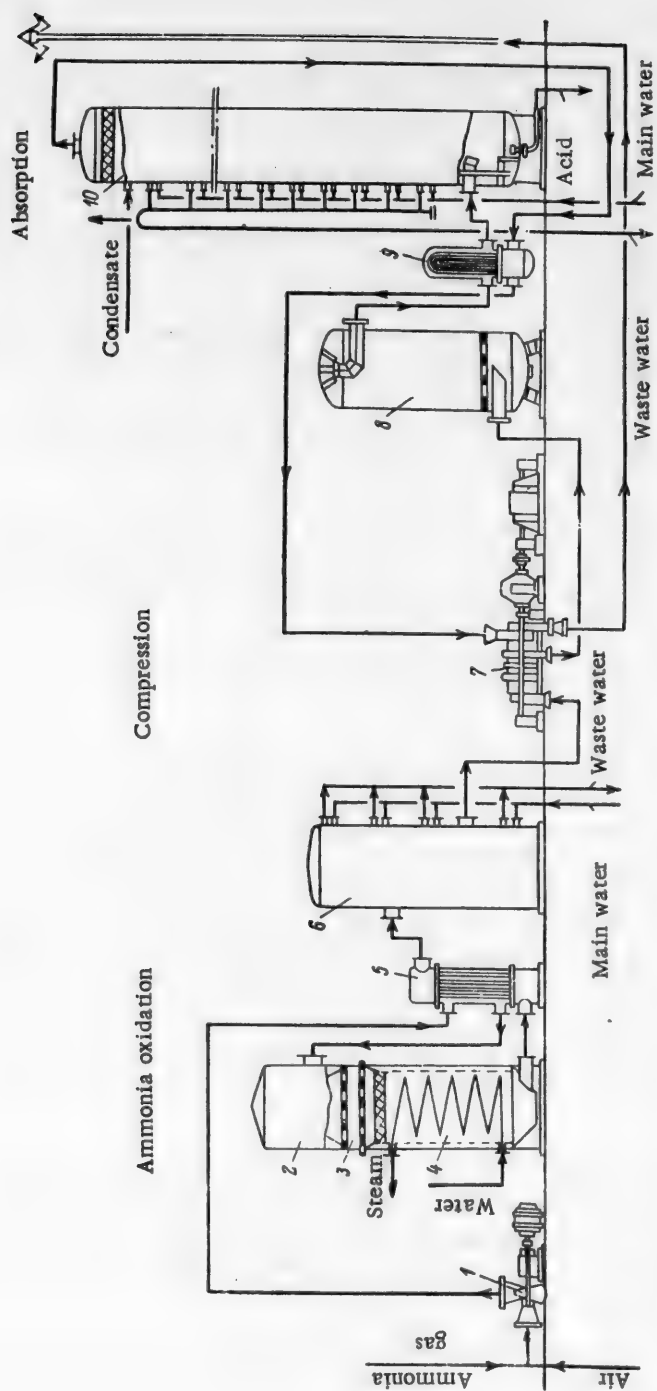
Fig. 2. Flow sheet for the combined process for the production of dilute nitric acid. 1) Air-ammonia blower; 2) filter; 3) contact unit; 4) waste-heat boiler; 5) preheater for ammonia–air mixture; 6) gas cooler and washer; 7) compressor for nitrogen oxides; 8) oxidation vessel; 9) waste gas preheater; 10) absorption tower.
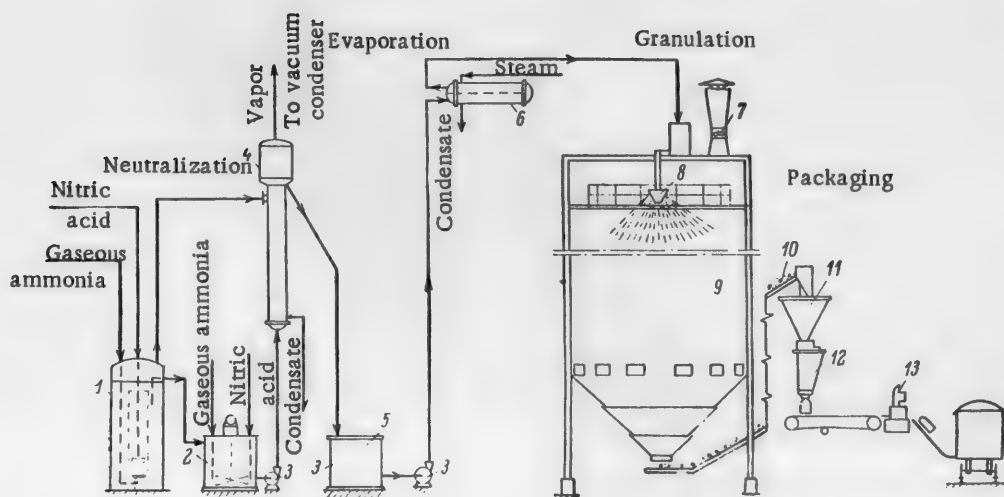
Fig. 3. Flow sheet for the production of granulated ammonium nitrate.
1) Neutralization tower; 2) additional neutralizer; 3) centrifugal pump;
4) first-stage evaporator; 5) hydraulic seal tank; 6) second-stage evapora-
tor; 7) ventilator; 8) granulator; 9) granulation tower; 10) conveyor;
11) hopper; 12) weighing machine; 13) bagging machine.

On the 40th anniversary of the Great October Socialist Revolution the nitrogen industry of the Soviet Union is a large, advanced, and rapidly growing branch of chemical industry, with numerous and highly qualified ranks of research, planning, and operational workers; this guarantees the successful execution of the tasks placed before it.

LITERATURE CITED

[1] The Great Soviet Encylopedia 2, 430 (1950).*

[2] N. A. Klyukvin and S. S. Klyukvina, J. Chem. Ind. 7, 13, 877 (1930).

[3] V. A. Karzhavin, I. M. Bogulsavsky and Z. M. Smirnova, J. Chem. Ind. 10, 8, 31 (1933).

[4] V. A. Karzhavin and A. G. Leibush, J. Chem. Ind. 11, 1, 34 (1934).

[5] The Industry of the USSR. Statistical Handbook (State Statistical Press, 1957) p. 192.*

[6] N. M. Zhavoronkov, Chem. Sci. and Ind. 1, 6, 609 (1956).

[7] N. A. Simulin, Chem. Sci. and Ind. 1, 6, 648-649 (1956).

[8] M. A. Miniovich and N. I. Belyaev, Chem. Sci. and Ind. 1, 6, 666 (1956).

Received July 22, 1957

* In Russian.

CERTAIN ASPECTS OF THE PRESENT STATE OF KNOWLEDGE RELATING TO PROCESSES AND EQUIPMENT IN CHEMICAL TECHNOLOGY

V. V. Kafarov

The October Revolution opened up unprecendented potentialities for the development of chemical industry in our country. During the years of Soviet rule the weakly developed industry of Tsarist Russia has grown into a giant chemical industry.

This industry is founded on the science of processes and equipment of chemical technology, which is based on the laws of thermodynamics, hydrodynamics, and physical chemistry; it is a young branch of the technical sciences, which has existed for hardly more than 25-30 years. Despite its youth, it has developed enormously during recent years, and the results of its practical application have largely determined the present status of the modern chemical, petroleum, and allied industrues.

In recent years industrial practice has demanded considerable intensification of processes, the design of high-output systems, systems with maximum output per unit volume of equipment.

Searches for the most efficient methods of utilization of equipment have greatly influenced the formation and development of concepts of the nature and mechanism of industrial processes, and assisted the extension and deepening of these concepts.

Much experimental materials is now available, there is an extensive literature on different types of processes and equipment in chemical technology, and the theory of standardized processes is being developed. The results of theoretical generalizations and experimental data are used for the design and construction of modern process equipment in chemical factories, and form the basis of further development and improvement of technology.

It is not possible in a single review to present the contents of the enormous number of investigations in the field of processes and equipment; it is not even possible to list them briefly. In this review we merely attempted to present a brief summary of the vast volume of work which has determined the modern state of the science and its practical results. It was also necessary to discuss briefly the modern methods of analysis and approach to the solution of practical problems relating to the most important typical processes in chemical technology.

Method of Analysis of the Principal Processes in Chemical Technology

In the eraly stages of development, any course on the fundamental processes of chemical technology consisted of a collection of individual, disconnected examples of calculations relating to certain processes and equipment of chemical technology. Such examples are collected in books such as A. K. Krupskii's Russian Chemical Works in Their Domestic Environment and External Circumstances (1873); L. F. Fokin's Methods and Apparatus of Chemical Technology (1923); L. F. Fokin and K. F. Pavlov's Calculation Methods for Standard Chemical Equipment (1929); A. G. Kasatkin's Processes and Apparatus of Chemical Technology (1937) (the book subsequently ran into six editions); Walker, Lewis, and McAdams's Principles of Chemical Engineering (1923); Badger and McCabe's Elements of Chemical Engineering (1931); the science of processes and equipment was not unified by a single method of analysis of different processes in chemical technology, and comprised a collection of disjointed examples of calculations rather than an elaborate scientific system.

Chemical engineering developed into an independent science only after the theory of similarity had been applied to analysis of the fundamental processes.

The main processes of chemical technology are generally of great complexity, often combining hydrodynamic, thermal, and diffusion processes. It is evident that difficulties of fundamental principle arise in analysis of such processes. Analysis based on assumption of fixed boundary conditions must be rejected owing to the extreme sensitivity of the fluid streams, especially in turbulent motion, to external influences and therefore to the slightest changes of the conditions of interaction between the stream and the surroundings, to say nothing of the influence of heat and mass-transfer effects.

However, even purely statistical methods, which were brilliantly justified in the development of the kinetic theory of matter, encountered considerable difficulties in relation to the study of turbulence, and of course there is no hope of extensive utilization of statistical methods for analysis of turbulent processes complicated by heat and mass transfer.

The investigator is therefore only left with semiempirical methods, among which is the method of the theory of similarity. This is now becoming the principal method for analysis of chemical engineering processes, with experimental data as its main support. The similarity method, like no other, utilizes theory and experiment simultaneously; experimental results are used for solution of differential equations or relationships of the most general type which describe a given process.

The method is essentially as follows: conditions are found such that out of a whole class of phenomena (such as the phenomena of fluid flow) a group of processes similar to each other are selected; these processes obey the same law within the limits of this group. The principle problem in the theory of similarity is to find conditions in which processes become similar to each other and conform to the same laws. Process similarity is of two kinds: geometrical similarity, as any process is carried out in equipment of definite geometrical configuration, and physical similarity in time and space, which characterizes the physical phenomenon as such. In geometrical similarity one of the geometrical dimensions of the apparatus is taken as determining, and all the other dimensions are compared with it. If the ratios of these dimensions to the determining dimension remain the same in some other apparatus, the two units are geometrically similar. Physical similarity is determined analogously: some quantity is taken as determining in a given physical phenomenon, and all the other quantities characterizing the phenomenon are compared with it. Processes are similar if the ratios of these quantities to the determining quantities remain the same when processes are carried out under other conditions. The ratios between the physical quantities and the determining quantity are usually dimensionless. Such dimensionless ratios of physical quantities are termed similarity criteria, and from the mathematical aspect the theory of similarity essentially consists of the derivation of such criteria. Similarity criteria may be derived directly from differential equations representing a given effect, or, in absence of a differential equation, by dimensional analysis of the quantities determining a given process.

The criteria of hydrodynamic similarity are obtained directly from the differential equation of motion which interrelates the forces acting in the liquid. One of the forces is taken as determining and all other forces are compared with it; this gives dimensionless ratios of forces. If these dimensionless ratios retain the same values in the systems under comparison, they become similarity criteria, and the systems themselves become similar with respect to the forces acting in them. For example, the following similarity criteria are found for hydrodynamic processes: $\dfrac{w^2}{gl}$ = Fr, the Froude criterion, representing the ratio of inertia forces to gravity forces; $\dfrac{wl}{\nu}$ = Re, the Reynolds criterion, representing the ratio of inertia forces to frictional forces (viscosity), etc.

Similarity criteria for thermal and diffusion processes are derived by comparison of thermal and diffusion flows with determining flows, and not of forces with determining forces. For example, the following similarity criteria are derived for thermal and diffusion processes: $\dfrac{al}{\lambda}$ = Nu, the Nusselt thermal criterion, representing the ratio of heat flow by convection to heat flow by conduction; $\dfrac{kl}{D}$ = Nu$_d$, the Nusselt diffusion criterion, representing the ratio of flow by convective diffusion to flow by molecular diffusion, etc.

For derivation of calculation formulas it is necessary to find the relationships between the similarity criteria and to determine the form of the criterial equations. This is done by means of experiments carried out under conditions of similarity (modeling of processes), within the limits of which the criterial equation, to be used subsequently for process calculations, is valid.

Criterial equations representing all the basic processes are used in modern chemical engineering. This science in its modern state can be defined as the science of the general laws of processes of chemical technology, expressed in the form of dimensionless criteria.

Individual processes in chemical industry are represented by combinations of similarity criteria with numerical values specific for the particular branch of industry substituted for the physical quantities.

At the present time the whole diverse range of chemical engineering processes may be classified in five principal groups: 1) hydrodynamic, 2) thermal, 3) diffusional, 4) chemical, and 5) mechanical processes.

The group of hydrodynamic processes includes processes of the motion of liquids and gases in pipes and equipment, machines for moving them, and treatment of liquid and gaseous heterogeneous systems (removal of dusts and mists from gases, separation of suspensions and emulsions, agitation in liquid media).

The group of thermal processes includes heat-transfer processes, heat-exchange equipment, evaporation processes, processes of moderate and deep refrigeration.

The group of diffusional or mass-transfer processes includes processes of absorption, adsorption, distillation, extraction, crystallization, solution, drying, sublimation, humidification, etc.

Chemical processes are at the present time generally considered in courses of specialized chemical technology, in a disjointed manner, in application to particular problems of different branches of chemistry; the only explanation for this is that the theory of similarity of chemical processes is in its early stages of development, and simple and reliable methods for generalization of the similarity of chemical processes are not yet available. Development of a theory of similarity of chemical processes is an urgent task for contemporary chemical engineers.

The group of mechanical processes includes processes of comminution and screening of materials, and feeding, classification, and conveying processes.

Owing to lack of space, only a few of the characteristic processes of chemical technology are examined in this review.

Process Mechanisms

The course of thermal, diffusion, and chemical processes is determined to a considerable extent by hydrodynamic relationships, and therefore the transfer of motion, heat, and mass depends on the hydrodynamic conditions in which a given process takes place. This idea is directly related to the concept of the mechanism of motion, heat, and mass transfer. The idea of two transfer mechanisms — molecular and turbulent — is now firmly established. Correspondingly, the concepts of molecular viscosity, molecular heat transfer, and molecular diffusion have been introduced for molecular transfer; and of turbulent or eddy viscosity, turbulent heat transfer, and turbulent diffusion for turbulent transfer. The meaning of these concepts is made clear by consideration of longitudinal and transverse transfer in turbulent flow.

In molecular transfer (laminar flow) energy and mass are transferred longitudinally only, whereas in turbulent flow both longitudinal and transverse transfer occur, so that an additional tangential stress arises and additional mass transfer occurs. This situation may be schematically represented as follows (Fig. 1).

Consider the motion of streams a and b with longitudinal velocities w_a and w_b. The velocity difference $\Delta w = w_a - w_b$ produces the usual tangential stress, given by the equation

Fig. 1. Origin of transverse transfer.

$$\tau_M = \mu \frac{dw}{dy} . \tag{1}$$

As the motion in this case is turbulent, there is transverse motion with velocity u in addition to the longi-
tudinal. This transverse motion will produce changes in the motion of particles situated between streams a
and b. If the surface area f between the streams and the transverse transfer across this boundary are uniform,
then uf is the volume transferred per second, and ρuf is the mass transferred from a to b in unit time. The
force induced by this transfer may be written as ρuf Δw, and the tangential stress per unit area as

$$\tau_T = \rho u \Delta w. \tag{2}$$

It follows from this equation that the tangential stress in turbulent flow is proportional to the square of
the velocity.

To reduce Equation (2) to a form analogous to Equation (1), Prandtl [1] introduced the concept of the
"mixture length" l over which the liquid particles (finite masses or eddies) lose their individuality in trans-
verse transfer from a to b. •   These finite masses of liquid — "moles" — move independently (relative to the
stream), and, in contrast to molecules (in molecular transfer), are continuously forming and breaking down
at the beginning of the path they separate from the surrounding medium, and after traversing the path l they
become completely mixed with the surroundings. Energy and mass are transferred by molecules in molecular
transfer, and by "moles" (finite masses of liquid) in turbulent transfer.

The relationship between the "mixture length" l, the axial velocity increase, and the radial change is
represented by the expression

$$\Delta w = l \frac{dw}{dy}. \tag{3}$$

By the law of conservation of momentum, the product of the final mass of liquid and the velocity is con-
stant in any cross section of the stream. In the stream under consideration it is always possible to find, in any
cross section (Fig. 1) a finite mass of liquid moving with transverse velocity u numerically equal to Δw; then,
according to Equations (2) and (3) and the law of conservation of momentum, we may write

$$\tau_T = \rho u \Delta w = \rho \left(l \frac{dw}{dy} \right) \cdot \left(l \frac{dw}{dy} \right) = \rho l^2 \left(\frac{dw}{dy} \right)^2. \tag{4}$$

If we put $\rho l^2 \frac{dw}{dy} = \epsilon_p$, Equation (4) reduces to the form of Equation (1):

$$\tau_T = \epsilon_p \frac{dw}{dy}, \tag{5}$$

where ϵ_p, by analogy with μ, acquires the meaning of viscosity, defined in this case as turbulent viscosity.
In contrast to molecular viscosity, turbulent viscosity is not a physical constant, and its numerical value de-
pends on the hydrodynamic conditions, and primarily on the velocity of the stream.

In the region of free turbulence it is quite legitimate to neglect effects of a molecular nature, as they
disappear entirely by comparison with turbulent transfer effects, the latter being thousands and even tens of
thousands of times as great. However, turbulence gradually diminishes as a solid surface is approached, and
in a certain thin wall layer the flow becomes laminar. In absence of a solid wall and with a free boundary
between two phases, turbulence at the boundary may even increase within the limits of each phase rather
than degenerate, and if finite masses of one phase penetrate into the other, free turbulence may develop.
This occurs because the boundary surface between streams with velocities differing in magnitude and direc-
tion is unstable, and may itself be a source of turbulence [3].

Goncharov [4] analyzed the motion of a liquid in interaction with the soil and concluded that turbulence
does not die down at the solid boundary, but the wall itself is a source of turbulence, which spreads from the
wall into the stream.

• Taylor [2] used "vorticity" and not momentum as the mechanical property transferred in turbulent flow.
In this case pressure pulsation in flow is taken into account.

In presence of both molecular and turbulent transfer, the total tangential stress may be represented, on the basis of Equations (1) and (5), in the following form:

$$\tau_M + \tau_T = (\mu + \epsilon_p) \frac{dw}{dy} . \tag{6}$$

Analogous equations may be derived for transfer of heat and mass. We then have; for total heat flow:

$$q_M + q_T = c\gamma (a + \epsilon_k) \frac{dt}{dy} , \tag{7}$$

and for total diffusional flow:

$$q'_M + q'_T = (D + \epsilon_d) \frac{dc}{dy} . \tag{8}$$

The predominance of one kind of energy and mass transfer over another is determined by the process conditions. Thus, when $\epsilon_p = 0$ and $\epsilon_d = 0$ we have pure molecular transfer (laminar regime); when $\epsilon_p = \mu$ and $\epsilon_d < D$ we have an intermediate regime; and when $\epsilon_p > \mu$ and $\epsilon_d > D$—a turbulent regime; when $\mu \rightarrow 0$, $D \rightarrow 0)$ and $\epsilon_p \rightarrow \infty$ and $\epsilon_d \rightarrow \infty$ we have a free turbulence regime (in a two-phase stream).

These energy- and mass-transfer regimes may be characterized by the appropriate similarity criteria (Fig. 2).

It follows from Fig. 2 that the Reynolds criterion (R_e) acquires the meaning of a quantitative measure of the ratio of the turbulent and molecular friction forces, or, which is the same thing, of the rates of turbulent ("molar") and the molecular transfer of momentum. This concept is interrelated with the concept of the Reynolds number as a quantitative measure of the ratio of the inertia forces and the forces of internal friction.

Since the motion of a medium develops under the action of two opposing influences — forces of internal friction, which maintain an ordered form of motion, and inertia forces, which assist the growth of any disturbances introduced into the stream, the ultimate nature of the motion is determined by the relationship between these mutually opposing influences.

The Nusselt criterion (Nu) is a quantitative measure of the increase of mass transfer due to turbulence, relative to purely molecular transfer. It is clear that Nu should increase with increase of Re, tending to infinity at free turbulence. This relationship was established earlier for diffusion processes [5]. The function Nu = f (Re) is represented diagrammatically in Fig. 3.

Free turbulence regimes (Regime IV, Fig. 3), in which the influence of molecular transfer is absent, have been determined in the case of pipes with distinctly rough surfaces [6], agitation in liquid media [7], diffusion in gas and liquid streams in packed tubes [8], extraction processes with agitation by means of stirrers [9], and absorption and recitification processes in packed towers [5].

Figure 2 shows that the Peclet criterion (Pe) is a quantitative measure of the ratio of the rates of turbulent ("molar") and molecular heat transfer (Pe heat criterion) and mass transfer (Pe_d diffusion criterion). In this sense the Pe criterion is the thermal or diffusional analog of the Re criterion. Both in Pe and in Re the numerators contain geometrical and regime parameters, and the denominators contain determining characteristics of molecular transfer, and therefore one criterion may be obtained from the other by appropriate substitution of physical constants in the denominator. Simultaneous elimination of geometrical and regime parameters from both criteria gives a criterion which contains only physical parameters, which also reflect the nature of the exchange — the Prandtl criterion. The Peclet criterion for purely turbulent transfer may be represented as $Pe = \frac{wl}{\epsilon_k}$, $Pe_d = \frac{wl}{\epsilon_d}$; it becomes constant at free turbulence. Therefore molecular and turbulent transfer respectively can often be represented by the Prandtl criteria (see Fig. 2) for molecular $Pr_d = \frac{v}{D}$ and turbulent $Pr_{d.T} = \frac{\epsilon_p}{\epsilon_d}$ transfer, which represent the ratio of friction to mass transfer, or velocity and concentration

profiles, or velocity and temperature profiles (the thermal criterion $Pr = \dfrac{\nu}{a}$).

In condition of free turbulence $Pe_{dT} = \dfrac{wl}{\varepsilon_d} = \text{const}$ and $Pr_{dT} = \text{const}$; hence it follows that a knowledge of the law governing the distribtuion of the average velocity across the section is sufficient basis for solution of the problem of turbulent mass (or heat) transfer, provided that the mass-transfer (or heat-transfer) process does not have a distorting effect on the hydrodynamic conditions of the process. These conclusions were confirmed experimentally by measurements of temperature profiles in pipes [10] and by measurements of concentrations [8, 11], in which good agreement was obtained with the calculated values.
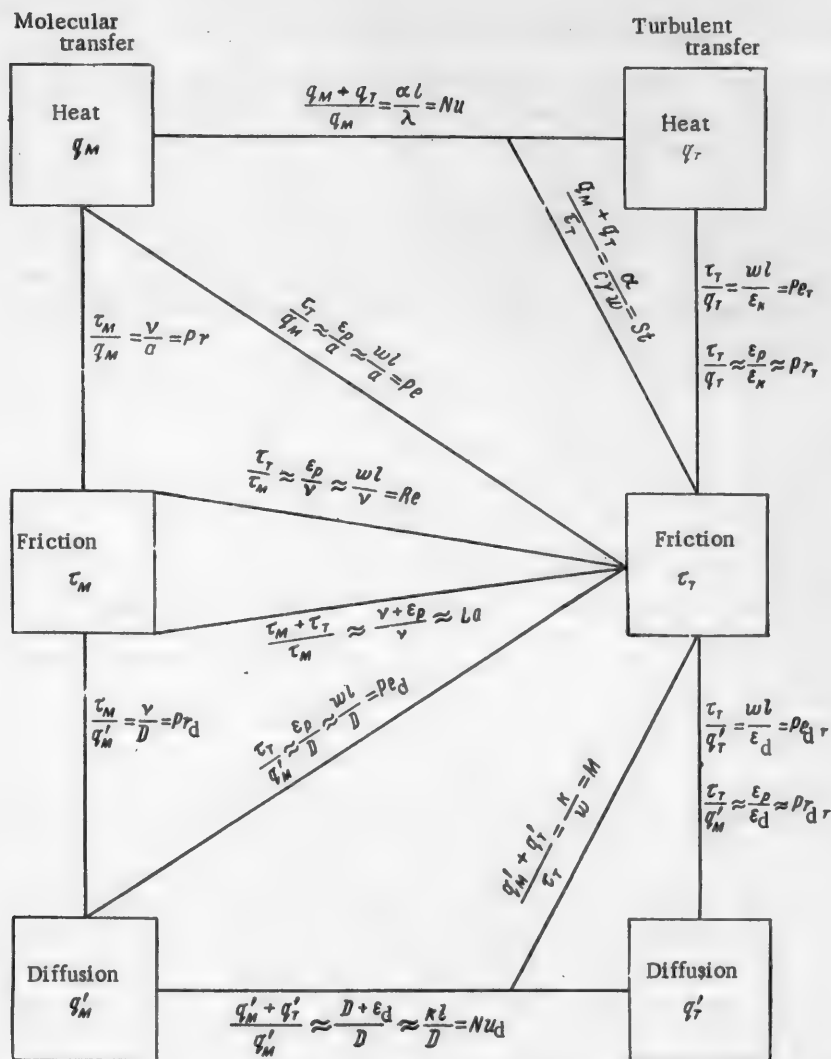

Fig. 2. Principal similarity criteria and process mechanisms.

Mechanism of Transfer in Two-Phase Streams

The presence of two-phase streams is characteristic of diffusional and of many thermal and chemical processes.

The hydrodynamics of two-phase streams has begun to be studied only very recently, and the results are

still very scanty owing to the exceptional complexity of the effects involved. Since there is no rigid theoretical description of the turbulence effect even for one-phase streams, but only semiempirical hypotheses (those of Prandtl, Taylor, and Goncharov), the lack of theoretically substantiated views on the motion of two-phase streams and their interactions is all the more understandable. The only results of practical significance have been obtained with the aid of the theory of similarity. Quantitative evaluation of energy and mass transfer in two-phase streams presupposes the acceptance of a definite transfer mechanism, which determines the rate of the process at the interphase boundary in a two-phase system.

In 1926 Lewis and Whitman [12] postulated a mechanism for molecular transfer of a substance between two phases on the assumption of the formation of "films" on the side of each phase at the interphase boundary; the rate of mass transfer through these films determines the rate of the whole mass-transfer process. The mechanism of mass transfer through the films was assumed to be molecular. Thus the rate of transfer of the substance from one phase into the other was determined entirely by molecular diffusion.

This theory is essentially an interpretation of Nernst's [13] and Brunner's [14] theory of solution, which is valid to a fair degree of accuracy in solution of problems involving solid boundary surfaces, where the existence of stationary films can be justified in some way.

The views advanced by Lewis and Whitman were given the name of the two-film or the film theory, and became widely accepted. This theory yielded practical results in cases involving processes occurring at fixed solid boundaries. For example, the film theory was used to derive equations for the evaporation of a liquid from wet tube walls into a turbulent air stream [15], in cooling towers [16], and for solution of solids in liquids [17, 18]. The equations derived on the basis of the film theory have the following general form:

$$Nu_{\mathrm{d}} = ARe^m \cdot Pr_{\mathrm{d}}^n \tag{9}$$

or

$$\frac{kl}{D} = A \left(\frac{wl}{\nu} \right)^m \cdot \left(\frac{\nu}{D} \right)^n . \tag{10}$$

It follows from this last equation that all the process characteristics are referred to molecular parameters (ν and D) which is evidently jusitified if the influence of molecular transfer is appreciable. However, as was shown above, in some hydrodynamic states of the systems exchange conditions may arise in which turbulent ("molar") exchange begins to predominate, and therefore under these conditions reference of all the process characteristics to molecular parameters leads to large errors, and in conditions of free turbulence it leads to absurd conclusions. This probably explains why in more than 30 years of existence the film theory has not yielded generalized equations for processes taking place not at fixed but at free interfaces, such as the boundary between moving gases and liquids (absorption), vapors and liquids (distillation), or pairs of liquids (extraction). In our opinion, these most important practical processes cannot be represented by equations of the type of Equation (9). Equation (9) contains an uncertainty in relation to the choice of criteria owing to the presence of a second phase and to the fact that it is necessary to have a relationship not among three quantities, but among at least six (for the two phases, gas and liquid). The main reason why Equation (9) is not applicable for analysis of processes at free boundaries between phases is that the surfaces, in contrast to solid-phase boundaries, are unstable, and under certain hydrodynamic conditions (at relatively high flow velocities in different directions) may themselves be the source of turbulence [3]. Under such conditions stationary films, with transfer of a molecular character in them, cannot exist, and molecular transfer effects vanish in comparison with "molar" (turbulent) transfer effects, being much less intense than the latter.

In this case the main question is that of the nature of the formation of the interphase boundary and of its stability.

Under certain hydrodynamic conditions, at maximum flow velocities, the interphase boundary becomes unstable, the phases themselves undergo continuous inversion, alternately becoming continuous and disperse, and the liquid is "emulsified" by the gas or vapor stream. Interpenetration of minute eddies of one phase into the other occurs — a regime of free turbulence is established, with turbulent transfer predominant (Fig. 3, Regime IV) [5]. It has been shown by Prandtl [1], Schlichting [19], Abramovich [20], and others, that the nature of free turbulence is itself different from the nature of the turbulence which results in presence of a

solid wall surface. In free turbulence, eddies with their axes perpendicular to the axis of the stream predominate, and cause additional transfer of energy and mass in a transverse direction.

In turbulent conditions the concentration gradients are determined not only by the course of the physicochemical process, but also by turbulent transfer, when the distribution of concentrations at the boundaries of the mixing masses depends on turbulent mixing.

There are only indirect methods for proving that the influence of molecular transfer under these conditions is negligible.
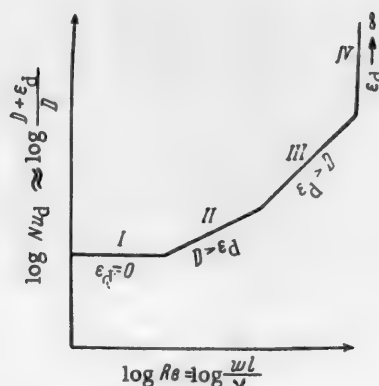
Fig. 3. Effect of hydrodynamic conditions on the mechanism of transfer.

It has been shown that in conditions of free turbulence in scarfy tubes [6] $\Delta_p \sim \mu^0$, in agitation by means of mechanical stirrers [7] $\Delta_p \sim \mu^0$, and for two-phase streams in packed towers [5] $\Delta_p \sim \left(\dfrac{\mu_L}{\mu_G}\right)^{0.045}$ in extraction in equipment with stirrers the coefficient of mass transfer [9] $k \sim D^0$. Sigwart and Nassenstein [21] used an optical method to prove the absence of stable films in extraction from drops, and showed that intense motion of the streams occurs in the boundary layers, accompanied by formation of vortices and separation of vortex rings from the moving drops.

Kishinevsky et al., [22, 23], in experiments on the chemisorption of gases by mechanically stirred liquids, proved that molecular diffusion has no influence on transfer.

As was stated above, Equation (9) is not valid in conditions of free turbulence in presence of free surfaces. The stream velocity $\underline{w}$ in conditions of free turbulence, for a given type of apparatus (of given configuration) and of definite dimensions d_e may be represented by the dimensionless expression $\sqrt{gd_e}$. This expression is a function of purely hydrodynamic parameters: the ratio of the liquid rate L to the gas (or vapor) rate G, and the ratio γ_G/γ_L of the densities of these phases, i.e.,

$$\frac{w}{\sqrt{gd}_e} = f_0\left(\frac{L}{G} \cdot \frac{\gamma_G}{\gamma_L}\right). \tag{11}$$

For conditions of free turbulence, the relative values of the volume coefficients of mass transfer for two systems can be found from a general equation, which includes only the hydrodynamic characteristics of turbulent flow [24]:

$$\frac{k_{v_1}}{k_{v_2}} = \frac{\varphi_1}{\varphi_2}\left[\frac{(L/G)_1}{(L/G)_2} \cdot \frac{(\gamma_G/\gamma_L)_1}{(\gamma_G/\gamma_L)_2}\right]^n, \tag{12}$$

where φ_1 and φ_2 are the absorption coefficients (Henry constants). For a two-phase stream this equation follows directly from the condition $Pe_{d.T} = \dfrac{wl}{\epsilon_d} = $ const. The constancy of Pe_{dT} was demonstrated by experiments on the diffusion of dyes into CO_2 and water, and in a number of other investigations [25].

The fact that in conditions of free turbulence $Pe_{d.T} = \dfrac{wl}{\epsilon_d} = $ const. opens up wide possibilities for modeling of processes, as in such cases, as already stated, the velocity and concentration profiles become similar. For two-phase streams, the constancy of Pe_{dT} may be expressed as the constant value of the ratio of a determining hydrodynamic characteristic (such as the velocity, $\underline{w}$) to a determining diffusional parameter (such as the length of the zone of phase interaction $\underline{h}$), i.e., as w/h.

In addition to these concepts of free turbulence in two-phase streams, concepts based on analysis of the state of the interphase boundary have also appeared.

Danckwerts [27], who continued Higbe's work [28], and Kishinevsky [23] independently of these authors, introduced the concept of renewal time of the phase-contact surface. According to Danckwerts, the rate of absorption is determined by the time of saturation of the surface. This is based on the assumption that the saturation time and the "age" of the surface are the same thing. The "age" of the surface is reckoned from the instant of its formation. The highest rate of diffusion is attained just at the instant of formation of the interphase boundary.

Kishinevsky [22, 23] demonstrated the inadequacy of Danckwert's method of analysis, where only molecular diffusion is considered, and developed a theory of surface renewal with turbulent diffusion taken into account; this theory was found to be in good agreement with experimental results for chemisorption.

Sherwood and Pigford [15] introduced the concept of nonsteady diffusion to explain diffusional effects in two-phase streams.

In a recent paper, Hanratty [29] criticized the Higbe —Dankwerts theory and postulated a "discontinous film" in mass transfer at solid—liquid interfaces. For confirmation of his views, Hanratty calculated the velocity profile near the wall, and obtained good agreement with Deissler's results. He also confirmed the applicability of Taylor's theory of turbulence [2] to mass transfer.

To summarize this discussion of transfer mechanisms in two-phase streams, we conclude that, depending on the hydrodynamic conditions of the process, molecular, turbulent, or mixed transfer may predominate in the transfer mechanism. Therefore the analysis of processes in two-phase systems must be based on analysis of actual hydrodynamic conditions; if hydrodynamic considerations are disregarded, no significant results or generalizations can be reached.

Advances in the Fields of Individual Processes

Hydrodynamic processes. The science of hydrodynamics originated in the St. Petersburg Academy of Sciences in the first half of the 18th century. Its founder were Active Members of the Russian Academy of Sciences, M. V. Lomonosov (1711-1765), L. Euler (1707-1783), and D. Bernoulli (1700-1782). They prepared the ground for the rapid development of the science of liquids and gases. Here enormous advanced were made by our famous compatriots M. V. Ostrogradsky, N. P. Petrov, N. E. Zhukovsky, S. A. Chaplygin, and A. N. Krylov.

Many Soviet scientists participated in the modern formulation of hydrodynamics as used in chemical engineering processes: L. S. Leibenzon, L. G. Loitsiansky, G. N. Abramovich, M. A. Velikanov, N. E. Kochin, V. N. Makaveev, L. I. Sedov, N. N. Pavlovski, A. N. Kolmogorov, and L. D. Landau.

V. G. Levich wrote the monograph "Physicochemical Hydrodynamics" [30]. P. G. Romankov's monograph contains a presentation of the hydrodynamic principles of chemical technology based on the theory of similarity [31]. Individual hydrodynamic processes are described in a number of monographs [32-38].

Analysis and calculations relating to hydrodynamic processes in chemical technology essentially consist of simultaneous consideration of the forces acting and counteracting in a given process. Such consideration makes it possible to determine the rate of the process and hence the principal dimensions of the equipment.

In hydrodynamic processes of chemical technology it is usual to consider forces acting against forces of resistance or friction in a given liquid stream or in the motion of bodies in liquids. The resistance force is expressed in terms of one general law in all cases, whereas the forces acting against it are expressed in different ways according to their nature, and this difference betweentthe acting forces determines the method of analysis used. Intensification of hydrodynamic processes thus consists of the selection of the most effective forces used to overcome resistance.

The interaction of forces in such cases is represented by the following criterial equation:

$$Eu = f_0 (Re) \tag{13}$$

or

$$\frac{\Delta p}{\rho w^2} = f_0\left(\frac{wl}{\nu}\right),$$ (14)

or

$$\frac{\Delta p}{\rho w^2} = A\left(\frac{wl}{\nu}\right)^m.$$ (15)

It follows from this last equation that a pressure force, created in one way or another and expressed in dimensionless form, acts against a frictional force, also expressed in dimensionless form.

The Euler criterion (Eu) is usually given in the form of the coefficient of friction, and then Equation (15), with the characteristic of geometric similarity l/d taken into account, reduces to the form

$$\Delta p = \lambda \frac{l}{d} \frac{w^2\gamma}{2g} \ \text{kg/m}^2$$ (16)

$$\Delta p = \xi \frac{w^2\gamma}{2g} \ \text{kg/m}^2$$ (17)

where

$$\xi = \lambda \frac{l}{d},$$ (18)

$$\lambda = 2Eu.$$ (19)

Then the analysis and calculation of a hydrodynamic process reduce to determination of the form of the relationship.

$$\lambda = f(Re).$$ (20)

The above-mentioned monograph on hydrodynamic processes, compiled by Romankov [31], contains a large amount of experimental material obtained up to 1948 on the form of the relationship (20) for various processes. Here we shall only consider the most important hydrodynamic relationships established in recent years.

The resistance in a two-phase stream at the limiting gas (or vapor) velocities at the inversion point (absorption or rectification processes) in packed towers was represented as the general equation [39]:

$$\left(\frac{\Delta p}{l}\right)_{G\,L} = \left(\frac{\Delta p}{l}\right)_{G}\left[1 + A\left(\frac{L}{G}\right)^m \cdot \left(\frac{\gamma_G}{\gamma_L}\right)^n \cdot \left(\frac{\mu_L}{\mu_G}\right)^c\right],$$ (21)

where L is the liquid rate (in $\text{kg/m}^2 \cdot \text{hour}$): G is the gas rate in the tower (in $\text{kg/m}^2 \cdot \text{hour}$); γ_G and γ_L are the densities of the gas and liquid; μ_G and μ_L are the viscosities of the gas and liquid; $(\Delta p/l)_G$ is the pressure drop across the dry packing (in mm H_2O/m); $(\Delta p/l)_{G\,L}$ is the pressure drop in presence of liquid (in mm H_2O/m).

The constants A, $\underline{m}$, $\underline{n}$, and $\underline{c}$ have the following values:

System	Values of constants			
	A	m	n	c
Gas—liquid	8.4	0.405	0.225	0.045
Vapor—liquid	5.15	0.342	0.190	0.038

The relationship (20) was found to take the following forms for the motion of vapors through packing without liquid spray [40];

$$\text{when} \quad Re = \frac{w d_L \rho}{\mu} < 80 \quad \lambda = \frac{400}{Re^{0.85}}, \tag{22}$$

$$\text{when} \quad 80 < Re < 400 \quad \lambda = \frac{70}{Re^{0.45}}, \tag{23}$$

$$\text{when} \quad Re > 400 \quad \lambda = \frac{16.5}{Re^{0.2}}. \tag{24}$$

Hydrodynamic calculations of sieve-plate towers have been given by Akselrod [41], and of bubble-cap towers by Atkins [42].

The greatest advances in recent years were made in the field of the hydrodynamics of granular layers.

The hydrodynamics of granular layers attained exceptional importance in relation to acceleration of processes in heterogeneous gas—solid systems [43]. Possible ways of accelerating such processes were indicated as long ago as 1885 by one of the founders of chemical engineering, Krupsky [44, 45]. He considered that one of the most important factors is increase of the area of phase contact, which is effected by the maximum possible subdivision of the solid phase (catalyst, sorbent, or solid fuel). The development of hydrodynamics revealed another most important factor in the intensification of processes in gas—solid systems; this is the conversion of a stationary into a moving layer, which greatly accelerates processes such as sorption, catalysis, cracking, and others, owing to rapid restoration of the activity of the layer, better heat-transfer conditions, and easier conveying of the material.
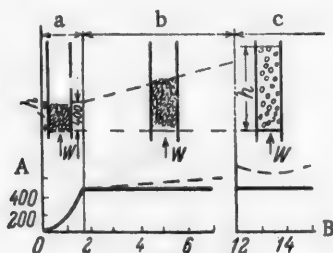

Fig. 4. States of a granular layer. a) Stationary layer; b) fluidized layer; c) pneumatic conveying. A) Height of layer (in mm); B) gas velocity (in m/sec.).

Three fundamentally different states of a layer of solid phase with a gas passing through it can now be distinguished: 1) immobile, stationary layer; 2) fluidized layer,* 3) pneumatic conveying. These states are illustrated in Fig. 4, which represents layers of uniform spherical particles, 5 mm diameter, density 2000 kg/m³, porosity $\epsilon = 0.4$, with gas density 1.2 kg/m³. The lower part of the diagram represents variations of the resistance of the layer in different states with the gas velocity [46].

The penetration of a gas through a stationary layer may be defined as filtration of the gas through the layer. The resistance of such layers was studied and the experimental data analyzed by Fedorov [47], Zhavoronkov [48], Boreskov and Ritter [49], Zakharov and Frost [50], Chilton and Colburn [51], Carman [52], Oman and Watson [53] and others [54-58].

The resistance in the filtration regime may be calculated from the general hydrodynamic equation:

*Fluidized layers are also described in the (Russian) literature as "boiling" and "suspended" layers.

$$\Delta p = \lambda \frac{h}{d_e} \frac{w^2 \gamma G}{\epsilon^2 2g_d} \, \text{kg/m}^2 \tag{25}$$

where ϵ is the porosity of the layer.

The form in which Equation (25) is given by different workers depends on the choice of the determining dimension — the particle diameter or the equivalent diameter. In our opinion it is more correct to use the equivalent diameter as the determining dimension.

When the gas velocity reaches a certain critical value, the layer enters into a mobile state, as if "fluidized;" this is the fluidization regime, in which the total upthrust acting on the layer is equal to the weight of layer. This is equivalent to the condition that the time-average upthrust exerted by the stream on each particle is equal to the weight of the particle [43]. Therefore any given value of the space velocity of the stream corresponds to a perfectly definite layer height $\underline{h}$ (Fig. 4), which increases with the velocity. When the velocity $\underline{w}$ increases, the upthrust acting on each particle becomes greater than its weight, and the layer begins to expand. With expansion of the layer and increase of its porosity ϵ, the velocity w/ϵ in its open section decreases, the upthrust decreases also, and when it again becomes equal to the particle weight further expansion ceases. It follows from the above that a fluidized layer automatically regulates its height. While a fluidized layer is dynamically stable, each individual particle in it is in a dynamically unstable state, so that the particles are in random motion and collide with each other.

Syromiatnikov [59] derived the connection between the height of a layer and its weight in the fluidized state. Smirnov and Li De Ep [60] established a relationship between the pressure difference and expansion of the layer. According to Todes [43], the critical velocity at which the layer passes into the fluidized state is determined from the general equation:

$$Re_{cr} = f \, (Ar), \tag{26}$$

where
$$Re_{cr} = \frac{w_{cr} d_e}{\epsilon \nu}, \quad Ar = \frac{1 - \epsilon}{2} \cdot \frac{g d_e^3}{\nu^2} \cdot \frac{\gamma_s}{\gamma_G} \, .$$

If the layer consists of fairly small particles (Ar < 5000) it passes into the fluidized state at

$$Re_{cr} = \frac{1}{36.5} \, Ar. \tag{27}$$

For larger particles, when, Ar > 5000

$$Re_{cr} = 0.5 Ar^{s/s} \, . \tag{28}$$

The total pressure drop in a fluidized layer, in the general case, is the sum of three terms:

$$\Delta p_{total} = \Delta p_1 + \Delta p_2 + \Delta p_3, \tag{29}$$

where Δp_1 is the weight of the solid particles in the gaseous medium, Δp_2 is the friction of the stream against the walls of the apparatus, and Δp_3 represents collisions of the particles with each other and the walls.

For approximate calculations it is now assumed that

$$\Delta p_{total} = \Delta p_1, \tag{30}$$

$$\Delta p_1 = h\,(1 - \epsilon)\,(\gamma_3 - \gamma_G)\ \text{kg/m}^2 \tag{31}$$

With further increase of velocity beyond the fluidization limit, some of the layer is carried out of the column; this is described as the pneumatic conveying regime (Fig. 4). This limiting velocity of fluidization is represented by a general expression of the form

$$\operatorname{Re}_{\lim} = f\,(\operatorname{Ar}_{\lim}), \tag{32}$$

where $\operatorname{Re}_{\lim} = \dfrac{w_{\lim}d}{\nu}$, $\operatorname{Ar}_{\lim} = g\,\dfrac{d^3\gamma_3}{\nu^2\,\gamma_{\lim}}$, where $\underline{d}$ is the particle diameter. For small particles, when $\operatorname{Re}_{\lim} < 2$ and $\operatorname{Ar}_{\lim} < 9$, according to Todes [43],

$$\operatorname{Re}_{\lim} \cong \frac{1}{18}\,Ar; \tag{33}$$

here the limiting velocity $w_{\lim} \gtrsim 50\,w_{cr}$.

For denser initial packing of the layer ($\epsilon < 0.476$), the ratio $\dfrac{w_{\lim}}{w_{cr}}$ may $\cong 100$, i.e., the fluidized layer may exist over a fairly wide range of stream velocities $w_{cr} < w < w_{\lim}$.

In solid-phase catalysis, cracking processes, hypersorption, etc., the two-phase system gas—solid may exist in different states at different points in the system. These states can be represented by means of diagrams [61] shown in Figs. 5-10.
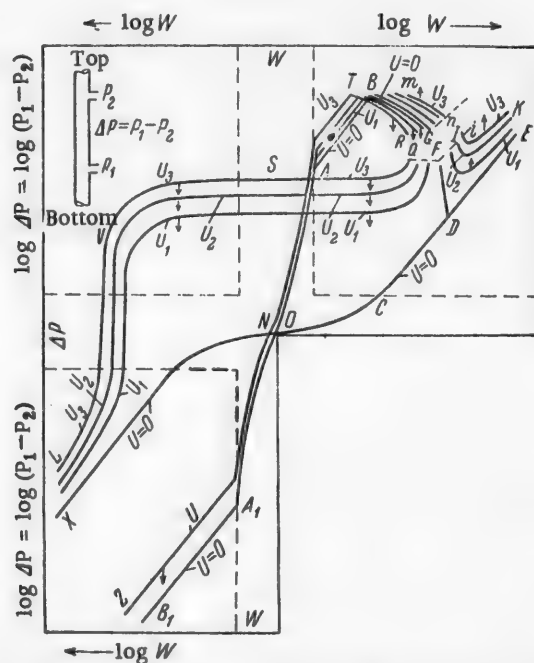

Fig. 5. Diagram of the hydrodynamic state of gas—solid system in a vertical pipe.

Figure 5 is a simplified diagram of the hydrodynamic state of a gas—solid system in a vertical pipe. The diagram consists of three sections, plotted in logarithmic coordinates and enclosed by dash lines. Each section contains: one curve for the gas velocity $\underline{w}$ referred to the full section of the pipe without solid phase, when $u = O$, and three curves representing constant gravimetric flow rates of the solid phase referred to the full section of the pipe, such that $u_3 > u_2 > u_1$. The arrows denote the directions of the upward and downward motion of the the solid particles in the stream. The point $\underline{o}$ is the coordinate origin. The abscissas to the right of $\underline{o}$ show the increase of the gas velocity upward in the pipe, and to the left of $\underline{o}$ they represent gas velocity increases down the pipe. At the point $\underline{o}$ the gas velocity nominally has the value of zero (there is no gas flow at the top or bottom of the pipe). The ordinates upward of $\underline{o}$ represent positive increases of the pressure differences per unit length of pipe, $\Delta P = P_1 - P_2$, and downward of $\underline{o}$ they represent increases of the negative value of ΔP or, which is the same thing, increases of the difference $P_2 - P_1$. The upper right-hand section shows regimes corresponding to solid and gas flows in the same direction, and also opposing (countercurrent) flows. The left-hand upper and lower sections represent regimes of unidirectional flow toward the bottom of the pipe. The regimes which arise in the motion of the gas and the solid phase can be easily determined from the diagram in Fig. 5. We place our reference points P_1 and P_2 in the middle of the stationary layer and follow the variations of ΔP with with variations of the gas velocity. The regime of filtration through a fixed layer is represented in the form of the Curve OAB. At the point B the pressure of the gas becomes equal to the weight of the layer, and fluidization commences beyond this point; further increase of velocity causes expansion of the layer (Curve BG). Curve OCDE represents the resistance to the upward flow of the gas through the empty pipe, and Curve OX, the corresponding resistance in downward flow. Curve OAB represents resistance to upward motion of the gas through the stationary layer (filtration regime), and Curve OA_1B_1, the corresponding resistance in downward flow. Curve BG represents expansion of the layer. At the point G, the diameter of the gas bubbles reaches the same magnitude as the pipe diameter before emerging from the layer, and causes plug motion of the layer. Point F represents the maximum attainable concentration of solid particles in the gas before they begin to settle into the layer. Point D represents almost total absence of solid particles in the gas. The Curve IK represents the pneumatic-conveying regime, which has been studied by a number of workers [62-69]. The region II of the curve is characterized by the presence of some deposited particles in the pipe. The dash line IF is the line of constant porosity of the disperse phase, corresponding to the minimum distance between the particles before they agglomerate into a layer. The Curve mn represents the resistance to the passage of the gas through a continuous layer of the solid phase (with gravimetric flow rate u_3) in upward flow unidirectional with the gas phase. This may be defined as the fluidization regime in a moving layer.

The point S represents the free fall of particles when the gas velocity is zero.

Curve SQ characterizes settling of the particles for a relatively low velocity of the countercurrent gas. Point Q is defined as the "choking" point [65, 68]. Curve RT corresponds to a regime of settling in a countercurrently moving gas passing through the layer in the form of bubbles. Curve TN characterizes a very slow rate of movement of the fixed layer countercurrent to the gas stream. The pressure difference practically coincides with the pressure drop across a stationary layer [55].

The regime corresponding to Curve TN is widely used in hypersorption, regenerators, in the Houdry process, etc.

Curve NZ characterizes resistance in unidirectional motion of the solid and gas streams down the pipe, ΔP being calculated as for a stationary layer.

If the gas is introduced at the top of the pipe with free settling of the particles, ΔP varies as indicated by Curve SV, and with further increase of gas velocity it follows the Curve VL; friction of the gas against the pipe walls then predominates.

Figure 6 is a simplified diagram of the hydrodynamic state of a gas—solid system in a horizontal pipe. The diagram is plotted in logarithmic coordinates; the linear velocity $\underline{w}$ of the gas stream referred to the full section of the pipe is taken along the abscissa axis, and $\Delta P = P_1 - P_2$ along the ordinate axis. The straight line AB represents the resistance of the empty pipe, calculated by means of the usual equations (see p. 1526-1527).

The straight lines DC represent the resistance to motion of the solid phase at velocities $u_3 > u_2 > u_1$ respectively. At point D the particles settle in the lower part of the pipe, and are in a pulsating state; accordingly the gas velocity corresponding to the point D is termed the pulsation velocity. This velocity is determined by the amount of solid phase in the pipe. Line DC represents the motion of the solid phase in the gas stream in presence of

some settled solid phase. The quantitative relationships corresponding to the course of the line CD have been studied by a number of workers [64, 67, 69-73]. The presence of a stationary solid layer in the lower end of the pipe results in an increase of the pressure difference (point E).

The straight lines EF characterize the increase of resistance caused by increase in the number of settled particles and the corresponding raising of the layer in the pipe owing to decrease of the gas velocity.

Kalinushkin's experiments [43] showed that in the transport of fine particles along a horizontal pipe the particle concentration varies significantly over the vertical cross section of the pipe. This distribution was statistically calculated by Todes [43].
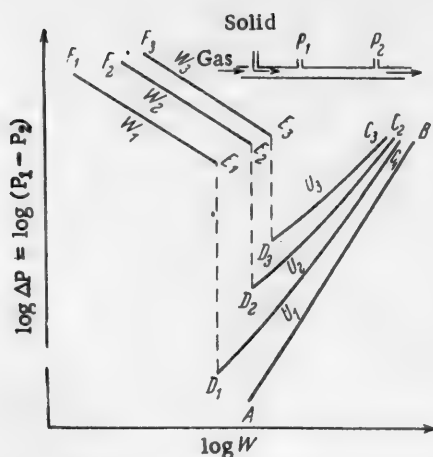

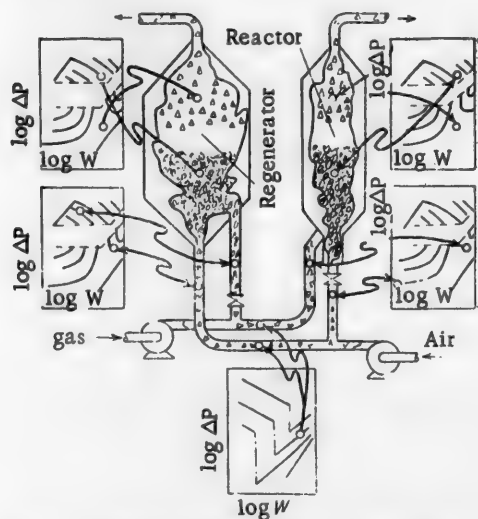Fig. 6. Diagram of the hydrodynamic state of a gas—solid system in a horizontal pipe.

Fig. 7. Hydrodynamic states of a gas—solid system in a catalytic-cracking reactor and regenerator.

Figures 7, 8, and 9 illustrate the above-mentioned regimes for gas—solid systems in catalytic cracking (Fig. 7), in reactors for the synthesis of hydrocarbons from H_2 and CO (Fig. 8), and in cracking in a moving bed — the Houdriflow process (Fig. 9).

It was shown in a study of transfer mechanisms in a hollow pipe and a granular layer [25] that eddy diffusion passes through a maximum (the Peclet turbulent number $Pe_{d.T} = \dfrac{wd'}{d.T}$ passes through a minimum) when the layer is in the fluidized state and the porosity ϵ reaches a value of about 0.65. This is illustrated in Fig. 10, where the values of the turbulence criterion $Pe_{dT} = \dfrac{wd'}{d.T}$ (here d' is the particle size) are taken along the ordinate axis, and $(1 - \epsilon)$ along the abscissa axis.

In view of the development of processes involving treatment of heterogeneous systems (gas purification, separation of suspensions and emulsions), results based on the solution of the so-called external hydrodynamic problem — determination of the resistance in the motion of a body in a medium — are becoming of great importance. The law governing the resistance remains the same (Equation 20), and only the nature of the forces applied to overcome the resistance changes. The methods used for purification or separation vary according to the nature of the applied forces: purification or separation by the action of gravity (sedimentation), purification or separation by the action of centrifugal force (cyclones, centrifuges), purification or separation in an electric field (electrostatic separation), purification or separation under the action of a pressure difference between two sides of a filtering partition (filtration).

The rates of separation of heterogeneous systems — rates of gas purification or a separation of suspensions — can be determined by simultaneous solution of equations for the applied forces and the forces of resistance.

In all cases the resistance is expressed in terms of the general law of resistance

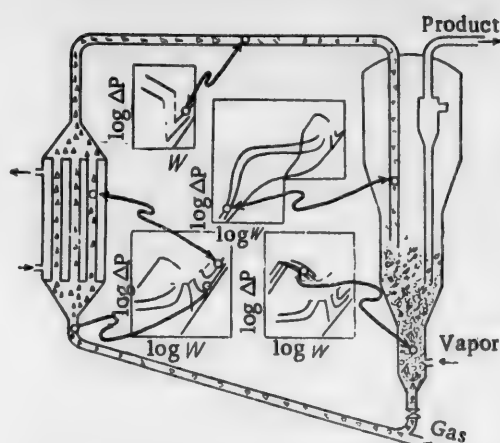$$S = \zeta F \frac{w_0^2 \gamma}{2g} G \ \ \text{kg} \tag{34}$$

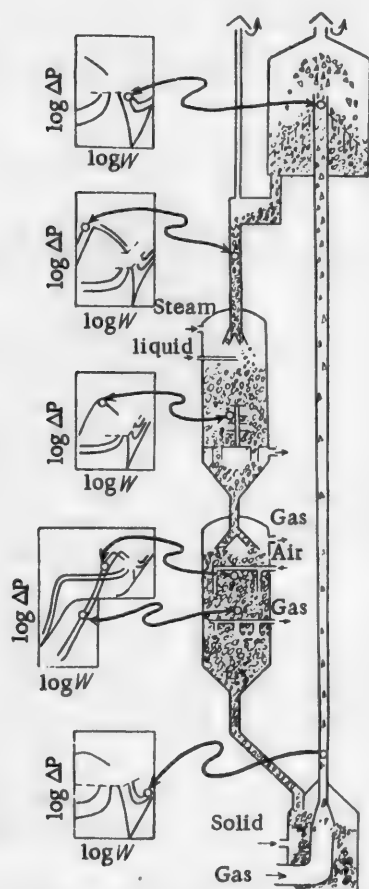Fig. 8. Hydrodynamic regimes for the gas—solid system in a hydrocarbon-synthesis reactor.

Fig. 9. Hydrodynamic regimes for a gas—solid system in a reactor with a moving bed.

by the following equations: when $Re = \dfrac{w_0 d \gamma_G}{\mu \cdot g} \le 2$

($\underline{d}$ is the particle diameter), F is the area of the middle cross section (Stokes' law)

$$\zeta = \frac{24}{Re},\qquad(35)$$

when $Re = 2 - 500$ (Allen's law)

$$\zeta = \frac{18.5}{Re^{0.6}},\qquad(36)$$

when $Re > 500$ (Newton's law)

$$\zeta = \mathrm{const} = 0.44.\qquad(37)$$

For nonspherical particles a shape factor $\varphi < 1$ is introduced into the above equations.

During recent years methods of purification based on the use of centrifugal force, filtration, scrubbing, etc., have been developed considerably. Centrifugal separation by means of cyclones has recently been extended to the extensive use of hydrocyclones for the separation of suspensions [74].

The main field of application of hydrocyclones is size classification of suspensions, mainly in the 15-100 μ range. They are used for classification and beneficiation of ores, including uranium ores [75-79].

The use of hydrocyclones in evaporation units, with return of the overflow to the evaporators, has been described [80]. Hydrocyclones are used as classifiers in conjunction with crushers [81-85].

The principal dimensions of hydrocyclones have been determined and calculated by Povarov [86], Moder and Dahlstrom [87], and Fitch and Johnson [88]. Velocity distributions in hydrocyclones have been studied most fully by Kelsall [89].

Wet cleaning (scrubbing) of gases is now extensively used. The foam method of scrubbing, developed by Pozin, Mukhlenov, Tarat, Tumarkina, and others [36], has been introduced into scrubbing practice. The foam method essentially involves the creation of an operating regime on a perforated plate such that a mobile foam is formed, consisting of a semisuspended liquid layer in the form of films and steams intermingled with bubbles and streams of gas. A mobile foam is formed when the gas is passed through the liquid at 0.7-3.5 m/second in the open section of the apparatus, which is higher than the velocity of free ascent of the gas bubbles in the liquid layer. The
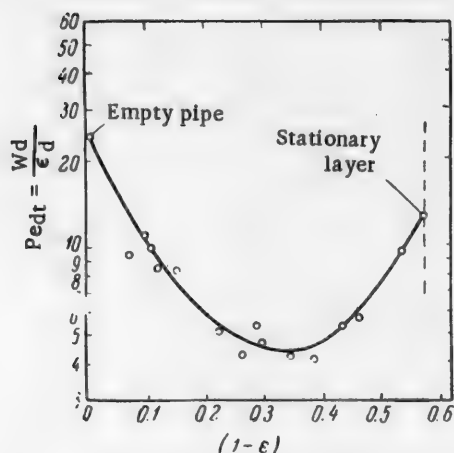
efficiency of the grid of a foam scrubber in dust removal reaches 99%.

The injection-nozzle method of wet cleaning by means of Venturi tubes is becoming widely used [90].

Filtration is one of the commonest and least studied methods for the separation of suspensions. The reason is that the rate of the process is determined by the specific properties of the suspension and the specific structure of the solid layer. Analyses of the filtration process and calculations relating to industrial filters are usually based on various modifications of the equation put forward by Lewis [91, 92] and modified by Sperry [93], Ruth [94], and others.

This equation has the following general form

Fig. 10. Variation of turbulent transfer with the state of the layer.

$$U = \frac{dQ}{F d\tau} = \frac{\Delta p}{\mu \rho l + R}, \qquad (38)$$

where U is the filtration rate (in m/second), Q is the volume of filtrate (in m³), τ is the filtration time (in seconds), F is the cross-sectional area of the filter (in m²), Δp is the pressure drop in filtration (in kg/m²), μ is the viscosity of the filtrate (in kg·sec/m², l is the thickness of the cake (in m), ρ is the specific resistance of the cake (1/m²), and R is the resistance of the filter membrane.

Despite the apparent simplicity of Equation (38) in practice its use is very difficult, as the quantities ρ and R are themselves complex and vary with the filtration conditions.

The specific resistance ρ of the cake includes all the usually unknown structural characteristics of the cake: the diameter and true length of the capillaries; quantities characterizing their convolution and form of cross section; the number of capillaries per unit cross section of the cake, etc.

The value of ρ may be found from Equation (38) under definite filtration conditions, provided that the resistance R of the filter membrane is known. However, in practice the values of ρ show poor reproducibility even for the same pressure difference. The problem becomes more complicated in attempts to transfer the results of experiments performed under one set of conditions to filters operating under different conditions. Attempts to take into account changes in the cake structure by determination of the $\rho = f(\Delta p)$ relationship, such as were made first by Lewis and later by others, have merely yielded numerous empirical equations, valid only for certain substances and within narrow ranges of pressure differences. The evident reason for this is that ρ is a complex quantity, consisting of several structural characteristics, which do not all change similarly with changes of pressure.

The resistance R of the filter membrane, which is usually assumed to be constant, is in reality a variable quantity, which greatly depends on the properties of the solid particles of the suspension, which penetrate to indefinite depths into the pores of the filter and thereby increase its resistance severalfold. The depth of penetration of the particles into the filter pores, and therefore the resistance of the filter, depend on the pressure difference in filtration.

It is therefore clear that it is not possible to model the filtration process with the aid of Equation (38), as it does not reflect the quantities which directly characterize the structure of the cake, while the quantities ρ and R are complex and vary with the filtration conditions.

During recent years there have been some different approaches to the analysis of industrial filtration, analogous to the methods used in the hydrodynamics of granular beds. These methods have provided solutions to a number of complex industrial problems such as the percolation of liquids through soil, motion of liquids

In packed towers, determinations of the characteristics of fluidized layers, etc. In our opinion the reason for the success in these branches of hydrodynamics is that the velocity of the liquid in the cake was directly correlated with the cake structure.

Several attempts have been made to correlate the specific resistance of a compressible cake with its structural characteristics [95-99].

It has been shown by a number of workers [96, 100-102] that the structural characteristics of the cake formed during filtration may be determined by means of experiments on the percolation of pure filtrate through a previously-formed cake. This makes it possible to write the filtration equation, in full harmony with the modern theory of hydrodynamics, in the following form:

$$\Delta p = \lambda \frac{w_0^2 \gamma l}{2 g d_e},$$ (39)

where Δp is the pressure loss in filtration (in kg/m^2); λ is the coefficient of friction in the cake capillaries (a dimensionless quantity); w_0 is the true flow rate of the liquid in the capillaries (in $m^3/m^2 \cdot sec$), γ is the density of the liquid (in kg/m^3); l is the thickness of the cake (in m); g is the acceleration due to gravity (in m/sec^2); d_e is the equivalent diameter of the cake (in m).

In Equation (39) λ is the coefficient of friction, defined by the equation

$$\lambda = f_0 (Re).$$ (40)

In this case Re can be written as

$$Re = \frac{w_0 \rho d_e}{\mu}.$$ (41)

Since the true velocity of the liquid in the cake (w_0) in Equations (39-41) is unknown, we refer the velocity to the total cross section of the filter. The velocity then becomes

$$w_0 = \frac{w}{\epsilon},$$ (42)

where ϵ is the porosity of the cake; w is the velocity of the liquid relative to the total cross section of the filter (in $m^3/m^2 \cdot sec$).

The equivalent diameter of the cake may be represented as follows:

$$d_e = \frac{4\epsilon}{S (1 - \epsilon)},$$ (43)

where S is the specific surface of the particles in the cake, i.e., the surface area of the particles present in unit volume of the solid particles in the cake (in m^2/m^3).

Introducing the values of w_0 and d_e into Equation (39) and solving it for λ, we find:

$$\lambda = \frac{8 g \Delta p \epsilon^3}{\gamma l w^2 S (1 - \epsilon)}.$$ (44)

Correspondingly, we obtain the following expression for Re:

$$Re = \frac{4 \gamma w}{g \mu (1 - \epsilon) S}.$$ (45)

According to a number of authors [103, 104], a compressible cake may be considered as consisting of agglomerates formed from fine crystalline particles. If so, then for any pressure difference the same form of functional relationship (40) should be valid for a compressible cake as for an incompressible cake, if in Equations (44) and (45) the values for the specific surface of the agglomerates are substituted for the specific surface S of the particles in the cake.

The porosity of the cake can in all cases be represented by the following expression:

$$\varepsilon = \frac{v_c - v_s}{v_c} = \frac{\dfrac{G_s}{\gamma_b} - \dfrac{G_s}{\gamma_s}}{\dfrac{G_s}{\gamma_b}} = \frac{\gamma_s - \gamma_b}{\gamma_s}, \tag{46}$$

where v_c is the volume of the cake at the instant of penetration of the liquid (in m³); v_s is the volume of the solid phase in the cake (in m³); G_s is the weight of the solid phase in the cake (in kg); γ_s is the density of the solid phase in the cake (in kg/m³); γ_b may be defined as the "bulk density" of the cake, as it is found by division of the weight of the dried cake by the volume occupied by the cake when the filtration rate was being determined at the given pressure difference.

In filtration through a compressible cake, γ_b increases and therefore the porosity decreases with increasing pressure difference. However, as the high porosities of many cakes are due to formation of agglomerates, when the cakes are compressed the decrease of porosity will occur both as the result of closer packing of the agglomerates, and as the result of deformation and destruction of the latter.

The deformation and destruction of agglomerates evidently leads to an increase of their specific surface, which in the limit approaches the value of the specific surface found for the individual particles. Since the compression of the cake is directly proportional to variations of its "bulk density" γ_b, it may be assumed as a first approximation that the specific surface also varies in direct proportion to variations of γ_b. With this assumption it is possible to relate the specific surface S_0, calculated from experimental data for a pressure difference Δp_0, to its changed value in any other experiment for a pressure difference Δp. If the bulk densities in experiments with pressure differences Δp_0 and Δp are represented by γ_{b0} and γ_b respectively, we obtain the following expression for the specific surfaces:

$$S = \frac{S_0 \gamma_b}{\gamma_{b0}}, \tag{47}$$

and then we have, from Equations (46) and (47):

$$S = \frac{S_0 \gamma_s (1 - \varepsilon)}{\gamma_{b0}} \tag{48}$$

If the values of S_0 and γ_{b0} for a pressure difference Δp_0 are taken as the initial constant values for a given suspension, the specific surface S for any other pressure difference, for a known value of ε corresponding to this pressure, can be found from Equation (48).

Thus, the process of filtration through a given compressible cake is determined by the values of three quantities: $\underline{w}$, Δp, and ε. The relationship between these quantities may be established by means of an expression of the form

$$\lambda = \frac{C}{Re}, \tag{49}$$

where C is a constant; this is in agreement with published investigations of filtration in which a laminar filtration law is assumed.

The relationship between the pressure difference and porosity is represented by the following expression:

$$\frac{\varepsilon^3}{(1-\varepsilon)^4} = f(\Delta p). \tag{50}$$

Analysis of numerous experimental data on the filtration of various suspensions giving compressible and incompressible cakes yielded the following equation [105], valid for the range $Re = 10^{-6} -10$, for a constant cake

$$\lambda = \frac{160}{Re} . \tag{51}$$

For compressible cakes, the following general expression was found:

$$\frac{\varepsilon^3}{(1-\varepsilon)^4} = A\Delta p^n, \tag{52}$$

where the constant $\underline{n}$ characterizes the compressibility of a given cake, and the constant A characterizes the structure of the uncompressed cake.

The rate of filtration with constant cake is 55-65% of the average filtration rate with a growing cake.

Agitation in mechanical mixers is a very common process in the chemical and allied industries. This process presents one of the most difficult hydrodynamic problems, complicated by the diversity of the currents created in the liquid by rotation of the impeller; these depend both on the design of the mixer and the agitation conditions. Analysis of the performance of mixers is complicated still further by the additional processes taking place during the agitation: solution, heating or cooling, introduction of a second phase, and the nonsteady character of the agitation process itself. At the present time two problems are usually solved in analysis of agitation processes. These are the power consumption required (a purely hydrodynamic problem), and the efficiency, determined by the specific conditions of the process, attained with the use of a given mixer. Joint solution of the two problems makes possible a complete calculation and selection of mixing devices.

The first problem has been solved only very recently, with the aid of the similarity principle. The general law of resistance $Eu = f(Re)$ was applied to mixers, and the following expressions were established [7]:

$$Eu_M = \frac{N}{d^5 n^3 \rho} = \xi = f(Re_M) \tag{53}$$

or

$$N = \xi d^5 n^3 \rho, \tag{54}$$

within the "laminar" region:

$$\xi = \frac{C_0}{Re_M} = \frac{C_0}{\frac{nd^2}{\mu}\rho} , \tag{55}$$

within the turbulent region:

$$\xi = \frac{C_1}{Re_M^m} ; \ m < 1 \ \ (m \cong 0.15 -0.25) \tag{56}$$

in the range of developed turbulence:

$$\xi = C_2 = \text{const.} \tag{57}$$

The limits of the different hydrodynamic regimes and the values of the constants C and m depend on the design of the mixer and on the presence or absence of baffles. * Most workers have recently concluded that scale modeling of mixers is possible only in presence of baffles which break down the vortex and waves, i.e., which eliminate the superposition of a gravity field or the influence of the Froude number on the centrifugal-force field. Otherwise the Re and Fr criteria must be kept constant simultaneously, which is impossible in most cases.

Solution of the problem of mixer efficiency is directly associated with analysis of the actual processes for which the agitation is used. This question has been studied very little.

Up to now, relationships for determination of the homogeneity of suspensions and emulsions formed have been derived [106, 107]; equations have been given for calculation of the coefficient of heat transfer from the wall to the agitated liquid [108]; an approximate expression for the dissolution time of a solid during stirring has been found [109]; the determining parameters in agitation in gas—liquid [110] and liquid—liquid [111] systems have been defined.

Mixer efficiency in chemical processes has been considered only in relation to analysis of continuous processes [112].

A detailed review of agitation processes and modeling of mixers has been published fairly recently by Green [113].

Heat-transfer processes. Since the Great October Revolution the Soviet school of heat technologists has taken one of the leading positions in the world, and has in many respects determined the development of the science of heat transfer. Academician M. V. Kirpichev and his school developed the theory of similarity and the theory of heat modeling, which provided wide possibilities for generalization of experimental data and studies of processes taking place in heat-exchange equipment. A brilliant interpretation of the physical nature of heat-transfer processes in the light of the theory of similarity is given by Gukhman in his well-known monograph [114].

The work of Mikheev, Styrikovich, Kruzhilin, Kosterin, Kutateladze, Kichigin, Kostenko, Tobilevich, Tolubinsky, Gukhman, Gudemchuk, Berman, Kondratyev, Chukhanov, Eigenson, Sterman, and others led to the development of original methods of calculation and experimental study of heat transfer; these methods are the most advanced in world science [115].

Soviet science has priority and the leading role both in the general formulation of the heat-transfer problem during variations of the state of aggregation of the heat-transfer medium, and in solution of the great majority of particular problems. We need only mention the remarkable monographs by Kutateladze [116] and Kichigin and Kostenko [117], and Mikheev's well-known textbook [118].

Much research has been done in the USSR on heat transfer and hydraulic resistance in smooth pipes. Special mention must be made of the most detailed investigations carried out by Antufyev, Beletsky, Kozachenko, Kuznetsov, Lokshin, and Ornatsky [119].

Gurvich [120] and Konakov [121] published extensive experimental data obtained by Soviet workers and theoretical analysis of such data on transfer by radiation.

For calculations relating to processes of heat transfer in nonsteady conditions, Vanichev [122] proposed an original method of elementary heat balances; this is preferable to the method of finite differences, which is essentially a consequence of Vanichev's method.

Kondratyev [123] developed the method of the regular regime; this is a general method for the mathematical solution of the problem of the relationship between the heat of cooling of a body of any configuration, the physical and geometric characteristics of the body, and the external cooling conditions.

It is not possible in this review to deal with the large number of particular solutions of individual heat-transfer problems or to give the numerous equations which have been derived; we shall therefore only indicate the general tendencies which have appeared in recent years in the theory and practice of heat transfer.

In chemical technology it is often necessary to calculate the area of the heat-transfer surface, given by the general heat-transfer equation

*Geometric ratios which take into account the influence of various geometric factors are usually introduced into Equations (53-57).

$$F = \frac{Q}{K\Delta t_{av}^{\tau}} \ m^2, \tag{58}$$

where Q is the quantity of heat transferred (in kcal.), K is the coefficient of heat transfer between two media (in kcal /$m^2 \cdot$ hr $\cdot$ °C), Δt_{av} is the average temperature difference between the media (in °C), and τ is the heat-transfer time (in hours).

The rate of heat transfer is determined by the coefficient of heat transfer K, which depends on the numerical values of the local coefficients of heat transfer on each side of the wall of the apparatus (α_1 and α_2). The latter, in their turn, are determined by the hydrodynamic conditions at the wall. In the case of heat exchange at a solid boundary (wall) analysis is considerably complicated by the presence of a boundary layer, as the velocity and temperature profiles in the core of the stream and in the boundary layers are different.

Analysis and calculation of thermal processes reduce to consideration of the flow of heat between the heat source and the receiving medium. The relationship between heat flow and the hydrodynamic conditions of the process is revealed through the relationships between the criteria of thermal similarity. The meaning of the principle criteria of thermal similarity from the aspect of heat-transfer mechanism is clear from the scheme given earlier (Fig. 2).
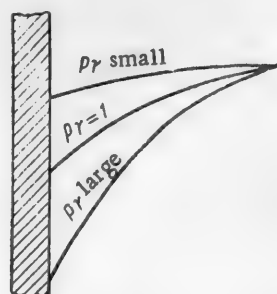

Fig. 11. Influence of the Prandtl number Pr on the temperature profile.

In accordance with the earlier discussion of the mechanism of processes, the temperature profile at a solid wall, where turbulent pulsations are damped, is determined by the influence of the value of the criterion which relates molecular friction to molecular heat conductance (thermal conductivity). Such a criterion is the Prandtl thermal criterion (see Fig. 2) $Pr = \dfrac{\nu}{a}$, where ν is the kinematic viscosity, $\underline{a}$ is the coefficient of temperature conductivity defined as $a = \dfrac{\lambda}{c\gamma}$ (λ is the thermal conductivity of the medium, $\underline{c}$ is its heat capacity, and γ is its density).

When Pr is considerably less than unity, the molecular conductance is great and the temperature gradient is small; when Pr = 1, the momentum due to molecular transfer is equal to the quantity of heat transferred by molecular transfer (heat conductivity), and therefore the temperature profile is the same as the velocity profile at high values of Pr heat transfer by conduction is small relative to the transfer of the quantity of motion, and the temperature gradient is large, i.e.,

$$\left(\frac{dt}{dr}\right)_{Pr_{small}} < \left(\frac{dt}{dr}\right)_{Pr=1} < \left(\frac{dt}{dr}\right)_{Pr_{large}}. \tag{59}$$

These relationships are illustrated in Fig. 11. A theoretical analysis is given in the monograph by Knudsen and Katz [124].

Liquid metals have small Prandtl numbers (of the order 0.01-0.001). When they are used as heat-transfer media, heat is transferred to the walls by conduction, and turbulent transfer has no appreciable influence. Conversly, when liquids with large Prandtl numbers are used as heat-transfer media, turbulent transfer has a significant effect. These facts have a direct bearing on methods for increasing the efficiency of heat exchangers.

From our earlier discussion of process mechanisms, two ways of intensifying the performance of heat exchangers can be derived — by increase of turbulent transfer, and by the use of liquids with small Prandtl numbers as heat-transfer media.

The first way is achieved by increase of the turbulence or of Re = $\dfrac{w}{\nu}$. Examination of the quantities which constitute Re shows that Re can only be increased by an increase of the stream velocity, since increase of $\underline{l}$ would produce exactly the opposite effect, because of a given value of Nu the coefficient of heat transfer is inversely proportional to $\underline{l}$. However, increase of the velocity involves an increase of the pressure difference for driving the liquid; this may be taken as proportional to $w^{1.74}$ for turbulent flow; consequently, the expenditure of energy for movement of the liquid is increased. This question is directly related to rational design of the heat-transfer surface in contact with the liquid. In his solution of this problem, Chukhanov [125] considers two types of surface — of the "bundle" and "canal" types — on the assumption that the temperature conditions of the process are identical (for the same temperatures of the medium at the entry and exit respectively, and the same wall temperature). The relative evaluation of the surfaces is based on the value of the pressure difference Δp required to attain a certain value of the heat-transfer coefficient α. As the result of appropriate calculations Chukhanov concludes that surfaces of the "bundle" type are definitely superior, as such surfaces give considerably lower pressure differences at all values of the parameters possible in practice. The same question is considered in detail in an interesting review by Gukhman [115].

In the design of modern heat exchangers, turbulence is effected by introduction of partitions, fins, baffles, etc. In a recent paper, Grass [126] proposed the use of the coefficient $\eta = \left(\dfrac{\alpha_{mv}}{\alpha_\infty}\right) : \left(\dfrac{\varphi_0}{\varphi_R}\right)$, and; α_{mv} for evaluation of heat-exchanger efficiency ; here α_∞ is the average value of the heat-transfer coefficient for pipes with baffles, α_∞ is the heat-transfer coefficient in smooth pipes with developed turbulence, and φ_0 and φ_R are the resistance coefficients for pipes with baffles and smooth pipes respectively.

Questions of rational heat-exchanger design are considered in a number of papers [127-131].

In recent years a considerable number of papers have been published, dealing with the influence of turbulent transfer on heat exchange [115, 132-135]. Most of these papers consider questions of the relationship between temperature and velocity profiles, and between coefficients of turbulent transfer of heat and momentum.

The second way of intensifying heat transfer follows directly from the influence of the Prandtl number, considered earlier. As was stated previously, the temperature profile levels out rapidly for liquids with low Pr, and the flow of heat is determined by the high value of λ . Consideration of the quantities comprising the Nusselt number Nu = $\dfrac{\alpha l}{\lambda}$, shows that the coefficient of heat transfer is directly proportional to λ :

$$\alpha = \frac{\lambda}{l} Nu. \tag{60}$$

It was shown by analysis of the exchange mechanism (Fig. 3) that the Nusselt number must be constant in laminar flow. This is confirmed experimentally. For example, values of Nu between 7 and 8 were obtained for liquid metals [124], and Nu = 2 was found for heat transfer in a granular bed [136].

It is therefore possibel to obtain relatively high values of the heat-transfer coefficient at very low flow velocities in laminar flow. The use of liquid metals as heat-transfer media in the production of atomic energy is based on these considerations [137].

It also follows from Equation (60) that the coefficient of heat transfer can by increased by decrease of linear dimensions. This is effected in modern equipment by the use of granular beds for heat transfer. The theory of this question has been discussed by Chukhanov [138], Chudnovsky [139], and others.

Moving granular beds can be used for considerable intensification of heat exchange, owing to increased turbulence of the gas stream; they are widely used for the heating of gases [140].

Heat transfer in fluidized beds is widely used in the metallurgy of zinc, in the burning of pyrites, for gasification of fuels, etc. [141].

One of the most important problems to be studied in the field of heat transfer during recent years is the question of ebullition. This problem is also associated with questions of atomic-energy technology [137]. Many papers dealing with ebullition were presented at the Geneva Conference in 1955 on the peaceful uses of atomic energy [137].

In an interesting recent paper, Rychkov [142] derived generalized equations for calculation of coefficients of heat transfer in the boiling of pure liquids and aqueous solutions.

For liquids at $P/P_{cr} < 0.35$:

$$\frac{\alpha E}{q} = 0.19 \ (q/q_{cr})^{-0.25} \cdot (P/P_{cr})^{0.33}. \tag{61}$$

For aqueous solutions of salts:

$$\frac{\alpha \cdot E}{q} = 0.095 \left(\frac{q}{q_{n.cr.}}\right)^{-n} \cdot \left(\frac{P_{osm}}{P^*_{osm}}\right)^{0.875}, \tag{62}$$

where α is the coefficient of heat transfer (in kcal /m$^2 \cdot$hour), E is the ebulliscopic constant, $\underline{q}$ is the rate of heat flow, q_{cr} is the critical rate of heat flow, $q_{n.cr}$ is the nominal critical rate; P is the pressure during boiling, P_{cr} is the critical pressure, P_{osm} is the osmotic pressure of a solution of the given concentration at the boiling point and the given external pressure, P^*_{osm} is the same, at saturation, and $\underline{n}$ is a constant for the given solution.

The ratio q/q_{cr} required for the calculation is found from the graph given by Chichelli and Bonilla

[143] as the function $\dfrac{q_{cr}}{P_{cr}} = f \left(\dfrac{P}{P_{cr}}\right)$.

Pramuk and Westwater [134] obtained significant results on the variations of the critical difference of temperatures during ebullition with changes of the hydrodynamic conditions (in agitation by mechanical stirrers). They showed that Δt_{cr} (for methanol) can be increased by 25% with the use of a propeller stirrer.

Much work is being done on the analysis, calculation, and practical aspects of evaporation processes. The above-mentioned monograph by Kichigin and Kostenko [117] deals with evaporation processes, and design calculations for evaporators; evaporation equipment is also described in Gelperin's monograph [144]; a classical method for design calculations of multiple-effect evaporators (later published as a separate brochure) was given by Tishchenko [145] as long ago as 1924. Other procedures for exact calculation [146-148] were developed later; these were based, in one way or another, on the work of Tishchenko, to whom great credit is due in the field of evaporator design calculations.

In evaporation technology increasing use is being made of evaporators with the heaters immersed directly in the solution to be evaporated [149, 150]. Hydrogen is used as fuel for evaporation of electrolytic caustic soda. For evaporation of sulfuric acid, calcium chloride, hydrochloric acid, etc., by submerged combustion, graphite is successfully used as the burner material, and heavy oil (mazut) as fuel.

Mass-transfer processes. Research on mass-transfer processes has made considerable progress in our country.

The work of Konovalov [151] and Vrevsky [152], the founders of the modern theory of rectification and separation of azeotropic mixtures, is the pride of Russian Science.

The thermodynamic theory of distillation and rectification processes was developed further by Tregubov [153], Obryadchikov [154], Badaturov [155], and others.

The well-known work of Stabnikov, which is partially detailed in the monograph compiled by him jointly with Kharin [156], deals with the theory of distillation and rectification processes and the solution of a number of practical problems. Stabnikov formulated the general principles relating to the economy of steam consumption in distillation [157].

The separation of gaseous mixture by rectification of the liquified gases is discussed in Fastovsky's monograph [158].

Distillation and rectification processes are also considered in the monograph by Gelperin [159].

Zhavoronkov, Maliusov and others [160, 161] studied molecular and film vacuum distillation.

Extractive and azeotropic distillation processes are considered in papers by Gelperin and Novkova, Gordievsky [163], and Kogan [164].

The theory of absorption processes has been advanced by the work of Shabalin [165], and the theory of chemisorption, by the work of Belopolsky, Turkhan [167], Pozin [168], and Kishinevsky [22, 23].

Zhavoronkov analyzed the scrubber process [48]. Absorption is also discussed in Ramm's monograph [169].

The development of drying technology was greatly advanced by the work of Ramzin who published, as long ago as 1918, a J—d diagram for moist air and developed a graphical method of calculation for different drying procedures [170].

Heat and mass transfer in drying processes are discussed in a number of monographs by A. V. Lykov, and in papers by his associates (P. D. Lebedev, A. V. Nestrenko, A. P. Voroshilov, M. V. Lykov, N. M. Mikhailov, A. S. Ginzburg, and others). The present state of drying technology is described in detail in Lykov's recent monograph [171].

Drying and adsorption processes are being studied by Romankov and his school [172].

The solution of solids in liquids and the present status of the problem are considered in Zdanorsky's monograph [173].

Among the typical investigations carried out by Soviet scientists in recent years in the field of mass transfer are studies of the principles of acceleration of mass-transfer processes, and researches in the light of the theory of accelerated processes and perfected equipment; in many respects this work is in advance of foreign research [174÷176].

Reviews of the present status and development of individual diffusion processes were published relatively recently in our literature [117-179]; the volume of the present review can be reduced considerably in consequence.

The following three aspects are always considered in calculation and analysis of mass-transfer processes.

1. The necessary and sufficient conditions for the existence of a given number of phases, and the laws governing the distribution of the components in them, determined by the phase rule and the laws of equilibrium.

2. The necessary and sufficient conditions created for the conduct of a process, the so-called operating conditions, which are predetermined by the initial and final concentrations and quantities of the substances involved in the process. The connection between the given quantities and concentrations is established by means of a material balance, which ultimately gives rise to the so-called operating lines for the process.

3. The necessary and sufficient conditions which determine the rate of transfer of a substance from one phase into another; these depend on the difference between the equilibrium and operating concentration (the driving force of the process), the physical properties of the systems, and the hydrodynamic conditions. The connection between these factors is established with the aid of equations of diffusion kinetics.

By simultaneous consideration of these three aspects of mass transfer the design and dimensions of diffusion equipment may be rationally determined.

The hydrodynamic conditions in a diffusion process in turn depend on the design characteristics of the equipment, which impose definite conditions on the geometric relationships between the determining dimensions. Therefore, while the first two aspects of analysis of mass-transfer processes can be examined without reference to the design characteristics of the diffusion equipment (static aspects of the process are not considered in the present review), the last aspect, kinetics, must be directly correlated with the actual design of the equipment used for the mass-transfer process.

It was pointed out in the general section of this review that the existence of a two-phase stream, characteristic of diffusion processes, introduces considerably complications into analysis of the effects, and it is not permissible to apply the laws of velocity and concentration distributions applicable in presence of a solid wall to free boundaries between streams.

However, the presence of a solid wall may in some cases exert a considerable influence in fixing the interphase boundary, for example in equipment such as wetted-wall towers, various types of film equipment, etc.

All the great variety of diffusion equipment can be divided into two large groups, according to the conditions for formation of the phase-contact surface—equipment with fixed geometric phase-contact surface (surface absorbers, film equipment, bubbling equipment with fixed interphase boundaries, etc.), and equipment in which the phase-contact surface is created by moving streams (equipment with fluid jets, emulsification towers, foam equipment).

In harmony with Fig. 2, the performance of equipment of the first group may be analyzed with the aid of criteria for molecular and mixed transfer, by means of the general Equations (9-10).

Analysis and modeling of equipment of the second group may be carried out with the aid of criteria for turbulent transfer. In the latter case Equations (11-12) are also applicable.

In conditions of free turbulence $Pe_{dT} = $ const or $\epsilon_p / \epsilon_d = $ const, and therefore the variations of the determining hydrodynamic characteristics and of the determining diffusional characteristics are of the same nature; variations of the pressure difference and of the mass-transfer coefficients are of the same character. This corresponds to the fact that in conditions of developed free turbulence the molecular-diffusion characteristics have no influence on mass transfer and, in particular, that the exponents of Pr_L and Pr_G tend to zero.

Since the ratio $w \underline{1}/\epsilon_d$ is constant, it is possible to calculate the quantity of substance transferred from known by hydrodynamic parameters, i.e., to make a complete design calculation for the equipment.

The condition $w \underline{1}/\epsilon_d = $ const is equivalent to a constant output per unit volume of the equipment, $w/h = $ const, if the equipment operates in conditions of free turbulence.

The present tendency in equipment design is to concentrate on equipment of the second group.

The theory and design of foam equipment [177], emulsification towers [179], nozzle extractors [180, 181], and nozzle absorbers [182] have been developed in our country.

In foreign practice, the following equipment has been introduced: bubble-cap plate towers, operating on the principle of nozzle equipment (with float-valves [183], with free disk valves [184], Uniflux [185], and Turbogrid sieve-plate towers) with dropping of the liquid through the perforations and countercurrent flow of gas [186].

Pulsation [187, 188] and vibration [189] towers, and packed towers with stirrers [190] have been devised for intensification of extraction processes.

The energy efficiency of diffusion equipment can in principle be evaluated in terms of the ratio

$$\eta_e = \frac{\Delta p_{G.L.} - \Delta p_G}{\Delta p_{G.L.}},\tag{63}$$

where $\Delta p_{G.L}$ and Δp_G are the resistances in a two-phase stream and a single-phase stream respectively.

The values of η_e are lower for equipment of the first than of the second group; in the first group η_e decreases and in the second it increases with increase of velocity. The efficiencies of equipment of different design are conveniently compared in terms of output per unit volume of the equipment and of the pressure difference per unit height of the interaction zone [179].

The output per unit volume of the equipment may be expressed as the ratio of the space velocity of the stream per unit cross section of the apparatus (w, $m^3/m^2 \cdot$ second) to the length of the zone of the apparatus (h_M) over which the interaction occurs. For towers, the length $\underline{h}$ of the zone is conveniently evaluated

in terms of the height equivalent to a theoretical plate. For extraction columns it is convenient to introduce the equivalent ratio $1/t_c$, where t_c is time required to effect one theoretical contact step in an extractor of the given type. This contact time is connected with the holdup time t_0 of the liquid in the extractor by the expression $t_c = t_0/n$, where $\underline{n}$ is the number of theoretical steps.

A second characteristic of the apparatus is the pressure difference Δp per unit length $\underline{h}$ of the contact zone; or, for towers, it is convenient to use the ratio of the pressure difference per theoretical step, $\Delta p/n$.

Comparative evaluations of diffusion equipment [179, 191] have shown the greater outputs per unit volume are obtained with equipment of the second group. The specific energy consumption $\Delta p/n$ may be of the same order for equipment of both groups, or a little lower for equipment of the first group.

By analogy with heat transfer in the laminar region, the efficiency of equipment of the first group is higher in cases when the Prandtl numbers for the determining phases are small and the concentration profile is level, i.e., when the magnitude of the molecular-diffusion coefficients is considerable. Kuhn's column [192] proved to be the most efficient apparatus of this kind.

The principal types of industrial equipment for mass-transfer processes used at the present time are bubble-cap towers of various designs, sieve-plate towers, grid towers, and packed towers. Centrifuges and stirred extractors are used in extraction processes. In recent years the efficiency of bubble-cap towers of old design has been raised by 30%.

Bubble-cap towers of new design, with floating valves or with Uniflux plates, give 2-3 times the output per unit volume (w/h) given by columns of older design.

Calculations of the most rational operating conditions of bubble-cap columns are given in the paper by Atkins [42].

In general, sieve-plate towers have higher efficiencies than bubble-cap towers, and are being increasingly used.

The performance of sieve-plate and grid towers has been studied by many workers in our country. Mention has already been made of the introduction, by Pozin, Mukhlenov, Tumarkina, and Tarat, of foam equipment which uses sieve or grid plates operating with a mobile-foam regime. The operation of foam equipment is discussed in detail in the monograph by these authors [193]. Noskov [194] has studied for a number of years the operation of sieve-plate rectification columns, with the aid of the theory of similarity.

The hydrodynamics of the operation of sieve-plate columns has been discussed by Akselrod [41, 195]. Akselrod used the results of hydrodynamic studies of the performance of sieve-plate columns used for separation of liquid air to derive methods for calculation and design of sieve plates. The plate diameter is determined from known liquid and vapor or gas rates, for a predetermined vapor velocity in the column; the suitable design is chosen; the area occupied by the overflow devices without perforations is determined, and the type of the latter selected. An equation derived by Akselrod is then used to determine the vapor velocity in the perforations, the pressure difference being calculated. Graphs and monograms are used to simplify the calculations necessary for determinations of the dimensions of the overflow devices, distances between the plates, etc. Akselrod has reviewed the equipment used for separation of liquefied gases [196].

Grid plates without overflow pipes are being increasingly used. Detailed investigations of such plates were carried out by Aerov and Darovskikh [197]; Aerov and Bystrova [198] reported a comparative evaluation of the performance of grid plates.

Similar plates with round holes were treated by Kuzminykh [199]. The use of grid plates without outflow tubes gives a considerable increase of output per unit volume of the apparatus, and permits considerable fluctuations in the operating loads.

Jones and Pyle [200] compared sieve-plate and bubble-cap rectification columns, and Kelley [201] similarly compared absorption towers.

Different designs of sieve-plate columns have been adopted in extraction technology [178]. Sieve-plate columns can be used as pulsation columns for extraction.

Packed towers may be used both under film conditions, and in emulsification conditions [179]. In the latter case packed towers are the most effective equipment, giving the maximum output per unit volume at $\Delta p/n$ within the usual pressure limits. Calculations relating to the design of packed emulsification towers are discussed fully in the literature [179].

Information concerning the use of packed towers under emulsification conditions has recently appeared in the foreign literature [202].

Emulsification in extraction columns produces the same effects as the use of pulsations and vibrations.

A common equation has been derived for the limiting flow rates in packed absorption and rectification columns [203].

In laboratory practice packed columns are usually operated under film conditions, and in such cases efficiency is ensured by suitable choice of the packing, with good flow and effective wetting. However, this method has not justified itself in industrial practice.

High-speed operation in packed columns with plane-parallel packing is found to be very effective [204].

In our country, the fullest investigations of equipment with plane-parallel packing have been carried out by Semenov and Shvartsshtein [205], and by Zhavoronkov, Maliusov, and Malofeev [206].

The advantage of equipment with plane-parallel packing is the relatively low value of $\Delta p/n$ with considerable output per unit volume (w/h) owing to the high permissible gas velocities $\underline{w}$.

The use of nozzle equipment proved very effective in extraction processes. Thus, Gelperin [180] described tests of an injection extractor, with injection of the continuous and disperse phases, which proved highly efficient.

A recent paper [181] describes a study of the principal operating characteristics of a nozzle extractor (pressure loss, suction coefficient liquid rate, efficiency of the extractor). Such extractors are most suitable for extraction in systems requiring a short time of exposure at a fairly high distribution coefficient.

Adsorption processes are based on modern hydrodynamics of granular layers. Such processes are accelerated by the use of fluidized or moving beds, etc. Adsorption and regeneration of the adsorbent are effected in a continuous process.

Consideration of the present state of the theory of adsorption is beyond the scope of the present review. The fundamental problems of adsorption and catalysis in moving and fluidized beds are considered in the review by Todes [43]. Here we shall only refer to a recent paper by Romankov, Lepilin, and Nemet [207] which is of practical interest. They plotted experimental data on adsorption in a fluidized bed, in adsorption rate—time $\left(\dfrac{dA}{d\tau} - \tau \right)$ and adsorption rate—amount of substance adsorbed $\left(\dfrac{dA}{d\tau} - A \right)$ coordinates; the curves obtained were analogous to drying curves (period of constant rate and period of decreasing rate). Calculation formulas were derived for both periods.

The technology of adsorption on fixed beds is discussed in Serpionova's monograph [208].

In conclusion, mention should be made of a recent monograph by Treyball [209], dealing with various mass-transfer operations.

The theory of continuous chemical processes has been developed by Planovsky [210]. Pozin put forward generalized equations for determination of the efficiency of different types of chemical equipment [211].

Further investigations in the field of chemical engineering processes and equipment must be directed toward theoretical development of accelerated processes and work on the design of equipment giving the highest output per unit volume.

LITERATURE CITED

[1] L. Prandtl, Hydro- and Aeromechanics (Russian translation) (IL, Moscow, 1949).

[2] G. J. Taylor, Proc. Roy. Soc., A, 135, 485 (1932).

[3] N. E. Kochin, I. A. Kibel and N. V. Roze, Theoretical Hydromechanics (GITTL, 1955). *

[4] V. N. Goncharov, Principles of the Dynamics of River Flow (Hydrometeorological Press, 1954).*

[5] V. V. Kafarov, Collected Papers on Processes and Equipment (Goskhimizdat, 1953); *J. Appl. Chem. 29, 1, 40 (1956).* *

[6] I. Nikuradse, Proc. 3rd Int. Cong. Appl. Mech. 1, 239 (1930).

[7] V. V. Kafarov, Agitation Processes in Liquid Media (Goskhimizdat, 1949). *

[8] R. H. Wilhelm, Chem. Eng. Progress 49, 3, 152 (1953).

[9] I. B. Lewis, Chem. Eng. Sci. 3, 248 (1954).

[10] E. V. Murphree, Ind. Eng. Ch. 24, 72 (1932).

[11] T. K. Sherwood, Tr. Am. Inst. Chem. Eng. 36, 817 (1940).

[12] W. K. Lewis and W. G. Whitman, Ind. Eng. Ch. 16, 1, 15 (1924).

[13] W. Nernst, Z. phys. ch. 47, 52 (1904).

[14] E. Brunner, Z. phys. ch. 47, 56 (1904).

[15] T. K. Sherwood and R. L. Pigford, Absorption and Extraction (1952).

[16] L. D. Berman, J. Tech. Phys. 9, 2 (1939).

[17] A. W. Hixson and S. I. Baum, Ind. Eng. Ch. 33, 478 (1941); 34, 120 (1942).

[18] N. I. Litunovsky, I. I. Petrenko and O. M. Todes, J. Tech. Phys. 23, 8, 1321 (1953).

[19] H. Schlichting, Boundary Layer Theory (Russian translation) (IL, 1956).

[20] G. N. Abramovich, Turbulent Free Streams of Liquids and Gases (Gosenergoizdat, 1948). *

[21] K. Sigwart and H. Nassenstein, Ver. deut. Ing. Z. 98, 453 (1956).

[22] M. Kh. Kishinevsky, J. Appl. Chem. 22, 1173, 1183 (1949).

[23] M. Kh. Kishinevsky, J. Appl. Chem. 24, 413, 542 (1951); * * 28, 9 (1955), * * 30, 2 (1957). * *

[24] V. V. Kafarov and V. I. Trofimov, J. Appl. Chem. 30, 211 (1957). * *

[25] T. J. Hanratty, J. G. Latinen and R. H. Wilhelm, A. I. Ch. E. Journal 2, 372 (1956).

[26] V. V. Kafarov, J. Appl. Chem. 28, 1234 (1955).* *

[27] P. V. Danckwerts, Tr. Far. Soc. 46, 300, 701 (1950); Ind. Eng. Ch. 43, 6 (1951).

[28] R. Higbe, Tr. Am. Inst. Chem. Eng. 31, 365 (1935).

[29] T. J. Hanratty, A. I. Ch. E. Journal 2, 359 (1956); 2, 42 (1956).

[30] V. G. Levich, Physicochemical Hydrodynamics (Izd. AN SSSR, 1952). *

[31] P. G. Romankov, Hydraulic Processes of Chemical Technology (Goskhimizdat, 1948). *

[32] N. G. Zalogin and O. M. Shukher, Purification of Flue Gases (Gosenergoizdat, 1954). *

[33] G. M. Gordon and I. A. Aladzhalov, Gas Purification by Bag Filters (Metallurgy Press, 1949). *

[34] B. L. Shneerson, Electrical Purification of Gases (Gosenergoizdat, 1950). *

[35] S. P. Zhebrovsky, Electrofilters (Gosenergoizdat, 1950). *

---

*In Russian.

**Original Russian pagination. See C. B. Translation.

[36] M. E. Pozin, I. P. Mukhlenov, and E. Ya. Tarat, The Foam Method of Dust and Mist Removal From Gases (Goskhimizdat, 1953).*

[37] N. V. Shpanov, Continuous-Action Filters (Mashgiz, 1949).*

[38] V. I. Sokolov, Centrifuges (Mashgiz, 1950).*

[39] V. V. Kafarov, J. Chem. Ind. 5 (1953).

[40] V. V. Kafarov and L. I. Blyakhman, J. Appl. Chem. 24, 1274 (1951).**

[41] L. S. Akselrod, Trans. VNIIK I Mash. 1, 22 (1956).

[42] G. T. Atkins, Chem. Eng. Progr. 50, 116 (1954).

[43] O. M. Todes, in the book: Methods and Processes of Chemical Technolgy (Izd. AN SSSR, 1955).*

[44] A. K. Krupsky, Bulletin of Industry 2, 1; 3, 19; 11, 1 (1885).

[45] A. K. Krupsky, Fundamental Principles of Planning in Chemical Technlogy, 2 (1915).*

[46] W. Barth, Chem. Ing. Techn. 26, 1, 29 (1954).

[47] I. M. Fedorov, in the book: Modern Problems of Drying Technology, 2 (Gosenergoizdat, 1941).*

[48] N. M. Zhavoronkov, Hydraulic Principles of the Scrubber Process and Heat Transfer in Scrubbers (Soviet Science, 1944).*

[49] G. K. Boreskov and L. G. Ritter, J. Chem. Ind. 6 (1946).

[50] B. A. Zakharov and A. V. Frost, Bull. Acad. Sci. USSR 3 (1946).

[51] T. N. Chilton and A. P. Colburn, Ind. Eng. Ch. 23, 23, 913 (1931).

[52] P. C. Carman, Tr. Am. Inst. Chem. Eng. 15, 150 (1937).

[53] A. O. Oman and K. M. Watson, Nat. Petr. News 36, R 795-802 (1944).

[54] J. M. Campbell and R. L. Huntington, Petr. Refiner 30, 12, 127 (1951).

[55] J. M. Coulson, Tr. Am. Inst. Chem. Eng. 27, 237 (1949.

[56] I. Happel, Ind. Eng. Ch. 41, 1161 (1949).

[57] M. Lewa, Chem. Eng. 56, 5, 115 (1949).

[58] I. I. Martin, W. L. McCabe and C. C. Monard, Chem. Eng. Progr. 47, 2, 91 (1951).

[59] N. I. Syromyatnikov, Proc. Acad. Sci. USSR 93, 3 (1953).

[60] N. I. Smirnov and Li De Ep, J. Appl. Chem. 24, 56, 383, 439 (1951).**

[61] F. A. Zenz, Petr. Refiner 37, 7, 123 (1953).

[62] D. H. Belden and L. S. Kassel, Ind. Eng. Ch. 41, 1174-1178 (1949).

[63] W. Camp and A. Priestley, The Engineer 137, 34 (1924).

[64] I. Farbar, Ind. Eng. Ch. 41, 1184-1191 (1949).

[65] H. Gasterstadt, Zeit. VDY 68, 24, 617-624 (1924).

[66] O. Harin and M. C. Molstad, Ind. Eng. Ch. 41, 1148-1160 (1949).

[67] E. G. Vogt and R. R. White, Ind. Eng. Ch. 40, 1731-1738 (1948).

[68] R. H. Wilhelm and S. Valentine, Ind. Eng. Ch. 43, 1199-1203 (1951).

[69] F. A. Zenz, Ind. Eng. Ch. 41, 2801-2806 (1949).

[70] G. N. Khudyakov and Z. F. Chukhanov, Proc. Acad. Sci. USSR 78, 681 (1951).

*In Russian.
**Original Russian pagination. See C. B. Translation.

[71] Segler, Zeit. VDY, 79, 558 (1935).

[72] V. A. Uspensky, Fuel Economy 3, 26 (1951).

[73] S. A. Wood and A. Babley, Proc. Inst. Mech. Engrs. (London) 142, 149 (1939).

[74] S. Z. Kagan, J. Chem. Ind. 6 (1956).

[75] I. N. Kachan, Refractories 6, 499 (1951).

[76] H. Trawinski, Z. Erz. Met. 7, 537 (1954).

[77] D. I. Nedogovorov and N. T. Klimenko, Nonferrous Metals 1 (1956).

[78] R. Köhler, Z. angew. Geol. 2, 33 (1956).

[79] E. O. Lilge, J. G. Edwards and H. H. McGreedy, Can. Min. Met. Bull. 48, 515, 133 (1955).

[80] O. F. Taugel and R. I. Brison, Chem. Eng. 62, 234 (1955).

[81] A. I. Povarov, Bull. Central Inst. Inf. Min. Nonferrous Metals 6, 5 (1955).

[82] C. G. Peachey, J. Chem. Met. Min. Soc. S. Africa 56, 107 (1955).

[83] R. J. Adamson, ibid. 56, 169 (1955).

[84] R. Berline, Genie Chim. 73, 134 (1955).

[85] C. Krijgsmann, Chem. Eng. Techn. 23, 540 (1951).

[86] A. I. Povarov, Trans. Sci. Res. Inst. for Mechanical Concentration of Minerals (Metallurgy Press, 1952). *

[87] I. I. Moder and D. A. Dahlstrom, Chem. Eng. Progress 48, 75 (1952).

[88] E. B. Fitch and E. C. Johnson, Min. Eng. 5, 304 (1953).

[89] D. F. Kelsall, Tr. Inst. Chem. Eng. (London) 30, 87, 103 (1952).

[90] R. M. G. Bucher , M. L. Franck and W. Fortman, Ind. Chemist 33, 385, 113 (1957).

[91] W. K. Lewis and C. Almey, J. Ind. Chem. 4, 528 (1912).

[92] W. K. Lewis, B. W. H. Walker and W. H. McAdams, Principles of Chem. Eng. New York (1923).

[93] D. K. Sperry, Ind. Eng. Ch. 36, 323 (1944).

[94] B. F. Rutha and L. L. Kempe, Trans. Am. Inst. Chem. Eng. 33, 34 (1937).

[95] S. M. Walas, ibid. 42, 783 (1946).

[96] L. G. Belkin, J. Chem. Ind. 7-8 (1946).

[97] G. I. Znamensky, Trans. Mikoyan Technol. Inst. Food Ind. Kiev 6 (1947).

[98] V. D. Ponomarev and A. P. Ni, Bull. Acad. Sci. Kazakh SSR, Chem. Ser. 118, 3, 11 (1953).

[99] B. F. Ruth, Ind. Eng. Ch. 38, 564 (1946).

[100] V. A. Zhuzhikov, J. Chem. Ind. 9 (1948).

[101] E. H. Hoffing and E. I. Lockart, Chem. Eng. Progr. 47, 3 (1951).

[102] W. L. Ingmanson, ibid. 49, 577 (1953).

[103] B. W. Wilson, Australian J. Appl. Sci. 2, 4 (1953).

[104] H. P. Grace, Chem. Eng. Progr. 49, 303 (1953).

[105] V. V. Kafarov and T. A. Malinovskaya, J. Chem. Ind. 8 (1956).

[106] I. S. Pavlushenko and N. M. Kostin, Inform. Bull. Abstracts of Sci. Res. Papers, 1, Lensoviet Inst. Chem. Tech. Leningrad (Goskhimizdat, 1954).

*In Russian.

[107] S. A. Miller and C. A. Mann, Tr. Am. Inst. Chem. Eng. 40, 709 (1944).

[108] T. H. Chilton, T. B. Drew and R. H. Lebens, Ind. Eng. Ch. 36, 510 (1944).

[109] V. V. Kafarov and V. D. Podolma, J. Chem. Ind. 2 (1957).

[110] V. V. Kafarov, M. I. Goldfarb , and N. G. Ivanova, J. Chem. Ind. 7 (1954).

[111] W. A. Padger, V. G. Trice and J. H. Rushton, Chem. Eng. Progr. 52, 515 (1956).

[112] M. F. Nagiev, Chemistry, Technology, and Calculations in the Synthesis of Motor Fuels (Izd. AN SSSR, 1955). •

[113] S. L. Green, Tr. Inst. Chem. Eng. (London) 31, 327 (1953).

[114] A. A. Gukhman, Physical Principles of Heat Transfer (Gosenergoizdat, 1934). •

[115] A. A. Gukhman, J. Tech. Phys. 23, 6, 1064 (1953).

[116] S. S. Kutateladze, Heat Transfer in Condensation and Ebullition (Mashgiz, 1952). •

[117] M. A. Kichigin and G. N. Kostenko, Heat Exchangers and Evaporators (Gosenergoizdat, 1955). •

[118] M. A. Mikheev, Fundamentals of Heat Transfer (Gosenergoizdat, 1954). •

[119] M. A. Kichigin, Rationalization of the Heat Economy in Industrial Undertakings (State Tech. Press, Ukrainian SSSR, 1953). •

[120] A. M. Gurvich, Heat Transfer in Boiler Furnaces (Gosenergoizdat, 1950). •

[121] P. K. Konakov, Bull. Acad. Sci. USSR, OTN 3 (1952).

[122] A. P. Vanichev, Bull. Acad. Sci. USSR, OTN 12 (1946).

[123] G. M. Kondratiev, Heat Conductivity Tests by the Regular-Regime Method (State Standards Press, 1936). •

[124] J. G. Knudsen and D. L. Katz, Fluid Dynamics and Heat Transfer Eng. Res. Inst. Univ. Michigan (1954).

[125] Z. F. Chukhanov, Bull. Acad. Sci. USSR, OTN 1 (1948).

[126] G. Grass, Allgem. Wärmetechnik 7, 4, 73 (1956).

[127] B. G. A. Skrotzki and S. S. Waldron, Power 98, 75 (1954).

[128] E. Schmidt, Chem. Ing. Tech. 25, 221 (1953).

[129] C. H. Gilmour, Chem. Eng. 61, 3, 190 (1954).

[130] R. L. Callard, Chem. Eng. 63, 196 (1956).

[131] O. E. Dwyer, Ind. Eng. Ch. 48, 1836 (1956).

[132] H. Ludwig, Z. Flugwiss 4, 73 (1956).

[133] W. D. Raunie, J. Aeronaut. Sci. 23, 485 (1956).

[134] F. S. Pramuk and J. H. Westwater, Chem. Eng. Progr. Symposium Series, Heat Transfer Louisville, 82, 8, 79 (1957).

[135] W. H. Corcoran and B. H. Sage, Am. Inst. Chem. Eng. J. 2, 251 (1956).

[136] B. W. Gamson, G. T. Thodos and O. A. Hougen, Tr. Am. Inst. Chem. Eng. 39, 1 (1943).

[137] Atomic Energy Research, Estab. (Harwell) ED/M. 20 (1955).

[138] Z. F. Chukhanov, Bull. Acad. Sci. USSR, OTN 7-8 (1945); 4 (1946).

[139] A. F. Chudnovsky, Heat Transfer in Granular Materials (Gosenergoizdat, 1952). •

•In Russian.

[140] B. W. Gamson, Chem. Eng. Progr. 47, 19 (1951).

[141] Summaries of Papers at the All-Union Sci. Tech. Conference on Heterogeneous Processes in Solid Phases in Fluidized Beds (State Tech. Press, 1957).*

[142] A. I. Pychkov , Calculation Formula for Determination of Heat-Transfer Coefficients in Ebullition of Liquids and Solutions MIKhM, Moscow (1956).*

[143] M. F. Chichelli and C. F. Bonilla, Tr. Am. Inst. Chem. Eng. 41, 755 (1945).

[144] N. I. Gelperin , Evaporators (State Chem. Press, 1947). *

[145] I. A. Tishchenko, Calculations of Multiple-Effect Evaporators (ONTI, 1938).*

[146] N. A. Ushatinsky , Chemical Machine Construction 2 (1937).

[147] B. V. Florinsky , Chemical Machine Construction 5 (1938).

[148] A. N. Planovsky , A. I. Rychkov and V. M. Lekae, J. Chem. Ind. 3 (1947).

[149] P. D. V. Manning and S. D. Kirpatrick, Chem. Met. Eng. 51, 5, 92, 137 (1949).

[150] C. S. Cronan, Chem. Eng. 63, 2, 163 (1956).

[151] D. P. Konovalov, The Vapor Pressure of Solutions (St. Petersburg,1884 and 1909; Leningrad, 1928).

[152] M. S. Vrevsky , Collected Works, edited by K. P. Mishchenko (Moscow-Leningrad, 1954).*

[153] A. M. Tregubov, Theory of Distillation and Rectification, 3rd Edn. (State Fuel Tech. Press, Baku, 1946). *

[154] S. N. Obryadchitov , Principles of Petroleum Distillation (State Fuel Tech. Press, 1939).*

[155] S. A. Bagaturov, Textbook on the Theory of Distillation and Rectification (State Fuel Tech. Press, 1954).*

[156] V. N. Stabnikov and S. E. Kharin, Theoretical Principles of Distillation and Rectification of Alcohol (Food Industry Press, 1951). *

[157] V. N. Stabnikov, Industrial Power 5 (1957).

[158] V. G. Gastovsky , Separation of Gaseous Mixtures (State United Press, 1947). *

[159] N. I. Gelperin , Distillation and Rectification (Goskhimizdat, 1947).*

[160] N. M. Zhavoronkov and A. I. Maier, "Separation of Mixtures by Molecular Distillation," in the book: Methods and Processes of Chemical Technology (Izd. AN SSSR, 1955). *

[161] N. M. Zhavoronkov, V. A. Malyusov and N. N. Umnik, "Separation of Mixtures by High-Vacuum Rectification," in the book: Methods and Processes of Chemical Technology (Izd. AN SSSR, 1955). *

[162] N. I. Gelperin and K. E. Novikova, J. Appl. Chem. 26, 912 (1953).**

[163] V. V. Kafarov and L. A. Gordievsky , J. Appl. Chem. 29, 3 (1956); 4 (1956); 5 (1956).* *

[164] V. B. Kogan, J. Phys. Chem. 29, 11, 1984 (1955).

[165] K. N. Shabalin, Friction Between Gases and Liquids in Technical Absorption Processes (Metallurgy Press, 1943). *

[166] A. P. Belopolsky, J. Appl. Chem. 19, 1181 (1946).

[167] E. Ya. Turkhan, J. Appl. Chem. 21, 927 (1948).

[168] M. E. Pozin, J. Appl. Chem. 19, 1201, 1319 (1946); 20, 205, 345, 353, 523, 754, 963 (1947); 21, 58, 218, 708 (1948).

[169] V. M. Ramm, Absorption Processes in Chemical Industry (Goskhimizdat, 1951). *

* In Russian.
* *Original Russian pagination. See C. B. Translation.

[170] L. K. Ramzin, Design of Driers and the J-d Diagram (VTI, Moscow, 1930).*

[171] A. V. Lykov, Heat and Mass Transfer in Drying Processes (Gosenergoizdat, 1956). *

[172] P. G. Romankov et al., Abstracts of Sci. Res. Papers, Lensoviet, Inst. Chem. Tech. Leningrad (1956); 2 (1957).*

[173] A. B. Zdanovsky, Kinetics of the Solution of Natural Salts in Conditions of Forced Convection, Trans. Sci. Res. Inst. Halurgy, 33 (Goskhimizdat, 1956).*

[174] Trans. All-Union Sci.-Methodol. Conf. on Mass Transfer (Moscow, 1956). *

[175] Summaries of Papers at the Conference on Separation of Mixtures by Distillation, Rectification, and Absorption (Ministry of Chemical Industry, Moscow, 1956).*

[176] Summaries of Papers at the All-Union Scientific-Technical Conference on Process Rates and Improvement of the Quality of Materials During Drying in the Principal Branches of Industry and Agriculture (Moscow, 1956). *

[177] M. E. Pozin, "Methods of Intensification of the Interaction of Liquids and Gases," in the book: Methods and Processes of Chemical Technology (Izd. AN SSSR, 1955). *

[178] V. V. Kafarov and S. A. Zhukovskaya, J. Chem. Ind. 2 (1956).

[179] V. V. Kafarov, Chem. Sci. and Ind. 1 (1957).

[180] N. I. Gelperin, Chem. Sci. and Ind. 5 (1956).

[181] V. V. Kafarov and S. A. Zhukovskaya, Medical Ind. 5 (1957).

[182] A. N. Ternovskaya and A. M. Malets (see Ref. [175]).

[183] I. E. Nutter, Petr. Eng., 26, 5 (1954); Oil and Gas J., 4, 165 (1954).

[184] G. C. Trift, Oil and Gas J. 4, 190 (1954); Chem. Eng. 61, 177 (1954); Petr. Eng. 26, 5 (1954).

[185] V. P. Bowles, Oil and Gas J. 4, 176 (1954); Chem. Eng. 61, 5, 174 (1954); Petr. Eng. 26, 5 (1954).

[186] Chem. Eng. Progr. 50, 2, 57 (1954).

[187] G. Sege and F. W. Woodfield, Chem. Eng. Progr. 50, 8 (1954).

[188] H. F. Wiegandt and R. L. von Berg, Chem. Eng. 61, 183 (1954).

[189] V. S. Morello and N. Poffenberger, Ind. Eng. Ch. 42, 1021 (1950).

[190] F. G. Scheibel, Chem. Eng. Progr. 44, 681, 771 (1948).

[191] Yu.I. Dytnersky, Study of the Performance of Packed Absorption Emulsification Towers, Dissertation (MKhTI, 1956).*

[192] I. Kuhn, Chem. Ing. Techn. 11, (1953).

[193] M. E. Pozin, I. P. Mukhlenov, E. S. Tumarkina and E. Ya.Tarat, Trans. Lensoviet Chem. Tech. Inst. Leningrad 31 (Goskhimizdat, 1955).*

[194] A. A. Noskov (see Ref. [171]).

[195] L. S. Akselrod and V. V. Dilman, J. Chem. Ind. 1 (1954).

[196] L. S. Akselrod, Chem. Sci. and Ind. 1 (1957).

[197] M. E. Aerov and E. P. Darovskikh, J. Chem. Ind. 2 (1957).

[198] M. E. Aerov and T. A. Bystrova, J. Chem. Ind. 1 (1957).

[199] I. N. Kuzminykh, J. Chem. Ind. 4, 234 (1956).

[200] J. B. Jones and C. Pyle, Chem. Eng. Progr. 51, 9, 424 (1955).

---

* In Russian.

[201] R. E. Kelley, Petr. Refiner 34, 5, 188 (1954).

[202] A. J. Teller, Chem. Eng. 61, 9, 188 (1954).

[203] V. V. Kafarov and Yu. I. Dytnersky, Trans. MKhTI 23 (1957).

[204] G. Adolphi and R. Fleischer, Chem. Techn. 11, 638 (1955).

[205] P. A. Semenov and Ya.V. Shvartsshtein, J. Chem. Ind. 9 (1952) ; 7 (1953).

[206] N. M. Zhavoronkov, V. A. Malyusov and N. A. Malafeev, J. Chem. Ind. 8 (1951).

[207] P. G. Romankov, V. N. Lepilin and E. S. Nemet, J. Appl. Chem. 29 (1956).*

[208] E. N. Serpionova, Industrial Adsorption of Gases and Vapors (Goskhimizdat, 1956).* *

[209] R. Treyball, Mass- Transfer Operations (New York, 1956).

[210] A. N. Planovsky, J. Chem. Ind. 5 (1944).

[211] M. E. Pozin, J. Appl. Chem. 29, 9, 1336 (1956).*

* Original Russian pagination. See C. B. translation.
* * In Russian.

DEVELOPMENT OF THE ELECTROCHEMICAL INDUSTRY IN THE USSR IN 40 YEARS

A. F. Alabyshev

The Great October Socialist Revolution, which heralded the start of a new epoch in the history of mankind and radically changed the social and economic situation, had a remarkably beneficial influence on the development of culture, science, and technology in the USSR. The great masses of workers of the economically weak country were handed the countless riches of their native land and, under changed social conditions, commenced the giant task of assimilation of this wealth under the guidance of the Communist Party. From the very start of the new social-economic system, industry advanced rapidly along the path of new revolutionary technology. The latter includes the development of electrochemistry.

Among the first attempts to apply electrical energy to chemical and metallurgical processes are Davy's well-known qualitative experiments at the beginning of the 19th century. The discovery by Faraday, in 1831, of the laws of electrolysis and the introduction of electrochemical terminology may be regarded as the beginning of quantitative electrochemistry. However, the adoption of electrochemical methods in technology only became possible with the development of electrical engineering and the creation of current generators sufficiently powerful and economical to make the transition from laboratory experiments to industrial electrochemistry possible. Therefore the development of applied electrochemistry began almost 50 years after the discovery of the fundamental laws of electrolysis.

In order to give an accurate picture of the development of the electrochemical industry in the USSR during the 40 years after the Great October Socialist Revolution, it is necessary to give a brief description of the state of the electrochemical industry at the time of the revolution, in the world as a whole and in Tsarist Russia in particular.

The first industrial application of electrochemistry in the world was the invention, by Academician of the Russian Academy of Sciences B. S. Jacoby in 1836, of an electroforming process for the production of copper copies of relief originals, and his practical utilization of this process for the production of printing blocks in the Department for the Production of State Papers in Peterburg.

B. S. Jacoby's invention found a variety of practical applications; in particular, it formed the basis of the electrolytic refining of copper, silver, gold, and other metals. Copper was first refined electrolytically in 1847 in Russia. However, this process was developed on the large industrial scale in England, America, and Germany in the 1870's.

It must be pointed out that Russian scientists played an important part in the development of many other industrial applications of electrolysis. Here it is appropriate to mention the discovery, by the Russian Academician Lenz in 1842, of the law of equivalence of electrical and thermal energy, which was of great importance in the development of applied electrochemistry. The work of Bagration and Sosnovsky (1866) on "dry" galvanic cells, of E. Klein (1869) on the electrolytic deposition of iron, F. Vashchuk and N. Glukhov's invention (1879) of the first cell for the production of chlorine, alkali, and hydrogen by electrolysis of aqueous solutions of common salt, the work of D. A. Lachinov (1888) on the electrolysis of water, of Lidov and Tikhomirov on the electrolytic production of bleaching liquors (1883), of Lashchinsky on the electrometallurgical extraction of copper from its ores and other work by Russian scientists and inventors laid the foundations of many electrochemical industries [1, 2].

However, owing to the technical and economic backwardness of prerevolutionary Russia, electrochemistry was not extensively used in our industry. The practical significance of electrolysis as a method which opens up new industries and radically changes old techniques was utilized much more extensively in Western Europe and America. The rapid development of applied electrochemistry abroad began in the last decade of the 19th century.

During this period there were started, in Europe and America, large electrochemical industries for the production of chlorine and alkalies, bleaching liquors, aluminum, magnesium, and sodium; the electrolytic refining of copper and precious metals was greatly developed. In a short time many chemical methods were replaced by electrochemical processes, and these became the only methods used for the production of such substances as chlorine, peroxides, aluminum, magnesium, sodium, etc.

The growth of applied electrochemistry was aided by the considerable expansion at that time of the electric-power resources in the technically advanced countries, and by achievements in the field of electrical engineering.

The demand for various strategic products and materials during the First World War of 1914-1918 provided a new impetus for the further expansion of the electrochemical industries, both in magnitude and in the range of products.

The status of some of the most important chemical and metallurgical applications of the electrochemical industries in the 1920's in Europe and America may be characterized by the following data [3]. Nearly all chlorine compounds were by then being made by electrolysis of alkali chlorides, despite the fact that the method used most widely in Europe for the production of chlorine was a very imperfect electrolytic process, the Griesheim—Elektron process, with a stationary-electrolyte diaphragm cell. The mercury cell method, which originated in England in 1901, and the use of bell-jar type cells for electrolysis of alkali chlorides were used less extensively.

The use of new types of circulating-electrolyte diaphragm cells resulted in rapid technological improvements, especially in the U.S.A. The development of new techniques in chlorine production was accompanied by developments in the production of new high-quality varieties of graphitized anodes and new types of diaphragm materials. The total power of all the chlorine units in Europe reached 35,000-40,000 kw, and the output was over 600 tons of chlorine per day or 20,000 tons per annum. The production of chlorine in U.S.A. reached exceptional dimensions for those times. By the end of the 1914-1918 war the chlorine output of the U.S.A. exceeded that of all Europe, reaching 640-650 tons/day. It is true that in the postwar years the production of chlorine in the U.S.A. and Europe fell at first owing to difficulties in finding a market for it; however, numerous customers were soon found and the production of chlorine began to rise again.

At that time the production of potassium chlorate was an important branch of the electrochemical industry. Other electrochemical processes to be developed were for the production of permanganate, perborate, persulfates, and hydrogen peroxide. It is interesting to note that what is now one of the most important electrochemical processes — the electrolysis of water to give hydrogen and oxygen — was not developed industrially until the 1920's, as hydrogen was of almost no importance as an industrial raw material. Nevertheless, the first industrial units for the electrolytic production of hydrogen and oxygen appeared as long ago as the 1890's. The consumption of hydrogen was confined to very small amounts for soldering of lead, illumination, airships, and hydrogenation of fats. The hydrogen obtained as a byproduct in the electrolytic production of chlorine was sufficient for these requirements, and the units for electrolysis of water were few and of very low capacity.

Electrometallurgy, and especially the electrolytic refining of copper, developed greatly by 1920. The production fo electrolytic copper in 1918 exceeded 1,400,000 tons, 60% of which was produced in the U.S.A. The electrolytic refining of silver and gold, and the use of electrolysis for the recovery of tin from scrap tinplate, came into extensive use. No particular advances had been made in the field of electrolytic refining of nickel or zinc, and the production of zinc by electrolysis of sulfate solutions only began to increase during the 1914-1918 war. Of the 1,000,000 tons of zinc produced in 1923, about 150,000 tons or 15% was made electrochemically.

The production of light metals — sodium, magnesium, aluminum, and others — reached the industrial scale only as the result of the development and extensive application of electrochemical methods. Even now the electrolysis of fused salts is the principal method for the production of these metals and their alloys.

By the end of the First World War the annual production of sodium reached about 10,000 tons, of magnesium, about 2500-3000 tons, and of aluminum, over 150,000 tons. The main producers of these metals were Germany (sodium and magnesium) and U.S.A. (aluminum). Of the 150,000 tons of aluminum supplied in 1923, the U.S.A contribution was 63,000 tons [4]. It is noteworthy that while the total production of the chemical and metallurgical industries declined during the first years after the 1914-1918 war, the production of aluminum steadily increased.

The electrochemical industry of Russia was very weakly developed before the October revolution, and was largely in the hands of foreign capital.

Chlorine and its compounds were made in two Southern plants — in Slaviansk (the Griesheim—Elektron process), near Lisichansk (mercury process), and in one plant in Poland, in Zembkovice*(Griesheim—Elektron process). Although the capacity of the plants was almost doubled during the War, the first two plants produced only 22 tons of chlorine per day, or less than 2% of the total world production. The two plants built toward the end of the 1914-1918 war, near Samara and at Rubezhnaya(Donbas), produced 8 tons per day each [3]. During 1920-1922, large-scale production of potassium chlorate, with an annual output of 150 tons, with a proposed expansion to 600 tons per annum, was started with the participation of Engineer N. N. Voronin (later Professor in the Kiev Polytechnic Institute).

Before the war, copper was refined electrolytically in five plants: in Peterburg, in Moscow, in the Urals (the Kyshtymsky and Bogoslovsky Works), and in the Caucasus (Alaverdy Works), with a total production of about 20,000-23,000 tons of pure copper. During the Civil War the last two plants were severely damaged, while the first three continued to operate at a low level, particularly on the conversion of copper alloys.

There were also two units for the electrolytic refining of silver and gold, three low-output plants for the production of storage batteries (two in Peterburg), and several electroplating units.

Thus, prerevolutionary Russia occupied one of the last places in the world by the scale of its electrochemical industry; this corresponded to the low capacity of the Russian power plants, which reached 1,100,000 kw in 1913, and produced 1,900,000,000 kw-hrs per annum.

The most important step in the development of the Soviet electrochemical industry was the decision in 1920 to accept V. I. Lenin's proposal for adoption of the plan for electrification of Russia, the historic plan of GOELRO (State Commission for the Electrification of Russia).

The GOELRO plan provided for the utilization of a substantial proportion of the output of the new power plants for the needs of the chemical and metallurgical industries. As the GOELRO plan came into effect, it became possible to establish our own electrochemical industries in the USSR; their origin can be dated to the end of the first decade of the existence of Soviet Russia.

In the almost total absence of technical aid from the technically and economically developed capitalist countries, Soviet scientists and technologists were faced with the difficult task of the independent creation of a powerful electrochemical industry. As is known, this task was successfully accomplished. However, in addition to the problem of Soviet power supplies, the creation of the new electrochemical industry required a supply of our own electrochemists, scientists, engineers, and technologists. The successful and rapid solution of the personnel problem was greatly influenced by two factors — the new facilities, under a socialist government, for training personnel from the ranks of workers, peasants, and intellectuals and the earlier prerevolutionary activity of leading progressive Russian scientists.

The doors of the educational establishments were opened to the masses by a number of important measures taken by the USSR Government and the Communist Party in the field of education, and in particular of advanced technical training.

Special mention must be made of the role of the progressive Russian intellectuals in the creation of a socialist culture and economy. Despite the weakness of the electrochemical industry in Tsarist Russia, our leading scientists clearly understood how important for the economic development of our country was the creation of our own flourishing industry, including electrochemical production. This is shown clearly by the considerable number of important scientific investigations in the field of electrochemistry, carried out by Russian scientists at the end of the 19th and in the first two decades of the 20th century [5].

---

* Transliteration of Russian — Publisher's note.

This understanding is also shown by the considerable efforts made by scientists in the training of Russian electrochemists during those years. Two main large schools of electrochemistry arose in Russia during that period. The teaching of electrochemistry and training of specialist electrochemists began in 1898 in the Peterburg Electrotechnical Institute at the initiative of Professor A. A. Krakau, with the active participation of Prof. A. A. Pushin [6]. The first Russian textbook of electrochemistry was written there by Professor A. A. Krakau in 1902, and published in a lithographic edition. By the 1920's this school had trained several eminent electro-chemists, who later led the organization of Soviet electrochemical teaching and scientific activity. Among these were Professors I. V. Grebenshchikov, M. S. Maksimenko, P. F. Antipin, I. V. Shcherbakov, K. K. Khrenov, and others [7].

During this period many important scientific investigations were carried out in the Electrotechnical Insti-on the electrolytic production of copper, sodium, magnesium, aluminum, and a number of other substances. It is significant that nearly every issue of the Bulletin of the Electrotechnical Institute during that period contained papers on electrochemistry, while of the 8 papers in issue No. 4, 1910, 7 dealt with electrochemical questions; these included such important papers as "Calculation of the Economic Current Density in the Electrolytic Re-fining of Metals" by P. M. Avaev, and "Potentials and Nature of Metallic Alloys" by N. A. Pushin. The notable research on aluminum, carried out during 1909-1912 [8], also belongs to this group of investigations.

The other important electrochemical school arose in the Peterburg Polytechnic Institute where the train-ing of specialist electrochemists began in 1904 at the initiative and under the guidance of the eminent Russian electrochemist, Professor P. P. Fedotyev; Professor V. V. Kistiakovsky played an important role in the training of the electrochemists of this school. Numerous scientific investigations in the field of electrochemistry were also carried out during the period up to 1920 in the Peterburg Polytechnic Institute [9]. These included funda-mental researches on the theory and practice of the electrolytic production of aluminum, magnesium, zinc, chlorine, chlorine compounds, etc. [1, 10].

By the 1920's this school had trained specialist electrochmists who likewise played a leading role in the development of the Soviet electrochemical industry. They include Professors Yu. V. Baimakov, N. P. Fedotyev, V. V. Stender, N. N. Voronin, and others.

The efforts of the scientists of both schools of Russian electrochemists were directed at that time not only toward further scientific research and training of future specialists, but also toward solutions of problems of organization. Thus, in the early 1900's a Chemical Committee was established in conjunction with the Main Artillery Administration; among the tasks of this Committee was study of the aluminum question and establish-ment of a national aluminum industry.

This Committee directed and financed a number of geological surveys in search of aluminum ores, and a series of scientific investigations. Eminent scientists of the time, including the above-mentioned groups of electrochemists from the Peterburg Polytechnic and Electrotechnical Insitutes, participated in the work of the Committee.

The Society of Electrical Engineers and the Russian Physicochemical Society did much work in the field of scientific publicity for electrochemistry. Many of the papers presented to these societies during the early part of the 20th century give a vivid picture of the sincere patriotic feelings of progressive Russian scientists, and of their deep understanding of the necessity to create a national industry based on advanced electrochemi-cal and other techniques [11].

This can be illustrated by a quotation from a paper by P. M. Avaev [11] presented at a public meeting of the Society of Electrical Engineers in December 1914, devoted to the question of freeing the Russian electro-chemical industries from foreign imports and capital: "Russian scientists and technologists must abandon blind imitation of foreign methods of production of various substances, but must take into account the special charac-teristics of Russian raw materials ..." The paper concluded with the following words: "... independent politi-cal existence of the state is an empty sound while economic slavery exists."

At the start of the First World War a Military Chemical Committee was established in association with the Russian Physicochemical Society. With moral and financial support from the Chemical Committee of the Main Artillery Administration, the members of the Military Chemical Committee established an experimental plant on Vatnyi Island in Petrograd; the first task of this plant was to produce, on a pilot scale, the chemical products needed for defense purposes which were not produced in Russia. From 1916 until the revolution a group

of eminent chemists and electrochemists joined in the work of the experimental plant, and pilot-scale production of electrolytic magnesium and sodium, red phosphorus, and a number of other materials was organized [12].

The prolific activity of these scientists, and of a number of other workers in the field of electrochemistry (Professor N. A. Izgaryshev in Moscow, Professors A. E. Makovetsky and I. V. Shcherbakov in the Urals, etc.) prepared the ground for the rapid growth of applied electrochemistry during the fulfillment of the first five-year plan .

The period 1921-1923 saw the start of mass training of young specialist electrochemists in the Petrograd Polytechnic and Electrotechnical Institutes, the Mendeleev Institute and the Nonferrous Metals and Gold Institute in Moscow, the centers of higher education in the Ukraine, the Urals, etc.

These specialists formed the backbone and the driving force of research, planning, and experimental work on a broad front in applied electrochemistry, and in organization of the electrochemical industry of the USSR during fulfillment of the early five-year plans.

An important part in the training of personnel, theoretical understanding, and creation of an electrochemical industry in the USSR was played by the publication, during the first few years of Soviet rule, of a number of Russian textbooks on theoretical and technical electrochemistry, by Professors P. P. Fedotyev, V. V. Kistiakovsky, M. S. Maksimenko, I. V. Grebenshchikov, and N. A. Izgaryshev, the translation of a number of foreign works on electrochemistry (Allmand, Le Blanc, Grube, etc.), the publication of a number of monographs (Yu. V. Baimakov's Electrolysis of Copper, 1920), the same author's Electrolytic Deposition of Metals (1924), etc.

The successful fulfillment of the GOELRO plan and the general rapid growth of industry faced the Soviet Republic in the late 1920's with the urgent task of organizing high-power electrochemical and other industries.

The status and growth of the electrochemical industry abroad by 1930 can be illustrated by the power (in kw) of the stations serving the needs of electrochemistry, according to J. Billiter's data [13].

	1914	1930
Electrolysis of aqueous solutions		
Copper refining	45000	50000
Extraction of copper from ores	—	100000
Zinc production	1000	100000
Chlorine, hypochlorites, chlorates	250000	380000
Decomposition of water (production of		
hydrogen and oxygen)	10000	260000
Electrolysis of fused salts		
Aluminum	240000	600000
Sodium	20000	50000
Magnesium, calcium, etc.	5000	10000
Total	571000	1550000

The increases in the production of zinc, chlorine, and especially of aluminum and hydrogen, are noteworthy.

One of the first stages in the rapid growth of Soviet applied electrochemistry was the great increase in the volume of research and experimental work in the universities which were already in existence in the 1920's in the scientific research institutes, and in some leading industrial undertakings.

The work of the State Institute of Applied Chemistry (GIPKh, Leningrad) was of the foremost importance in the field of applications of electrochemical methods in the chemical industry. The activity of the scientists of this team began even in the years of the first imperialist war, when the first pilot-plant production of magnesium and sodium was organized in Russia at the experimental plant of the Military Chemical Committee, which subsequently became the GIPKh Pilot Plant.

However, it was only during the years of the First Five-Year Plan that GIPKh and its Pilot Plant really began important scientific and experimental work on the electrolytic production of chlorine and alkalies, the production of magnesium, sodium, and peroxide compounds (including persulfates, perchlorates, and manganese dioxide), on electroplating, the hydroelectrometallurgy of nickel, and the development of more efficient chemical sources of current.

During the same period, work in the field of diaphragm materials and graphitized electrodes was developed in GIPKh. The laboratory and pilot-plant work of GIPKh on the extraction of alumina from domestic raw materials was of the greatest importance fro the further development of the aluminum industry of the USSR, while its extensive research on the production of organic and inorganic chlorine compounds was significant in relation to the chlorine industry. It is not possible here to give even a brief description of all this research carried out in GIPKh and its Pilot Plant, or of the work of other teams of Soviet scientists and institutes named below. This information is contained in the collected transactions of the institutes; only partial bibliographies are as yet available in some jubilee publications and subject monographs. It must be noted, however, that by attracting all the eminent electrochemists of Leningrad and numerous young specialists GIPKh has laid the foundations of a mighty Soviet Industry for the production of chlorine and alkalies, chlorine compounds, aluminum, magnesium, higher oxy-compounds, and for many types of electroplating, electrometallurgy of aqueous solutions, and chemical sources of current [14].

The success of the research work of GIPKh was aided by the extensive participation of the State Planning Institutes (Giprokhim, for the chemical industry, Giprotsvetmet for the nonferrous metals industry, Giproaliuminii for the aluminum industry, etc.) and the staffs of a number of plants (the chlorine plants of the Donbas, the North Urals (UAZ), Volga, Volkhov, and Dnieper aluminum plants, etc.).

The creative cooperation of the workers of different undertakings on the foundation of a common mighty growth of Soviet industry and electrification ensured rapid development of the electrochemical industry of the USSR, unprecendented in the history of applied electrochemistry.

Highly significant contributions to the development of Soviet applied electrochemistry and electrometallurgy were made by the scientific research work of the Ural Chemical Scientific Research Institute (UNIKhIM) in Sverdlovsk, on magnesium and on compounds in higher states of oxidation; of the Ukrainian Institute of Applied Chemistry (UIPKh, Kharkov), on chlorine, alkalies, sodium and potassium and their peroxides; of the State Institute of Nonferrous Metals (GINTSVETMET) and the Northern State Institute of Nonferrous Metals (SEVGINTSVETMET), on electrometallurgy; and of the Karpov Institute (Moscow), on electrolysis of water and on compounds in higher states of oxidation.

A decisive role in the development of the Soviet aluminum and magnesium industries was played by the institutes established in the 1930's (VAMI—the All-Union Aluminum—Magnesium Institute, and Giproaluminii); by Gipronikel (the State Institute for Planning of the Nickel Industry) in the development of nickel and tin production, and by GIREDMET (State Rare Metals Scientific Research Institute) in the production of rare metals. The work of a number of newly established specialized institutes (the Nitrogen Institute, Giproazot — the State Institute for the Planning of Nitrogen Plants, GSPI-Z, the Storage Battery and Electric Cell Institutes, etc.) ensured the rapid growth of the production of hydrogen, oxygen, chlorine, and alkalies, and efficient production of chemical sources of current.

As the result of the successful fulfillment of the first three five-year plans, by the start of the Great Patriotic War the USSR had mighty reserves of electric power. The GOELRO plan of 1921 provided for an increase of the power of the power stations from 1,000,000 kw in 1913 to 2,500,000 kw during a period of 10 years.

In fact, by October 1, 1931, the power capacity of all the power stations of the USSR was already 3,500,000 kw. By the beginning of 1941 it had increased 11-fold in comparison with 1913, and the output of energy increased 25-fold, thus satisfying the basic requirement for the growth of a mighty electrochemical industry. In regions where electric power is cheap and the necessary raw materials were available, numerous industrial combines were established, with electrochemical and electrometallurgical plants for the production of aluminum, magnesium, zinc, nickel, hydrogen, and peroxide compounds. Among these were the Volkhov aluminum plant (started in 1932), a group of industries associated with the Dnieper Hydroelectric Power Plant in Zaprozhye,

the Zerezniki and Solikamsk plants in the Northern Urals, the Chirchik Electrochemical Combine in the Uzbek SSR, and electrochemical plants in the Gorky province, in the Central Volga region, and in the Central Urals. The older electrochemical plants (for chlorine production, copper refining, and production of cells and storage batteries) in the Donbas, Urals, Moscow, and Leningrad regions were considerably expanded.

It must be pointed out that the Soviet applied electrochemistry developed largely by independent means, without any substantial technical aid from abroad. Naturally, use was made of published foreign information, but this generally reflected the state of electrochemistry at stages which had already been passed, and required an attentive and critical approach.

The development of the most important electrochemical industries of the USSR reached a very low level by the start of the Second World War, in comparison with the prerevolutionary era [1, 2]. Several new plants for the electrochemical production of chlorine and alkalies had been built. Many foreign cell designs had been tested, the techniques of the production of asbestos diaphragms (board and sheet) and high-quality graphitized anodes had been developed, and manufacture of these was organized.

A rational and original cell design for electrolysis of sodium and potassium chloride solutions was developed.

The electrolysis of water was developed on the industrial scale following the production of powerful and compact units of low energy consumption. An original cell of the filter-press type of electrolysis of water under pressure was designed.

The production was organized, although in modest quantities, of electrolytic manganese dioxide by the GIPKh original method [14] of persulfates, and of hydrogen peroxide.

The production of metallic potassium and sodium was started; an original powerful cell for the electrolysis of fused alkali was designed, considerably superior in performance to the equipment described in the literature.

The greatest achievement of Soviet electrochemistry during this period was the creation of our own aluminum and magnesium industries in plants which were superior by the level of their technology and the scale of production to many foreign plants of that time.

In the field of hydroelectrometallurgy, two powerful plants were established for the production of electrolytic zinc from the zinc ores of the Urals and Northern Caucasus. The production of electrolytic nickel was established anew, with extraction of cobalt compounds and metals of the platinum group as byproducts The production of electrolytic copper was expanded considerably when the biggest electrolytic copper plant in the world was started in the Urals in 1934. The electrolytic refining of lead and the production of metallic manganese by electrolysis of aqueous manganese sulfate solutions were also organized.

Large electroplating sections, with mechanization and automation of many operations, were established in numerous old and new plants in which metal-finishing operations were performed.

The scale and technical level of production of lead storage cells and primary cells were raised. New and improved types of cells and dry batteries were produced. Soviet designs of alkaline storage cells were developed, and their industrial production was organized.

The war of 1941-1945 and the temporary occupation of a considerable part of the European USSR stopped the work of many large electrochemical undertakings. For example, the first plants of the Soviet aluminum industry — the Volkhov and Dnieper plants, the Dnieper magnesium plant, a group of chlorine plants in the Donbas, and the only existing units for the production of metallic sodium and potassium, were all destroyed or dismantled. The electrochemical plants of Leningrad, and partly of Moscow, stopped normal production.

However, from the very first months of the War, at the call and under the guidance of the Communist Party, the Soviet people began the most extensive increase of the productive capacity of the undertakings in the unoccupied part of the USSR, and rapid construction of new plants.

The whole previous history of the development of Soviet electrochemistry, in conjunction with the mighty potentialities of the Socialist State assured by the fulfillment and overfulfillment of the preceding five-year plans for the development of the national economy and culture, played a significant role in this

creative work. The existence of powerful specialized scientific research institutes, and the numerous ranks of specialists nurtured in the spirit of patriotism and love of their country, made it possible within the first six months of the War to replace the loss of productive capacity of the occupied territories in a number of industries, and even to increase production in some cases. During the war years the production of aluminum in the Urals Aluminum Plant was increased, new plants (Bogoslovsky, Stalin and others) were started, the production of magnesium at the Solikamsk plant was increased, and a new plant was built in Berezniki. The production of metallic sodium near Moscow, in Berezniki, and in Chirchik was organized very quickly on a scale above the prewar level. A new unit was organized for the production, by an original process, of lead—sodium— potassium alloy used for making tetraethyllead. The capacities of plants for chlorine production and electrolysis of water were considerably increased. Two units were set up, in Berezniki and near Moscow, for production of electrolytic manganese dioxide and hopcalite, and a high-purity electrolytic manganese unit was started in the Caucasus. The output of electrolytic copper, zinc, and lead increased considerably, especially in Kazakhstan. The work of the scientific and planning organizations on the further development of Soviet applied electrochemistry was not stopped.

However, the difficult war situation and the losses suffered during the 1941-1945 war could not fail to influence the rate of development of the USSR industry in general and of the electrochemical industry in particular. The scale and technical level of production of some products decreased somewhat [15]. However, the vigorous activity of the Soviet people during the war years prepared the ground for new and even more fruitful development of industry during the postwar years. As is known, the industrial production of USSR increased 4-fold in 1956 relative to the 1940 level. The output of electrical energy rose from 1,900,000,000 kw-hr in 1913 to 192,000,000,000-kw-hr in 1956, which is a 100-fold increase [15]. The electrochemical section of industry also developed at a high rate. For example, the production of caustic soda, which was 55,100 tons in 1913 and 190,400 tons in 1940, rose to 563,000 tons in 1955 [15].

The Fourth Five-Year Plan for the period 1946-1950 provided for a 2-fold increase of aluminum production, and 2.7-fold, 2.5-fold, and 1.6-fold increases in the production of magnesium, zinc, and copper. The Fifth Five-Year Plan provided for further increases by 1955, as compared with 1950, of 90% in the production of refined copper, 2.7-fold, 2.6-fold, and 2.5-fold increases in the production of lead, aluminum, and zinc respectively, and 53% increase in the production of nickel. Special attention was devoted to the development of advanced production methods, including electrolysis.

Thus, the postwar years marked the most fruitful stage in the growth of Soviet electrochemical industry. It is not possible to give in a single article even a partial account of the achievements of this period. We can only indicate the principle trends in the development of applied electrochemistry.

During the past decade the electrochemical industry developed not only by growth of its productive capacity and the creation of new undertakings, but also by adoption of more advanced methods. The struggle to increase the output of individual electrochemical units, to raise labor productivity, to introduce automation and process control, to ensure more complete and varied utilization of raw materials, and to improve the industrial health conditions and safety techniques, is characteristic of the progress of applied electrochemistry during the period under review.

As an illustration of this progress, let us consider the production of aluminum, which is one of the greatest energy consumers among the electrochemical industries. About 35% of the electrical energy used for electrochemical processes is used by the aluminum industry. As is known, the production of aluminum is a very complex technological process. In addition to the actual extraction of aluminum, the process involves the production of pure aluminum oxides, fluorides, and carbon electrodes. Plant production of aluminum in the USSR began 25 years ago, when the first Soviet aluminum plant, the Volkhov plant, now named after S. M. Kirov, started production on May 14, 1932. A combine was built near the Tikhvin bauxite deposits; the technology of the process was largely developed by Russian and Soviet scientists and technologists and the power was supplied from one of the pioneer units in the electrification of the USSR — the Volkhov hydroelectric power plant. Only the electrolytic section, in the early stages, used French equipment and technical aid kindly supplied by French firms. This equipment consisted of 23,000 amp -cells with 14-16 baked carbon electrodes, the metal being produced by the "pot" method. With a cell voltage of 4.5-5 v and a current efficiency of 80-85%, one ton of aluminum requires about 20,000 kw-hr from a direct-current supply.

Similar cells were installed in the second Soviet aluminum plant on the Dnieper (DAZ), at that time the largest aluminum plant in Europe, which started operation in June 1933. However, in a short time Soviet engineers introduced many improvements into the electrochemical equipment, increased the cell amperage by a factor of 1.5, lowered production costs, and improved the industrial health conditions. The production of carbon anodes, lining blocks, and of alumina by the original process devised by the Soviet scientists Professors A. N. Kuznetsov and E. I. Zhukovsky, was also organized at DAZ.

It is not possible to describe all the technological processes involved in the production of aluminum; we shall merely note that during the 40 years the USSR has been in existence the raw material resources of the aluminum industry have been greatly expanded. With the discovery of sources of bauxite in the Urals, Siberia, and other localities, and with the development of new economic and ingenious methods for the processing of bauxite and other forms of aluminum ores, the sources of alumina in the USSR have become virtually inexhaustible [16, 17].

Let us consider the technical progress of the electrochemical part of the process for aluminum production, during the 25 years since the Volkhov plant was started. The control of multianode cells, even with their increased capacity, is a very laborious task, which moreover requires the organization of separate production of baked carbon anodes, also a very laborious and costly operation. The tonnage of this auxiliary production is at least half of the tonnage of the electrolytic aluminum produced. By the successful efforts of Soviet technologists it was possible by the start of the 1941-1945 War to switch to the use of improved single-anode cells with continuous self-baking anodes; among the plants to adopt these was the new large Urals plant. Apart from the fact that the production of baked anodes became unnecessary, it became possible to increase the load on the individual units to 50,000-100,000 amps and over, to introduce mechanization and automation in many of the operations, to lower costs and to improve the hygienic conditions. All these means toward technical progress were widely utilized by the Soviet aluminum industry during the postwar years.

As a result, on its 40th anniversary the Soviet Union has the most advanced aluminum industry in the world, both in technical equipment and in productivity. Naturally, not all the potentialities have been exhausted, and the workers of the aluminum industry, from the scientists and engineers to the foremen and workmen, continue along the glorious path of technical progress of the aluminum industry of the USSR.

The technical progress in other electrochemical industries during the postwar years has followed a similar course. The most important factor in the economics of many electrochemical processes is the specific consumption of electrical energy. The tendency is to increase the output of individual cells by increase of current load and sometimes of electrode current density; this is accompanied by a tendency to lower the energy consumption. Therefore the main ways of improving the techniques and equipment of the electrochemical industries have involved decreases of the cell voltages [18] and increases of current efficiency. In the new cell designs for the electrolysis of water, production of chlorine, alkalies, oxidizing agents, and other chemical products and metals much attention was devoted to improvements of electrode shape and materials, decreases of the interelectrode distances, decrease of gas saturation, improvements of electrode contacts, choice of suitable electrolytes, and other conditions of electrolysis. A high degree of mechanization in operations which are very laborious or demand a high degree of precision has been achieved in the production of chemical sources of current such as cells and storage batteries. The same applies to electroplating, which is extensively used in all branches of the Soviet industry for treatment and finishing of metallic machine, equipment, and instrument parts. Semiautomatic and automatic machines and whole production lines are usual in our factories. Considerable extensions have been made to the range of metals and alloys used for galvanic coatings, and of other methods for electrochemical treatment of metals (anodizing, electropolishing, anodic mechanical spark treatment). The technical potentialities of galvanic processes have been much improved and extended by the use of pulsating and reversible current.

It must be noted that in recent years applied electrochemistry has been making use of improved and more efficient direct-current sources — mercury-type and other rectifiers, instead of rotary motor-generators. Soviet electrical engineers have greatly influenced the successful course of electrochemistry and electrometallurgy in this respect.

In conclusion, reference must be made to the changes which have taken place in the geographical distribution of the electrochemical industry of the USSR. Whereas in 1955 the industrial output of the country as a whole was 3.2 times the 1940 level, the corresponding increases were 5.2 times in the Volga and Urals regions, 5.6 in Western Siberia, 3.4 in Eastern Siberia, and 4.2 in the Kazakh SSR [15].

The electrochemical industry of the USSR followed a similar course in its growth; an illustration of this is the development of the electrochemical industry in Kazakhstan [17]. During the period of the Sixth Five-Year Plan new electrochemical undertakings will be built mainly in eastern regions. For example, new large aluminum plants will be built in the Irkutsk province, in the Krasnoyar region, in the Kuznetsk Basin, and in Pavlodar; the raw materials will be Uzhur nephelines from the Minusinsk depression and Turgai bauxites from the Kustanai province of Kazakhstan [19].

During the 40 years of existence of the USSR a mighty electrochemical industry has been created, satisfying the demands of all branches of the Soviet economy. However, the great advance of modem technology cannot be content with the existing state of electrochemistry. The directives of the Sixth Five-Year Plan for the development of the national economy of the USSR indicate the main directions in which applied electrochemistry is to develop. For example, the directives provide for the following increases in 1960 as compared with 1955: 60% in the output of refined copper, 2.1-fold in the production of aluminum, 42% in the production of lead, 64% in the production of nickel, 2.1-fold in the production of commercial manganese, and 77% in the production of zinc. Considerable increases in the production of titanium and rare metals such as germanium, niobium, zirconium, etc. are planned. It is proposed to increase the output of nonferrous and rare metals of a high degree of purity, to be used for further development of electronics, radio engineering, and the production of heat-resisting alloys; to increase the extraction of metals, and to organize multiple processes for treatment of raw materials. Applied electrochemistry has a large share in the solution of these problems. Soviet electrochemists have also achieved much success in the development of new electrochemical processes — the extraction of rare metals, organic chemicals, new highly effective oxidizing agents, etc. However, these processes are yet to be widely adopted by industry.

It must be pointed out in this context that, together with the solution of purely electrochemical problems, Soviet science also has the important task of developing auxiliary materials such as special electrodes and diaphragms, ceramics, and plastics for electrochemical equipment, without which further technical progress of Soviet applied electrochemistry is unthinkable.

The actual achievements of the Soviet people during 40 years of work under the guidance of the Communist Party of the USSR have far exceeded the dreams of the best representatives of Soviet sciences who wished their country success.

LITERATURE CITED

[1] N. P. Fedotiev, J. Appl. Chem. 22, 10, 1045 (1949).

[2] V. G. Khomyakov, V. P. Mashovets and L. L. Kuzmin, Technology of Electrochemical Processes (Goskhimizdat, 1949).*

[3] P. P. Fedotiev, The Heavy Mineral, Chemical, and Electrochemical Industries During the Past Decade (Sci. Chem.-Tech. Press, Leningrad, 1925).*

[4] P. P. Fedotiev, Essays in Chemical Technology (Leningrad, 1930).*

[5] Bull. Peterburg Electrotech. Inst. (1890-1920); Bull. Peterburg Polytech. Inst. (1904-1920).

[6] Bull. Electrotech. Inst. 2 (1904).

[7] Symposium, 50 Years of the Leningrad Electrotechnical Institute (Gosenergoizdat, 1948).*

[8] N. A. Pushin and M. A. Baskov, Bull. Electrotech. Inst. 7 (1912).

[9] Trans. Leningrad Polytech. Inst. 1 (1948).

[10] P. P. Fedotiev, Collected Research Papers (Chem. Theoret. Press, 1936).*

[11] P. M. Avaev, Bull. Electrotech. Inst. 12, 175 (1915).

[12] The Pilot Plant of the Institute of Applied Chemistry, 1916-1926 (1927).*

[13] J. Billiter, Die neueren Fortschritte der Technischen Elektrolyse. Halle (1930).

[14] Jubilee Collections of the State Institute of Applied Chemistry [20th Anniversary (1940) and 25th Anniversary (1944)].*

* In Russian.

[15] Central Statistical Administration USSR. The Industry of the USSR (State Statistical Press, Moscow 1957). *

[16] I. L. Talmud, Science and Life 4 (1957).

[17] V. V. Stender, Bull. Acad. Sci. Kazakh SSR 11, 3-7 (1956).

[18] V. G. Khomyakov and M. Ya. Fioshin, J. Chem. Ind. 1, 30 (1957).

[19] V. F. Vasyutin, All-Union Society for the Propagation of Political and Scientific Knowledge, Series 2, 43 (Knowledge Press, 1956).*

---
*In Russian.

OXIDATION OF AMMONIUM SULFITE—BISULFITE SOLUTIONS

B. A. Chertkov

Scientific Research Insitute for Industrial and Sanitary Purification of Gases (NIIOGAZ)

The removal of sulfur dioxide from waste gases, such as the waste gases from nonferrous metallurgical processes, or flue gases from power plants burning sulfurous coal, is accompanied by a parallel process of partial oxidation of the sulfur dioxide. The oxidation takes place in the liquid phase by the reaction of sulfurous acid or its salts with the oxygen which is always present in these gases.

In the ammonia continuous process for the removal of SO_2 from flue gases and its recovery as the 100% gas [1], where the absorbent is ammonium sulfite—bisulfite solution, ammonium sulfate is formed as a by-product as the result of oxidation. About 0.1% by weight of technical p-phenylenediamine is added to the absorbent, to serve as an inhibitor of oxidation.

Preliminary laboratory [2,3] and pilot-plant [4] investigations with the use of pure gases and solutions showed that this inhibitor is very effective, decreasing oxidation severalfold. However, in the initial stages of operation of the first industrial unit for the removal of SO_2 from flue gases, p-phenylenediamine did not produce the expected effect, and the liquor was oxidized fairly rapidly [1] — about 20% of hth absorbed SO_2 was converted into ammonium sulfate. This was attributed to the influence of impurities present in the flue gas — solid particles of ash, soot, and products of incomplete combustion including hydrogen sulfide.

At the same time, the course of the oxidation process is determined to a considerable extent by the composition of the absorbent solution; the variations of this composition are intensified with increasing rate of oxidation.

Our purpose was to obtain the necessary data on the role and significance of individual factors in the oxi- of ammonium sulfite—bisulfite, and in particular, data on the role of the composition of the solution, which are of the greatest interest from the practical aspect. *

Many investigators have studied the oxidation of sulfites. There cannot be many reactions which have aroused as much interest and stimulated so much research* * as this apparently simple reaction, represented by the over-all equation

$$O_2 + 2SO_3^{2-} \rightarrow 2SO_4^{2-}, \tag{a}$$
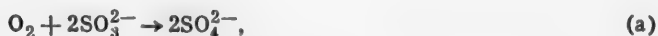
The object of most of the researches was to elucidate the mechanism of the intermediate reactions in the oxidation process, or the mechanism of action of positive and negative catalysts, and the experiments were carried out with very dilute solutions under specific laboratory conditions. The results of these investigations are difficult to reproduce, they are often contradictory, and therefore cannot be used for elucidation of the oxidation kinetics of the highly concentrated solutions used in practice.

---

* The experimental work was carried out by D. L. Pukilna, T. I. Pekareva, and T. T. Spiridonova.

* * Recent literature reviews on this subject are given in a paper by Abel [5], who postulated a new mechanism for the oxidation of sulfites, and in Rozenknop's book [6].

A static method was used in the present work; samples of solution in open vessels, merely protected from access of accidental solid impurities, were oxidized by the oxygen of the surrounding air. The partial pressure of oxygen was therefore constant, while the composition of the solution gradually changed during oxidation; this was recorded by periodic analyses of the liquid phase. In the static method the area of phase contact remains strictly constant, equal to the open surface of the vessel, and diffusion of the oxidation products from this surface into the depth of the liquid, and the countercurrent diffusion of fresh molecules toward the boundary layer, occur freely, without external interference.*

By variations of the ratio of the contact area F and the sample volume $\underline{v}$ it was possible to obtain quicker or slower variations of the composition of the solution in the samples, according to the problem in question.

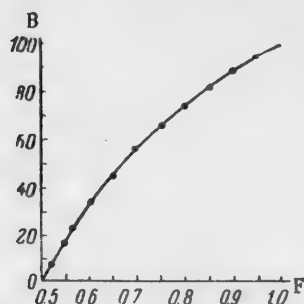The composition of the absorbent solution is represented in terms of the following notation: S is the SO_2 content of the ammonium sulfite and bisulfite (in moles/liter); C is the NH_3 content of the ammonium sulfite and bisulfite (in moles/liter); A is the NH_3 content in ammonium sulfite (in moles/liter); NH_{3total} is the total NH_3 present in solution as ammonium sulfite, bisulfite, sulfate, thiosulfate, and trithionate (in moles/liter); in absence of thiosulfate and trithionate NH_{3total} = A + C; G_{O_2} is the rate of oxygen absorption, equivalent to the formation rate of ammonium sulfate (in $g/m^2 \cdot hour$); S/C is a quantity which represents the ratio of the amounts of sulfite and bisulfite in the solution. In the limiting cases, if the solution contains sulfite only, S/C = 0.5, and if it contains bisulfite only, S/C = 1.

Fig. 1. The S/C ratio as a function of ammonium bisulfite content in solution. B) Bisulfite content (molar %), F) S/C ratio.

It can be shown that in this notation the molar content of ammonium bisulfite is 2S − C, and the molar content of ammonium sulfite is C − S. Hence the percentage content of ammonium bisulfite in the solution is $\dfrac{(2S - C)\,100}{S}$ or $\left(2 - \dfrac{1}{S/C}\right)100$. The relationship between the percentage of bisulfite in solution and the S/C ratio is plotted in Fig. 1.

The solutions were analyzed by the standard method developed in NIIOGAZ by S. M. Goliand and A. E. Strakhova for the ammonia continuous process for recovery of SO_2 from flue gases.

EXPERIMENTAL METHODS

Curves for the oxidation kinetics of pure sulfite−bisulfite solution, containing no other substances, with total ammonia concentration NH_{3total} = 8.42 moles/liter and initial S/C ratio = 0.8,** in contact with air at room temperature, are given in Fig. 2.

It follows from Fig. 2 that the concentration of ammonium sulfate increases continuously (Curve A), with corresponding decreases of the ammonium sulfite and bisulfite concentrations (Curve C). However, the average rate of formation of ammonium sulfate, and correspondingly G_{O_2}, the average rate of oxygen absorption, differs over the different periods into which the whole course of oxidation of the given sample is subdivided. The solution is oxidized slowly at first, with a simultaneous increase of the S/C ratio. The oxidation rate then increases, passes through a maximum (the S/C ratio reaches a maximum simultaneously), and decreases again.

*In dynamic methods the results of oxidation are influenced by the nature and magnitude of the area of contact between the air and solution ; these factors generally do not remain constant with variation of the solution composition and other experimental conditions. This accounts for the fact that various workers who used dynamic methods obtained results which were contradictory and difficult to reproduce.
** This is close to the composition of the regenerated liquor used in the last absorption stage of the ammonia continuous process for the recovery of SO_2 from flue gases.

The oxidation of sulfite and bisulfite is accompanied by spontaneous decomposition of the solution, with appearance of ammonium trithionate and thiosulfate. However, these reactions develop very slowly, and the thiosulfate and trithionate contents increase at a negligible rate.
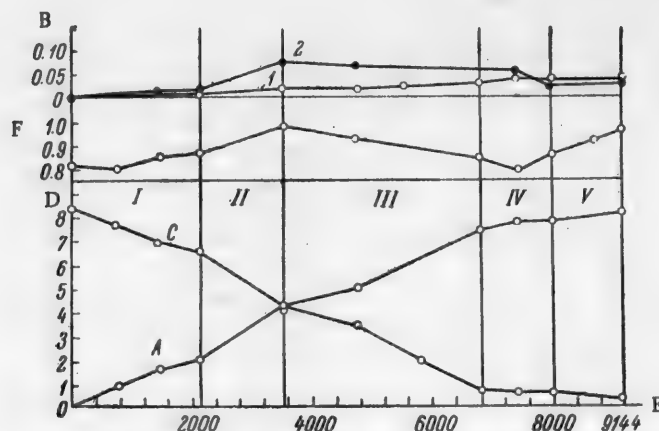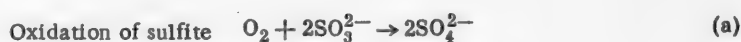

Fig. 2. Course of oxidation and variations in the composition of the solution in contact with air.
NH_{3total} = 8.4 moles/liter, S/C (initial) = 0.8, temperature 20-22°.
B) Contents of $(NH_4)_2S_2O_3$ (Curve 1) and $(NH_4)_2S_3O_6$ (Curve 2) (in moles/liter); D) concentrations of ammonium sulfate (A) and ammonum sulfite and bisulfite (C) (in moles/liter); E) time (hours); F) S/C ratio. Rate of oxygen absorption G_{O_2} (in g/m²·hour) at various periods: I) 0.68; II) 1.20; III) 0.73; IV) 0.36; V) 0.12.

The variations of the S/C ratio during the oxidation, and the formation of thiosulfate and trithionate in the solution, can be explained as follows.

When a mixture of sulfite and bisulfite is oxidized, the final result is represented by the same equation, irrespective of which of these salts reacts with oxygen:

Oxidation of sulfite $\qquad O_2 + 2SO_3^{2-} \rightarrow 2SO_4^{2-}$ (a)

Oxidation of bisulfite $\qquad O_2 + 2HSO_3^{-} \rightarrow 2HSO_4^{-}$ (b)

$$\frac{2HSO_4^{-} + 2SO_3^{2-} \rightarrow 2HSO_3^{-} + 2SO_4^{2-}}{O_2 + 2SO_3^{2-} \rightarrow 2SO_4^{2-}}$$

(c)

(a)

This is because bisulfate, which is a much stronger acid than bisulfite,* reacts according to Equation (c) with an equivalent amount of sulfite, converting it into bisulfite. Thus the bisulfite content remains constant during the oxidation, and only the sulfite content decreases, giving the false impression that sulfite undergoes perferential oxidation. Decrease of the sulfite concentration naturally results in an increase of the S/C ratio. On the other hand, contact of the sulfite—bisulfite solution with air results in a continuous decrease of the S/C ratio owing to desorption of SO_2, in view of the existence of a definite partial pressure of SO_2 vapor, P_{SO_2}, over these solutions.

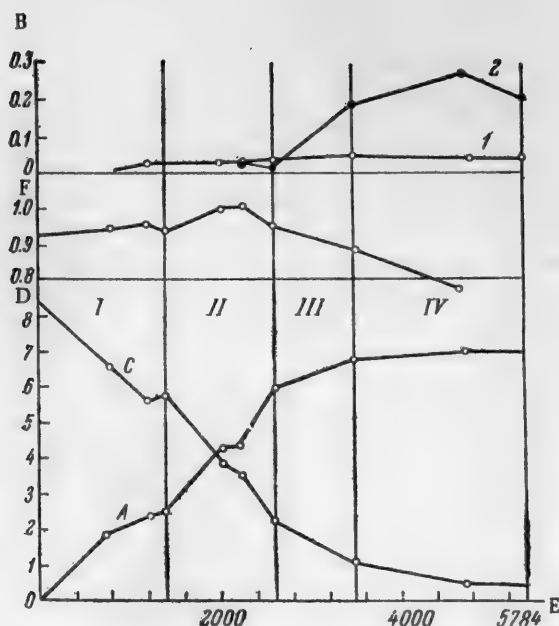---

* $K_{HSO_4^-}$ = 1.2·10⁻²; $K_{HSO_3^-}$ = 6.4·10⁻⁸.

Fig. 3. Course of oxidation and variations in the composition of the solution in contact with air.
$NH_{3 total} = 8.2$ moles/liter, $S/C = 0.92$, temperature 20-22°.
Designations as in Fig. 2. Rate of oxygen absorption G_{O_2} (in $g/m^2 \cdot hour$) at various periods: I) 1.30, II) 2.17, III) 0.43, IV) 0.04.

The over-all variation of the S/C ratio as the result of oxidation and desorption of SO_2 may be either positive or negative, depending on which of these processes is predominant.*

Ammonium trithionate and thiosulfate appear in the solution because bisulfite solutions have a tendency to spontaneous decomposition owing to their thermodynamic instability. The initial stage of the spontaneous decomposition, according to Foerster [7], occurs according to the equation:

$$4HSO_3^- \rightarrow SO_4^{2-} + S_3O_6^{2-} + 2H_2O; \qquad (d)$$

the trithionate formed then undergoes hydrolysis and is converted into thiosulfate:

$$S_3O_6^{2-} + H_2O \rightarrow SO_4^{2-} + S_2O_3^{2-} + 2H^+. \qquad (e)$$

Under normal conditions these reactions are extremely slow. They are accelerated with increase of the S/C ratio, with increase of temperature, and on addition of certain catalysts to the solution.

Figure 3 shows the course of oxidation of a solution which differed from the preceding one only in that its initial S/C ratio was 0.92** and not 0.8. In this case the oxidation proceeded at a higher rate than in the previous instance right from the start; this is undoubtedly due to the higher initial S/C ratio. Here again the

* The S/C ratio can also vary owing to the existence of a partial pressure of NH_3 over the ammonium sulfite—bisulfite solution, and to the formation of trithionate from bisulfite (the reaction is given below). In the former case C decreases, in the latter, S decreases. However, because of the extremely low partial pressure of NH_3 over the solutions generally used, and the slow rate of the spontaneous-decomposition reaction, these factors have almost no influence on the S/C ratio during oxidation, and they may be neglected without serious error.
** Close to the composition of the saturated solution formed in the ammonia continuous process for recovery of SO_2 from flue gases.

oxidation rate reaches a maximum, which coincides with the maximum value of the S/C ratio; it is noteworthy that there is a short region of almost complete inhibition of oxidation during the period when the S/C ratio became a little greater than 1*.

There is no doubt that the progressive increase of the thiosulfate and trithionate contents also influences the oxidation rate of the solution. For a clearer idea of the extent of this influence, and experiment was carried out on the oxidation of a solution to which 0.25 mole/liter of sodium thiosulfate** had been added at once (Fig. 4).

It is clear from Fig. 4. that here the situation is totally different. When a large quantity of sodium thiosulfate was added at once, the oxidation rate increased rapidly, with a corresponding increase of the S/C ratio. The average rate of oxygen absorption in the initial period was several times as high as in the experiments without addition of thiosulfate. In this instance there was again a maximum point, beyond which the rate of oxygen absorption began to decrease, evidently because of the decrease in the sulfite—bisulfite concentration.
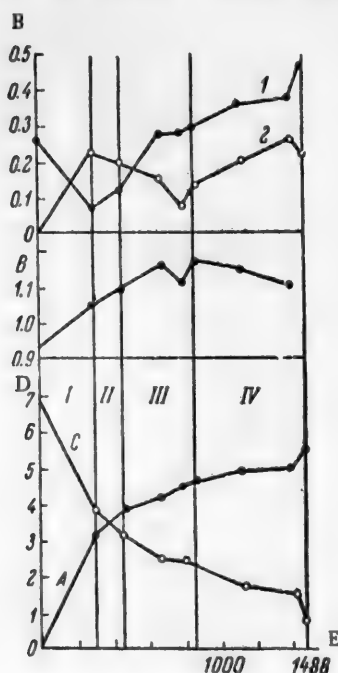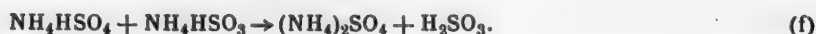

Fig. 4. Course of oxidation and variations in the composition of the solution in contact with air, with addition of 0.25 mole of sodium thiosulfate per liter.
NH_{stotal} = 7.10 moles/liter, S/C = 0.93, temperature 20-22°. Rate of oxygen absorption G_{O_2} (in $g/m^2 \cdot hour$) ar various periods: I) 7.90; II) 4.03; III) 1.46; IV) 1.33. Remaining designations as in Fig. 2.

It also follows from Fig. 4 that there is continuous interaction between thiosulfate and trithionate. On the one hand, in presence of bisulfite the thiosulfate is oxidized to trithionate (Fig. 4). This reaction probably proceeds according to the equation:

$$2NH_4HSO_3 + (NH_4)_2S_2O_3 + O_2 \rightarrow$$
$$\rightarrow (NH_4)_2S_3O_6 + (NH_4)_2SO_4 + H_2O. \tag{g}$$

At the same time trithionate is continuously converted into thiosulfate by hydrolysis, according to Equation (e).

In our opinion, this interconversion is the basis of the catalytic action of thiosulfate in the oxidation of sulfite—bisulfite by oxygen.

This action is intensified on increase of the thiosulfate and trithionate concentrations in the solution, as is clear from Fig. 4; despite the fact that the S/C ratio was considerably in excess of 1, the oxidation was very rapid. In contrast to this, at low thiosulfate concentration increase of the S/C ratio above 1 resulted in a sharp decrease of the oxidation rate (Fig. 3).

The decrease in the oxidation rate for solutions in which the S/C ratio is greater than 1, i.e., which contain some free sulfurous acid in excess of the bisulfite, is probably the consequence of the sharp decrease of the pH of such solutions.***

Figure 5 shows the course of oxidation of a solution in which the S/C ratio was maintained for a long time above 1 by addition of 100% SO_2. It is seen that in the early stages, when the concentrations of the thiosulfate and trithionate are still low and their catalytic action is not fully manifested, the oxidation of the
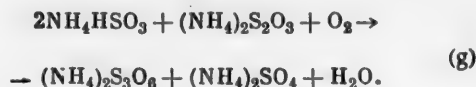
* In addition to bisulfite, free sulfurous acid was formed by the reaction

$$NH_4HSO_4 + NH_4HSO_3 \rightarrow (NH_4)_2SO_4 + H_2SO_3. \tag{f}$$

** This is an average value for the concentration of sodium thiosulfate in the liquor used in the ammonia continuous process for recovery of SO_2 from flue gases.
*** The pH value of ammonium bisulfite is 4.5. The pH of sulfurous acid is 2. The cessation or great retardation of the oxidation of sulfite solutions on addition of acids has been observed by numerous workers (for example, Basset and Parker [8]).

solution is very slow; this confirms the above-mentioned influence of free sulfurous acid in suppressing the oxidation of bisulfite when the two are present simultaneously in solution.

In the sulfite—bisulfite system, when the S/C ratio is below 1, increase of this ratio produces, on the contrary, an increase of the oxidation rate of the solution, as was already noted earlier.
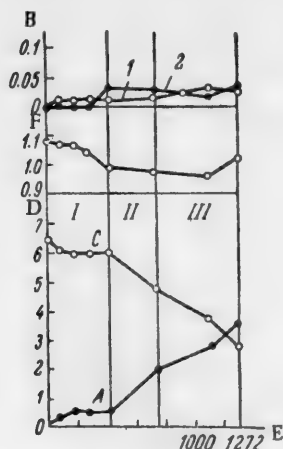
Fig. 5. Course of oxidation and variations in the composition of the solution in contact with air. NH_{3total} = 6.6 moles/liter, S/C = 1.08, temperature 20-22°. Rate of oxygen absorption G_{O_2} (in g/m^2·hour) at various periods: I) 0.63; II) 3.92; III) 3.70. Remaining designations as in Fig. 2.

The nature of the variation of G_{O_2} with the S/C ratio in the 0.75-1 range of the latter, which is the range of practical significance, is illustrated in Fig. 6. It is seen that the relationship between G_{O_2} and the S/C ratio is complex, and cannot be represented as a definite function without regard for the varying concentration of ammonium sulfite—bisulfite.* However, for values of C between 7.5 and 3.0 moles/liter, at constant NH_{3total}, which was 8.0 moles/liter in this instance, the results may be smoothed to give Curve 1 in Fig. 6.

The relationship between G_{O_2} and S/C according to this curve may be represented by the equation:

$$\log G_{O_2} = 6\log S/C + 0.325. \qquad (1)$$

Further decrease of C (below 3.0 moles/liter) at the same NH_{3total} produces a sharp decrease in the oxygen absorption rate, as is shown by Curve 2 in Fig. 6. The relationship between G_{O_2} and S/C according to Curve 2 corresponds to the equation

$$\log G_{O_2} = 6\log S/C + 0.118. \qquad (2)$$

Despite a certain difference between the curves in Fig. 6, they both show convincingly that the oxidation rate of the solution increases continuously with increase of the relative content of bisulfite from 63% (S/C = 0.73) to 100% (S/C = 1). This shows that ammonium bisulfite is oxidized considerably more rapidly than ammonium sulfite. It is interesting to compare this result with the results obtained by others. It is stated in Gmelins Handbuch [9] that aqueous solutions of ammonium bisulfite are oxidized less rapidly in air than sulfite solutions, but more rapidly than sulfurous acid solutions. The concentrations of the solutions are not given.

Teres and Heinsen [10] found that in dilute solutions ammonium sulfite and bisulfite are oxidized very similarly. As in our experiments, they found that in concentrated solutions bisulfite was oxidized much more rapidly than sulfite.

Wartman [11], on the contrary, concluded that ammonium bisulfite is oxidized much more slowly than sulfite (in dilute solutions, on addition of a sample of the original solution to water previously saturated with oxygen), and considered that the determining factor in the oxidation of sulfite is the rate of solution of oxygen, and in the oxidation of bisulfite, the rate of reaction between the dissolved oxygen and the salt.

Fuller and Crist [12], who used very dilute solutions of sodium sulfite, found that the degree of oxidation decreased with increasing bisulfite content, and the oxidation was almost zero in presence of pure bisulfite. They could only explain their results on the assumption that the oxidation rate is determined by the concentration of sulfite ions SO_3^{2-} and hydrogen ions H^+, and is independent of the concentration of bisulfite ions HSO_3^-.

Abel [5] interpreted Fuller and Crist's results differently, and showed that only the bisulfite ions and not the sulfite ions are oxidized. According to Abel, the oxidation rate is proportional to the HSO_3^- ion concentration and inversely proportional to the square root of the H^+ ion concentration. Such contradictory conclusions

* The thiosulfate and trithionate contents, determined at the end of experiments in samples with high S/C ratios, did not exceed 0.015 mole/liter, while in the samples with low S/C ratios only traces were detected.

drawn by different workers can be attributed to differences in the experimental conditions, and primarily to differences in the concentrations of the solutions. It seems that the situation is not the same in solutions of low concentrations as in concentrated solutions, and analogies between the two are impossible.
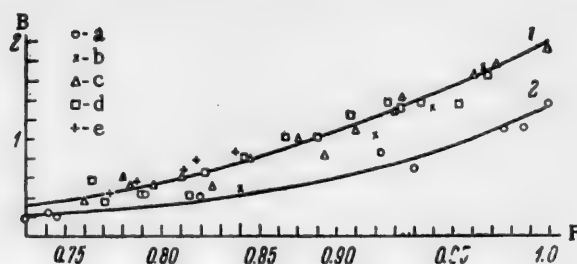

Fig. 6. Effect of variations of the S/C ratio on the oxidation rate of the solution in contact with air.
NH_{3total} = 7.8-8.2 moles/liter, average 8.0 moles/liter, temperature 20-22°. B) Oxidation rate G_{O_2} (in g/m² · hour), F) S/C ratio. NH_3 contents in ammonium sulfite and bisulfite (C) (in moles/liter): a) 1.5-2.8; b) 3.2-3.8; c) 4.5-5.5; d) 6.0-6.8; e) 7.0-7.8. The curves are explained in the text.
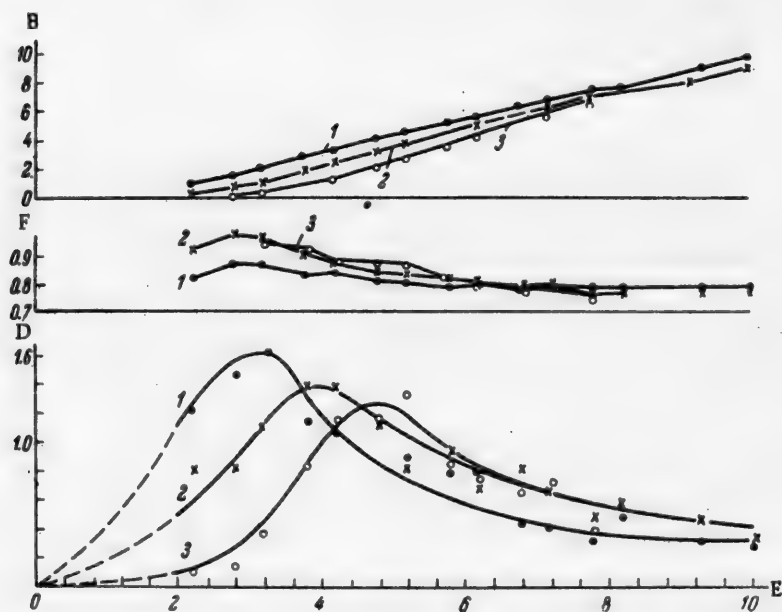

Fig. 7. Influence of total salt concentration NH_{3total} on the rate of oxygen absorption on contact with air at 20-22°. S/C ratio (initial) = 0.78-0.80. B) Concentration of ammonium sulfite and bisulfite (C) (in moles/liter), D) rate of oxygen absorption G_{O_2} (in g/m² · hour), E) NH_3total concentration = A + C (in moles/liter), F) S/C ratio. Curves 1, 2, and 3 represent the results of successive analyses.

Moreover, in our opinion, the investigators who ascribed a low oxidation rate to the bisulfite ion erred in ignoring the changes in the composition of the solution during oxidation. When bisulfite was added to water saturated with oxygen, as was done by Wartman, free sulfurous acid was immediately formed (owing to the reaction between NH_4HSO_4 and NH_4HSO_3), and the oxidation proceeded in the system bisulfite—sulfurous acid, at an S/C ratio considerably higher than 1 when, as was stated above, oxidation is retarded considerably.

Figure 7 represents the results of experiments on the influence of total concentration of the salts in solution on the oxidation rate. The results of successive analyses of the solutions are plotted in Curves 1, 2, and 3; the values of C and S/C ratio given are the average values for the intervals between the analyses.

Thus, for each value of $NH_{3\ total}$ the variations of G_{O_2} were determined with decrease of the ammonium sulfite—bisulfite concentration and corresponding increase of the ammonium sulfate concentration.

The course of the curves in Fig. 7 is highly significant. First, all the curves are the same shape with clearly-defined maxima, indicating a complex relationship between the total concentration of the solution and its oxidation rate. In dilute solutions, at very low salt concentrations, the oxidation rate is at a mimimum. It increases with increasing concentration and reaches a maximum, beyond which it decreases slowly and again becomes very low at high concentrations.

The region of NH_{3total} concentrations between 7 and 9 moles/liter, which is particularly important in practice, is seen to be on the descending branch of the curve in Fig. 7, beyond the maximum, i.e., in conditions which are relatively favorable with regard to the oxidation rate.*

With decrease of C (and corresponding increase of A) the maximum points on the Curves 1, 2, and 3 gradually shift to the right, in the direction of higher NH_{3total} concentrations. It is noteworthy, however, that the oxidation maximum on each curve corresponds to a definite sulfite—bisulfite concentration (C = 2-3 moles/liter).** This is probably a boundary concentration, above and below which the influence of different factors on the oxidation changes. At higher sulfite—bisulfite concentrations the rate of absorption of oxygen from the air is the determining factor. Below this concentration the determining factor is the rate of reaction between the dissolved oxygen and the sulfite—bisulfite (generally speaking, this rate is proportional to the sulfite—bisulfite concentration), and the rate of access of oxygen no longer plays its former role. This explains the presence of maxima on the curves in Fig. 7. The oxidation rate decreases to the left of the maximum because C decreases with decrease of NH_{3total}. To the right of the maximum the oxidation rate decreases because the solubility of oxygen in the solution decreases with increase of its total concentration.
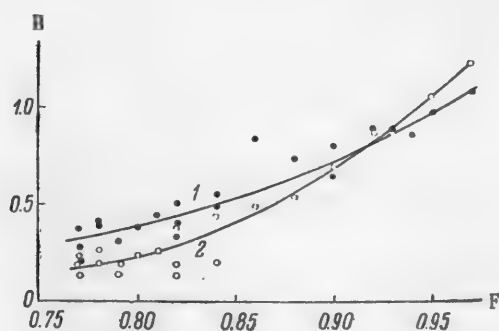
Volfkovich and Tsirlin [13] studied in detail the oxidation of ammonium sulfite, and found that oxidation is greatly accelerated with decrease of concentration. Terres and Heinsen [10] and Wartman [11] reached the same conclusion with regard to ammonium bisulfite.

Our data for mixtures consisting predominantly of ammonium bisulfite (75% and over) introduce the following modification into these conclusions: the oxidation rate increase with dilution only down to a definite sulfite—bisulfite concentration (C = 2-3 moles/liter); below this the situation changes and further dilution leads to a decrease of the oxidation rate.

The amounts of oxidized and desorbed SO_2 (in moles/liter of solution) for various values of the S/C ratio are compared in Fig. 8.

Within the ranges of S/C and C given in Fig. 8, with undisturbed diffusion of the components both in the gaseous and in the liquid phase, the rate of SO_2 desorption was found to be comparable to the oxidation rate of the solution.

Fig. 8. Variations of the amounts of SO_2 oxidized and desorbed, with the S/C ratio of sulfite bisulfite solution in contact with air at 20-22°. NH_{3total} from 8.1 to 8.2 moles/liter, C from 5.5 to 7.5 moles/liter. B) Amounts of oxidized (Curve 1) and desorbed (Curve 2) SO_2 (in moles/liter), F) S/C ratio.

* This is the operating concentration of the ammonium sulfite—bisulfite solution in the ammonia continuous process for recovery of SO_2 from flue gases.
** Trithionate and thiosulfate were almost absent in these experiments. Only traces of them were detected.

These results show that oxidation of ammonium sulfite—bisulfite solution by means of a current of pure air, which is sometimes suggested as a method for the production of ammonium sulfate, cannot be realized, as even at low values of the S/C ratio, of the order of 0.75-0.8, the loss of SO_2 by desorption would be almost equal to the amount of SO_2 oxidized, and it might be even higher at high air speeds.

SUMMARY

1. The influence of the composition of ammonium sulfite—bisulfite solutions on their oxidation rate by atmospheric oxygen was studied, and it was found that in a mixture of these salts ammonium bisulfite is oxidized perferentially.

In the range of bisulfite contents from 63 to 100%, which is the range of practical importance, the oxidation rate of the solution increases approximately 6-fold. If free sulfurous acid is present in the solution in addition to bisulfite, the oxidation rate falls, down to complete cessation of oxidation, because of the sharp decrease of pH.

2. Concentration of the solution has a complex influence on the oxidation rate; it depends on the factor which controls the oxidation process — the rate of access of oxygen from the air, or the rate of reaction of the dissolved oxygen with the sulfite and bisulfite.

At a definite concentration of sulfite and bisulfite (from 2 to 3 moles/liter) the oxidation rate is at a maximum. Above and below this concentration the oxidation rate decreases continuously, reaching minimum values both in highly concentrated and in very dilute solutions.

3. The oxidation of sulfite and bisulfite is accompanied by reactions of spontaneous decomposition, leading to appearance of thiosulfate and trithionate in the solution. At first these reactions develop extremely slowly but ultimately become a factor which greatly influences the oxidation process as the products of these reactions — thiosulfate and trithionate — can catalyze the oxidation reaction.

4. The amount of SO_2 desorbed from ammonium sulfite—bisulfite solutions in contact with air is comparable with the amount of SO_2 oxidized.

LITERATURE CITED

[1] A. P. Andrianov and B. A. Chertkov, J. Chem. Ind. 7, 10 (1954).

[2] Ya. I. Zilberman and P. T. Ivanov, J. Appl. Chem. 14, 541 (1940).

[3] T. D. Averbukh, J. Chem. Ind. 11, 14 (1948).

[4] B. A. Chertkov, Dissertation (1950).

[5] E. Abel, Monatsh. 82, 815 (1951).

[6] Z. P. Rozenknop, Extraction of Sulfur Dioxide from Gases (Goskhimizdat, 1952).*

[7] F. Foerster and E. Haufe, Z. anorg. Ch. 177, 17-41 (1928).

[8] H. Basset and W. G. Parker, J. Am. Chem. Soc. 1540-60 (1951).

[9] Gmelins Handbuch anorg. Chem., 23, 259.

[10] E. Terres and A. Heinsen, Gas u. Wasserfach 994 (1929).

[11] F. S. Wartman, Rep. Invest. U. S. Bur. Mines No. 3339 (1937).

[12] E. C. Fuller and R. H. Crist, J. Amer. Chem. Soc. 63, 6, 1644 (1941).

[13] S. I. Volfkovich and D. L. Tsirlin, J. Chem. Ind. 6, 1323-1331 (1929).

* In Russian.

INVESTIGATION OF THE THERMOCHEMICAL DECOMPOSITION OF ALUMINUM SULFATE

V. V. Pechkovsky and A. N. Ketov

The A. M. Gorky State Institute, Molotov

The thermochemical decomposition of aluminum sulfate is of interest as one method for the processing of alunite [1]. It must also be emphasized that the alumina formed by thermochemical decomposition of aluminum sulfate is highly disperse and has a very defective crystal lattice, with consequent higher sintering power [2]. For this reason alumina made by this method is an excellent raw material for products with a high content of Al_2O_3.

Such products, which are usually made by so-called solid-phase reactions, are being used to an increasing extent in the metallurgical, chemical, electrotechnical, and other industries.

Kukolev and Leve [2] showed that the alumina formed by decomposition of aluminum sulfate is inferior only to the alumina made by calcination of aluminum acetate with regard to ease of sintering.

These authors found that the sintering of alumina is assisted by additions of various oxides, the most effective of which were the oxides of titanium, iron, manganese, chromium, and certain other metals.

The purpose of the present investigation was to study the influence of various factors on the rate of thermochemical decomposition of aluminum sulfate.

The object of the work was to find conditions in which the thermochemical decomposition of aluminum sulfate is fairly rapid and complete at the lowest possible temperature. It has already been shown [3, 4] that the most important factors influencing the rate and degree of decomposition of sulfates are the temperature, duration of heating, the oxygen content of the original gas, the presence of additives in the charge, and of reducing agents in the reaction zone.

The influence of these factors on the rate of thermochemical decomposition of aluminum sulfate was therefore studied.

EXPERIMENTAL METHODS

The materials used for the experiments were thoroughly dehydrated analytical-grade aluminum sulfate, chemically pure TiO_2, Fe_2O_3, and Cr_2O_3, and pure, dry oxygen, nitrogen, and carbon monoxide.

Aluminum sulfate, and its mixtures with various additives, were heated in a laboratory tubular furnace in a stream of dry gas in the 700-900° range. The furnace temperature was measured by means of a thermocouple and galvanometer, and regulated by means of an LATR-1 autotransformer. 1 g of aluminum sulfate was taken for each experiment; the average particle size, by sieve analysis, was 0.1-0.14 mm.

The gas rate in the system was 3.5 liters/hour in all experiments. To study the influence of oxygen in the gas on the decomposition rate of aluminum sulfate, the latter was heated in currents of nitrogen, oxygen, air, and a mixture of nitrogen and air containing 10% of oxygen. In addition, aluminum sulfate was heated in a current of pure carbon monoxide.

In studies of the decomposition rate of aluminum sulfate, some difficulties were met with regard to analysis. The known methods for analysis of the decomposition products of sulfates [3, 4] proved to be unsuitable.

Determination of aluminum oxide in the solid decomposition products proved difficult because basic sulfates are formed when a mixture of alumina and aluminum sulfate is dissolved. Difficulties arose in the analysis of the gaseous decomposition products of aluminum sulfate because the gas phase contains considerable amounts of sulfur trioxide, which condenses in the cold part of the reaction tube. Therefore the total amount of aluminum sulfate decomposed was determined from the loss of weight of the sample taken. For determination of total sulfur in the gaseous decomposition products, a continuous method of analysis was devised, similar to the continuous method of analysis used for sulfur dioxide. The apparatus used for this is shown in Fig. 1.
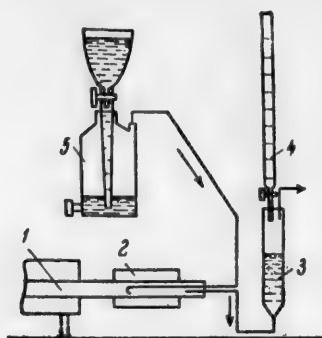

Fig. 1. Diagram of the apparatus.
1) Reaction tube; 2) additional heater; 3) absorption vessel; 4) buret; 5) gas holder.

TABLE 1

Effects of Temperature and Time on the Degree of Decomposition of Aluminum Sulfate in a Current of Air

τ *	Degree of decomposition of aluminum sulfate (in %) at temperature (°C)			
	750°	800°	850°	900°
15	4.6	8.8	20.0	55.2
30	6.8	12.0	32.1	87.4
45	7.9	13.8	43.2	99.4
60	9.2	15.4	54.4	100.0

TABLE 2

Effects of Temperature and the Oxygen Content of the Original Gas on the Degree of Decomposition of Aluminum Sulfate (τ = 30 minutes)

Temperature (°C)	Degree of decomposition of aluminum sulfate (in %) at oxygen concentrations in the original gas (in vol. %)			
	0	10	21	100
750	9.1	7.6	6.8	6.6
800	17.9	14.3	12.0	10.9
850	43.1	34.5	32.1	30.5
900	100.0	96.6	87.4	85.1

* Here and subsequently τ represents the time in minutes.

The method of analysis was as follows. The gas formed by decomposition of aluminum sulfate, containing a mixture of sulfur trioxide and dioxide, passes along the reaction tube, at the right-hand extension of which is an electric heater which maintains a temperature of 650-750° in this part of the tube. Carbon monoxide is fed from a gas holder into the middle of this part of the reaction tube; under these conditions it is drawn along with the stream of the reaction gas and readily reduces sulfur trioxide to the dioxide. The sulfur dioxide leaving the reaction tube then enters the absorption vessel, where it is continuously titrated with 0.1 N iodine solution added dropwise. The amount of iodine taken for the titration gives the degree of decomposition of aluminum sulfate at any given instant.

Stasifactory agreement was obtained between the results found by the loss-of-weight method and by the method described above.

The principal experimental results are given in Tables 1-5 and Figs. 2 and 3.

It follows from the data in Table 1 and Fig. 2 and 3 that the rate of thermochemical decomposition of pure aluminum sulfate increases with temperature; pure aluminum sulfate decomposes at a rate acceptable for practical purposes only at temperatures above 900°.

Examination of the data in Tables 2 and 5 and Fig. 2 leads to the conclusion that the decomposition rate increases somewhat with decrease of the concentration of oxygen in the gas passed over the sulfate. It should be noted, however, that variation of the oxygen concentration in the gas is not an important factor in the rate of the process.

Data on the influence of various additives on the rate of thermochemical decomposition of aluminum sulfate are given in Tables 3 and 5 and in Fig. 2.

These results show that some additives significantly increase the decomposition rate of aluminum sulfate, especially above 800°. The most active additives were oxides of chromium and iron. For example the degree of decomposition of pure aluminum sulfate and of aluminum sulfate with added Cr_2O_3 at 850° in 30 minutes was 32.1 and 83.0% respectively.

TABLE 3

Effects of Nature and Contents of Additives on the Degree of Decomposition of Aluminum Sulfate in a Current of Air (τ = 30 minutes) Additives: 1) Fe_2O_3; 2) Cr_2O_3; 3) TiO_2

Contents of additives in mixtures (%)	Degree of decomposition of aluminum sulfate (in %) in presence of additive at temperatures (°C)								
	750°			800°			850°		
	1	2	3	1	2	3	1	2	3
5	8.7	9.1	7.1	18.6	20.8	11.1	71.4	83.0	30.9
10	9.7	10.8	6.7	18.2	23.1	12.4	74.8	80.3	30.9

TABLE 4

Effect of Temperature on the Degree of Decomposition of Aluminum Sulfate in a Current of Carbon Monoxide (τ = 10 minutes)

Temperature (°C)	Conversion of sulfate sulfur into gaseous products (%) in the form of:		
	SO_2	$COS+CS_2+S_2$	total
750	6.4	—	6.4
800	70.3	8.1	78.4
850	86.2	6.8	93.0

TABLE 5

Effect of Duration of Heating on the Degree of Decomposition of Aluminum Sulfate (Temperature 750°) Degree of decomposition of aluminum sulfate (in %): 1) in a current of nitrogen; 2) in a current of carbon monoxide; 3) with addition of Fe_2O_3

τ	Degree of decomposition of aluminum sulfate (%)		
	1	2	3
15	6.9	9.6	6.4
30	9.1	16.1	8.7
45	11.2	19.7	10.3
60	12.1	23.2	11.8

Fig. 2. Effect of temperature on the degree of decomposition of aluminum sulfate (τ = 30 minutes). A) Degree of decomposition of aluminum sulfate (%), B) temperature (°C) Decomposition of $Al_2(SO_4)_3$ in a current of: 1) oxygen, 2) air, 3) nitrogen, 6) carbon monoxide. Decomposition of $Al_2(SO_4)_3$ in presence of additives: 4) Fe_2O_3; 5) Cr_2O_3.

The data in Table 3 show that additions of TiO_2 have little or no effect on the decomposition rate of aluminum sulfate.

The fact that oxides of metals of variable valence had an accelerating effect on the thermochemical decomposition of aluminum sulfate, and also that this action is almost independent of the amount added, shows that these additives catalyze the decomposition of aluminum sulfate.

It may be concluded from these results that if Fe_2O_3 is added to aluminum sulfate for decomposition not only is the process accelerated, but sintering may also be accelerated if the alumina formed is to be used for the production of various materials containing Al_2O_3:

Data on the reduction of aluminum sulfate by carbon monoxide are given in Tables 4 and 5 and in Fig. 2.

It follows from the data in Tables 4 and 5 that carbon monoxide actively reduces aluminum sulfate.
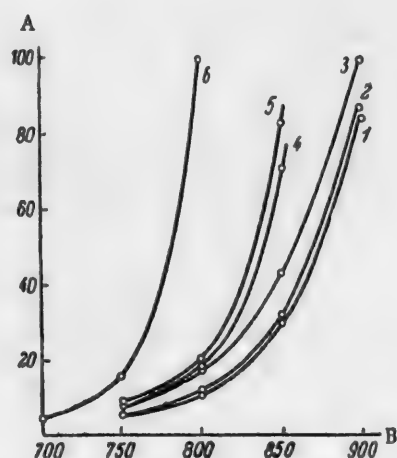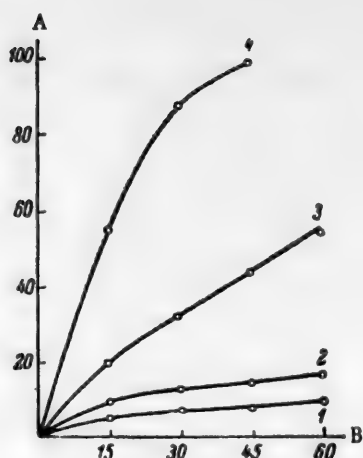
Fig. 3. Effect of heating time on the degree of decomposition of aluminum sulfate in a current of air. A) Degree of decomposition of aluminum sulfate (%), B) heating time (minutes). Temperature (°C): 1) 750; 2) 800; 3) 850; 4) 900.

Thus, at 800°, in experiments lasting 15 minutes, the degree of decomposition of aluminum sulfate in a current of air and of carbon monoxide is 8.8 and 78.4% respectively. The solid product formed by the reduction of aluminum sulfate by carbon monoxide is Al_2O_3. Sulfur is present in the gaseous reduction products largely in the form of sulfur dioxide.

It follows from Table 4 that relatively small amounts of other sulfur compounds are present in the gas.

SUMMARY

1. The thermochemical decomposition of aluminum sulfate in a current of dry air proceeds at a rate high enough for practical purposes at temperatures above 900°.

2. The decomposition rate of pure aluminum sulfate increases somewhat with decrease of the oxygen content of the gas entering the reaction zone.

3. Addition of the oxides of iron or chromium appreciably accelerates the thermochemical decomposition of aluminum sulfate.

4. The decomposition of aluminum sulfate is particularly accelerated with the use of gaseous reducing agents. In a current of carbon monoxide, aluminum sulfate decomposes at a rate acceptable for practical purposes even at 800°. The solid decomposition product is alumina, and the sulfur is present in the gas mainly as sulfur dioxide.

LITERATURE CITED

[1] I. L. Bagbanly and A. K. Posadovskaya, Bull. Acad. Sci. Azerbaidzhan SSR 1, 13 (1955).

[2] G. V. Kukolev and E. N. Leve, J. Appl. Chem. 28, 909 (1955).*

[3] M. E. Pozin and A. M. Ginstling, J. Appl. Chem. 24, 134 (1951).*

[4] V. V. Pechkovsky, J. Appl. Chem. 28, 237 (1955). *

Received February 24, 1956

REGENERATION OF ARSENICAL SODA LIQUORS *

N. I. Brodskaya, M. I. Gerber, and V. P. Teodorovich

The Leningrad Scientific Research Institute of Petroleum Processing and the Production of
Synthetic Liquid Fuel

The arsenical soda process for removal of hydrogen sulfide from gases is one of the leading methods of gas purification.** The reason for the wide field of application of this process is the possibility of using it for gases containing different amounts of hydrogen sulfide; the presence of considerable amounts of carbon dioxide and oxygen in the gases does not interfere. Moreover, it is possible to obtain the sulfur extracted from the gas as a commercial product. However, despite the extensive use of this method in industry and the apparent simplicity of the chemical reactions taking place in the process, its nature has remained obscure, and at some undertakings periodic deterioration of the purification has been repeatedly observed without any apparent changes in the conditions.

The behavior of the liquors in the stage of hydrogen sulfide absorption and in the regeneration stage was studied in order to elucidate the chemistry of the processes taking place in arsenical soda solutions both during normal operation and during disturbances of the normal course of purification.

Shebalin, Mikhelson and others [1] postulated the following reaction scheme for the processes occurring in the removal of hydrogen sulfide from gases by the arsenical soda method.

$$Na_3AsS_3O + H_2S = Na_3AsS_4 + H_2O \text{ (absorption stage)}, \tag{1}$$

$$Na_3AsS_4 + \frac{1}{2}O_2 = Na_3AsS_3O + S \text{ (regeneration stage)}. \tag{2}$$

The principal reactions in the liquor are always accompanied by side reactions, often undesirable:

$$\tag{3}$$

$$Na_2CO_3 + H_2S = NaHS + NaHCO_3,$$

$$2NaHS + 2O_2 = Na_2S_2O_3 + H_2O. \tag{4}$$
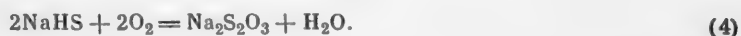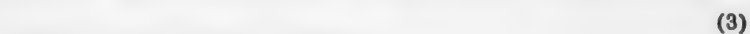
Formation of thiosulfate in the side reactions increases the consumption of soda and decreases the sulfur yield. Moreover, accumulation of thiosulfate in the liquor makes periodic regeneration of the liquor necessary. Because of the insufficient demand, thiosulfate is extracted as a commercial product at only a few plants.

Studies of the regeneration of arsenical soda solutions are described in this paper.

EXPERIMENTAL METHODS

The liquor for regeneration contained 10.8 g of As_2O_3 and 12.5 g of Na_2CO_3 per liter, corresponding to a 1.15 ratio of nominal soda [2] to arsenious anhydride. This solution was saturated with hydrogen sulfide to

* Communication I in the series of investigations of the oxidation of oxythioarsenates in aqueous solutions.

This work was carried out under the guidance of V. V. Ipatyev and reported at the Conference on Sulfur Removal held at the State Institute of the Nitrogen Industry, June 18-20 1952.

** Thylox process — Publisher's note.

initial pH 6.8. The temperature during the experiment was maintained at 20°. The pH of the solution was determined by means of an electronic pH-meter, made by the All-Union Scientific Research Institute of the Hydrolysis Industry, to within 0.1 unit. For investigations of the regeneration process, the arsenical soda liquors were oxidized by means of oxygen in a special laboratory regenerator [3]. The quality of the liquor being regenerated was estimated both by the rate of oxygen absorption and by the amount of sulfur liberated during regeneration.

Effect of dilution on the regeneration of arsenical soda solutions. The object of the first series of experiments was to determine the influence of dilution of the arsenical soda solution on the rate of oxygen absorption. The results are given in Table 1. The oxygen consumed during regeneration is used both in liberation of sulfur and in formation of thiosulfate.

TABLE 1

Effect of Dilution on Regeneration of Arsenical Soda Solution

Taken for oxidation (in ml)		Amount of sulfur liberated (in g/liter)	Amount of oxygen absorbed by 100 ml of solution (in ml)	Amount of oxygen consumed for liberation of elemental sulfur (%)	pH of solution		Amount of S liberated in g-atoms per 1 g-atom As
solution	water				initial	after regeneration	
80	0	2.888	123.6	87.6	6.8	8.3	1.03
80	20	2.603	120.0	81.3	6.8	8.5	0.93
60	40	1.970	92.3	80.1	6.8	8.3	0.94
40	60	1.333	61.4	81.3	6.8	8.5	0.95
20	80	>0.622	30.0	—	6.8	8.5	0.89
10	90	>0.262	12.9	—	6.8	8.5	0.75

The results show that the regeneration of the arsenical soda solutions is always practically complete in 15-20 minutes, and that the amount of oxygen absorbed gradually decreases with increasing dilution. The amount of sulfur liberated during regeneration, expressed in g-atoms per 1 g-atom of arsenic, remains constant, the value being close to unity.*

Effect of addition of Na₂S on the regeneration of arsenical soda solutions. The results of experiments on the regeneration of arsenical soda solution in presence of various amounts of Na₂S are given in Table 2 and Fig. 1. It is seen that the oxidation curves fall into two quite distinct groups: the first group contains Curves 1, 2, and 3, and the second, Curves 4, 5, 6, and 7. When sodium sulfide is added in 0.75 N, 0.37 N, and 0.07 N concentrations, the sulfide is apparently oxidized first (to thiosulfate), and the amount of oxygen absorbed gradually decreases with decreasing concentration of the Na₂S added; sulfur is not liberated. The solution pH after regeneration remains above 9. It can also be seen that the higher the sulfide concentration, the higher does the curve lie, and the more oxygen is absorbed. For comparison, Fig. 1 includes a curve for the oxidation of pure sulfide (0.25 N solution, Curve 9) in absence of arsenical soda solution. This curve lies between Curves 2 and 3, corresponding to added sodium sulfide concentrations of 0.37 N and 0.07 N respectively. At added sodium sulfide concentrations of 0.056 N and less, the course of the oxidation changes abruptly, maxima appear on the curves, sulfur is liberated, and the course of the curves virtually coincides with the course of the curve for the regeneration of arsenical soda solution without additives (Fig. 1, Curve 8).

Effect of addition of Na₂CO₃ on the regeneration of arsenical soda solutions. The influence of added Na₂CO₃ on the regeneration of arsenical soda solutions is shown by the data in Table 3. It is seen that the effect of sodium carbonate on regeneration is somewhat different from that of sodium sulfide. Sulfur is liberated even at 1 N concentration of sodium carbonate. However, this liberation occurs progressively later with increasing concentration of the added sodium carbonate (see Column 3, Table 3). Moreover, the amount of oxygen absorbed is more than equivalent to the amount of sulfur liberated. this discrepancy increases with increasing concentration of the added carbonate (see Column 6, Table 3). Finally, and this is perhaps the most significant feature, the absolute amount of liberated sulfur decreases sharply with increasing concentration of the carbonate added. It is interesting to note that liberation of sulfur coincides with the appearance of a maximum on the absorption curve.

* In Experiments 5 and 6 of Table 1 part of the sulfur was lost during filtration owing to formation of a colloidal solution.
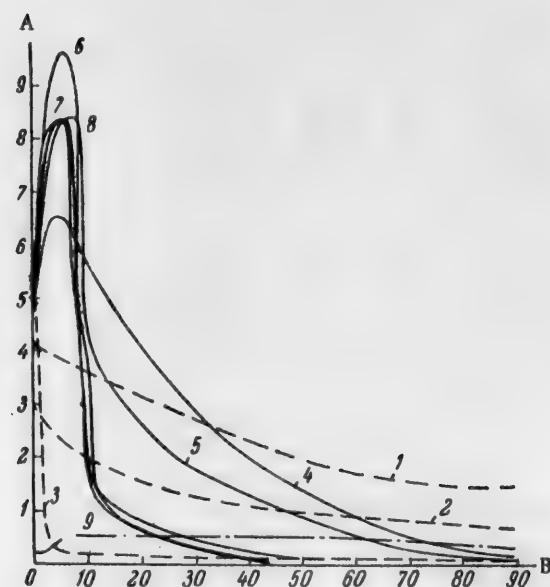
Fig. 1. Effect of additions of sodium sulfide on regeneration of arsenical soda solution.
A) Rate of oxygen absorption (in ml/minute), B) time (minutes). Additions of Na_2S (in g-equiv. per 1 g-atom of arsenic): 1) 8.3; 2) 4.2; 3) 0.83; 4) 0.63; 5) 0.42; 6) 0.08; 7) 0.008; 8) 0; 9) 0.25 N. Na_2S without arsenical soda solution.

Effect of additions of NaHS and $NaHCO_3$ on the regeneration of the recovery liquor at constant pH of the original solution. In all the previous experiments the introduction of additives resulted in sharp changes of composition and the pH of the solutions. A special series of experiments was therefore performed, with the use of original solutions (NaHS, $NaHCO_3$ and partially-regenerated arsenical soda solution) with pH constant at 8.45, in order to study the effect of solution composition. The solutions for regeneration were mixtures of these three solutions in different proportions (Table 4, Fig. 2), but such that the total concentration of the additive was 0.25 g-equiv/liter.

The results indicate that the liberation of sulfur is increasingly rapid (the maxima on the oxidation curves are shifted to the left) with progressive replacement of sodium hydrosulfide by bicarbonate. Evidently, in presence of sodium hydrosulfide there are two possibilities in the absorption of oxygen: 1) oxidation of NaHS with formation of sodium thiosulfate, and 2) reaction between sodium hydrosulfide and sodium oxythioarsenate to give sodium thioarsenate, with subsequent oxidation of sodium thioarsenate according to Equation (2).

These results indicate that the regeneration of arsenical soda liquors is a highly complex process, the rate of which depends on the amount of free alkali (nominal soda) in the solution; in other words, on the pH of the solution.

TABLE 2

Effect of Added Sodium Sulfide on the Regeneration of Arsenical Soda Solution

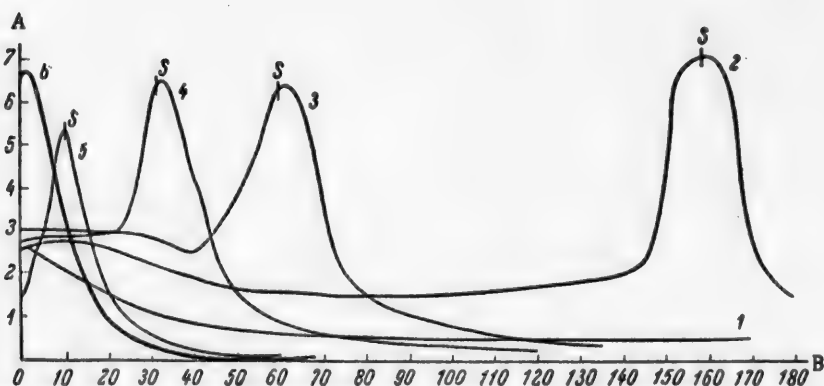| Amount added, in g-equiv. Na per 1 g-equiv As	Concentration of added Na_2S in the liquor ($\frac{g\text{-equiv.}}{liter}$)	Amount of sulfur liberated (in g/liter)	Amount of oxygen absorbed by 100 ml of liquor (in ml)	Oxygen consumed in formation of elemental sulfur (%)	pH of solution original	pH of solution after regeneration	Amount of S liberated in g-atoms per 1 g-atom As
8.3	0.73	0	298	—	—	—	—.
4.2	0.37	0	130	—	—	10.2	—
0.83	0.07	0	30	—	8.75	9.5	—
0.63	0.056	1.548	202	29	7.5	8.3	0.55
0.42	0.037	1.552	159	36	7.3	8.3	0.55
0.08	0.007	1.683	98	64	7.0	8.2	0.60
0.008	0.0007	1.915	84	85	6.9	8.2	0.68
0	0	2.951	93	88	6.8	8.3	0.84

TABLE 3

Effect of Added Sodium Carbonate on Regeneration of Arsenical Soda Solution

Amount added, in g-equiv. Na per 1 g-equiv. As	Concentration of added carbonate in the liquor (g-equiv./liter)	Start of sulfur liberation (min.)	Amount of sulfur liberated (in g/liter)	Amount of oxygen absorbed by 100 ml of liquor (in ml)	Oxygen consumed in formation of elemental sulfur (%)	pH of solution		Amount of S liberated in g-atoms per 1 g-atom As
						original	after regeneration	
11.40	1.0	42	0.2420	208	4	10.0	9.1	0.09
8.55	0.75	20	0.8880	153	28	9.9	8.8	0.82
5.70	0.5	12	1.4270	113	47	9.5	9.4	0.51
1.14	0.1	7	2.4060	142	63	6.8	8.2	0.85
0	0	3	2.6030	120	83	6.6	8.7	0.92

TABLE 4

Effect of Additions of NaHS and $NaHCO_3$ on Regeneration of Arsenical Soda Solution of Constant Initial pH

Amount added, in g-equiv. Na per 1 g-equiv. As	Concentration of additives in liquor (in g-equiv./liter)		Start of sulfur liberation (in min)	Amount of sulfur liberated (in g/liter)	Amount of oxygen absorbed by 100 ml of liquor (in ml)	pH of solution		Amount of S liberated in g-atoms per 1 g-atom As
	NaHS	$NaHCO_3$				original	after regeneration	
4.5	0.25	0	—	0	245	8.45	9.3	—
	0.20	0.05	158	0.936	459		8.8	0.52
	0.15	0.10	59	1.109	306		9.2	0.62
	0.10	0.15	31	1.188	212		9.2	0.66
	0.05	0.20	10	0.804	76		9.1	0.45
	0	0.25	3	0.080	81.7		8.8	0.045
0	0	0	4	1.651	76.6	6.6	8.4	0.93

Fig. 2. Effect of additions of NaHS and $NaHCO_3$ on regeneration of arsenical soda solution of initial pH 8.45.
A) Rate of oxygen absorption (in ml/minute), B) time (minutes). Respective concentrations of NaHS and $NaHCO_3$ in the liquor (in g-equiv/liter: 1) 0.25 and 0; 2) 0.20 and 0.05; 3) 0.15 and 0.10; 4) 0.10 and 0.15; 5) 0.05 and 0.20; 6) without additives.
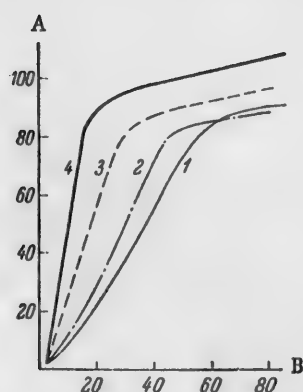
Fig. 3. Time variation of the total amount of oxygen absorbed by arsenical soda solution (pH = 7.1) at different partial pressures of oxygen in the regenerator.
A) Amount of oxygen absorbed (in ml), B) time (minutes). Oxygen content in the regenerator (%): 1) 20; 2) 36; 3) 50; 4) 100.

Regeneration of sodium thioarsenate solution under different partial pressures of oxygen. A series of experiments was performed to determine the effect of oxygen partial pressure on the regeneration rate; the following method was used to establish different partial pressures, constant during a given experiment. Nitrogen containing a definite amount of oxygen was passed for 10-15 minutes through an empty laboratory regenerator. The solution was then poured into the regenerator, the gas supply was stopped, and the regenerator was connected to a gas buret containing 100% oxygen. Thus, the partial pressure of oxygen over the solution remained constant during absorption of oxygen in the course of regeneration, as the absorbed oxygen was replaced from the buret. The total pressure was maintained at 1 atm.

The time variation of the total amount of oxygen absorbed is plotted in Fig. 3. It is seen that the rate of regeneration increases with increase of the oxygen partial pressure in the regenerator.

SUMMARY

The oxidation of arsenical soda solutions by oxygen in a laboratory regenerator, and the influence of sodium carbonate and sodium hydrosulfide on the oxidation rate of thioarsenates, were studied; it is shown that for higher rates of regeneration and sulfur yields the regeneration must be carried out at low ratios of nominal soda to arsenious anhydride, and at low pH values.

LITERATURE CITED

[1] K. N. Shebalin, J. Chem. Ind. 9 (1933).

[2] M. I. Gerber, S. S. Iordan and V. P. Teodorovich, Factory Labs. 7, 823 (1954).

[3] M. I. Gerber, V. P. Teodorovich, N. I. Brodskaya and V. V. Ipatiev, J. Appl. Chem. 26, 657 (1953).*

*Original Russian pagination. See C. B. Translation.

HYDROLYSIS OF MANGANESE CHLORIDE IN THE SOLID PHASE

G. I. Zvorykina

The Gorky Polytechnic Institute

Powder metallurgy is becoming increasingly important, and is being used for the solution of many important problems. One such problem is the production of electrical and radio components with special magnetic and electrical properties.

As is known, raw materials for the production of metallic powders can be obtained from the wastes of many industries: scale from metallurgical industries, turnings from metal-working processes, and pyrite cinders from the chemical industries, although pyrite cinders are not yet used for the production of iron powder.

One method for the production of iron powder from steel turnings is by chloride hydrolysis [1-2]; this could be successfully used for the production of metallic powders from pyrite cinders.

Any method for the production of iron powder from steel turnings involves the following problems: 1) production of a powder containing all the components present in the steel turnings; 2) production of a powder of an exact predetermined composition; and 3) production of pure iron powder. To solve any of these problems it is necessary to study the behavior of all the components of the steel turnings at all stages of treatment.

Manganese is a component of most carbon steels; our task was to study the behavior of manganese at all stages of the chloride hydrolysis process for the conversion of steel turnings into iron powder. The influence of various factors on the rate of hydrolysis of manganese chloride in the solid phase was studied. The results may be of some theoretical interest, as the solid-phase hydrolysis of manganese chloride is a solid-phase heterogeneous reaction, and interest in such reactions has recently increased considerably.

There have been several investigations of the reactions between steam and metal chlorides [3-9], but the studies were purely preparative, and question of kinetics were not considered at all.

Attempts to study kinetic aspects of such reactions were made by Ivanov [8] and Ivantsov [9]. The purpose of the first investigation was synthesis of metal oxides, including manganese oxide, from solid metal chlorides by the action of superheated steam. Only one kinetic curve, for 400°, is given for each reaction in the paper, and neither the influence of the temperature nor the influence of other factors are considered.

The question is examined somewhat more fully in Ivantsov's paper [9].

Ivantsov studied the reactivity of superheated steam toward a number of metal chlorides in the 250-400° range, but did not consider the influence of other factors on the rate of the process.

EXPERIMENTAL METHODS

Pure manganese chloride of analytical-reagent grade was used. The salt was recrystallized twice from water, and analyzed for manganese; the manganese content was 26.93%. The crystalline hydrate and the anhydrous chloride were used in the experiments; to obtain the latter, the crystalline hydrate was dehydrated by heat at 230°.

The anhydrous chloride contained 42.81% of manganese. Both samples were ground in a mortar and sifted. Fractions between 0.25 and 0.5 mm were taken for the experiments.

The apparatus used for the hydrolysis studies (Fig. 1) consisted of two tubular furnaces 1, steam generator 2, reaction tube 3, flow meter 4, condenser 5, graduated receiver for condensate 6, and wash bottles 7.
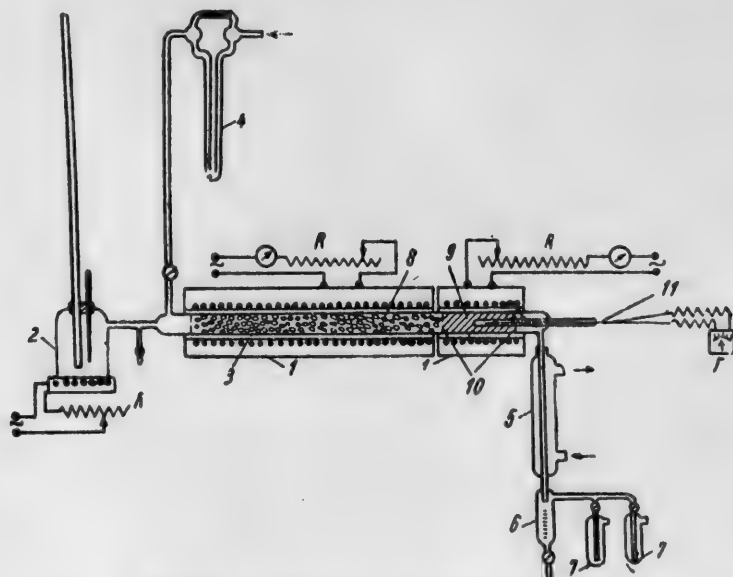

Fig. 1. Diagram of apparatus. Explanation in text.

An iron or porcelain tube was inserted into the furnaces; part of the tube was packed with pieces of porcelain 8, and acted as superheater for the steam. Another part of the tube was completely filled with manganese chloride; to ensure this, metal or porcelain grids 10 were inserted in the tube always at the same distance apart; a definite weight of the salt—either 40 g of $MnCl_2 \cdot 4H_2O$, or 26 g of $MnCl_2$ — was placed between them. A thermocouple 11 was inserted in the reaction zone of the tube for determination of the temperature in that zone.

The steam supply was regulated by means of the heater used for the steam generator and partial release of steam into the air; the amount of steam was found from the amount of condensate formed.

Air was supplied from a blower, and the amount was recorded by means of the flow meter.

The hydrolysis rate was determined from the amount of hydrogen chloride formed The condensate was collected every 10 minutes and analyzed for hydrogen chloride. To check that the hydrogen chloride was completely absorbed in the condensate, wash bottles containing 0.1 N alkali solution were used; their contents were titrated with hydrochloric acid every 10 minutes. It was found that the hydrogen chloride was completely absorbed in the condensate in nearly every case.

The experiments were performed in steam at 400, 450, 500, 550, and 600° at a steam rate of 6.27 liters/minute, and in a steam—air medium under the same conditions, at an air rate of 34 liters/hour.

The results of the experiments are given in Figs. 2 and 3, which show the conversion of hydrated manganese chloride in steam and steam—air mixture, and Figs. 4 and 5, which show the time variations of the hydrolysis rate.

The percentage conversion of the manganese chloride was calculated from the amount of hydrogen chloride formed, and the reaction rate was calculated as the degree of conversion of manganese chloride during 10 minutes.

It follows from the diagrams that the hydrolysis rate is lower in steam than in steam—air mixture. At 400-450° the hydrolysis rate is low, and in 2.5 hours the conversion only reaches 23.3% in steam and 23-24.2% in steam—air mixture.
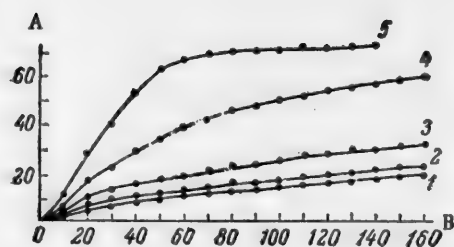
Fig. 2. Conversion of manganese chloride in steam at various temperatures.
A) Degree of conversion (%), B) time (minutes). Temperature (°C): 1) 400; 2) 450; 3) 500; 4) 550; 5) 600.
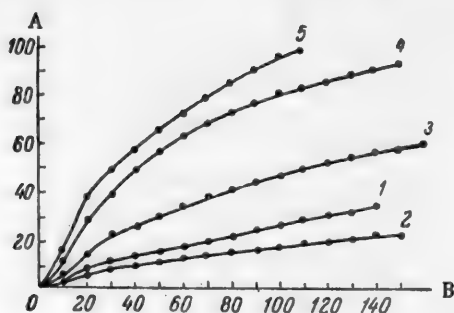

Fig. 3. Conversion of manganese chloride in steam—air mixture at various temperatures.
A) Degree of conversion (%), B) time (minutes). Temperature (°C): 1) 450; 2) 400; 3) 500; 4) 550; 5) 600.

The hydrolysis rate increases considerably with temperature; at 600° the conversion reaches 73% in 2.5 hours in steam, and 99% in 2 hours in steam—air mixture.

Each rate curve has a maximum, which is reached at the 20th minute from the start of the reaction. The greatest maximum is found at 600°, when the conversion of manganese chloride is 26% in steam and 36.8% in steam—air mixture.
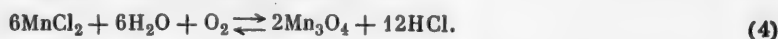
The difference between the hydrolysis rates of the crystalline and anhydrous manganese chlorides is shown in Fig. 6, which gives the time variations of the hydrolysis rate in a number of experiments. The dash lines represent the hydrolysis rate of anhydrous manganese chloride, and the continuous lines, that of the hydrated salt. It is seen that the difference between the rates is not large, being only a few per cent. A possible explanation for the somewhat higher hydrolysis rate of anhydrous manganese chloride is that in removal of the water of crystallization the breakdown on the crystal lattice (which has a favorable effect on the hydrolysis rate) is accompanied by partial sintering of the crystalline mass, which hinders somewhat the passage of steam through the reaction mass.

To determine the effect of the air rate on the rate of hydrolysis, experiments were performed with the air fed in at 380, 150, 50, and 34 liters/hour, at a steam rate of 6.47 liters/minute and 500°; for comparison, experiments were performed under the same conditions, but in a current of nitrogen fed in at 34 liters/hour. The results of these experiments are given in Fig. 7, which shows the time variations of the reaction rate at different air rates. A curve for the reaction rate in steam is shown for comparison. It is seen that the air rate has a considerable influence on the rate of hydrolysis of manganese chloride. This influence is especially pronounced at an air rate of 380 liters/hour.

Analysis of this effect from the kinetic aspect should lead to the opposite conclusion, since increase of the air rate decreases the steam concentration in the reaction zone, and this should lower the rate of reaction. Hence it may be concluded that the hydrolysis rate of manganese chloride is determined not only by the rate of the chemical reaction, but is also influenced by a number of other processes, such as diffusion, as is the case in many topochemical reactions. It will be shown later that the hydrolysis of manganese chloride in steam is represented by the equations;

$$2MnCl_2 + 3H_2O \rightleftarrows Mn_2O_3 + 4HCl + H_2, \tag{1}$$

$$3MnCl_2 + 4H_2O \rightleftarrows Mn_3O_4 + 6HCl + H_2; \tag{2}$$

and in steam—air mixture, by the equations;

$$4MnCl_2 + 4H_2O + O_2 \rightleftarrows 2Mn_2O_3 + 8HCl, \tag{3}$$

$$6MnCl_2 + 6H_2O + O_2 \rightleftarrows 2Mn_3O_4 + 12HCl. \tag{4}$$

Although the system did not reach equilibrium in the conditions of our experiments, nevertheless the rate of the over-all process is greatly influenced by the rate of the reverse reactions in Equations (1 and 2); clearly, the higher this rate, the less HCl will be formed and the lower the rate of the over-all process will be.

The hydrolysis reaction in presence of air may be represented as:

$$4MnCl_2 + 6H_2O \rightleftarrows 2Mn_2O_3 + 6HCl + 2H_2, \tag{a}$$

$$2H_2 + O_2 \rightleftarrows 2H_2O. \tag{b}$$

In the conditions of our experiments (high temperature, in presence of manganese oxides as catalysts), Reaction (b), the oxidation of hydrogen by atmospheric oxygen, is very rapid and does not influence the over-all rate of the process. However, this reaction removes one of the reactants in the reverse reaction of Equation (a), and its rate therefore decreases. Moreover, increase of the air rate increases the rate of diffusion of HCl and H_2 from the reaction zone (from the solid surface) owing to the considerable decrease of their concentration in the gas phase. This also accounts for the influence of nitrogen on the reaction rate. The influence of the amount of air supplied on the rate of hydrolysis was also studied at 400 and 500°. The variation of the maximum rate of hydrolysis with the air rate at these temperatures is plotted in Fig. 8. The greatest increase of the rate of hydrolysis is found at an air rate of 380 liters/hour. At low temperatures (400-500°) the maximum rate of hydrolysis is increased almost fivefold as compared with hydrolysis in absence of air. At high temperatures the rate of hydrolysis is influenced considerably even by air fed at the low rate of 34 liters/hour, when the maximum rate of hydrolysis is almost doubled, but further increase of the air rate has much less effect. It must be pointed out that a substantial increase of the air rate (above 150 liters/hour) complicates the process, as manganese chloride and the hydrolysis products, which are formed in a state of finer subdivision, are blown out of the reaction zone. Moreover, a more complicated system is needed for the cooling of the exit gas in order to condense water vapor and hydrogen chloride.
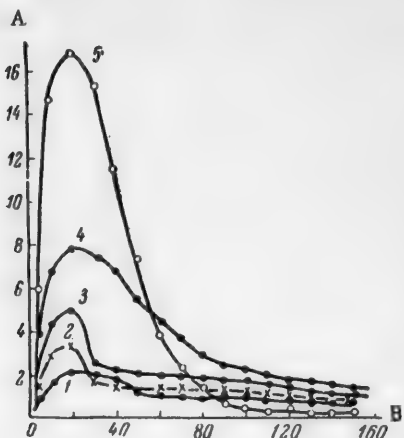

Fig. 4. Time variation of the hydrolysis rate in steam. A) Hydrolysis rate (in %/10 minutes), B) time (minutes). Temperature (°C): 1) 400; 2) 450; 3) 500; 4) 550; 5) 600.

For mathematical analysis of the data obtained at different temperature the following equation [10-13] was used:

$$\alpha = \left(1 - e^{-k \cdot t^n}\right).$$

According to Kazeev [11] and a number of other authors [13] a value of n > 1 indicates that the reaction is a kinetic process; a value of n between 0.5 and 1 indicates that the reaction is a kinetic-diffusional process, and n < 0.5 indicates that it is diffusional.

For determination of these parameters for the hydrolysis of manganese chloride, the experimental data were plotted in log [− log(1−α)]/log t coordinates in Figs. 9 and 10. It is clearly seen that the experimental data fit broken rather than straight lines, the breaks being at the 30th minute of the experiments in most cases. The first part of the line corresponds to the beginning of the process up to the maximum rate. The second part corresponds to the final stage of the process, when a certain amount of hydrolysis products has accumulated.

The value of n is found from the slopes of these lines. The values of n and k for different temperatures are given in Tables 1 and 2.

It is seen that the value of n at the start of the reaction in steam is close to unity, and increases some-what with temperature. Beyond the rate maximum the value of n becomes less than unity, and decreases with
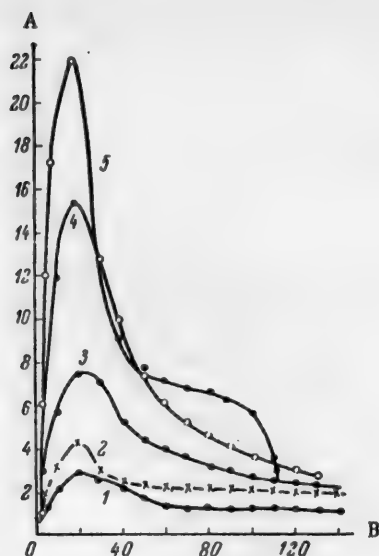
Fig. 5. Time variation of the hydrolysis rate in steam—air mixture. A) Hydrolysis rate (in %/10 minute), B) time (minutes). Temperature (°C): 1) 400; 2) 450; 3) 500; 4) 550; 5) 600.

Fig. 6. Hydrolysis rates of hydrated and anhydrous manganese chloride in steam at various temperatures. A) Hydrolysis rate (in %/10 minutes), B) time (minutes). Temperature (°C): 1, 3) 450; 2, 4) 500.
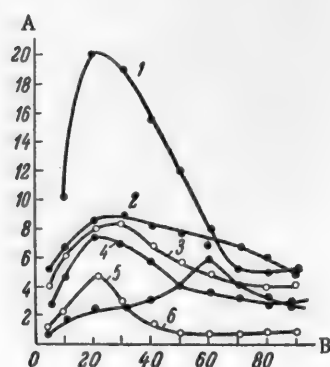

Fig. 7. Effect of air rate on the rate of hydrolysis at 500°. A) Hydrolysis rate (in %/10 minutes), B) time (minutes). Air rate (in liters/hour): 1) 380; 2) 150; 3) 60; 4) 34; 5) nitrogen rate 34 liters/hour, 6) without air.
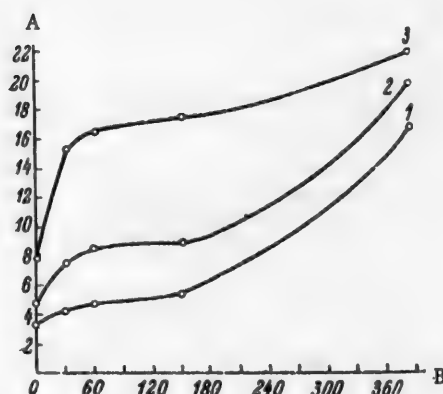
Fig. 8. Effect of air rate at different temperatures on the maximum rate of hydrolysis. A) Maximum rate of hydrolysis (in %/10 minutes) B), air rate (in liters/hour). Temperature (°C): 1) 400; 2) 500; 3) 550.

temperature; the decrease at 600° is particularly rapid. The values of $\underline{n}$ and $\underline{k}$ are somewhat higher for the reaction in steam—air mixture than in steam. The value of $\underline{n}$ is greater than unity and again increases with temperature. Beyond the maximum $\underline{n}$ is less than unity, but it does not decrease with temperature, as in the reaction in steam, but increases and approaches unity.

The values of the rate constants were used to calculate the activation energy for the initial stage of the reaction. The Arrhenius equation

$$k = ce^{-\frac{A}{RT}}$$

was used, and the data were plotted in $\ln k / \frac{1}{T}$, coordinates, as shown in Fig. 11. It is seen that the experimental points fit satisfactorily on a straight line only at low temperatures. At 550-600° the points are scattered,
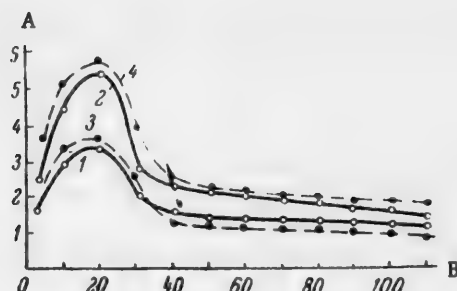
Fig. 9. Determination of the parameter $\underline{n}$ for the reaction in steam. A) $\log[-\log(1-\alpha)]$, B) $\log \underline{t}$. Temperature (°C): 1) 400; 2) 450; 3) 500; 4) 550; 5) 600.

Fig. 10. Determination of the parameter $\underline{n}$ for the reaction in steam—air mixture. A) $\log[-\log(1-\alpha)]$, B) $\log \underline{t}$. Temperature (°C): 1) 400; 2) 450; 3) 500; 4) 550; 5) 600.

Fig. 11. Variation of $\ln \underline{k}$ with $1/T$ for the hydrolysis of manganese chloride. A) $\ln k \cdot 10^{-3}$, B) $\dfrac{1}{T} \cdot 10^{-4}$. 1) In steam, 2) in steam—air mixture.

the discrepancy being so great that it cannot be attributed to experimental error. At these temperatures the reaction rate increases so sharply that evidently the Arrhenius equation is not applicable. The values of the activation energy are given below:
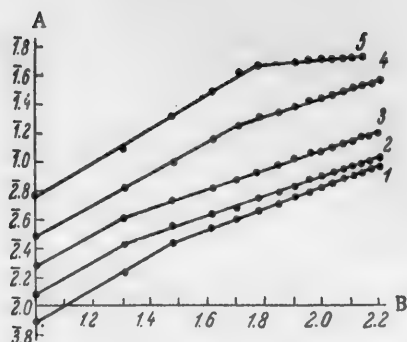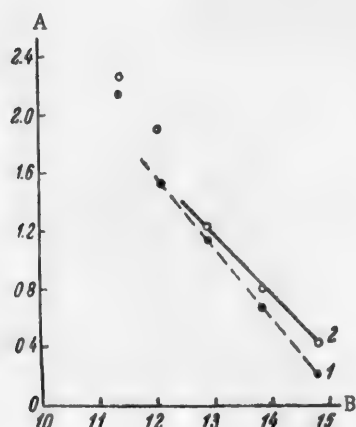
TABLE 1

Values of $\underline{n}$ and $\underline{k}$ for the Reaction in Steam

Before the maximum					
t (in °C)	400	450	500	550	600
n . . .	1.15	1.16	1.16	1.18	1.19
$k \cdot 10^{-3}$	1.25	1.975	3.1	4.58	8.151

After the maximum					
t (in °C)	400	450	500	550	600
n . . .	0.16	0.7	0.68	0.65	0.174
$k \cdot 10^{-3}$	4.14	9.77	21.88	73.11	583.4

TABLE 2

Values of $\underline{n}$ and $\underline{k}$ for the Reaction in Steam—Air Mixture

Before the maximum					
t (in °C)	400	450	500	550	600
n . . .	1.16	1.2	1.25	1.28	1.29
$k \cdot 10^{-3}$	1.53	2.19	3.39	6.67	9.66

After the maximum					
t (in °C)	400	450	500	550	600
n . . .	0.75	0.8	0.85	0.97	0.98
$k \cdot 10^{-3}$	6.16	8.55	12.52	19.36	23.44

Experimental conditions	t (in °C)	A (in cal.)
In steam	400-500	9575
In steam—air mixture	400-500	8080

Composition of the solid products of hydrolysis. In addition to the studies of the rate of hydrolysis, we investigated the nature of the manganese oxides formed in the hydrolysis of manganese chloride.

Very scanty data are available in the literature on the hydrolysis products of manganese chloride, as this question has not been studied directly. The existing data are extremely contradictory. Some authors [8, 9] consider that the product of interaction of manganese chloride with steam is MnO, others [14] that it is Mn_2O_3 and yet others [15, 16] that it is Mn_3O_4.

Our experiments showed that pure MnO cannot be formed under the conditions used, as all the hydrolysis products were brown or brownish black in all cases, whereas MnO is green.

Therefore it may be assumed that the hydrolysis products consist either of pure Mn_2O_3 and Mn_3O_4, or a mixtures of all three oxides.

There are several methods for the chemical analysis of manganese oxides in their simultaneous presence [17-19]. However, our experiments showed that these methods do not give sufficiently reliable results.

It is known that the most reliable methods for the analysis of solid multicomponent systems are physico-chemical methods, and in particular, thermal analysis. Pure manganese oxides and their mixtures have all been studied fully, and exhaustive data on them are available in the literature. We therefore used the thermal curves for manganese oxides given in Rode's book [20], and compared these with thermograms for our hydrolysis products obtained at different temperatures.
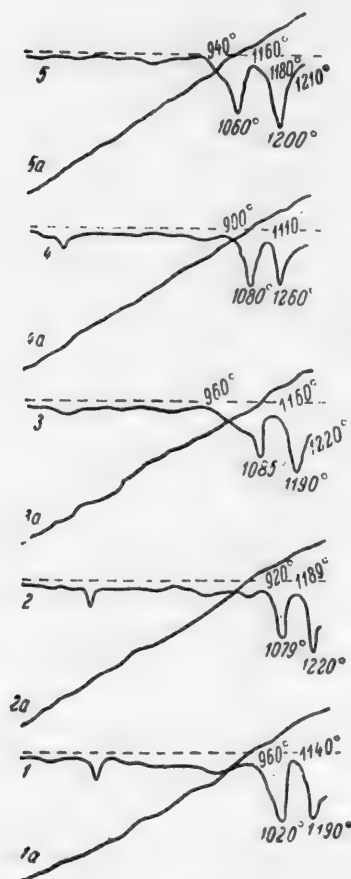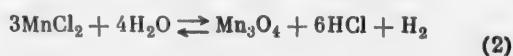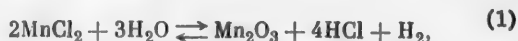

Fig. 12. Thermograms of hydrolysis products formed at different temperatures. Temperature (°C): 1) 400; 2) 450; 3) 500; 4) 550; 5) 600. Reaction medium: 1, 4, 5) steam—air mixture, 2, 3) steam.

The thermograms were obtained in air, with the aid of Kurnakov's pyrometer. The samples were previously washed with water acidified with hydrochloric acid, to remove unhydrolyzed manganese chloride, and then water to remove chloride ions. they were then dried at 230°.

Some of the thermograms are shown in Fig. 12. It is seen that each has two endothermic effects, the first in the 920–1080° range, and the second in the 1160-1200° range, the second being reversible. The thermograms of samples obtained at lower temperatures, 400- 450°, have a small endothermic effect in the 310-400° range, this may be attributed to incomplete removal of manganese chloride owing to the low degree of hydrolysis at these temperatures.

Comparison of these curves with the thermograms in Rode's book [20] shows that such a curve is given by β -Mn_2O_3, which at 940-1060° passes into β -Mn_3O_4, while at 1180-1220° β -Mn_3O_4, is converted into γ -Mn_3O_4. This last thermal effect is reversible. However, such a curve does not exclude the presence of β -Mn_3O_4, which has an endothermic effect at 1180-1220°. Chemical analysis for total manganese (Table 3) showed that the composition of the hydrolysis products approximates to a stoichiometric mixture of Mn_2O_3 and Mn_3O_4, with a slight excess of Mn_2O_3 is some cases. Hence it may be concluded that hydrolysis of manganese chloride, both in steam and in steam—air mixture, gives a mixture of the oxides β -Mn_2O_3 and β -Mn_3O_4, and the hydrolysis reactions may be represented as

$$2MnCl_2 + 3H_2O \rightleftarrows Mn_2O_3 + 4HCl + H_2, \quad (1)$$

$$3MnCl_2 + 4H_2O \rightleftarrows Mn_3O_4 + 6HCl + H_2 \quad (2)$$

for the reaction in steam, and as

$$4MnCl_2 + 4H_2O + O_2 \rightleftarrows 2Mn_2O_3 + 8HCl, \tag{3}$$

$$6MnCl_2 + 6H_2O + O_2 \rightleftarrows 2Mn_3O_4 + 12HCl \tag{4}$$

for the reaction in steam—air mixture.

TABLE 3

Manganese Contents of the Hydrolysis Products

Formation conditions of hydrolysis products	Mn content (%)
Pure MnO	77.5
Pure Mn_3O_4	72.1
Pure Mn_2O_3	69.4
Pure MnO_2	63.9
Steam—air mixture, 600°	70.9
Steam, 600°	70.1
Steam—air mixture, 350°	70.5
Steam—air mixture, 500°	70.7
Steam, 500°	71.1
Steam—air mixture, 450°	69.6
Steam, 450°	70.3
Steam—air mixture, 400°	69.8
Steam, 400°	71.2

DISCUSSION OF RESULTS

Analysis of the experimental data obtained in the study of the hydrolysis rate of manganese chloride confirms that this reaction belongs to the group of topochemical reactions. It is known that the first stage in such reactions is an induction period. It follows from Figs. 4 and 5 that the induction period in this process is very short; the higher the reaction temperature, the steeper are the kinetic curves and the shorter is the induction period. At 550-600° it is totally absent.

The explanation for the absence of an induction period is that manganese chloride crystallizes in the form of a hydrate which, according to the views of a number of authors [21, 9] may be regarded as the complex compounds$[Mn(H_2O)_4]Cl_2$ with water in the inner group. When the compound is heated the water is removed and the crystal lattice of manganese chloride breaks down; the reactivity of the salt is thereby increased considerably. The higher the temperature, the more rapid this process is and the more active centers are formed on the salt surface.

Moreover, as was shown by our investigations of hydrated manganese chloride, and by the work of others [3, 7] on other chlorides, removal of water of crystallization is accompanied by partial hydrolysis with formation of metal oxides, which may subsequently catalyze the reaction.

The second stage of a topochemical reaction is the period of increase of the rate from zero to the maximum value. For the reaction under consideration, this period is 20 minutes, during which the hydrolysis rate reaches its maximum. During this time the extent of the reaction zone becomes fairly large, and covers all or most of the manganese chloride surface. This leads to the third stage — more or less rapid decrease of the reaction rate. The layer of hydrolysis products thickens, hinders diffusion of the gaseous reactant and reaction products, and thereby retards the reaction.

These views are confirmed by analysis of the values of the parameters $\underline{n}$ and $\underline{k}$ in the kinetic equation for the process. The values show that the rate of hydrolysis cannot be expressed uniquely for the temperatures chosen.

The value of $\underline{n}$ is greater in the initial than in the final stage at all temperatures. This shows that the hydrolysis occurs in different regions at the same temperature. In all cases the value of $\underline{n}$ in the initial stage of the reaction is greater than unity, and therefore the hydrolysis of manganese chloride occurs in the kinetic region. The rate of diffusion of steam to the chloride surface during this period has no

appreciable influence on the rate of the over-all process. Beyond the maximum the value of $\underline{n}$ decreases and becomes less than unity but more than 0.5; this indicates that the process is diffusional—kinetic. The explanation is that a considerable amount of manganese chloride reacts during the initial period and the product of hydrolysis hinders the penetration of steam and oxygen to the chloride; their concentration in the reaction zone decreases. The diffusion of the gaseous products of hydrolysis is also slowed down and their concentration in the reaction zone increases.

In steam, the values of $\underline{n}$ and $\underline{k}$ increase with temperature at the initial stage and decrease at the final stage. This indicates that at the start of the process the reaction rate increases with temperature, as is the case with most kinetic processes, and then decreases, because the chemical process is complicated by diffusion factors with accumulation of hydrolysis products. The higher the temperature, the more of the reaction products accumulate in the initial stage of the process, and hence the lower the reaction rate in the final stage will be.

In steam—air mixture, the situation with regard to $\underline{n}$ is somewhat different. The value of $\underline{n}$ increases with temperature both in the initial and in the final stage of the process. Evidently the presence of oxygen not only increases the rate of chemical reaction but favors the formation of a looser layer of the reaction products, so that diffusion is easier.

The somewhat lower activation energy than that found for the reaction in steam is further evidence for the above.

SUMMARY

1. It is shown that the hydrolysis product of manganese chloride is a mixture of the oxides β-Mn_2O_3 and β-Mn_3O_4.

2. The rate of hydrolysis is negligible at 400-450°, and increases greatly at 550-600°.

3. The rate of the hydrolysis reaction greatly increases in presence of oxygen, especially at high temperatures.

4. The hydrolysis of manganese chloride is a topochemical reaction; in the temperature region studied, it is a kinetic process at the initial stage, and a kinetic—diffusional process in the final stage.

LITERATURE CITED

[1] M. V. Ionin, Powder Metallurgy, Proceedings of a Scientific-Technical Session, 113 (Metallurgy Press, 1954).*

[2] H. Schulze, and C. Vogt. Zbl. 125, 6, 1342 (1954).

[3] Eschelmann, Chem. Ind., 12, 2, 25 (1889).

[4] W. Moldenhauer, Z. anorg. Ch., 51, 36, 9 (1906).

[5] B. Kosmann, Die Darstellung von Chlor und Chlorwasserstoffsäure aus Chlormagnesium. Berlin (1851).

[6] Zambonini, Atti dei Zine, 5, 15 (1906).

[7] I. A. Kablukov, Trans. Moscow Chemical Sci.-Res. Inst. 1035 (1925).

[8] G. V. Ivanov, Candidate's Dissertation (1946).

[9] V. P. Ivantsov, Trans. State Univ. Tomsk 126, 78 (1954); Candidate's Dissertation (1947).

[10] A. N. Kolmogorov, Bull. Acad. Sci. USSR, Div. Math. Sci. 3, 355 (1937).

[11] A. N. Kolmogorov, Metallurgist 6 (1936); Kinetic Principles of Metallurgical Processes (Leningrad, 1946). *

[12] B. V. Efrofeev, Proc. Acad. Sci. USSR 52, 515 (1946).

[13] M. M. Pavlyuchenko and G. A. Lazerko, J. Phys. Chem. 28, 102, 109 (1954).

[14] A. V. Zverev and V. E. Mitrofanov, Matl. Geol. Lab. Admin. Bull. 5 (29), 18 (1945).

*In Russian.

[15] V. A. Vanyukov, Affinities of the Elements at High Temperatures in Relation to Mendeleev's Periodic System (Moscow, 1916).

[16] Yu.V. Karyakin, Pure Chemical Reagents (ONTI, Moscow—Leningrad, 1947).*

[17] A. M. Zanko and V. F. Stefanovsky, J. Gen. Chem. 4, 404 (1934); J. Appl. Chem. 14, 9, 2192 (1936).

[18] E. I. Eristavi and D. N. Barnabashvili, Trans. Tbilisi Chem. Inst. 5, 9 (1942).

[19] A. K. Lavrukhina, J. Anal. Chem. 4, 40 (1949).

[20] E. Ya. Rode, Oxygen Compounds of Manganese (Moscow, 1952).*

[21] A. A. Grinberg, Introduction to the Chemistry of Complex Compounds (Moscow—Leningrad, 1951).*

---

* In Russian.

INFLUENCE OF FUNDAMENTAL PHYSICOCHEMICAL FACTORS ON THE ADSORPTION RATE OF NITROGEN OXIDES IN $Ca(OH)_2$ SOLUTION IN HIGH-SPEED MECHANICAL ABSORBERS*

S. N. Ganz and M. A. Lokshin

The Dnepropetrovsk Institute of Chemical Technology

The proceding communication [1] dealt with the influence of hydrodynamic conditions in high-speed mechanical absorbers on the rate of absorption of nitrogen oxides by $Ca(OH)_2$ solution.

The present paper contains the results of a study of the influence of fundamental physicochemical factors on the rate of this process.

A mechanical absorber of the pilot plant unit was used; the gas was supplied from the nitric acid plant.

The fundamental physicochemical factors which determine the rate of the process are: temperature; concentrations of CaO, nitrate, and nitrite in the solution; concentration and the degree of oxidation of nitrogen oxides in the gas.

Experimental data on the influence of temperature on the coefficients of absorption of nitrogen oxides by $Ca(OH)_2$ solution were published earlier [2]. These data indicate that the absorption coefficients remain almost constant with increase of temperature to 40°. The absorption rate decreases considerably with increase of temperature above 45-50°. Similar results were obtained by Kuzminykh et al., [3] in their studies of the absorption of nitrogen oxides by milk of lime in bubbling equipment.

Some data on the influence of the concentration of nitrogen oxides in the gas on the absorption rate are given in our earlier communication [1].

Here this factor is considered in greater detail in conjunction with other physicochemical factors.

Influence of the Concentrations of CaO, Nitrite, and Nitrate in the Solution on the Absorption Process

It was found in experiments with packed towers [4] that at certain proportions of calcium nitrite and nitrate and CaO in the solution precipitation of the basic salt $[Ca(OH_2)_2 \cdot Ca(NO_3)_2 \cdot 2H_2O]$ is possible. For example, it has been reported that rapid formation of basic salts occurs at a total nitrogen concentration of the solution of 11.75%, with nitrite—nitrate ratio 1.32:1, when 40-45 g/liter of CaO (about 3.3%) is added to the solution. With 6.5% total nitrogen and 2.8% nitrite nitrogen in the solution, addition of 1% CaO produces vigorous foaming of the solution and an appreciable increase of viscosity. A thick gelatinous mass is formed when the CaO content is further increased to 3%.

Therefore the concentrations of CaO and nitrite—nitrate in the absorption of nitrogen oxides must be such as to preclude the formation of a solid precipitate.

According to our results, appreciable thickening of the solution at rest begins when it contains 40-45 g CaO and 285-290 g of calcium nitrite + nitrate per liter. In our experiments with a mechanical absorber we worked in the region of the most dangerous concentrations of CaO and nitrite + nitrate (450-500 g/liter of $Ca(NO_3)_2 + Ca(NO_2)_2$ and 30-40 g/liter of CaO) without formation of a precipitate anywhere in the absorber; this was probably due to high turbulence of the liquid, which prevented aggregation of the individual particles into large agglomerates.

*Communication II.

Nevertheless, since there was a risk of formation of basic salts, many of the experiments were performed with solutions containing 3-4.5 g/liter of active CaO and up to 470-500 g/liter of nitrite + nitrate.

For packed towers, empirical relationships have been found between the degree of absorption and the concentration of calcium nitrite + nitrate in the solution [4]. These relationships are linear. For example, when the concentration of nitrogen oxides is in the range 0.8-1.2%, the degree of absorption is given by the equation

$$\alpha = 100 - 0.1042 \cdot C_L. \tag{1}$$

For 0.3-0.6% concentrations, the degree of absorption can be found from the equation:

$$\alpha = 100 - 0.1362 \cdot C_L. \tag{2}$$

where α is the degree of absorption (in %), and C_L is the total concentration of Ca nitrite + nitrate (in g/liter).

In practical plant conditions, the degrees of absorption are less than the calculated values given by Equations (1) and (2). However, it follows from these equations that the degree of absorption decreases with increasing concentration of calcium nitrite + nitrate in the solution, and with decreasing concentration of nitrogen oxides in the gas. Experiments in packed towers showed that increase of the calcium nitrite + nitrate concentration in the solution leads to a decrease of the degree of absorption in all cases.

The same experiments showed that the concentration of active CaO in the circulating liquor, if its content of calcium nitrite + nitrate is low has little or no influence on the degree of absorption.

The fundamental results of these investigations are confirmed by our experiments on absorption in mechanical absorbers. The following constant conditions were maintained in our experiments: gas rate $w = 400$ m^3/m$^3 \cdot$ hour, peripheral disk speed $v_d = 23$ m/second, and t = 65-75°.

The calcium nitrite + nitrate concentration increased from 0 to 480-500 g/liter. Separate series of experiments were carried out at the following concentrations of nitrogen oxides in the gas: 0.25-0.5%, 0.9-1%, and 2-2.25%.

In most of the experiments at these concentrations of nitrogen oxides the solution contained 3-5 g of active CaO per liter. A separate series of experiments was carried out with 1% of NO + NO$_2$ in the gas, and 30-35 g/liter of CaO in the solution.

The results of these experiments are given in Fig. 1. Table 1, for average concentrations of nitrogen oxides, contains the calculated values of the absorption rates, driving force, and absorption coefficients, for different concentrations of calcium nitrite + nitrate in the solution and NO + NO$_2$ * in the gas. These calculated data were used to plot K as a function of C_L and $\underline{x}$; the graphs are given in Fig. 2.

According to the experimental data (Fig. 1), increase of nitrite + nitrate concentration in the solution leads to a decrease of the degree of absorption in all cases. However, the relationship here is not linear, as is the case in packed towers; this is probably because used a wider range of nitrite + nitrate concentrations.
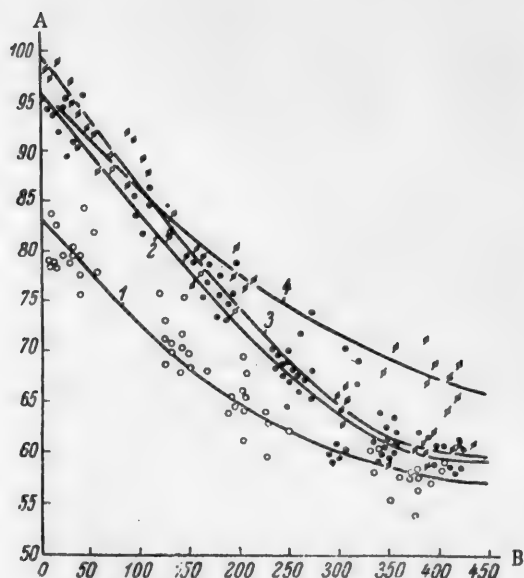
Fig. 1. Variation of the degree of absorption of nitrogen oxides by Ca(OH)$_2$ solution with the contents of CaO and nitrite + nitrate; w = 400 m^3/m$^3 \cdot$ hour, v_d = 23 m/second, t_{av} = 65°. A) Degree of absorption (in %), B) concentration of Ca(NO$_3$)$_2$ + Ca(NO$_2$)$_2$ (in g/liter). Concentrations of NO + NO$_2$ in the gas (in %): 1) 0.25-0.5; 2) 0.9-1.1; 3) 2-2.2; 4) 0.9-1.1 with CaO content 30-35 g/liter.

---

* With 60-65% oxidation of NO.

TABLE 1

Dependence of the Absorption Rate on the Concentrations of NO + NO$_2$[*] in the Gas and Calcium Nitrite + Nitrate in the Solution at w = 400 m^3/m$^3 \cdot$ hour, v_d = 23 m/second, and t = 60-65°

Contents of Ca(NO$_3$)$_2$ + +Ca(NO$_2$)$_2$	Average concentration of NO+NO$_2$ at		Degree of absorption	Absorption rate	Driving force of absorption	Absorption coefficient	CaO content of solution
	entry	exit					
C_L	x_1	x_2	α	$G/v \cdot \tau$	ΔP	K_g	g
g/liter	%	%	%	kg/m$^3 \cdot$ hour	atm.	kg/m$^3 \cdot$ hour $\cdot$ atm.	g/liter
50		0.105	77.9	1.850	0.00245	755	
150		0.150	68.4	1.625	0.00282	576	
250	0.475	0.180	62.2	1.475	0.00304	482	
350		0.195	59.0	1.400	0.00315	444	
450		0.205	56.9	1.350	0.00322	419	
50		0.105	89.5	4.475	0.00398	1124	
150		0.220	78.0	3.900	0.00516	756	
250	1.000	0.320	68.0	3.400	0.00597	570	3—5
350		0.390	61.0	3.050	0.00649	470	
450		0.400	60.0	3.000	0.00656	457	
50		0.150	92.9	9.875	0.00746	1324	
150		0.420	80.0	8.525	0.011053	810	
250	2.125	0.650	69.4	7.375	0.01247	591	
350		0.820	61.5	6.525	0.01355	482	
450		0.850	60.0	6.375	0.01393	458	
50		0.090	91.0	4.550	0.00378	1204	
150		0.185	81.5	4.075	0.00484	842	
250	1.000	0.255	74.5	3.725	0.00546	682	30—35
350		0.305	69.5	3.475	0.00586	593	
450		0.340	66.0	3.300	0.00621	531	

It is significant that at low concentrations of nitrite + nitrate in the solution the differences in the degree of absorption for different concentrations of nitrogen oxides are considerably greater than in the region of high concentrations of nitrite + nitrate. The curves converge steadily when the nitrite + nitrate concentration is 300-450 g/liter. It follows from Curve 4 in Fig. 1 that an approximately 10-fold increase of the CaO concentration (to 30-35 g/liter) in presence of high concentrations of calcium nitrite + nitrate increases the degree of absorption. The explanation is that in the conditions of vigorous agitation in mechanical absorbers the rate of solution of CaO is very considerable. At 40-50° the solubility of CaO in water is 1/932 to 1/1019 parts. In the tower process, the rate of solution of CaO in water lags behind the rate of interaction of Ca(OH)$_2$ with nitric and nitrous acids. In mechanical absorbers CaO dissolves rapidly and the solution process does not determine the rate of formation of nitrite + nitrate. Moreover, the presence of excess CaO in solution prevents or restricts the inversion of calcium nitrite, which decreases the degree of absorption of nitrogen oxides.

Therefore the presence of excess CaO, if considerable amounts of calcium nitrite + nitrate are present, accelerates the absorption process.

Our experimental data were used to derive empirical equations for determination of absorption coefficients for different concentrations of nitrite + nitrate in the solution and NO + NO$_2$ in the gas.

Individual coefficients (for the influence of any one factor on K) were determined for individual gas concentrations, and were then expressed in the general form

$$K = f(C_L, x),$$

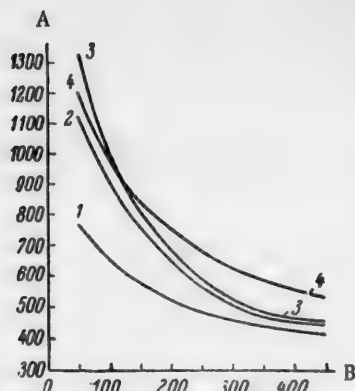[*] The degree of oxidation of NO was 60-65%.

Fig. 2. Variations of coefficients of absorption with $NO + NO_2$ concentration the gas and concentration of nitrite + nitrate in solution; $w = 400$ m³/m³·hour, $v_d = 23$ m/second, $t_{av} = 65°$. A) Absorption coefficient (in kg/m³·hour·atm), B) concentration of $Ca(NO_3)_2 + Ca(NO_2)_2$ in solution (in g/liter). Concentrations of $NO + NO_2$ in the gas (in %): 1) 0.25-0.5, 2) 0.9-1.1, 3) 2-2.5; 4) 0.9-1.1 with CaO content 30-35 g/liter.
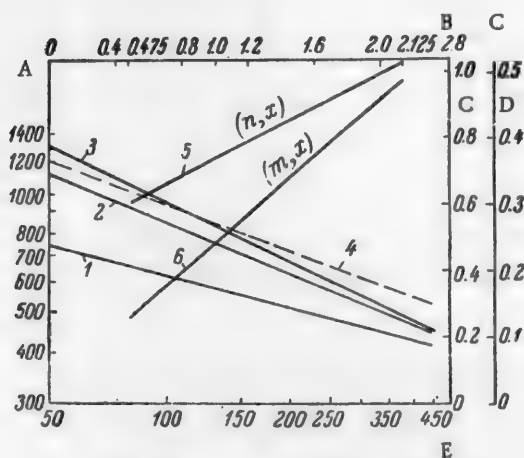

Fig. 3. Determination of absorption coefficients for different $NO + NO_2$ concentrations in the gas and concentrations of nitrite + nitrate in solution. A) Absorption coefficients on log K scale (kg/m³·hour·atm), B) concentration of $NO + NO_2$ in gas (%), C) values of the coefficient m, D) values of the coefficient n, E) concentration of $Ca(NO_3)_2 + Ca(NO_2)_2$ (in g/liter) on log C_L scale. Concentration of $NO + NO_2$ in gas (%): 1) 0.25-0.5, 1) 0.9-1.1; 3) 2-2.5; 4) 0.9-1.1; with CaO content 30-35 g/liter; 5) coefficients n and x; 6) coefficients m and α.

where C_L is the concentration of calcium nitrite + nitrate in the solution, and x is the initial concentration of $K = f(C_L, \underline{x}$ curves in Fig. 3 in rectangular coordinates, with logarithmic scales for both coordinate axes. The general form of the equation is:

$$K = m \cdot C_L^n. \qquad (3)$$

The following values were found for the coefficients $\underline{m}$ and $\underline{n}$:

$$
\begin{aligned}
m_1 &= 2154; & n_1 &= -0.268; \\
m_2 &= 5588; & n_2 &= -0.410; \\
m_3 &= 8760; & n_3 &= -0.483; \\
m_4 &= 5153; & n_4 &= -0.3717;
\end{aligned}
$$

for $x_1 = 0.475\%$
for $x_2 = 1\%$ } CaO contents 3-5 g/liter
for $x_3 = 2.125\%$
for $x_5 = 1\%$ with 30-35 g of CaO per liter

Thus, the individual coefficients of absorption are given by the equations:

$$K_{0.475} = 2154 \cdot C_L^{-0.268}, \qquad (4)$$

$$K_1 = 5588 \cdot C_L^{-0.410}, \qquad (5)$$

$$K_{2.125} = 8760 \cdot C_L^{-0.487}, \qquad (6)$$

and when $x = 1\%$ and the CaO content is 30-35 g/liter, after certain corrections.

$$K' = 5150 \cdot C_L^{-0.37} \qquad (7)$$

for $v_d = 23$ m/second, $w = 400$ m³/m³·hour, and $\underline{t}$ of gas = 60°.

To find the general formula for $x = 0.475$ to 2.125% and CaO = 3 to 4.7 g/liter, the functions $m = f_1(x)$ and $n = f_2(x)$ were plotted. Rectification gave the analytical relationship in the form:

$$
\begin{aligned}
m &= a \cdot x + b, \\
n &= a' \cdot x + b'.
\end{aligned}
$$

The following values were found graphically: a = 4400, b = 400, a' = − 0.13, b' = − 0.24.

Therefore, the values of $\underline{m}$ and $\underline{n}$ are given by the equations:

$$m = 4400x + 400,$$
$$n = -(0.13x + 0.24).$$

The general expression for the absorption coefficient as a function of the calcium nitrite + nitrate content in the solution and the $NO + NO_2$ in the gas becomes, after corrections

$$K_g = (4400x + 400) \cdot C_L^{-(0.13x+0.24)}. \tag{8}$$

This equation is valid for v_d = 23 m/second, w = 400 $m^3/m^3 \cdot$ hour, t = 60-70°, CaO = 3-5 g/liter, and x_{av} = 0.475-2.125%.

Comparison of the experimental data with values for K_g = f (C_L, x) calculated by Equation (8) gives deviations up to 2-3%, which may be caused by experimental error. Table 2 contains the values of K = f (C_L, x) calculated from Equation (8).

TABLE 2

Values of K_g (in kg /$m^3 \cdot$ hour $\cdot$ atm) for Curves 1, 2, and 3 in Fig. 1 at CaO = 3-5 g/liter, Calculated from Equation (8)

Calcium nitrate + nitrate contents (in g/liter)	K_g for $NO + NO_2$ concentration (in %)			Note
	0.475	1.0	2.125	
50	755	1124	1324	
150	576	756	810	
250	482	570	591	
350	447	470	482	Decreases at a lower rate
450	419	457	458	

Table 3 contains comparative values of K_g calculated from Equations (7) and (8), for evaluation of the absorption coefficient (from Curves 2 and 4) of Fig. 1, for different CaO contents in the solution.

TABLE 3

Values of K_g (in kg/$m^3 \cdot$ hour $\cdot$ atm) Calculated from Equations (7) and (8)

Calcium nitrite + nitrate contents (in g/liter)	K_g at CaO concentration (in g/liter)		Variation of Curve 4 (in %) relative to Curve 2	Note
	3−5	30−35		
	curve 2	curve 4		
50	1124	1204	+ 7.6	Average increase of K_g according to Curve 4 is ~ + 16%, while the CaO content is increased from 3-5 to 30-35 g/liter
150	756	842	+11.0	
250	570	682	+19.5	
350	470	593	+26.03	
450	457	531	+16.2	

The data in Table 3 were obtained at x = 1%, v_d = 23 m/second, w = 400 $m^3/m^3 \cdot$hour, t = 65-70°.

Effect of the degree of oxidation of NO on the rate of absorption of nitrogen oxides. Experience in the use of tower units showed that the lower the degree of the nitrogen oxides at the entry to the absorption tower, the lower is the degree of absorption in milk of lime. Thus, at the gas rate 11-12 m^3 per m^3 of tower per hour, at t = 27-35°, the percentage absorption of nitrogen oxides varied as follows with the initial degree of oxidation of NO: [*]

Degree of oxidation of NO (in %)	22	27	35	40	50
Absorption of NO + NO_2 (in %)	38-40	45-48	50-52	52-58	60-65

These results show that in packed towers the degree of absorption of nitrogen oxides by $Ca(OH)_2$ solution increases with increasing degree of oxidation of NO. To study the effect of the degree of oxidation of NO on absorption in mechanical absorbers, we included 5 pairs of pilot-unit acid-absorption towers before the alkaline absorption stage. By regulation of the liquor rate in the last acid tower, and by subsequent exclusion of this tower from the liquor system, we were able to vary the degree of oxidation of NO between 25 and 85%, and to study the degree of absorption NO + NO_2 by $Ca(OH)_2$ solution in this range. The following conditions were kept constant during the experiments: t_{gas} = 30-35°, gas rate w = 300-320 $m^3/m^3 \cdot$hour, peripheral disk speed 23 m/second, CaO content 4-6 g/liter, calcium nitrite + nitrate content 200-250 g/liter. Thus, the conditions of absorption in the mechanical absorber were identical to those in the tower system, except that the gas rate in our experiments was 22-25 times that in the towers.

The experiments were carried out at two gas concentrations, 0.5-0.7 and 1-1.3%.

The results are tabulated in Table 4 and plotted in Fig. 4.

TABLE 4

Variation of the Degree of Absorption of Nitrogen Oxides by $Ca(OH)_2$ Solutions with the Degree of Oxidation of NO at w = 300 $m^3/m^3 \cdot$hour

Average NO + NO_2 content at entry (%)	Average degree of oxidation of NO (%)	Content of NO + NO_2 at exit (%)	Degree of absorption (%)	Average NO + NO_2 content at entry (%)	Average degree of oxidation of NO (%)	Content of NO + NO_2 at exit (%)	Degree of absorption (%)
2.2	30	0.371	69.8	0.6	32	0.228	62.0
	42	0.288	76.6		40	0.202	67.0
	50	0.264	78.4		52	0.177	71.5
	65	0.260	81.6		60	0.175	72.5
	70	0.258	82.1		68	0.172	73.2

The following conclusions may be drawn from the data in Table 4.

1) The rate of the process depends to a considerable extent on the concentration of nitrogen oxides in the gas. Apart from the direct influence of the concentration factor, the oxidation rate of NO in the gas phase is proportional to the square of its concentration. Therefore the over-all absorption process is more rapid with more highly concentrated gases.

2) The rate of absorption of nitrogen oxides depends to a considerable extent on the degree of oxidation of NO.

At first, as the degree of oxidation of NO increases to 45-50% the absorption rate increases rapidly, but subsequently the rate of increase diminishes (Fig. 4). The absorption of N_2O_3 is accompanied by absorption of NO_2. Zhavoronkov et al., [5] reached the same conclusion. These authors reported that at the end of the process the relative content of NO is considerably higher than that of NO_2 in the gas as a consequence of the parallel absorption of N_2O_3 and NO_2. In our experiments analysis of the exit gases likewise showed that the relative

[*] The CaO content of the solution was 4-6 g/liter, and the final $Ca(NO_3)_2$ + $Ca(NO_2)_2$ content was 200-210 g/liter.

content of NO in the gas is higher than that of NO_2, even when the nitric oxide (before entry into the apparatus) was 50-55% oxidized. This indicates that absorption of NO_2 accompanies absorption of N_2O_3.

The simultaneous absorption of NO_2 and N_2O_3 accounts for the fact that in the absorption of gases of a low degree of oxidation ($NO_2 < 50\%$) calcium nitrate is formed as well as nitrite. In pilot-plant tests calcium nitrate was formed in solution when the degree of oxidation was less than 30%. Fig. 5 shows the relative proportions of calcium nitrate and nitrite in a solution formed in a pilot-plant mechanical absorber.
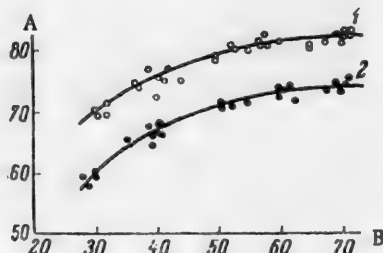

Fig. 4. Variation of the degree of absorption of nitrogen oxides by $Ca(OH)_2$ solution with the degree of oxidation of NO. $w = 300$ $m^3/m^3 \cdot$ hour, $v_d = 23$ m/second, $t_{av} = 32°$. Oxygen content of exit gas 4-5%. CaO content 6-8 g/liter. A) Degree of absorption (%), B) degree of oxidation of NO (%). Concentration of NO + NO_2 (in %): 1) 1.2; 2) 0.6.
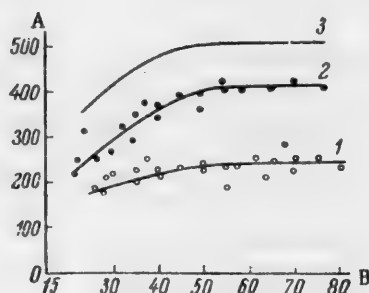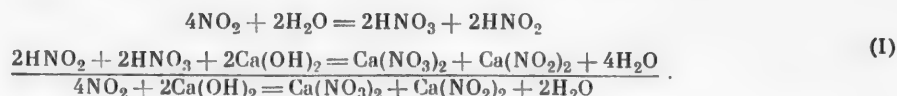
Fig. 5. Relative proportions fo calcium nitrite and nitrate in solution for different degrees of oxidation of NO. $w = 300$-320 $m^3/m^3 \cdot$ hour, $v_d = 23$ m/second, CaO 6-8 g/liter, oxygen in exit gas, 4-5%. A) Content of $Ca(NO_3)_2 + Ca(NO_2)_2$ (in g/liter), B) Degree of oxidation of NO (%). 1) $Ca(NO_2)_2$; 2) $Ca(NO_3)_2 + Ca(NO_2)_2$; 3) theoretical content of $Ca(NO_3)_2$ with absorption of NO_2 only.

Curve 1 (Fig. 5) represents the calcium nitrite content, and Curve 2 represents the total nitrogen present in the solution as calcium nitrite and nitrate. Curve 3 was found by calculation; it shows the amount of $Ca(NO_3)_2$ which would be formed in the solution if only NO_2 was absorbed.

The results plotted in Fig. 5 were obtained at gas rate $w = 300$ $m^3/m^3 \cdot$ hour, which corresponds to a contact time of 8.4 seconds for the gas in the absorber.

Comparison of the experimental data in Fig. 5 with values calculated for homogeneous oxidation of NO in the gas phase leads to the conclusion that the oxidation of NO is more rapid in conditions of high turbulence. With increase of the peripheral disk speed above 22-23 m/second the rate of absorption of NO_2 becomes equal to the rate of absorption of N_2O_3.

<u>Mechanism of formation of calcium nitrite + nitrate in conditions of high turbulence</u>. The formation of nitrite + nitrate by the reaction of $Ca(OH)_2$ with NO_2 can be represented by the equations:

$$4NO_2 + 2H_2O = 2HNO_3 + 2HNO_2$$
$$\frac{2HNO_2 + 2HNO_3 + 2Ca(OH)_2 = Ca(NO_3)_2 + Ca(NO_2)_2 + 4H_2O}{4NO_2 + 2Ca(OH)_2 = Ca(NO_3)_2 + Ca(NO_2)_2 + 2H_2O} \; . \tag{I}$$

According to Equation (I), if nitrogen oxides are present in the gas as NO_2 only, equimolecular amounts of $Ca(NO_3)_2$ and $Ca(NO_2)_2$ are formed, and 132 g of $Ca(NO_2)_2$ is formed per 164 g of $Ca(NO_3)_2$. Consequently, the weight ratio of calcium nitrate to nitrite is $164:132 = 1.24$. We shall use this value as the conversion factor. If $Ca(OH)_2$ reacts with N_2O_3, only $Ca(NO_2)_2$ is formed, according to the equation

$$N_2O_3 + Ca(OH)_2 = Ca(NO_2)_2 + H_2O. \tag{II}$$

In the pilot-plant experiments, the degree of oxidation of NO at the entry into the absorber was 65-70%. Calculated on the free volume of the absorber, the gas remained in it for 6-6.5 seconds (at $w = 400 \text{ m}^3/\text{m}^3 \cdot \text{hour}$). During this time, at $t = 60-70°$, with 1% NO + NO_2 and 15-16% O_2 in the gas, the maximum degree of oxidation of NO could reach 90%, while at concentrations below 1% it would be still less. Nevertheless, the results of the experiments show that more nitrate than nitrite was formed. This indicates that the oxidation of NO is more rapid than an equation for a reaction of the third order suggests.

With continuous operation of the unit and recycling of the liquor, nitrite + nitrate accumulated in the solution. At first the system was filled with 5 m^3 of $Ca(OH)_2$ solution containing 75-80 g CaO per liter. The solution was then recycled through the mechanical absorber. As nitrite + nitrate accumulated in the solution, part of the solution was withdrawn from the system, which was replenished with fresh $Ca(OH)_2$. The accumulation of nitrite + nitrate in the solution is shown graphically in Fig. 6. Curve 1 represents total $Ca(NO_3)_2$ + $Ca(NO_2)_2$ determined by the Devarda method, Curve 2 represents accumulation of calcium nitrite in the solution, and Curve 3 was found by calculation — by multiplication of the weights of calcium nitrite by the conversion factor 1.24, to give the weights of calcium nitrate. Curve 4 was found by addition of the weights of calcium nitrite and nitrate, and thus represents the theoretical sum of equimolecular amounts of $Ca(NO_3)_2$ and $Ca(NO_2)_2$. However, as is seen in Fig. 6, the curve for the amount of nitrogen compounds (nitrite + nitrate) actually formed lies above the theoretical curve, which indicates a small degree of preferential accumulation of nitrate.
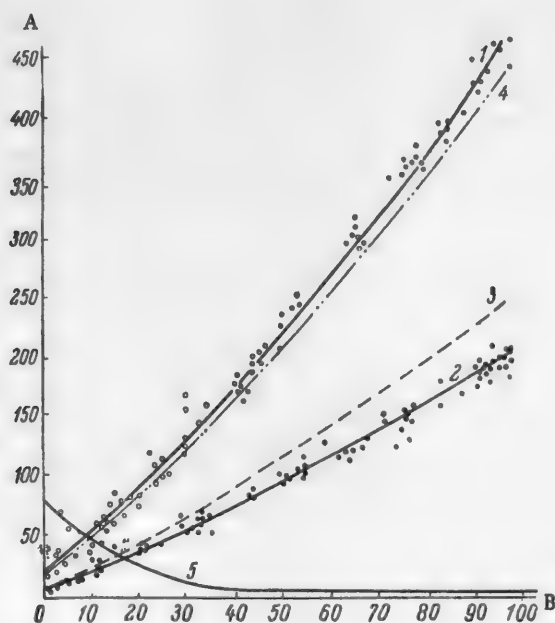
Fig. 6. Formation of calcium nitrite + nitrate as a function of the liquor circulation time.
A) Contents of $Ca(NO_3)_2$ + $Ca(NO_2)_2$ in solution (in g/liter), B) liquor circulation time (hours). 1) Sum of ($Ca(NO_3)_2$ + $Ca(NO_2)_2$ (in g/liter) actually formed; 2) calcium nitrite content (g/liter); 3) theoretical curve for $Ca(NO_3)_2$ (g/liter); 4) sum of equimolecular amounts of $Ca(NO_3)_2$ + $Ca(NO_2)_2$ (g/liter); 5) CaO content of solution (g/liter).

This result may be attributed to the following causes: a) the nitrogen oxides entering the absorber are oxidized almost completely in the liquid phase, with consequent formation of equimolecular amounts of calcium nitrite and nitrate; b) the calcium nitrite formed undergoes partial inversion by the action of nitrogen dioxide in the region where the gas enters and the liquid leaves, as here the concentration of nitrogen oxides and the degree of oxidation of NO are fairly high, while the alkalinity of the solution at the exit is virtually zero.

The nitric oxide liberated during the inversion reaction

$$Ca(NO_2)_2 + 2NO_2 = Ca(NO_3)_2 + 2NO,$$ (III)

is again oxidized to NO_2 in the liquid phase. It was stated earlier that the oxidation rate of NO in high-speed mechanical absorbers is considerably higher than the rate given by a third-order reaction equation [6]. Thus, the predominant accumulation of nitrate in solution can be attributed only to inversion.

Curve 5 in Fig. 6 represents the CaO content of the solution (in g/liter) during the entire experiment. Initially the CaO content was 75-80 g/liter, but the CaO content then decreased continuously as neutralization proceeded, and was then maintained at 3-5 g/liter.

The graph shows that when the CaO content is fairly high, and exceeds the nitrite content, the theoretical and practical curves for the total nitrogen almost coincide.

Under those conditions the reaction proceeds mainly according to Equations (I and II). However, when the CaO content is low and that of nitrite is high, the inversion of calcium nitrite, Reaction (III), is intensified.

SUMMARY

1. The influence of physicochemical factors on the rate of absorption of nitrogen oxides by $Ca(OH)_2$ solution was studied, and it was found that: a) the absorption rate decreases with increase of temperature above $45-50°$; b) in the hydrodynamic conditions used, increase of the concentration of nitrogen oxides accelerates absorption; c) in absence of nitrite + nitrate, variations of the CaO concentration have no practical effect on the rate of the process; and d) increase of the nitrite + nitrate concentration always leads to a decrease of the absorption rate. In this case, increase of the CaO concentration retards the decrease of the absorption rate.

2. It was found that in conditions of high turbulence the absorption rates of N_2O_3 and NO_2 are practically equal.

3. The predominant accumulation of nitrate in the solution is indicative of the rapid oxidation of NO to NO_2 in the liquid phase, and of the inversion reaction in the experimental conditions used.

LITERATURE CITED

[1] S. N. Ganz, J. Appl. Chem. 30, No. 9 (1957).•

[2] S. N. Ganz and S. B. Kravchinskaya, J. Appl. Chem. 28, No. 2 (1955).•

[3] I. N. Kuzminykh , E. P. Aigina and N. D. Babushkina, J. Appl. Chem. 26, No. 8 (1953).•

[4] V. E. Gorfunkel and Ya. I. Kilman, Trans. State Inst. Nitrogen Ind. 3 (Goskhimizdat, 1954).••

[5] N. M. Zhavoronkov, S. I. Bykov, Yu. M. Martynov and R. N. Chernykh, J. Chem. Ind. 7, 419 (1954).

[6] S. N. Ganz, J. Appl. Chem. 28, No. 10 (1955). •

•Original Russian pagination. See C. B. Translation.
••In Russian.

DETERMINATION OF THE RATE OF GROWTH OF HYDRARGILLITE PARTICLES IN AN ALUMINATE SOLUTION BY THE LINEAR GROWTH OF THE CRYSTAL FACES*

A. N. Lyapunov and E. P. Kholmogortseva

The first communication contained a discussion of a method for determination of the growth of crystalline particles in a supersaturated solution, based on the particle-size composition of the precipitates before and after growth of the particles. The present communication contains a description of the experiments and details of the results obtained in studies of the growth of hydrargillite particles in aluminate solutions.

EXPERIMENTAL METHODS

Particle-size analysis of hydrargillite precipitates. In the technical production of alumina, the particle-size composition of the hydrargillite precipitates is determined by means of areometric sedimentation analysis. The principle of the method, the measurement technique, and the calculation procedure are described in detail by Zverevich [1]. This method was convenient for our purpose on the following grounds. First, there is no need to use a graphical method for determination of the size-distribution curve from the sedimentation curve, based on construction of tangents at various points of the latter curve. The graphical construction introduces appreciable errors into the final result. Second, this method cannot be used for determination of the size distribution of particles smaller than 20μ. This limitation satisfies the condition that the particle-size distribution curve for hydrargillite should not reflect the distribution of "young" particles formed from nuclei. In our experimental conditions, these particles could not be larger than $20-25 \mu$.

The liquid used for areometric sedimentation analysis is water; the hydrargillite precipitate was air-dry and washed free from alkali. It should be noted in this connection that the properties of washed and air-dried hydrargillite precipitate differ somewhat from the properties of a precipitate not subjected to this treatment. For example, washed and air-dried precipitates are usually of low activity and readily dispersed in aluminate solution. These properties are much less pronounced in precipitates which had not been wholly separated from from the aluminate solution. Changes in the properties of the precipitate in the course of the sedimentation analysis could not be permitted, as the sediment formed in the cylinder after anlysis was transferred completely into aluminate solution for determination of the growth of the hydrargillite particles. For this reason, aluminate solution (the mother liquor after the decomposition) was used instead of water for sedimentation analysis.

The following procedure was used to test the use of the aluminate mother liquor as the liquid for areometric sedimentation analysis. The particle-size distributions of coarse hydrargillite precipitate and of the fine precipitate used for seeding were determined. Mixtures were then made up from these precipitates. The first mixture contained 25% of the production precipitate and 75% of the seeding precipitate. The secon mixture contained 52.4% of the production and 47.6% of the seeding precipitate. The third mixture contained 76.0 and 24.0% of the course and fine precipitates respectively. The particle-size composition of these mixtures was determined by direct sedimentation analysis. In Fig. 1, Curve 1 in each case represents the size distribution of the seeding hydrargillite; Curve 2, of the production precipitate; Curve 3, of the mixture, as determined by direct sedimentation analysis; and Curve 4, of the mixture, calculated from the distributions of the production and seeding hydrargillites (the calculated points are denoted by circles).

*Communication II.

The distribution curves for the mixtures show good agreement between the calculated values and the data of direct sedimentation analyses for particles between 30 and 70 μ. The agreement was particularly good for mixtures in which the fine precipitate was "coarsened" by addition of not more than 52.0% of the coarse precipitate.

This check also confirmed that the particles did not undergo aggregation or dispersion in the course of sedimentation analysis.

The hydrargillite precipitate circulating in the alumina unit of the Bogoslovskoe aluminum plant was used for the experiments. The hydrargillite precipitate was agitated with aluminate solution in glass flasks fixed in a cross piece rotating in an air thermostat. The temperature was measured to within ± 2°. The duration of each experiment was 12 hours. The aluminate solution was warmed to the temperature of the experiment on a water bath before being put into the flasks. The concentration of the hydrargillite precipitate used was low, 7-8 g/liter, rather than the 180-200 g/liter used in the production process. When the particle concentration is low, the probability of their growth by collision, coherence, and coalescence is less. Moreover, the degree of decomposition of the solution is low, and it may be assumed that particle growth occurs at constant supersaturation of the solution.
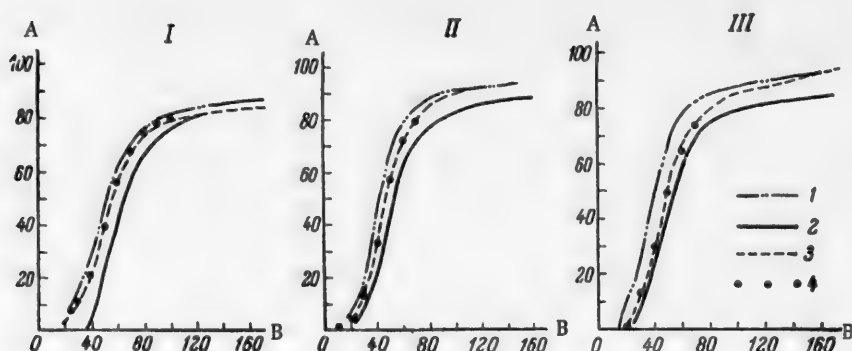

Fig. 1. Agreement between the particle-size distribution curves of hydrargillite mixtures, determined by direct sedimentation analysis, and curves calculated from the size-distribution characteristics of production and seeding hydrargillites. A) Contents of particles (wt. %), B) particle size (μ). 1) Seeds; 2) production precipitate; 3) mixture; 4) calculated data. Contents of production and seeding precipitates in the mixtures (%): I) 25 and 75; II) 52.4 and 47.6; III) 76 and 24.

In view of the fact that a hydrargillite precipitate becomes somewhat finer when introduced into a heated aluminate solution, the following steps were taken to prevent this effect from distorting the experimental results. Before introduction into the main bulk of the aluminate solution for determination of particle growth, the hydrargillite solution was kept for 1 hour in a small portion of the same heated aluminate solution. During this time the dispersion process was completed (this was confirmed by special experiments).

The precipitate was filtered off (but not pressed) to remove the aluminate solution in which it was kept, and put into the mother liquor ($Na_2O_{caustic} \simeq 125$ g/liter, $Al_2O_3 \simeq 56$ g/liter) for sedimentation analysis. The liquid was decanted from the sediment in the cylinder, the sediment was shaken in a small portion of the original aluminate solution, and the suspension was distributed uniformly between flasks containing the main bulk of the solution for the experiment.

Calculation of the increase in the particle size due to growth of the crystal faces. A specimen calculation for Experiment 1 is given. The original data, conditions, and results of this experiment are given in the Table. The same method of calculation was used for the other experiments listed in the Table. The particle-size distributions of the initial and final hydrargillite precipitates in Experiment 1 are given in Fig. 2.

The calculation was based on the balance equation and the formulas for the separate terms of this equation, which were derived in the first communication [2].

To form the balance equation

$$m_0 + \Delta_1 m + \Delta_2 m + \Delta_3 m - \Delta_4 m = m_1,$$

(where m_0 is the weight of the fraction of particles between p_1 and p_2 in the original precipitate; $\Delta_1 m$ is the initial weight of the particles between $(p_1 - v)$ and p_1 in the original precipitate; $\Delta_2 m$ is the weight increase of these particles during growth by v_{cm}; $\Delta_3 m$ is the weight increase of all the particles initially between p_1 and $(p_2 - v)$ owing to growth by v_{cm}; $\Delta_4 m$ is the weight of particles between $(p_2 - v)$ and p_2 in the original precipitate; m_1 is the weight of the fraction of particles between p_1 and p_2 in the precipitate after the experiment), the fraction with particles between $4 \cdot 10^{-3}$ and $6 \cdot 10^{-3}$ cm was chosen. It was assumed that the growth of the particles does not exceed $2 \cdot 10^{-3}$ cm. This assumption was quite legitimate, as if all the particles increased by 20μ in diameter, the amount of precipitate would be many times greater than that found in the experiment.

Results and Conditions of Experiments on the Determination of the Growth Rate of Hydrargillite Particles in Aluminate Solution

Experiment No.	Average composition of aluminate solution (in g/liter) during the experiment					Amount of original aluminate solution (liters)	Amount of seeding Al(OH)$_3$	Amount of Al(OH)$_3$ precipitated (in g)	Temperature of solution (°C)	Increase of particle size during experiment (in μ)	Increase of particle size (in μ/hour)	Number of particles with the sizes:	
	Na$_2$O$_{total}$	Na$_2$O$_{caustic}$	Al$_2$O$_3$	$\alpha_{caustic}$*	density							before experiment from $(4 \cdot 10^{-3} - v)$ to $6 \cdot 10^{-3}$ cm	after experiment from $4 \cdot 10^{-3}$ to $(6 \cdot 10^{-3} + v)$ cm
1	129.0	115.7	110.5	1.720	1.280	4.8	39.0	45.8	65	10.8	0.900	330 · 10^6	306 · 10^6
2	130.6	118.1	112.3	1.720	1.232	4.8	39.6	36.4	65	10.6	0.880	352 · 10^6	320 · 10^6
3	134.8	121.4	76.7	2.605	1.220	4.8	40.0	5.7	65	1.9	0.160	74 · 10^6	71 · 10^6
4	130.9	117.1	113.1	1.705	1.235	4.8	87.3	31.0	50	4.5	0.370	94 · 10^6	86.5 · 10^6
5	134.0	121.0	71.7	2.770	1.216	4.8	41.0	3.42	50	0.7	0.062	59 · 10^6	56 · 10^6

* $\alpha_{caustic}$ of the aluminate solution represents the molecular ratio of Na$_2$O$_{caustic}$ to Al$_2$O$_3$.
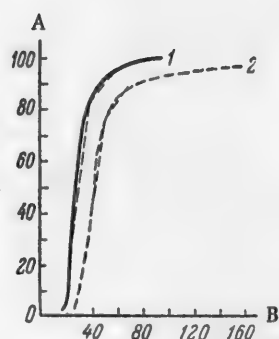
Fig. 2. Particle-size distribution of original hydrargillite seeding precipitate (Curve 1), and of the hydrargillite precipitate obtained after the experiment (Curve 2); t = 65°; $\alpha_{caustic}$ = 1.67. A) Content of particles (in wt. %), B) particle size (in μ)

The empirical equation for the section of the particle-size distribution curve of the original precipitate between $2 \cdot 10^{-3}$ and $6 \cdot 10^{-3}$ cm is rather complex, making the subsequent calculation difficult.

To avoid this difficulty, this section of the curve was replaced by two linear portions. One portion corresponds to particles between $2 \cdot 10^{-3}$ and $4 \cdot 10^{-3}$ cm, and is represented by the equation

$$q = 35.3 \cdot 10^3 p - 58.2; \quad dq = 35.3 \cdot 10^3 dp. \qquad (1)$$

the other portion corresponds to particles between $6 \cdot 10^{-3}$ cm, and is represented by the equation

$$q = 6 \cdot 10^3 p + 59; \quad dq = 6 \cdot 10^3 dp. \qquad (2)$$

We now calculate the terms of the balance equation for the fraction between $4 \cdot 10^{-3}$ and $6 \cdot 10^{-3}$ cm. The weight of the fraction of such particles in the original precipitate is $m_0 = \dfrac{39 \cdot 12}{100}$. The relative content of this fraction is 12% (see Fig. 2).

This fraction of the precipitate obtained at the end of the experiment contains particles which were between $(4 \cdot 10^{-3} - v)$ and $4 \cdot 10^{-3}$ cm in the original precipitate. The weight of these particles before growth, according to Equation (1), is:

$$\Delta_1 m = \frac{39}{100} \cdot \int\limits_{4 \cdot 10^{-3} - v}^{4 \cdot 10^{-3}} dq = \frac{39}{100} \cdot 35.3 \cdot 10^3 \cdot \int\limits_{4 \cdot 15^{-3} - v}^{4 \cdot 10^{-3}} dp = \frac{39}{100} \cdot 35.3 \cdot 10^{-3} v.$$

The increase in the weight of these particles during the experiment, according to the formula derived in the first communication, is:

$$\Delta_2 m = \frac{39}{100} \int\limits_{4 \cdot 10^{-3} - v}^{4 \cdot 10^{-3}} \left(3\frac{v}{p} + 3\frac{v^2}{p^2} + \frac{v^3}{p^3}\right) dq = \frac{39}{100} \cdot 35.3 \cdot 10^3 \int\limits_{4 \cdot 10^{-3} - v}^{4 \cdot 10^{-6}} \left(3\frac{v}{p} + 3\frac{v^2}{p^2} + \frac{v^3}{p^3}\right) dp$$

or

$$\Delta_2 m = \frac{39}{100} \cdot 35.3 \cdot 10^3 \cdot 6.9v[\log 4 \cdot 10^{-3} - \log(4 \cdot 10^{-3} - v)] -$$

$$- \frac{39}{100} \cdot 35.3 \cdot 10^3 \cdot 3v^2 \left(\frac{1}{4 \cdot 10^{-3}} - \frac{1}{4 \cdot 10^{-3} - v}\right) -$$

$$- \frac{39}{100} \cdot 35.3 \cdot 10^3 \cdot 0.5v^3 \left[\frac{1}{(4 \cdot 10^{-3})^2} - \frac{1}{(4 \cdot 10^{-3} - v)^2}\right].$$

An analogous expression gives the weight increase $\Delta_3 m$ of the particles which were between $4 \cdot 10^{-3}$ and $(6 \cdot 10^{-3} - v)$ in the original precipitate.

The expressions for $\Delta_3 m$ and for $\Delta_2 m$ differ in their integration limits; moreover, the value of dq from Equation (2) is used in the former.

$$\Delta_3 m = \frac{39}{100} \cdot \int\limits_{4 \cdot 10^{-3}}^{6 \cdot 10^{-3} - v} \left(3\frac{v}{p} + 3\frac{p^2}{p^2} + \frac{v^3}{p^3}\right) dq = \frac{39}{100} \cdot 6 \cdot 10^3 \int\limits_{4 \cdot 10^{-3}}^{6 \cdot 10^{-3} - v} \left(3\frac{v}{p} + 3\frac{v^2}{p^2} + \frac{v^3}{p^3}\right) dp$$

or

$$\Delta_3 m = \frac{39}{100} \cdot 6 \cdot 10^3 \cdot 6.9v[\log(6 \cdot 10^{-3} - v) - \lg 4 \cdot 10^{-3}] -$$

$$- \frac{39}{100} \cdot 6 \cdot 10^3 \cdot 3v^2 \left(\frac{1}{6 \cdot 10^{-3} - v} - \frac{1}{4 \cdot 10^{-3}}\right) -$$

$$- \frac{39}{100} \cdot 6 \cdot 10^3 \cdot 0.5v^3 \left[\frac{1}{(6 \cdot 10^{-3} - v)^2} - \frac{1}{(4 \cdot 10^{-3})^2}\right].$$

The particles which were between $(6 \cdot 10^{-3} - v)$ and $6 \cdot 10^{-3}$ cm in the original precipitate grew by $\underline{v}$ cm during the experiment, and left the fraction of particles between p_1 and p_2. The weight $\Delta_4 m$ of these particles, by Equation (2), is:

$$\Delta_4 m = \frac{39}{100} \cdot \int\limits_{6\cdot 10^{-3}-v}^{6\cdot 10^{-3}} dq = \frac{39}{100} \cdot 6 \cdot 10^3 \int\limits_{6\cdot 10^{-3}}^{6\cdot 10^{-3}} dp = \frac{39}{100} \cdot 6 \cdot 10^3 v.$$

The weight of the particles between $4 \cdot 10^{-3}$ and $6 \cdot 10^{-3}$ cm in the precipitate after the experiment is $m_1 = \dfrac{84.8 \cdot 45}{100} = 38$, where 45 is the percentage content of the fraction in the precipitate (see Fig. 2).

After substitution of the values of m_0, $\Delta_1 m$, $\Delta_2 m$, $\Delta_3 m$, $\Delta_4 m$, m_1 into the balance equation, we have:

$$41.4 \cdot 10^3 v \cdot \log(6 \cdot 10^{-3} - v) - 243 \cdot 10^3 v \cdot \log(4 \cdot 10^{-3} - v) +$$
$$+ \frac{105.9 \cdot 10^3 v^2}{4 \cdot 10^{-3} - v} - \frac{18 \cdot 10^3 v^2}{6 \cdot 10^{-3} - v} + \frac{17.6 \cdot 10^3 v^3}{(4 \cdot 10^3 - v)^2} -$$
$$- \frac{3 \cdot 10^3 \cdot v^3}{(6 \cdot 10^{-3} - v)^2} - 455.7 \cdot 10^3 v - 21.9 \cdot 10^6 v^2 - 0.915 \cdot 10^9 v^3 - 85.5 = 0. \qquad (3)$$

We solve this equation graphically for $\underline{v}$. Substitution of different values of $\underline{v}$ into the equation gives the values of the function $\underline{y}$ represented by this equation.

v	0	10^{-3}	$1.2 \cdot 10^{-3}$	$2 \cdot 10^{-3}$
y	-85.5	-12.7	17.1	248

The values of $\underline{v}$ and $\underline{y}$ are used to plot a curve which cuts the $\underline{v}$ axis at $v = 1.08 \cdot 10^{-3}$ cm or 10.8μ. This value of $\underline{v}$ is the required root of Equation (3). The curve does not cut the horizontal axis at any other logically admissible values of $\underline{v}$. This justifies the assumption that the value found for $v = 10.8\mu$ is the actual increase in size of the particles in the fraction from 30 to 60μ during the experiment. The growth rate of the particles is $\dfrac{10.8}{12} = 0.9\,\mu/\text{hour}$.

It now remains to examine the possibility of the growth, to some extent, of the particles as the result of collisions, adherence, and coalescence into aggregates and also of the possible entry into the fraction in question of "younger," more rapidly growing particles of initial size $< (4 \cdot 10^{-3} - v)$ cm. If these effects did not take place during the experiment, the number of particles between $(4 \cdot 10^{-3} - v)$ and $6 \cdot 10^{-3}$ cm in the original precipitate should be equal to the number of particles between $4 \cdot 10^{-3}$ and $(6 \cdot 10^{-3} + v)$ cm after the experiment. The number of particles in the original precipitate, between $4 \cdot 10^{-3} - v = 4 \cdot 10^{-3} - 1.08 \cdot 10^{-3} = 2.92 \cdot 10^{-3}$ cm and $4 \cdot 10^{-3}$ cm in size, according to Equation (1), is

$$\frac{39}{100} \cdot \frac{35.3 \cdot 10^3}{1.27} \int\limits_{2.92\cdot 10^{-3}}^{4\cdot 10^{-3}} p^{-3}\, dp.$$

The weight of one hydrargillite particle of size $\underline{p}$ is $1.27\,p^3$.

By Equation (2), the number of particles between $4 \cdot 10^{-3}$ and $6 \cdot 10^{-3}$ cm in the original precipitate is

$$\frac{39}{100} \cdot \frac{6 \cdot 10^3}{1.27} \int\limits_{4\cdot 10^{-3}}^{6\cdot 10^{-3}} p^{-3}\, dp.$$

The total number of particles between $2.92 \cdot 10^{-3}$ and $6 \cdot 10^{-3}$ cm in the seeding precipitate is

$$\frac{39 \cdot 10^3}{100 \cdot 1.27}\left[35.3 \cdot \int\limits_{2.92 \cdot 10^{-3}}^{4 \cdot 10^{-3}} p^{-3}\,dp + 6\int\limits_{4 \cdot 10^{-3}}^{6 \cdot 10^{-3}} p^{-3}\,dp\right] = 330 \cdot 10^6.$$

The section of the particle-size distribution curve for the precipitate obtained after the experiment (see Fig. 2), corresponding to particles between $4 \cdot 10^{-3}$ and $(6 \cdot 10^{-3} + v)$ cm, where $v = 1.08 \cdot 10^{-3}$ cm, is replaced by two linear portions. The first portion corresponds to particles between $4 \cdot 10^{-3}$ and $5.1 \cdot 10^{-3}$ cm. The equation for the first portion is:

$$q = 34.1 \cdot 10^3 p - 98.4; \quad dq = 34.1 \cdot 10^3 dp.$$

And for the second portion:

$$q = 5.05 \cdot 10^3 p + 53.7; \quad dq = 5.05 \cdot 10^3 dp.$$

The number of particles between $4 \cdot 10^{-3}$ and $7.08 \cdot 10^{-3}$ cm in the precipitate after the experiment is

$$\frac{84.8 \cdot 10^3}{100 \cdot 1.27}\left[34.1\int\limits_{4 \cdot 10^{-3}}^{5.1 \cdot 10^{-3}} p^{-3}\,dp + 5.05\int\limits_{5.1 \cdot 10^{-3}}^{7.08 \cdot 10^{-3}} p^{-3}\,dp\right] = 306 \cdot 10^6.$$

The number of particles for which the balance equation was formed was $330 \cdot 10^6$ before the experiment and $306 \cdot 10^6$ after the experiment, whereas the weight of the original precipitate was 39 g, and the weight of the precipitate after the decomposition was 84.8 g. The discrepancy between the numbers of particles is within the limits of experimental error and of error in analysis of the data. All the foregoing justifies the view that this method gives the true increase in the size of the hydrargillite particles as the result of the growth of crystal faces during the decomposition process.

Growth rate of hydrargillite particles as a function of the supersaturation of the aluminate solution. The Table contains data on the conditions and growth rates of hydrargillite particles in conditions other than those used in Experiment 1. The tabulated data were used to plot (Fig. 3) the growth rates of the hydrargillite particles against the degree of supersaturation of the aluminate solution. The degree of supersaturation was determined by the routine method, not described here.

The graphs show that the rate of growth of the hydrargillite particles greatly increases with supersaturation. This increase is greater at 65° than at 50°. The slope of the curve for 65° corresponds to 0.023 μ/hour per g Al_2O_3/liter of supersaturation, and that for the curve for 50°, to 0.011 μ/hour.

The growth rate of the hydrargillite particles depends to a very great extent on the temperature over the temperature range characteristic of the initial stage of the decomposition process in plant practice. For example, a growth rate of 0.3 μ/hour at 65° corresponds to a supersaturation of 15 g Al_2O_3 per liter. At 50° this same rate can only be reached at a considerably higher supersaturation, 50 g Al_2O_3 per liter.

These variations of the growth rate of the hydrargillite particles account for the fact, familiar in industrial practice, that if the initial temperature is lowered below 55° a sufficient absolute amount (the relative amount in % is not significant, as it reflects the appearance of new fine particles in the precipitate) of large particles cannot be obtained, despite high supersaturations.

The experimental data indicate that the growth kinetics of the hydrargillite particles is not determined by diffusion; this is shown by the very great influence of temperature on the growth rate.
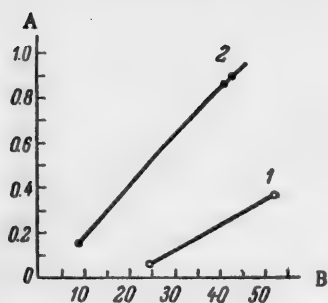
Fig. 3. Growth rate of hydrargillite particles as a function of the supersaturation of the aluminate solution. A) Particle-growth rate (in μ/hour) B) supersaturation (in g Al_2O_3 per liter). Temperature (°C): 1) 50; 2) 65.

These results also refute the view of Gerrman and Stipetisch [3] that the crystallization rate of hydrargillite is determined by steric factors. If this was the case, the rate of crystallization should decrease with increase of temperature, i.e., with increase of the intensity of thermal motion of the elementary particles constituting the crystal lattice. The experimental data show that the reverse is the case.

It must be pointed out that the growth of complex particles, consisting of concretions of small crystals and having convex and concave surfaces with various radii of curvature, is not constant but depends on the surface configuration. In this respect the proposed method for determination of the growth rate of hydrargillite particles can be used for characterization of the seeding activity of precipitates used for decomposition of aluminate solutions in alumina production.

SUMMARY

1. The growth rate of hydrargillite particles in aluminate solutions of equal degrees of supersaturation greatly increases with increase of temperature from 50 to 65°. The rate of growth of the hydrargillite particles increases with increase of the degree of supersaturation of the aluminate solution to a greater extent at 65° than at 50°.

2. The proposed method for determination of particle-growth rate may be used for estimation of the seeding activity of hydrargillite precipitates used for the decomposition of aluminate solutions in alumina production.

LITERATURE CITED

[1] V. V. Zverevich, Areometric Method for Determination of the Granulometric Composition of Finely-Divided Materials (Scientific Research Institute for Mechanical Concentration of Minerals OBVNTI).

[2] A. N. Lyapunov and E. P. Kholmogortseva, J. Appl. Chem. 30, No. 9, 1298 (1957).*

[3] L. Gerrman and J. Stipetisch, Z. allg. anorg. Ch., 262, 1-5, 258-287 (1950).

*Original Russian pagination. See C. B. Translation.

KINETICS OF GASEOUS CORROSION OF MAGNESIUM ALLOYS

I. A. Makolkin

G. V. Plekhanov Moscow Institute of National Economy

Study of the kinetics of gaseous corrosion of magnesium, the basic element of the most important alloys used in industry, is of great interest. The accumulation of reliable experimental data on the kinetics of corrosion in air and in different gases helped to develop a rational technology of heat treatment for cast magnesium alloys [1]. These data can also help us to understand the mechanism of gaseous corrosion.

Optical-mechanical and contact-interference methods, studies of electrical resistance [3] and weight loss during oxidation [4], applied to the investigation of the kinetics of the growth of oxide films at temperatures above 400°, showed that the corrosion rate of magnesium and its alloys (ML-4 and ML-5) in gaseous media is a linear function of time.

The present paper concerns the study of the gaseous corrosion of magnesium and its alloys ML-4 and ML-5 at temperatures below 400° and that of MA-1 in the range of 450-500°

The choice of the temperature range below 400° was determined by the consideration that the knowledge of the shape of the curves representing the corrosion rate within this range of temperatures is very important for the understanding of the mechanism of the corrosion process. The experiments showed that in the temperature range extending from room temperature to 400° the oxidation rate of magnesium and its alloys ML-4 and ML-5 in air follows a parabolic law. However, the effect of corrosion within this temperature range is very small and therefore it was difficult to determine systematically the loss of weight of the samples. Therefore, we chose 350° as the operating temperature; at this temperature the corrosion rate also follows the parabolic law, but its effects are sufficiently significant to allow one to perform the necessary measurements.

The experiments at 350° were performed with the aid of microbalance, according to the method described earlier [4].

Figure 1 represents the curves of gaseous corrosion rate of magnesium and its alloys ML-4 and ML-5.

The corrosion of MA-1 alloy in gases was studied with the adsorption balance described earlier [5].

Figure 2 represents the weight increase of the sample as the function of time and temperature.

Figure 2 shows that the corrosion rate of MA-1 in gases in the temperature range of 450-600° is a linear function of time except at the initial stage of the process at 600°, characterized by low corrosion rate.

As we shall see later, the addition of 2.5% Mn increases the heat resistance of magnesium; however, this addition does not affect the character of the curve representing the corrosion rate, the corrosion rate of the alloy is a linear function of time as in the case of pure magnesium.

Up to 550° all the curves are spread regularly; above this temperature, namely at 600°, the corrosion is so intense that the curve corresponding to this temperature is sharply separated from the rest of the group of curves. This curve consists of two branches: the first branch corresponds approximately to 6-7 hours of the initial oxidation; during this process the corrosion rate progressively increases and finally reaches the linear oxidation rate; the second branch is represented by straight line characterizing the constant rate of the process.
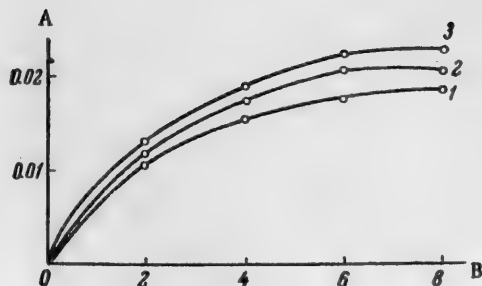
Fig. 1. Oxidation curves of Mg, ML-4 and ML-5 at 350° in air. A) Weight increase (in mg/cm^2). B) time (in hours). Curves: 1) Mg; 2) ML-4; 3) ML-5.
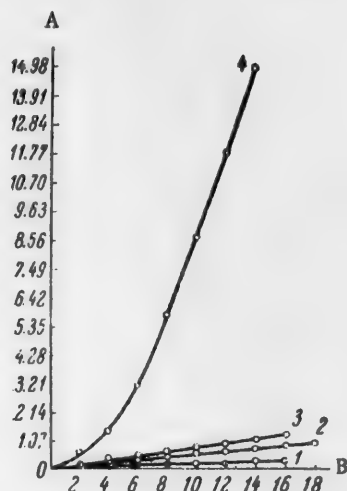

Fig. 2. Gaseous corrosion of MA-1 in air. A) Weight increase (in mg/cm^2), B) time (in hours). Temperature (in °C): 1) 450; 2) 500; 3) 550; 4) 600.

2) For the MA-1 allow:

The corrosion rate of magnesium and its alloys ML-4 and ML-5 in air at 350° follows a parabolic law and can be represented by the following equation:

$$q^2 = K\tau. \qquad (1)$$

The corrosion rate of magnesium and its alloys MA-1, ML-4 and ML-5 above 400° is best represented by the equation:

$$q = K\tau. \qquad (2)$$

In both equations q is the amount of oxygen or metal consumed during time τ and K is a constant depending only on temperature. To calculate the activation energy we shall use the results of the experiments performed at 400°. Figure 3 shows that the constant K varies with temperature according to an exponential law; this variation can be represented by the following relationship:

$$K = Ae^{-\frac{\Delta E}{RT}}, \qquad (3)$$

where K is the constant of the gaseous corrosion (in mg/cm$^2 \cdot$ min), A is the reaction constant, R is the gas constant (in calories), T is the absolute temperature and E is the activation energy.

Figure 4 represents the variation of the experimental value of log K as the function of the reciprocal of the absolute temperature (1/T).

This figure shows that the experimental points fall on a straight line, which indicates that log K varies linearly with 1/T. This relationship is expressed by the following equations: 1) for magnesium:

$$\log K = 3.8398 - \frac{5146}{T}, \qquad (4)$$

$$K = 6.883 \cdot 10^3 \cdot e^{-\frac{23550}{RT}};$$

$$\log K = 5.5276 - \frac{6613}{T}, \qquad (5)$$

$$K = 3.369 \cdot 10^5 \cdot e^{-\frac{30255}{RT}};$$
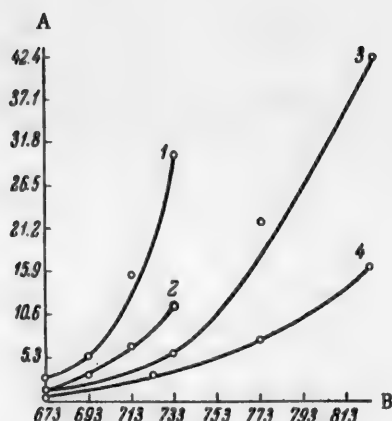
Fig. 3. Effect of temperature on the rate constant relative to gaseous corrosion. A) Constant of the reaction rate $K \cdot 10^4$, B) temperature (in °K). Curves: 1) ML-5; 2) ML-4; 3) Mg; 4) MA-1.
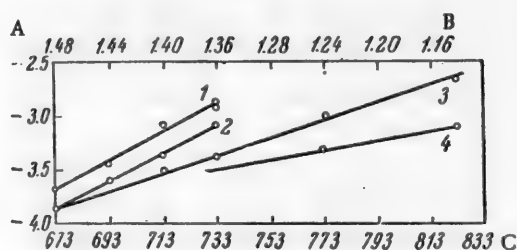
Fig. 4. Variation of log K as the function of 1/T in the case of gaseous corrosion of Mg, ML-4, ML-5, and MA-1 in air at 400° and above. A) Value of log K, B) value of 1000/T, C) temperature (°K). Curves: 1) ML-5; 2) ML-4; 3) Mg; 4) MA-1.

Heating in a Mixture of CO_2 and Air

Alloy ML-4

3) for the ML-4 allow:

$$\log K = 10.0267 - \frac{9369}{T}, \qquad (6)$$

$$K = 1.063 \cdot 10^{10} \cdot e^{-\frac{42860}{RT}};$$

4) for the ML-5 allow:

$$\log K = 10.167 - \frac{9245}{T}, \qquad (7)$$

$$K = 1.469 \cdot 10^{10} \cdot e^{-\frac{42300}{RT}}.$$

In these equations the numbers 23,550, 30,255, 42,860 and 42,300 represent the values of the activation energies for the corrosion processes occurring in air in the case of magnesium, MA-1, ML-4, and ML-5 allows.

In our earlier work [4] we have shown that the corrosion rate of ML-4 and ML-5 in nitrogen, mixtures of carbon dioxide and air, and sulfur dioxide and air, decreases with time. These processes can be described by the following equations:

Heating in Nitrogen

a) alloy ML-4

$$\log K = 15.000 - \frac{13610}{T}, \qquad (8)$$

$$K = 1 \cdot 10^{15} \cdot e^{-\frac{62270}{RT}};$$

b) alloy ML-5

$$\log K = 21.666 - \frac{18340}{T},$$

$$K = 4.634 \cdot 10^{21} \cdot e^{-\frac{83906}{RT}}. \qquad (9)$$

$$\log K = -0.2143 - \frac{2874}{T},$$

$$K = 1.638 \cdot 10^{-4} \cdot e^{-\frac{13150}{RT}}. \qquad (10)$$

Alloy ML-5

$$\log K = -3.357 - \frac{1197}{T},$$

(11)

$$K = 6.25 \cdot 10^4 \cdot e^{-\frac{5480}{kT}}.$$

The numbers 62270 and 83906 in equations (8) and (9) represent the activation energies of the gaseous corrosion of ML-4 and ML-5 in nitrogen and the numbers 13150 and 5480 in equations (10) and (11), the activation energies of the gaseous corrosion of ML-4 and ML-5 in CO$_2$ and SO$_2$.

DISCUSSION OF RESULTS

The curves of Fig. 1 show that the corrosion process at 350° follows a parabolic law. This seems to indicate that at this temperature a continuous protective oxide film is being formed on magnesium and its alloys ML-4 and ML-5, and that the corrosion process is slowed down by the diffusion of the reagents through the film. The curves show that as the film thickens its growth slows down. At lower temperatures, the protective property of the films on magnesium and its alloys ML-4 and ML-5 is even more evident. Thus it appears that on magnesium and its alloys the oxide film shows protective properties in the temperature range extending from room temperature up to 400° and only above 400° does the oxidation process assume a linear character [4].

The protective action of magnesium oxide is explained by the phenomenon of pseudomorphism in the primary oxide film; this was experimentally proven by Finch and Quarrell [6]. The phenomenon of pseudomorphism characteristic of magnesium and zinc became particularly clear in the light of the theory presented by Dankov [7], in which he formulated the principle of orientational and dimensional correspondence.

The principle of Dankov's crystallographic-chemical correspondence is expressed by the relationship:

$$\Delta a \approx \sqrt{\frac{2a\sigma}{c_{11} + c_{12}}},$$

which shows that between two phases in contact (metal and oxide film) an orientational correspondence takes place when the difference Δa between the linear dimensions of the original and the new phase is smaller than the square root of the ratio of $2a\sigma$ (twice the product of the parameter of the flat lattice of the new phase and its free surface energy) to the sum ($c_{11} + c_{12}$) of the elastic modulae in two crystallographic directions.

According to this principle, maximum similarity occurs at the plane of contact between the metal and oxide lattices because the atoms of the metal lattice are subjected to minimum displacement during the formation of the oxide lattice. This means that the primary oxide film on magnesium has a hexagonal structure and represents a crystallographic continuation of the metal lattice. This provides the continuity of the film and is responsible for its protective character. However, as the film grows, the difference in the geometry of both lattices becomes so great that the film breaks down and transforms into an ordinary cubic oxide due to the internal strain taking place in the film. As was shown previously [4], such films are incapable of slowing down the diffusion of the reagents in spite of their constantly growing thickness during the oxidation process of magnesium and its alloys.

Figure 3 shows that the addition of 2.5% of Mn to pure magnesium increases the heat resistance of magnesium while on the contrary the addition of aluminum and zinc decrease its heat resistance; the greater the concentration of aluminum, the greater the decrease of heat resistance. This can be explained by the fact that with magnesium, aluminum and zinc form intermetallic compounds MgZn, MgZn$_2$, MgZn$_5$, and Mg$_3$Al$_2$Zn$_3$ of very low melting points (340-342); as the result, the melting point of the total alloy decreases and the total vapor pressure above the solid phase increases, which leads to an increase of the gaseous corrosion rate of the alloys ML-4 and ML-5 as compared to pure magnesium.

The activation energy for the process of gaseous corrosion is greater for MA-1 than for magnesium, which shows that the heat resistance of MA-1 is greater than that of magnesium.

The comparison of the activation energies of the processes of gaseous corrosion for the alloys ML-4 and ML-5 in air and in nitrogen leads to the conclusion that in nitrogen the corrosion process is very slow while it is much faster in air. This indicates that nitrogen represents a good protective medium for the performance of heat treatments of magnesium alloys.

The corrosion rate of alloys in mixtures of air and CO_2, and SO_2, is rather high, which is borne out by the magnitude of the activation energies. The processes however are accompanied by the formation of protective layers on the metal surface; these layers are composed of carbonates and sulfates of magnesium and of the alloyed metal so that after 4-6 hours the corrosion process is practically stopped. Consequently, mixtures of these gases can be recommended as protective media [4]. The utilization of these mixtures as protective media leads to the development of the technology of faster heat treatment of cast magnesium alloys [1], which method has been applied in the machine tool industry.

SUMMARY

1. The study of the gaseous corrosion rate of magnesium and its alloys ML-4 and ML-5 at 350° in air allowed us to determine that this process follows a parabolic law while the gaseous corrosion of magnesium at 400° proceeds according to a linear law.

2. It was shown that the alloyed metals affect the gaseous corrosion rate of magnesium in a different way. Manganese increases the heat resistance of the alloy while zinc and aluminum decrease its heat resistance. The effect of aluminum and zinc is due to the fact that these metals form with magnesium a eutectic, decreasing the melting point of the alloy, and this increases the evaporation of magnesium; as a consequence the corrosin rate increases.

3. This corrosion rate of Mg and its alloys in nitrogen and in mixtures of air with CO_2 and SO_2 is considerably lower than in air.

LITERATURE CITED

[1] I. A. Makolkin, J. Appl. Chem. 27, No. 4, 421 (1954).*

[2] I. A. Makolkin, Z. L., 12, 1433 (1950).

[3] I. A. Makolkin, Sb. stat. USSR zaochn. polytechn. inst., 9, 43 (1955).

[4] I. A. Makolkin, J. Appl. Chem. (USSR) 24, No. 5, 460 (1951). *

[5] I. A. Makolkin, Z. L. 10, 1210 (1949).

[6] Finch and Quarrell, Nature 131, 877 (1933); Proc. Royal. Soc. (A) 141, 398 (1933); Proc. Phys. Soc. London, 46, 148 (1934).

[7] P. D. Dankov, Trudy 2nd Conference on Corrosion of Metals, 2, 121 (1943); Trudy of the Conference on Adsorption (1948); Doklady Akad. Nauk SSSR, 23, 458 (1939); Izvestia Akad. Nauk SSSR, Chemistry series 5-6 (1938).

*Original Russian pagination. See C. B. Translation.

CORROSION ACTIVITY OF A NITRATE-NITRITE MOLTEN MIXTURE

E. I. Gurovich and G. P. Shtokman

This investigation constitutes one part of a complex study, the goal of which is to determine the possibility of utilizing in industry the molten mixture of nitrates and nitrites composed of 55% (by weight) KNO_3, 40% $NaNO_3$, and 7% $NaNO_2$.*

The present study is directed toward the choice of steels for the equipment, pipes, etc., which would be suitable for use in industries utilizing molten salts (heat conductors, baths for tempering, baths for various heat treatments, etc.).

In the literature one can find data on the effect of molten nitrates and nitrites and their mixtures on metals and alloys. We shall mention here only the most important publications concerning this subject. Thus, for example, there exists information according to which aluminum remains practically unaltered when in contact with molten potassium or sodium nitrite [1]; however, this information is well known in the industries concerned with the manufacturing of light alloys. Iron in powder form melted together with potassium nitrate leads to the formation of potassium ferrate (K_2FeO_4) [2]. In vacuum, iron is oxidized by the mixture and partially restores potassium nitrite to the nitrate state; at white heat nitrogen, the oxide, and peroxide of potassium are formed [2]; some of these products react in turn with the metals with which they are in contact. In contact with copper the nitrate is partially transformed into oxide, while copper becomes covered with an irregular layer of copper oxide; the mixture contains the nitrite [4] also.

Metallic iron heated (500-600°) in vacuum with sodium nitrate becomes covered with a porous precipitate of magnetic iron oxide (burnishing) [3].

Lloyd and Chamberlain [5], as well as Box and Middleton [6], showed that the life of iron and steel containers for molten nitrates used in industry (in heat treatment of metals) is 1-2 years (particularly in the case of high grade nitrates). The welded seams, as far as corrosion resistance is concerned, do not differ from the other parts of the containers. When these containers are heated by direct flame, corrosion is usually somewhat higher in the areas of the inner surface corresponding to the outer parts exposed to the flame (local overheating in molten nitrate). The opinion (by analogy with aqueous solutions) that the presence of nitrites in nitrates decreases corrosion of metals is not confirmed in the case of molten nitrates. It was found that the corrosion rate increases with temperature. The increase in alkalinity during the utilization period of the bath has a beneficial effect on the resistance of steel containers to corrosion, while the presence of even traces of chlorides in molten nitrates increases their corrosion activity.

The effect of the concentration of carbon in steels on their corrosion resistance was also investigated [7]. The author came to the conclusion that the concentration of carbon in steel has practically no effect on its corrosion rate.

Aluminized containers (covered by an alloy of aluminum and iron) were also subjected to corrosion tests in molten nitrates [8].

Lloyd and Chamberlain [5] noted that studies of the mechanism of film formation on the surface of different steels are in progress, but the results are not yet published.

A great number of publications devoted to the problems of heat treatment of metals in nitrates, nitrites and their mixtures, contain data on the corrosion resistance of various metals and alloys [9-12].

We have investigated the effect of nitrates of alkaline metals on some metals and alloys, including steel [13].

*In the following we shall call this mixture either the molten mixture or simply mixture.

Some work on corrosion of metals in nitrate-nitrite mixtures was performed earlier in IONKh [14]. Thus, for example it was shown that the heat resistant steel −2 (Fe−Cr−Al type) is stable at 500°. The experiments were performed by allowing continuous contact with air for 52 days. Ravich and Frolov have maintained the nitrate-nitrite molten mixture in silver and in Armco iron crucibles in an atmosphere of nitrogen at 500° for 30 days. It was shown that in the first case (silver crucibles) the molten mixture remained stable, while in Armco iron crucibles it decomposed. Sokolov and Rassonskaya have investigated the behavior of Armco iron, Cr18/Ni9/Ti steel and 3−steel in nitrate-nitrite molten bath at 300, 450, and 500° in the presence of air and in the inert gases. The experiments were performed over a period of 200 hours in iron containers. The samples were separated by dividers made of corundum smoothed by surface melting. It was shown that in the presence of air the increase in weight of the samples is considerably smaller than in the presence of an inert medium. Thus, for example, the increase in weight of Cr18/Ni9/Ti steel in an inert medium was $+0.0106$ g/m$^2 \cdot$hour at 500°, $+0.0077$ g/m$^2 \cdot$hour at 450° and $+0.0044$ g/m$^2 \cdot$hour at 300°, while in the presence of air the increase of weight was only $+0.004$ g/m$^2 \cdot$hour at 500°.

For Armco iron in an inert medium the following results were obtained (at the corresponding temperatures): $+0.193$, $+0.060$, and $+0.014$ g/m$^2 \cdot$ hour while in the presence of air the increase of weight was $+0.072$ g/m$^2 \cdot$hour at 500°.

Analogous corrision tests of Armco iron, steel−5 and other alloys were performed in the Timiryazev Agricultural Academy. In these tests the corrosive medium was composed of a molten nitrate-nitrite alloy to which were added alkali, borates, silicates, and phosphates. The tests were made at 300, 450, and 500°.*

EXPERIMENTAL METHODS

Corrosion tests of samples were performed in a small autoclave made of Cr18/Ni9/Ti steel, which was found to be sufficiently resistant to molten nitrates [13].

The tests were performed in a molten mixture of nitrates-nitrites at 500, 550, and 600°, temperatures considerably higher than those investigated by other authors; the following steels were investigated: OCrNi3− M, 12Cr2FV, Cr5VF (two different batches, 76 and 77, somewhat different from each other), Cr18Ni9Ti, 12MFCr, 12CrMF, and Armco iron.

Besides that, the steels OCrNi3-M, 12CrMF, and 12MFCr were tested in melts of nitrate-nitrite mixtures containing 2% $K_2Cr_2O_7$, which acted as an inhibitor.

The surface of the OCrNi3-M samples was 14 cm^2; the surface of the other samples varied from 16 to 17 cm^2. Two samples of steel were used in each test. The majority of the steels investigated was obtained from Ts.N.I.I. of Chermet.

The chemical composition of the steels is given in the following table:

Name	C	Ni	Si	Mn	Cr	V	Nb	W	Mo
OCrNi3-M	0.4	2.84	0.24	0.49	1.04	−	−	−	present
12Cr2FB	0.12	−	0.53	0.2	2.16	0.81	0.99	−	−
Cr5VF (76)	0.10	−	0.56	0.24	5.44	0.85	−	0.37	−
Cr5VF (77)	0.11	−	0.55	0.21	5.48	0.58	−	0.57	−
12MFCr	0.09	−	−	−	0.5	0.2	−	−	0.35
12CrMF	0.09	−	−	−	0.92	0.24	−	−	0.38
Cr18Ni9Ti	−	9	−	−	18	(with 0.5% Ti)			

The tests were run for three hours every day during the necessary number of days. In these intermittent tests the time taken by the heating and the cooling was not taken into account. In addition, continuous tests were run over a period of a month on the 12CrMF steel.

* According to available data the corrosion of metal in nitrate-nitrite molten alloys was also studied in TsIATIM (Central Scientific Research Institute of Aviation Fuels and Lubricants).

Tests of steels containing high percentage of chromium. Figure 1 shows the curves illustrating the be-
havior of high-chromium-content steels in the nitrate-nitrite mixture. In the case of 12Cr2FB steel containing
over 2% chromium, the surface film initially formed falls off periodically. As the result of this loss of surface
film the molten mixture usually contains slime. The samples start to lose weight after 20 hours of testing. The
corrosion curve is limited to 60 hours, since after this period the loss of weight of the sample is catastrophically
large; this result indicates that this steel is unsuited for work with nitrate-nitrite molten mixtures. Naturally
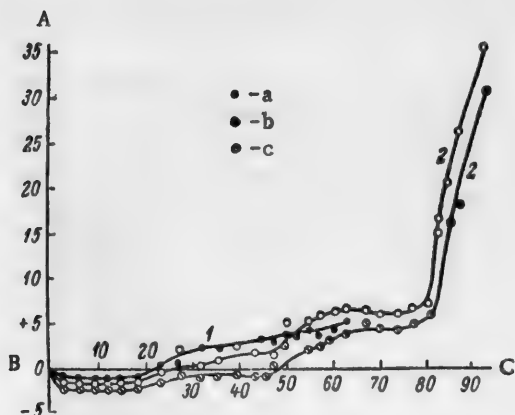this steel was not tested at higher temperatures since it is unacceptable at 500°.

Fig. 1. Effect of the nitrate-nitrite molten mixture
on the 12Cr2FB steel (a) Cr5VF (76) (b) and Cr5VF
(77) (c). A) Loss of weight (in g/m²), B) increase
in weight (in g/m²), C) time (in hours). Tempera-
ture (in °C): 1) 500; 2) 600.

Figure 1 also contains the curves relative to the
two Cr5VF steels (two different batches, 76 and 77,
slightly different from each other; see analysis of steels).
These steels contain an even higher percentage of chro-
mium (about 5.5%) and also contain vanadium and tung-
sten in different proportions. The testing of these steels
was performed at various temperatures up to and includ-
ing 600°.

Figure 1 represents only the corrosion curves cor-
responding to 600° and shows the variation of the resist-
ance with time. The tests made at 500 and 550° showed
that these steels can be satisfactorily used in contact
with nitrate-nitrite molten mixtures; in some cases the
loss of weight did not exceed 0.3 g/m² · hour and the
gain of weight, i.e., the growth of the surface film,
oscillated between 0.02 and 0.12 g/m² · hour. The
total increase in weight over the whole period of the
test is insignificant. In these cases the surface films
are strongly fixed to the surface of the metal. The
experimental curves obtained at these temperatures
are not represented because the scale of the figure is
too small for the results obtained (at the scale of Fig.
1 these curves almost fall on the axis of the abscissa).

Thus, the relatively high degree of corrosion,
which these steels undergo at 600° does not allow us
to recommend them for use at this temperature, but
these steels can be considered satisfactory for work
with nitrate-nitrite molten mixtures at 500 and 550°.

Chemical analysis of the mixture after the test-
ing of this group of steels revealed the presence of up
to 0.33% Cr (in the case of testing at 600°); iron was
not found to be present in the mixture. The increased
alkalinity of the mixture at high temperature affects
the steels containing chromium in such a way that
chromium becomes "extracted" from the steel. How-
ever, this extraction decreases with time.

Tests of steels containing a relatively low
percentage of chromium. Figure 2 shows corrosion
curves relative to the 12MFCr and 12CrMF steels in
the nitrate-nitrite molten mixture at 500 and 600°.
This group of steels is characterized by a relatively
low chromium content and furthermore, contains molyb-
denum and vanadium. The corrosion curves show that
these steels are inadequate in the case of periodic tests;
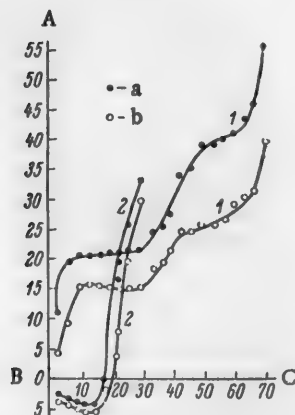however, long continuous tests show relatively low
losses by corrosion.

Fig. 2. Effect of nitrate-nitrite molten mixture on
a) 12MFCr steel and b) 12CrMF steel. A) Loss of
weight (in g/m²), B) gain of weight (in g/m²) C)
time (in hours). Temperature (in °C): 1) 500; 2)
600.

Chemical analysis of the mixture of salts after the tests showed that the concentration of chromium at 500° is about 0.15% CrO_4, and after the tests at 600° it is 0.23% CrO_4.

Fig. 3. Effect of Nitrate-Nitrite molten mixture on a) OCrNi$_3$-M, and b) EIa-I$_T$. A) Loss of weight (in g/m^2); B) increase in weight (in g/m^2); C) Time (in hours). Temperature (in °C): 1) 500; 2) 550; 3) 600.

Fig. 4. Liberation of gas resulting from the action of the nitrate-nitrite molten mixture on the 12CrMF steel. A) Rate of liberation of the gas 1 (in cc/hour); B) total amount of gas liberated 2 (in cc); C) time (in hours).

Tests of steels containing nickel. Figure 3 shows corrosion curves of steels containing nickel in various proportions. This group of steels includes OCrNi3-M steel and the Cr18Ni9Ti stainless steel.

OCrNi3-M steel was tested at 500, 550, and 600°. Cr18Ni9Ti steel was tested only at 600° since at lower temperatures (300, 450, and 500°) it was studied earlier by other authors.

These corrosion curves indicate that these steels are characterized as film-forming metals. As time increases, the curves assume a direction parallel to the axis of the ascissa. The films produced adhere solidly to the surface and tests over prolonged periods of time showed that these steels are completely adequate for the nitrate-nitrite molten mixtures.

Chemical analysis of the mixture of salts, performed after completion of the tests on OCrNi3-M steel, revealed the presence of CrO_4 up to 0.018%; no iron was found; nickel was also absent in the salt mixture. In spite of the high content of chromium and nickel in Cr18Ni9Ti steel, chemical analysis of the molten mixture of salts revealed only the presence of chromium, up to 0.03% CrO_4.

Other tests. Tests of Armco iron in nitrate-nitrite molten mixture showed that it is totally inadequate for this mixture since the film formed on the surface of the metal falls off easily.

In order to prevent some steels from selective "extraction" of chromium under the effect of the nitrate-nitrite molten mixture, (by analogy with water solutions) we made tests on low-chromium steels in molten salts containing 2% $K_2Cr_2O_7$ (which is an inhibitor in aqueous solutions). These tests showed that the corrosion of a number of steels (OCrNi3-M, 12MFCr, and 12CrMF) is somewhat more intense than in the case of pure nitrate-nitrite molten mixtures.

Prolonged continuous tests (during 30 days) were made on 12CrMF steel; in this case the steel samples were placed in specially prepared containers made of the same steel. The samples were suspended on hooks also made of the same steel. After the cover was sealed, about 145 g of finely ground nitrate-nitrite mixture was introduced through a tube. This tube connected the container with a buret (by a rubber hose) meant to collect the liberated gas; the container was placed in a crucible furnace heated to 500°. The rate of gas liberation was measured. The liberation of gas, very active at the beginning of the experiment, progressed at a decreasing rate (Fig. 4). The gas was analyzed for NO, O_2 and NO_2. It was found that the liberated gas consists essentially of nitrogen. At the end of the test the samples were again weighed and the salt mixture analyzed for Fe, Cr, Mo and V (using the colorimetric method). The detection of iron was made with KCNS. The amount of chromium was also determined by the gravimetric method, using barium acetate for the precipitation. The weight of the samples increased during the test due to formation of a porous oxide film which easily fell off. The film was removed by boiling the samples in a saturated solution of ammonium oxalate, after
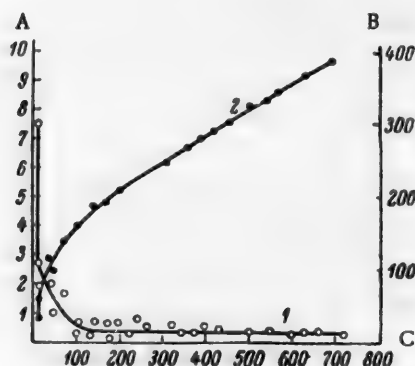
which samples were weighed again. The loss of weight was 0.76 $g/m^2 \cdot$ hour on the average, and during the whole time of the experiment the samples lost an average of 549 g/m^2 (duration of the experiment was 720 hours). After the completion of the test the salt mixture was dissolved in water and submitted to chemical analysis. The test for iron with KCNS gave negative results. We analyzed for chromium colorimetrically, using diphenylcarbaside in an acid medium. It was found that 0.0035% (by weight) of chromium passed into the molten mixture (calculated in terms of CrO_4, considering the total amount of the molten mixture). The amount of molybdenum was also determined colorimetrically using the rhodanin complex; only very small amounts were found — about 0.0012% by weight of the total amount of the salt mixture (0.002% MoO_4). An attempt was made to determine the amount of vanadium colorimetrically but the test gave negative results. Thus it was established that only insignificant amounts of chromium and molybdenum pass into the molten mixture.

We also studied the effect of the nitrate-nitrite molten mixture on nickel, one of the possible constituents of steel. Nickel was found to be very resistant to the mixture at temperatures below 600° (no tests were made above this temperature). This result apparently explains the resistance of the Cr18Ni9Ti (9% Ni) steel and the OCrNi3-M (about 3% Ni) steel in the nitrate-nitrite molten mixture.

Molybdenum and vanadium were also submitted to test as possible constituents of steel. Molybdenum was found to be very unstable in the nitrate-nitrite mixture: at 450-550° the oxidation of molybdenum is very strong, reaching inflammability. The reaction is very violent and as a result the metal dissolves very rapidly. Tungsten is even more unstable; it inflames at 400°.

SUMMARY

The OCrNi3-M and the Cr18Ni9Ti steels were found to be very resistant in the nitrate-nitrite molten mixture at temperatures below 600°. Armco iron, and the 12Cr2FB, 12CrMF, and 12MFCr steels were found to be unstable in the nitrate-nitrite mixture at 600°. The Cr5VF (batches 76 and 77) were found resistant to the molten mixture up to 550°. Molybdenum and tungsten, as possible constituents of steel, were found very unstable in the nitrate-nitrite mixture.

Nickel was found to be very resistant to the molten mixture of salts. The addition of $K_2Cr_2O_7$ to the nitrate-nitrite mixture increases the corrosion of steels.

LITERATURE CITED

[1] Büschlinger, Z. Metalkunde, 19, 105 (1927).

[2] L. Moeser, J. pr. Ch. [2] 55, 425 (1897).

[3] L. Hackspill and R. Grandadam, Ann. Chim. 10, 5, 232 (1926).

[4] C. Graf, Vierteljahresschr. pract. Pharm. 4, 65 (1885).

[5] P. B. A. Lloyd and E. A. Chamberlain, J. Iron and Steel Inst. (London) 142, 11, 141 (1940).

[6] R. J. Box and B. A. Middleton, J. Iron and Steel Inst. 151, 1, 71-78 (1945).

[7] C. A. Siebert, Trans. Am. Soc. Met. 27, 3, 752-757 (1939).

[8] Rollason, J. Inst. Metals 60, 45 (1937).

[9] E. L. Cady, Materials and Methods 35, 3, 9-114 (1947).

[10] L. F. Spencer, Steel Processing 39, 3, 120, 131 (1953).

[11] L. B. Rosseau, Steel 134, 7, 108-111 (1954).

[12] E. J. Eckel, R. M. Mayfield, G. W. Wensch and F. A. Rough, Industr. Heat 20, 8, 1482-1484, 1488 (1953).

[13] E. I. Gurovich, J. Appl. Chem. (USSR) 28, 9, 1358-1365 (1956).*

[14] Otchety IONKh Academy of Sciences, USSR (1941-1942).

CORROSION OF METALS IN HYDROGEN SULFIDE AT HIGH TEMPERATURES

Kh. L. Tseitlin, L. V. Merzloukhova and V. A. Strunkin

Institute of Organic Intermediates and Dyes

Hydrogen sulfide attacks metallic structures very strongly [1]. Low-nickel and carbon steels were submitted to corrosion at 200-500° in a circulating mixture of hydrogen (95%) and hydrogen sulfide (5%) under pressure. Aluminum and the 18/8 type stainless steels show good resistance [2]. The alloys "Fekhral" and "Chromal" are sufficiently resistant to sulfur vapor up to 700°; iron, chromium and nickel-chromium steels are strongly corroded [3]. Above 700°, H_2S attacks Inconel, iron, copper and 18/8 steel; tungsten, molybdenum and tantalum are the most resistant [4]. Small additions of silicon and particularly aluminum to chromium steels increase their chemical resistance to hot petroleum products containing sulfur [5]. The role of the nature of the metal is indicated also in other publications [6-11]. The wear of motor cylinders increases proportionally to the concentration of sulfur in the fuel [12-13]. It was shown that in the temperature range of 220 to 450° the corrosion rate of iron in hydrogen sulfide follows a parabolic law [14] (using the method of periodic weighing of samples without withdrawing them from the furnace). A medium composed of hydrogen sulfide and water vapor induces corrosion of metals at 40° [15], and high-chromium steels and nickel-chromium steels may disintegrate under the effect of this corrosion [16, 17].

The data concerning corrosion of metals by dilute hydrogen sulfide presented in the literature are usually calculated on the basis of the samples' gain in weight. It seems of interest to determine the resistance of metals by studying the loss of weight occurring in a stream of hydrogen sulfide and hydrogen sulfide mixed with water vapor and nitrogen.

EXPERIMENTAL METHODS

We used the testing method described earlier [18]. Hydrogen sulfide was obtained by the action of a 20% H_2SO_4 solution on sodium sulfide. The gas was first passed through wash bottles filled with water and glass wool, was then dried over calcium chloride enclosed in a glass tube, and then admitted into the quartz container where the metals were tested (in dry H_2S). For tests in a mixture of hydrogen sulfide and nitrogen, nitrogen from a bottle was simultaneously introduced into the glass tube of the system. Humidification was achieved by introducing measured quantities of distilled water into the system drop by drop (20 ml/hour).

The rate of flow of hydrogen sulfide was 250 ml/min. The rate of flow of the mixture of hydrogen sulfide and nitrogen was 250 and 20 ml/min respectively (this corresponded to a weight ratio of $N_2:H_2S \sim 1:10$). One must take into account the fact that at temperatures above 350° the corrosive medium becomes in effect a mixture of hydrogen sulfide and sulfur vapor [19]. The duration of the test was 6 hours. The chemical analysis of the metal investigated was given earlier [18].

The results of the experiments are summarized in tables and represented in the figure.

At high temperatures (Table 1) aluminum and the chromium-aluminum alloy of the EI595 type (containing 25% chromium, 5% aluminum and 0.1% carbon) show good resistance in a flow of dry hydrogen sulfide. Stainless steel (up to 360°), carbon steel and cast iron (up to 250°) have a satisfactory resistance. Water vapor has different effects: it has no significant effect on the corrosion rate of aluminum, steel and cast iron in the temperature range of 200° to 420°, nor on the corrosion rate of stainless steel above 550°; it slows down the corrosion rate of steel and cast iron above 420°, that of stainless steel within the temperature range of 200°

to 500°, and that of the EI595 alloy and copper; the corrosion of cast iron, carbon steel and stainless steel is somewhat accelerated below 200°, when the formation of an acid fog becomes possible. Dilution of hydrogen sulfide up to the proportion of 1:10 decreases the corrosion of steel, cast iron (up to 500°), chromium aluminum alloy, copper and stainless steel (particularly at temperatures above 400°). The slowing down of the corrosion process due to dilution with an inert gas can apparently be explained by the decrease of the diffusion rate of the hydrogen sulfide to the metal's surface. At high temperatures (Table 2) the corrosion of aluminum in hydrogen sulfide, water vapor, and strongly humidified chlorine is approximately the same; in all cases the corrosion is very slight. Carbon steel, stainless steel and cast iron undergo a much stronger attack by hydrogen sulfide than by water vapor or by a mixture of chlorine and water vapor. Even at about 310° copper corrodes in water vapor ten times less than in humid hydrogen sulfide or in chlorine [20]. This difference increases at high temperatures. Copper is the least resistant of all metal tested in hydrogen sulfide and its mixtures.

It was shown earlier that in the case of the formation of volatile products the corrosion of metals strongly increases with the rate of flow of the corroding gas [18].

The effect of this factor was checked in the case of dry hydrogen sulfide (Table 3). Iron sulfide is heat resistant and only slightly volatile. Therefore, as one would expect, the rate of flow of the gas has no significant effect on the corrosion of iron alloys up to a certain temperature (about 420°). When the temperature increases from 420° to 650° the effect of the rate of flow of the gas on the corrosion process of steel and cast iron increases somewhat. The increase of the rate of flow of hydrogen sulfide has practically no effect on the corrosion of stainless steel, but increases the corrosion of copper somewhat; this result is apparently related to the increased possibility of the destruction of surface films characteristic of copper.

Aluminum, steel and copper react violently with dry chlorine even below 300°; this can be explained by the high vapor pressure of the chlorides formed, their low melting points (copper chloride), and high thermal effect of the reaction, which in turn increases the reaction rate [20]. The reactions of the metals with dry hydrogen sulfide, within the tested temperature, are much slower than in the case of chlorine; this can be explained by the better protection of the surface films due to their lower vapor pressure and higher heat resistance. It must be noted however that at high temperatures hydrogen sulfide and its mixtures with water vapor and nitrogen strongly attack carbon steel, stainless steel, cast iron, and in particular copper.

It seems that sulfide films, and also the secondary oxides which can be formed during the decomposition of sulfur compounds in the presence of water vapor, are porous and do not offer adequate protection against corrosion. One may assume that the particularly strong corrosion of copper occurs because of the high porosity of the surface film and the presence of internal stresses in the surface film, and this leads to the destruction of its continuity. It is known that a characteristic rupture, indicating periodic destruction of the film, takes place at about 500° in the case of copper corroding in air [21]. Many authors have pointed out the poor protective properties of copper sulfide surface films [22, 23].

The maximum temperature limits of satisfactory corrosion resistance (in °C) are given below.

Metals	In dry hydrogen sulfide	In dry hydrogen sulfide greatly diluted with nitrogen	In mixtures of hydrogen sulfide and water vapor
Aluminum	425•	425•	425•
Carbon steel, cast iron	250	300	250
1Cr18Ni9Ti steel	360	420	420
EI595 type alloy	550	650	650

SUMMARY

1. Dry hydrogen sulfide induces considerable corrosion of cast iron and steel above 250° and the attack increases sharply at about 500° The increase of the corrosion rate of 1Cr18Ni9Ti stainless steel starts at 360°.

• The maximum temperature corresponding to a satisfactory chemical resistance of aluminum in a flow of hydrogen sulfide is higher than 425. The temperature of 425 determines the mechanical characteristics of aluminum, which melts at 600° [24].

TABLE 1

The Effect of Temperature on the Corrosion of Metals by Hydrogen Sulfide

Reagent	Corrosion of metals (in g/m² · hour) at different temperatures (in °C)								Characteristics of the resistance
	170	200	310	360	420	500	550	650	
Aluminum									
Hydrogen sulfide	0.0	0.0	0.0	0.0	0.1	0.1	0.2	—	Aluminum has good resistance.
Hydrogen sulfide and water vapor	0.0	0.0	0.0	0.0	0.1	0.1	0.2	—	Above 360° a dull film is formed on the sur-
Hydrogen sulfide diluted with nitrogen	—	—	0.0	—	0.0	0.1	0.1	—	face, this film is in- soluble in water. No H₂S is found in wash water.
Carbon Steel									
Hydrogen sulfide	0.6	0.7	3.2	8.6	14.8	89.6	239.0	340.4	Above 250° steel and cast iron are strongly
Hydrogen sulfide and water vapor	1.7	2.1	4.9	5.6	10.4	35.5	45.3	—	corroded. Below 200° water vapor increases somewhat the attack,
Hydrogen sulfide diluted with nitrogen	0.1	0.5	1.2	2.7	3.7	106.8	132.5	—	while at higher tem- perature it slows down the corrosion process.
Cast Iron									
Hydrogen sulfide	0.5	0.5	7.4	11.8	10.9	91.1	159.0	338.0	Up to 420° great dilu- tion of H₂S with nitro-
Hydrogen sulfide and water vapor	0.5	1.1	5.1	7.5	8.2	20.7	79.6	—	gen decreases corro- sion, while at 500-
Hydrogen sulfide diluted with nitrogen	0.2	0.3	0.8	1.4	5.7	120.3	—	—	550° it does not have any appreciable effect.
1Cr18Ni9Ti Steel									
Hydrogen sulfide	0.0	0.0	0.4	0.7	2.2	10.7	17.7	36.9	Stainless steel is stable up to 360°. Below 200°
Hydrogen sulfide and water vapor	0.1	0.2	—	—	0.2	1.8	21.4	27.0	water vapor somewhat increases corrosion,
Hydrogen sulfide diluted with nitrogen	—	—	0.1	0.6	0.9	—	0.4	0.4	while at higher tem- peratures it slows down the corrosion process.

At 500-650° there is no difference between the effects of dry and humid hydrogen sulfide. Great dilution of hydrogen sulfide with nitrogen decreases corrosion. In a number of cases a dangerous intercrystalline corrosion of unstressed steel takes place in hydrogen sulfide at 550-650°

TABLE 1 (continued)

Reagent	Corrosion of metals (in g/m² · hour) at different temperatures (in °C)								Characteristics of the resistance
	170	200	310	360	420	500	550	650	
Copper									
Hydrogen sulfide	73.7	106.4	350.5	—	659.4	—	1196.5	—	Copper is strongly corroded in all cases. The presence of water vapor and dilution of hydrogen sulfide with nitrogen decrease corrosion.
Hydrogen sulfide and water vapor	26.6	36.3	118.7	250.1	276.3	—	—	—	
Hydrogen sulfide diluted with nitrogen	—	8.8	—	88.8	132.3	—	—	—	
Chromium — Aluminum Alloy of the EI595 Type									
Hydrogen sulfide	—	—	—	—	0.4	—	0.4	6.5	The alloy has good resistance to corrosion. The presence of water vapor and the dilution of hydrogen sulfide with nitrogen increase the resistance to corrosion.
Hydrogen sulfide and water vapor	—	—	—	0.0	0.0	—	0.01	0.02	
Hydrogen sulfide diluted with nitrogen	—	—	—	0.0	0.0	—	—	0.0	

TABLE 2

Corrosion of Metals in Water Vapor, Hydrogen Sulfide and Humid Chlorine at 550°

Metal	Corrosion of metals (in g/m² · hour) in different media				
	water vapor	water vapor and chlorine	hydrogen sulfide	hydrogen sulfide and water vapor	hydrogen sulfide diluted with nitrogen
Aluminum	0.1	0.1	0.2	0.2	0.1
Carbon steel	7.6	7.4	239.0	45.3	132.5
Cast iron	—	48.5	159.0	79.6	—
1Cr18Ni9T steel	0.06	1.5	17.7	21.4	0.4
Copper (about 310°)	0.2	318.3	350.5	118.7	88.8 (360°)

TABLE 3

Effect of the Rate of Flow of Hydrogen Sulfide on the Corrosion of Metals

Metal	Corrosion (in g/m² · hour) at different temperatures (in °C)					
	420°		550°		650°	
	and different rates of flow (in ml/min)					
	20	250	20	250	20	250
Carbon steel	14.6	14.8	95.6	239.0	204.9	340.4
Cast iron	10.5	10.9	114.2	159.0	174.3	338.0
1Cr18Ni9Ti steel	—	2.2	15.8	17.7	34.2	36.9
Copper	417.8	659.4	832.1	> 1196.5	—	—

A

140
120
100
80
60
40
20
0

170 200   300   400   500   600   700   B

1   2   3   4 5
6
7
8
9
10
11
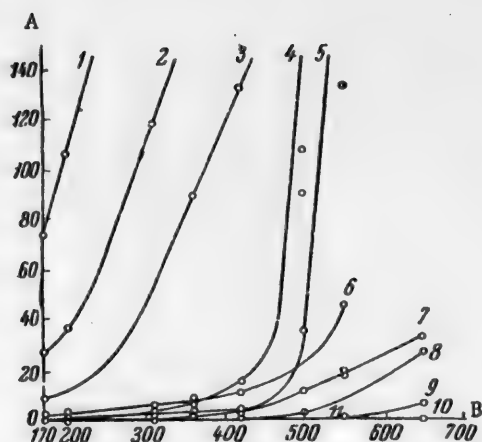
Effect of temperature on the corrosion of metals in hydrogen sulfide. A) Corrosion (in g/m$^2 \cdot$hour) B) temperature (in °C), 1) Cu, dry H$_2$S; 2) Cu, humid H$_2$S; 3) Cu, H$_2$S diluted with N$_2$; 4) Steel−3, dry H$_2$S; 5) Steel−3, H$_2$S diluted with N$_2$; 6) Steel−3, humid H$_2$S; 7) 1Cr18Ni9Ti steel, dry H$_2$S; 8) 1Cr18Ni9Ti steel, humid H$_2$S; 9) EI595 type alloy, dry H$_2$S; 10) EI595 type alloy, humid H$_2$S diluted with N$_2$; 1Cr18Ni9Ti steel, H$_2$S diluted with nitrogen; 11) Al, H$_2$S, dry, humid, and diluted with nitrogen.

Aluminum and chromium-aluminum alloys of the EI595 type have good resistance up to 500°C. Among all the metals tested in hydrogen sulfide, copper corrodes most strongly (even at 170°C).

2. In a number of cases the presence of water vapor in hydrogen sulfide slows down the corrosion of iron alloys at high temperatures. The resistance of aluminum is not affected by the presence of water vapor while the corrosion of copper is very high, although its absolute value decreases.

3. Strong dilution of hydrogen sulfide with nitrogen decreases the corrosion of iron alloys and copper. However, at about 500° the dilution of hydrogen sulfide has practically no effect on the corrosion rate of cast iron and steel, which reaches considerable values. Dilution of hydrogen sulfide with nitrogen does not affect the corrosion resistance of aluminum.

4. At high temperatures iron and its alloys corrode much more strongly in dry chlorine than in dry hydrogen sulfide. In the presence of water vapor a reverse situation occurs — hydrogen sulfide attacks the metals more strongly because the surface films apparently have a more porous structure than the oxide films formed on the surface under the effect of humid chlorine.

5. Maxima temperature limits of satisfactory corrosion resistance of metals in hydrogen sulfide are presented on the basis of short corrosion tests (6 hours).

LITERATURE CITED

[1] N. I. Dobroshtan, Second Conference on Corrosion of Metals, Academy of Sciences, USSR, II, 225 (1943).

[2] M. S. Perminov and A. A. Putilov, Corrosion and its Prevention, III, 1, 7 (1937). •

[3] V. K. Perchke, S. S. Gastev and I. V. Oknin, Chemical Mochinedesign (USSR) 4, 27 (1937).

[4] M. Farber and D. Ehrenberg, J. Electrochem. Soc. 99, 10, 427 (1952).

[5] S. I. Volfson, "Problems of Resistant to High Temperatures" State Scientific-Technical Press for Machine Construction Literature (1950). •

[6] A. White and L. Makrek, Ind. Eng. Chem. 24, 859 (1932).

[7] E. Dittrich, Chem. Fabrik, 11, 25 (1933).

[8] M. Pieri, Chim. ind. agr. biol., 10, 352 (1934).

[9] Jozsef Vero, Anyagvizsgalok Kozlonye, 19, 31 (1941).

[10] L. A. Aliavdina, Second Conference on Corrosion of Metals, Academy of Sciences, USSR, II, 251 (1943).

[11] "Corrosion of Metals" — series of articles translated under the editorship of V. V. Skorchelletti, II, 677 (1952).

[12] C. G. Williams, J. Inst. Automobile Engrs. London, 8, 728 (1940).

• In Russian.

[13] C. S. Bruce, J. T. Duck and A. R. Pierce, J. Research Nat. Bur. Standards 41, 44 (1948).

[14] V. V. Ipatyev and K. V. Kostriukova, "Rate of Scaleformation on Metals and Alloys" Series of articles published by Leningrad State University, Leningrad (1954).

[15] A. I. Akkerman, M. L. Tamarkina and A. I. Shultin, Corrosion and its Prevention IV, 5-6, 344 (1938).

[16] L. A. Glikman, Corrosion—Mechanical Resistance of Metals. State Scientific-Technical Press for Machine Construction Literature 8 (1955).

[17] B. M. Nikiforova, A. V. Riabchenkov and N. A. Reshetkina, "Effect of corrosive media on the resistance of steel," Series of articles published by the State Scientific-Technical Press for Machine Construction Literature, 58 (1955).

[18] Kh. L. Tseitlin, J. Appl. Chem. (USSR) 27, 9, 953 (1954).

[19] B. V. Nekrasov, Course of General Chemistry, State Chemistry Press (1955). *

[20] Kh. L. Tseitlin, J. Appl. Chem. (USSR) 29, 8, 1182 (1956). J. Appl. Chem. (USSR) 28, 5, 490 (1955).

[21] N. D. Tomashov, Theory of Corrosion — Metallurgy Press, 64 (1954).

[22] I. S. Shklovskii, "Investigations of the Corrosion of Metals" Academy of Sciences USSR (1951).

[23] Yu. R. Evans, Corrosion, Passivity and Protection of Metals. Translated from English under the editorship of G. B. Akimov, Metallurgy Press (1941).

[24] V. P. Batrakov, Corrosion of Structural Materials in Agressive Media — Defence Press, 58 (1952). *

---

* In Russian.

SOLUTION OF COPPER, IRON, AND LEAD IN NITRIC ACID*

A. G. Loshkarev

V. V. Vakhrushev Sverdlovsk Mining Institute

Free solution of metals in electrolytes, particularly in acids, constitutes the basis of a series of the most important phenomena relative to technological processes such as corrosion of metals and alloys, extraction of salts by dissolving metals in acids, etc.

The modern electrochemical theory of solution of metals was developed by Frumkin [1], Wagner and Traud [2], Durdin [3], Shultin [4], Akimov [5], and other investigators.

Tananaev [6] developed a new "shavingless" method of chemical analysis in which the samples are taken by bringing the solvent in immediate contact with the surface of the metal to be analyzed ("shavingless" dissolution). In this method the components of an alloy pass into the sample in the same proportion as they exist in the alloy. The sample is then submitted to quantitative and qualitative analysis.

Shavingless dissolution can be applied to the investigation of the corrosion of metals, of the thickness of protective surface films, etc.

In spite of the fact that shavingless dissolution presents great practical interest, its specific characteristics remained undetermined.

In the present work we shall investigate the kinetics of the shavingless solution of copper, iron, and lead in nitric acid.

EXPERIMENTAL METHODS

We investigated experimentally the kinetics of the shavingless dissolution of electrolytic copper (99.95% Cu), Armco iron, and electrolytic lead (99.99% Pb) in nitric acid whose concentration was varied from 2.6 to 13.0 N. These experiments were performed at 17, 27, and 37°.

Measurements of the corrosion rate as the function of time were performed in the following way: a small cup 3 mm deep and 8 mm in diameter was drilled in the surface of metal plates (100 × 3 × 8 mm). The inner surface of the cup was 1.22 cm². The surface of the cup was thoroughly degreased with hot alcohol, rinsed with water, etched with acid, then rinsed again and dried with filter paper. Then 0.124 ml of the solvent was poured into this prepared cup. The duration of the reaction was controlled with a stop watch.

The resulting solution was transported quantitatively in a small flask serving for the determination of the amount of dissolved metal. This determination was accomplished either by the photoelectrocolorimetric method (when the concentration was low), or by the volumetric method, using microburets, (when the concentration was high) [7, 8].

Conclusions on the kinetics of the process were based on the experimental results concerning the variation of the concentration of metal in the sample as the function of the duration of the reaction.

We also studied the variation of the potential of the meatl as the function of time. The diagram of the apparatus used is shown in Fig. 1. The metals were dissolved under the conditions described.

* This is the first of a series of communications devoted to the study of solubility of metals and alloys.
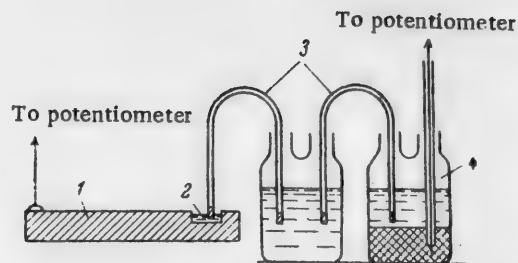
Fig. 1. Diagram of the experimental setup used to measure the solution potential of metals. 1)Metal under investigation; 2) solvent; 3) contact tubes; 4) reference electrode.

The solution potential was measured with respect to a saturated calomel electrode by the noncompensation method using a direct current balance cathode voltmeter described earlier [9].

Diffusion potentials were eliminated by using contact tubes filled with a saturated solution of potassium chloride. The end of the tube immersed in the solution in the cup was stuffed with clean asbestos wool previously treated with hydrochloric and nitric acids and thoroughly washed with distilled water. The other ends of these tubes were stuffed as usual with filter paper.

The solution potential was determined with a specially prepared galvanometer. One division of the galvanometer corresponded to 2.15 mv.

EXPERIMENTAL RESULTS

The results of the experiments on the kinetics of solution of copper, iron, and lead in nitric acid are summarized in the following table and in Figs. 2 and 3.

Kinetics of Shavingless Solution of Copper, Iron, and Lead in 0.124 ml, of a 6.50 N HNO$_3$ at 17°

Reaction time (in min.)	Amount dissolved (in mg)		
	Cu	Fe	Pb
0.5	5.0	7.4	—
1	9.1	12.1	4.0
2	16.0	15.9	4.2
3	17.0	16.4	4.0
5	18.6	17.5	4.2
7	19.0	18.0	4.5
10	19.1	18.5	4.5
15	19.0	18.8	5.0

Metals dissolving in acid liberate either nitrogen dioxide or nitrogen oxide, for example.

$$M^{II} + 4HNO_3 = M^{II}(NO_3)_2 + 2NO_2 + 2H_2O.$$

$$3M^{II} + 8HNO_3 = 3M^{II}(NO_3)_2 + 2NO + 4H_2O.$$
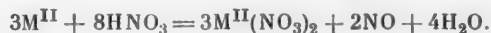
Theoretical calculations of the amount of copper passing into solution when 0.124 ml of acid at 17° is used show that according to the first reaction we should obtain 22.5 mg, and according to the second reaction we should obtain 33.7 mg of copper. After 15 minutes of reaction the pH of the 6.5 N HNO$_3$ solution is equal to 2, i.e., almost all the acid intervened in the reaction. The amount of copper dissolved under these conditions is equal to 19 mg (see Table)

The comparison of the theoretical and the experimental results shows that copper dissolves in nitric acid (2.6—13.0 N), liberating essentially nitrogen dioxide. Iron dissolves according to the same pattern.

Tananaev [6] came to the conclusion that during the shavingless dissolution of iron in nitric acid (6.5 N) iron passes into solution in the state of bivalent ions which later partially oxidize to the trivalent state. When the concentration of iron is 75-80%, iron is in the state of bivalent ions while when the concentration is 20-25% it is in the state of trivalent ions. Special experiments allowed us to confirm these results.

The kinetics of shavingless dissolution of the metals investigated in nitric acid is characterized by two consecutive processes: during the initial process the amount of metal dissolved is a linear function of time, then the solution rate decreases with time, dropping practically to zero. This result is clearly seen in the case of copper in nitric acid whose concentration varies within the range of 4.33—6.5 N (Fig. 2). In concentrated solutions (13 N) copper dissolves very rapidly during the first period of time (19 mg are dissolved within 1/2 minute); we can only suppose that in this case too the relationship is linear.

Iron behaves in an analogous manner. Lead follows the same pattern within the concentration limits of 3.25 — 4.33 N HNO$_3$.

The corrosion rate of the investigated metals in nitric acid during the linear period is characterized by the following values calculated from the results obtained at 17°:

	mg/cm$^2 \cdot$ min	A/cm^2
Cu (in 6.50 N HNO$_3$	6.4	0.32
Fe (in 6.50 N HNO$_3$	9.6	0.55
Pb (in 4.33 N HNO$_3$	3.4	0.05

Our experiments showed that within the concentration range of 6.50 — 13 N HNO$_3$, 70-85% of the total amount of copper, iron, and lead which dissolved during the 10-15 minutes of the reaction passed into the solution during the two to three minutes of the initial linear period of the reaction.

During the linear period of the reaction copper is dissolved most intensely by a 13.0 N HNO$_3$ solution, although part of the acid remains unused at the end of the reaction. The reason for this is apparently the formation of oxide films on the metal surface. As the concentration decreases, the solution rate decreases and a 3.25 N solution practically does not dissolve copper. After 15 minutes of contact with the acid, metallic copper could not be uncovered by treatment with hydroxide.

As the temperature increases up to 37°, the solution rate of copper remains practically constant. The solution rate of lead increases with temperature only slightly (Fig. 3).

These experimental facts can be explained by assuming that the limiting factor of the dissolution of copper, iron, and lead is the diffusion of nitric acid to the metal surface; although diffusion proceeds at a high rate, it is still lower than that of the anodic ionization of the metal and cathodic regeneration of nitric acid.

The density of the solution current (i_c) during the linear period of the reaction, i.e., for the stationary diffusion of ions of nitric acid to the metal surface, is determined by the equation:
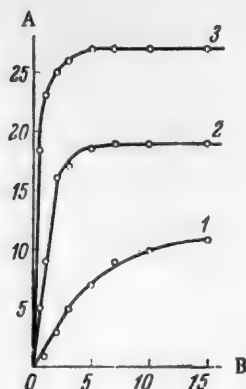

Fig. 2. Kinetics of shavingless solution of copper in nitric acid at 17°. A) Amount of copper passed into the solution (in mg) B) time (in minutes). Concentration of HNO$_3$ (in N): 1) 4.33; 2) 6.50; 3) 13.0.
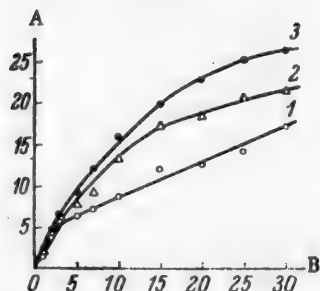
$$i_c = nFD \frac{C_0 - C}{\delta}, \qquad (1)$$

where $\underline{n}$ is the charge of the ion, F is the Faraday number, D is the diffusion coefficient, δ is the thickness of the diffusion layer, ($C_0 - C$) is the difference between the concentrations of the solution at the bottom and at the surface of the metal.

Fig. 3. Kinetics of shavingless solution of lead in a 2.60 N HNO$_3$ solution at different temperatures. A) Amount $\underline{q}$ of Pb passed into solution (in mg), B) time (in minutes). Temperature (in °C): 1) 17; 1) 27; 3) 37.

Since the density of the solution current remains constant at the beginning of the reaction, the difference between the concentrations at the bottom and at the surface of the metal remains practically constant.

The solution rate decreases with time. It is natural to assume that this decrease is due to the decrease of the diffusion of nitric acid to the metal surface. During this second period of the reaction, the solution rate is determined by the rate of the nonstationary diffusion. The analysis of our experimental results confirm this assumption.

The density of the solution current is determined by the equation relative to nonstationary diffusion given by Levich [10]:

$$i_c = \frac{nF\sqrt{D}}{\sqrt{\pi t}},\qquad (2)$$

where t is the duration of the reaction, $\pi = 3.14$. The amount of metal q dissolved during the time t is given by the equation:

$$q = \int_0^t i_c\, dt.\qquad (3)$$

Replacing the value of i_c from equation (2) into equation (3) and integrating, we obtain:

$$q = \frac{2nF\sqrt{D}}{\sqrt{\pi}}\sqrt{t}.\qquad (4)$$

Thus, during the period of nonstationary diffusion, the amount of dissolved metal is directly proportional to the square root of the reaction time.
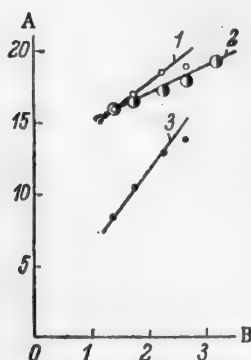

Fig. 4. The nonstationary period of the kinetics of shavingless solution of copper (1) and iron (2) in 6.50 N HNO_3 and of lead (3) in 4.33 N HNO_3 at 17°. A) Quantity of metal q (in mg) passed into solution B) $\sqrt{t}$ (t — time in minutes).
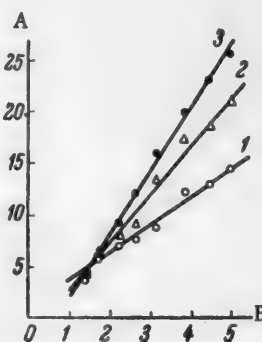
Fig. 5. The nonstationary period of the kinetics of shavingless solution of lead in 2.60 N HNO_3 at different temperatures. A) Quantity of lead q (in mg) passed into solution B) $\sqrt{t}$ (t — time in minutes). Temperature (in °C): 1) 17; 2) 27; 3) 37.

Equation (4) can be used for conclusions on the character of the solution reaction of the investigated metals in nitric acid succeeding the linear period.

Figures 4 and 5 represent the experimental results concerning the solution of copper, iron, and lead during the second period of the reaction; the results are represented in $q\sqrt{t}$ coordinates. As we can see, the linear relation between $q\sqrt{t}$ required by equation (4) is satisfactorily achieved.

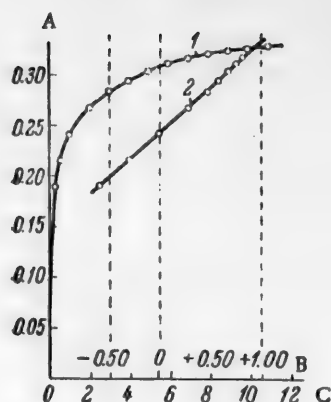Fig. 6. Variation of the shavingless solution of copper as the function of time in a 6.50 N HNO₃ at 17°. A) Potential (in volts), B) value of log t, C) time (in minutes). Curves: 1) $\varphi = f(t)$; 2) $\varphi = f(\log t)$.
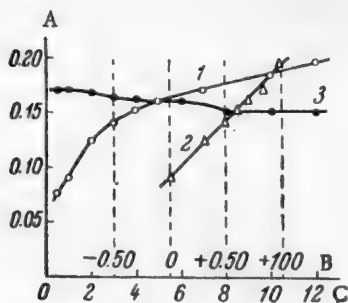

Fig. 7. Variation of the shavingless solution of iron in a 6.50 N HNO₃ solution and of lead in a 4.33 N HNO₃ solution at 17°. A) Negative potential (in volts), B) value of log t, C) time t (in minutes). Curves: 1) $\varphi_{Fe} = f(t)$; 2) $\varphi_{Fe} = f(\log t)$; 3) $\varphi_{Pb} = f(t)$.

The experimental results and their analysis show that copper, iron, and lead, and apparently many other metals, dissolve in nitric acid at a relatively high rate determined at the beginning of the reaction by the rate of stationary diffusion, and at the end by the rate of nonstationary diffusion.

During shavingless solution of metals in nitric acid, the electrochemical potential (solution potential) of the metals varies.

Measurements of the solution potential were performed by the method described. The amount of solvent used in this case was 0.08 ml of a 6.50 N HNO₃ solution. The measurements were performed at 17°. The results are presented in Fig. 6 and 7.

During dissolution the potentials of copper and lead increase (becomes more positive) while the potential of iron at the beginning of the reaction increases up to a certain maximum and then decreases (becomes more negative). At the end of the reaction the potentials change very little.

Under the conditions of shavingless dissolution, the potential of the metal is the function of many parameters — nature of the metal and of the solution, concentration and amount of the solution, temperature, reaction time, etc.

The variation of the solution potential of copper (φ_{Cu}) by the following empirical equation:

$$\varphi_{Cu} = a + b \log \cdot t, \qquad (5)$$

where a and b are constants (Fig. 6).

Our experimental results are well represented by this equation when a = 0.146, and b = 0.009 (φ_{Cu} is in volts and t in minutes).

The solution potential of lead in nitric acid remains almost constant at the beginning of the reaction and increases only after a certain time (Fig. 7). This is apparently due to two causes: the first cause is that the solution potential of lead is almost equal to its equilibrium potential in this solution. The second cause seems to be the fact that the lead ion concentration in pores of the oxide film, formed on lead in nitric acid, remains constant during the process of solution.

After a certain reaction time the potential of lead increases, apparently because of increased lead ion concentration in the solution.

The variation of the solution potential of iron in nitric acid during shavingless dissolution presents a number of peculiarities. The passage from a KCl solution to a nitric acid solution sharply increases the potential of iron (from −0.370 to −0.077 v), then during the subsequent dissolution the potential decreases (after 12 minutes it drops to −0.195 v).

Insofar as the value of the solution potential is always intermediate between that of the potential and anodic solution of the metal and that of the cathodic regeneration of the solution, the potential of iron in the nitric acid solution increases with time. The greater initial solution rate of iron, causing polarization, also contributes to this effect.

As the concentration of the acid and the solution rate decrease, the solution potential of iron decreases, but naturally remains quite different from its equilibrium potential in this solution, since the passivating oxide film formed under the effect of the acid prevents the potential from reaching its equilibrium value.

It is interesting to note that the decrease of solution potential of iron can be described by the following empirical equation:

$$\varphi_{Fe} = a + b \lg t, \tag{6}$$

analogous to equation (5), but the values of the constants in this case are: $a = 0.024$ and $b = -0.10$.

SUMMARY

The kinetics of shavingless solution of copper, iron and lead in nitric acid solutions varying from 2.60 N to 13.0 N at temperatures varying from 17 to 37° is limited by the diffusion rate of the solvent to the metal surface.

LITERATURE CITED

[1] A. N. Frumkin, Z. phys. Ch. 160, 116 (1932).

[2] C. Wagner and N. Traud, Z. Elektroch. 44, 391 (1938).

[3] Ya. V. Durdin, J. Org. Chem (USSR) 17, 844 (1947), 17, 862 (1947) 18, 345 (1948) 19, 2131 (1949) 21, 604 (1951).

[4] A. I. Shultin, J. Phys. Chem. (USSR) 15, 370, 399 (1941) 18, 61, 69 (1944).

[5] G. V. Akimov, The Theory and the Methods of Investigation of Corrosion, Academy of Sciences SSSR Press (1945).*

[6] N. A. Tannaaev, ZL, 13, 4, 389 (1947).

[7] A. K. Babko and A. T. Pilipenko, Colorimetric Analysis, State Chemistry Press (1951).*

[8] Method of Analysis of Electrolytic Baths. — VNIIAM. State Press of Defense Industry, Moscow (1944).*

[9] A. G. Loshkarev and G. V. Loshkareva, J. Appl. Chem (USSR) 27, 8, 866 (1954). * *

[10] V. G. Levich, J. Phys. Chem. (USSR) 18, 335 (1944) 22, 575, 711 (1948).

* In Russian.

* * Original Russian pagination. See C. B. Translation.

MECHANISM OF THE INHIBITORY ACTION OF HETEROCYCLIC NITROGEN BASES IN THE PICKLING OF STEEL IN SULFURIC ACID IN THE PRESENCE OF CERTAIN ANIONS

N. D. Rusyanova and M. V. Goftman

In a study of the possible use of coal-tar nitrogenous bases as inhibitors of acid corrosion it was found that they retard the dissolution of iron and steel in hydrochloric and sulfuric acid at room temperature, but have almost no influence on the action of sulfuric acid at 60-70°, i.e., under the normal pickling conditions.

Similar behavior had been observed previously in other compounds of nitrogen. At the same time, Beskov [1] found that certain nitrogen compounds retard the action of sulfuric acid also. One such substance is quinoline ethiodide, which dissociates in solution to give iodide ions.

The action of this compound on the solution rate of steel in acid depends on the content of the halide ions in the solution. From this, Iofa [2] concluded that when iron dissolves in sulfuric acid, the metal surface is positively charged, so that adsorption of positive ions of the nitrogeneous bases is hindered. If halide ions are present in the solution, they interact with the iron surface to form a chemical compound. The dipoles of this compound are directed with their negative ends toward the solution, creating an additional negative charge and facilitating adsorption of the positively charged ions of the nitrogeneous bases.

Ayazyan [3] tested and verified this hypothesis experimentally. He showed that the zero-charge potential of iron is on the negative side of the equilibrium potential, and therefore the surface of iron at the equilibrium potential is positively charged. Moreover, he postulated that halide ions not only displace the zero-charge potential but alter the forces which determine specific adsorption.

We found that the presence of SCN' ions in solution also greatly increases the inhibitory action of bases in sulfuric-acid pickling. Experiments were carried out with a number of negative ions in an attempt to extend the range of substances which have this effect.

The pickling on No. 3 steel was carried out in 12% sulfuric acid at 70-73° for 2 hours. The results are given in Table 1.

It follows from Table 1 that only SCN', I', and Br' ions had a good stimulating effect. These ions retard the dissolution of steel in acid even in absence of bases, which shows that they are adsorbed on the metal surface, but the activity of thiocyanate and Br' is much higher if they are used in mixtures with bases (the inhibitory effect γ is 3, 2, and 13 respectively for thiocyanate, and 9, 3, and 24 for Br').

The other ions studied increase the activity of bases only very slightly.

Another interesting fact is that the inhibitory effect of mixtures of thiocyanate with bases increases with increasing SCN' concentration up to a certain limit, and then remains almost constant, or decreases (see Figure).

It was thought that a complex of iron, base, and thiocyanate ions is formed. To test this hypothesis, we prepared the complexes, determined their composition, and tested their effects on the dissolution of No. 3 steel in sulfuric acid at 70°.

The complex with KSCN was prepared as follows: 2.5 g of $FeSO_4 \cdot 7H_2O$ was dissolved in 12 ml of 12% sulfuric acid, to this 2 g of quinoline was added, followed by a solution of 2 g of KSCN in 5 ml of water. Red oily drops of the complex compound separated out immediately; after some time they solidified to thin needle-like crystals with m. p. 93°.

TABLE 1

Effect of Additions of Salts on the Inhibitory Activity of Bases

Added to 12% H_2SO_4 (in %)		$\gamma = \dfrac{\rho_0{}^*}{\rho}$	ρ (in g/cm^2·hour)
bases	salts		
Quinoline 0.2		1.5	$30.8 \cdot 10^{-4}$
—	KSCN 0.2	2.8	$16.9 \cdot 10^{-4}$
Quinoline 0.2	KSCN 0.02	7.1	$6.8 \cdot 10^{-4}$
—	KSCN 0.2	3.2	$15 \cdot 10^{-4}$
Quinoline 0.2	KSCN 0.2	13	$4.4 \cdot 10^{-4}$
Basic fraction with b.p. 250-270°, 0.2	KSCN 0.2	34	$13.7 \cdot 10^{-5}$
	$K_4Fe(CN)_6$ 0.02	1.15	$40 \cdot 10^{-4}$
Quinoline 0.2	$K_4Fe(CN)_6$ 0.02	39	$12.5 \cdot 10^{-4}$
	$K_4Fe(CN)_6$ 0.2	1.2	$38 \cdot 10^{-4}$
Quinoline 0.2	$K_4Fe(CN)_6$ 0.2	2.1	$22.6 \cdot 10^{-4}$
—	$K_3Fe(CN)_6$ 0.02	0.45	$10.5 \cdot 10^{-3}$
Quinoline 0.2	$K_3Fe(CN)_6$ 0.02	3.6	$13 \cdot 10^{-4}$
	$K_3Fe(CN)_6$ 0.2	0.92	$49 \cdot 10^{-4}$
Quinoline 0.2	$K_3Fe(CN)_6$ 0.2	1.4	$3.4 \cdot 10^{-4}$
—	KI 0.2	16	$3.1 \cdot 10^{-4}$
Quinoline 0.2	KI 0.2	17.7	$2.8 \cdot 10^{-4}$
	KBr 0.2	9	$5.1 \cdot 10^{-4}$
Quinoline 0.2	KBr 0.2	15	$3.06 \cdot 10^{-4}$
—	NaCl 0.2	1.6	$31.1 \cdot 10^{-4}$
Quinoline 0.2	NaCl 0.2	2.5	$19 \cdot 10^{-4}$
—	KCN 0.2	0.5	$94 \cdot 10^{-3}$
Quinoline 0.2	KCN 0.2	0.56	$84 \cdot 10^{-3}$

$^* \rho = \dfrac{\Delta p}{cm^2 \cdot hr}$, Δp is the weight loss (in g), $\rho_0 = 46 \cdot 10^{-4}$.

To determine the composition of the complex, its nitrogen content was determined by the Kjeldahl method, and SCN' by the Volhardt method. The empirical formula was calculated from the results.

Found %: SCN 37.8, N 15.2. $Fe(SCN)_6(C_9H_8N)_4$. Calculated %: SCN 37.2, N 15.1.

The reaction of a solution of quinoline with potassium thiocyanate without iron salts gave a white complex, m. p. 138°

Its composition corresponds to the formula $C_9H_8N \cdot SCN$.

Found %: SCN 29.2, N 14.8. $C_9H_8N \cdot SCN$. Calculated %: SCN 28.8, N 14.3.

In analogous conditions quinoline does not form a complex with bivalent iron and iodine. A yellowish complex with m. p. 195° is formed; its composition corresponds to the formula $C_9H_8N \cdot I$.

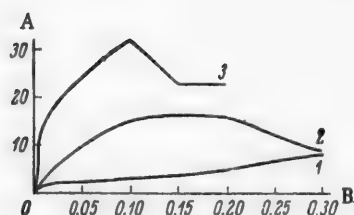Found %: I 48.9, N 5.2. $C_9H_8N \cdot I$. Calculated %: I 49.7, N 5.4.

A quinoline—bromine complex is also formed, but its melting point is considerably lower and its solubility higher than those of the above complexes; it is only deposited on cooling, in the form of oily yellow crystals.

The inhibitory activity of these complexes was tested in the pickling of No. 3 steel as described above. The results are given in Table 2.

TABLE 2

Results of Pickling in the Presence of Complexes

Inhibitor	Inhibitor concentration (%)	γ	$\rho \quad 10^{-4}$
Quinoline	0.2	} 16	2.9
KSCN	0.2		
Quinoline−thiocyanate complex of m.p. 138°	0.4	8	5.8
Complex of m.p. 138°	0.3	} 14	8.4
KSCN	0·2		
Quinoline−iron−thiocyanate complex, m.p. 93°	0.4	14	8.3
Quinoline	0.2	} 17.7	2.6
KI	0.2		
Quinoline−iodine complex, m.p. 195°	0.4	16.7	2.8
Quinaldine	0.2	} 16	2.9
Quinaldine−iron−KSCN complex	0.2		
	0.4	16.6	2.8
Quinaldine−bromine complex	0.4	14.5	8.3

Influence of KSCN concentration in solution of the inhibitor effect of bases. A) Inhibitory effect γ, B) KSCN concentration (in g). Pickling in presence of: 1) KSCN; 2) 0.1 g of quinoline and KSCN; 3) 0.1 g of fraction of bases with b. p. 250-270° and KSCN.

The complexes formed by the bases with iron and thiocyanate, and also with iodine or bromine without iron, have the same activity as mixtures of bases with these irons.

This suggests that when iron is dissolved in sulfuric acid in presence of bases and SCN', I', or Br' ions, a dense film of a complex compound is formed on the metal surface, preventing dissolution. That is why the same inhibitory effect is obtained if the complex compound itself is added to the pickling liquor.

However, as follows from the data in Table 2, the complex of the composition $C_9H_9N \cdot SCN$ proved less active. The probable reason is that it does not contain enough SCN' ions to form a complex with iron, as its activity increases when KSCN is added to the pickling liquor.
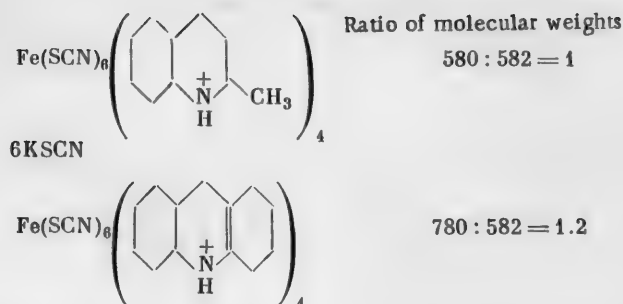
Therefore the cause of the increased activity of bases in presence of certain anions is the ability of these ions to form complex compounds with the bases, or with the bases and bivalent iron.

If the anions are incapable of reacting to form complex compounds, they have little or no effect on the ability of bases to retard the dissolution of iron in acids (Table 1).

This explanation accounts for the fact that I' and Br' greatly increase the inhibitory effect of bases, while Cl' increases their activity only slightly.

Our explanation is in harmony with Ayazyan's views on the changes in the forces determining specific adsorption, in presence of halide ions.

To test this view, the amounts of KSCN and bases of different molecular weight necessary for the formation of complex compounds were calculated. These calculations were carried out for quinaldine and acridine.

Fe(SCN)$_6$$\left(\begin{array}{c}\text{[quinaldinium structure]}\\ \overset{+}{\underset{H}{N}}\text{—CH}_3\end{array}\right)_4$ Ratio of molecular weights
                                                       $580 : 582 = 1$

6 KSCN

Fe(SCN)$_6$$\left(\begin{array}{c}\text{[acridinium structure]}\\ \overset{+}{\underset{H}{N}}\end{array}\right)_4$ $780 : 582 = 1.2$

The pickling was then carried out in presence of the bases and KSCN taken in the calculated quantities, and also in presence of the reagents in ratios above or below the calculated ratios.

It follows from the data in Table 3 that the greatest inhibitory effect is obtained when the quantities of bases and KSCN added correspond to the compositions of the complex compounds. The same result was obtained for the fraction of bases with b. p. 250-270°, the average molecular weight of which (determined by potentiometric titration) was 170, and the ratio $\dfrac{RN}{KSCN}$ = 1.02 (where RN represents a heterocyclic base).

TABLE 3

Effect of Component Ratio on Inhibitory Activity

Contents in solution (in g)		Component ratio	γ	Contents in solution (in g)		Component ratio	γ	Contents in solution (ing)		Component ratio	γ
quinaldine	KSCN			acridine	KSCN			250-270° fraction	KSCN		
0.1	0.1	1	16	0.12	0.1	1.2	11	0.1	0.01	10	13
0.1	0.2	0.5	16.8	0.12	0.2	0.6	11.8	0.1	0.05	2	23
0.1	0·3	0.33	11	0.12	0.3	0.4	12.0	0.1	0.1	1	31
0.05	0.3	0.17	9	0.06	0.1	0.6	5.7	0.1	0.15	0.67	18
0.2	0.1	2	4.5	0.24	0.1	2.4	9.1	—	—	—	—

For confirmation of these results, similar experiments were carried out with all the base fractions, the average molecular weights of which were determined by potentiometric titration (Table 4).

In all cases the inhibitory effect was higher in presence of the calculated quantities of bases and KSCN.

The results obtained (Tables 3 and 4) show convincingly that if the components are added to the pickling liquor in other than the calculated proportions the inhibitory activity is diminished. If the amounts of bases and KSCN are increased proportionately, this is not the case (see the last column in Table 4).

One possible explanation of this fact is as follows. At first SCN' and the bases form complexes of the composition $R\overset{+}{N}H \cdot SCN$, while the iron ions react with excess SCN' ions, forming Fe(SCN)$_2$, and this is followed by the reaction:

$$\text{Fe (SCN)}_2 + 4R\text{NH} \cdot \text{SCN} = \text{Fe (SCN)}_6 (R\overset{+}{N}H)_4.$$

A definite excess of SCN' ions must be present for this reaction to take place. If thiocyanate ions are not present in excess but, on the contrary, more base is added, the base combines with all the SCN' ions to give the compound RNH·SCN, so that the complex with iron cannot be formed. Complexes of the composition RN̈H·SCN, as was shown earlier, are less active, but their activity increases on addition of the necessary amount of SCN'.

TABLE 4

Pickling in Presence of Different Amounts of Components

Boiling range of fraction (°C)	Average molecular weight	Amount of KSCN (in g) per 0.1 g of base	γ in presence of the calculated amount of KSCN	γ in presence of 0.1 g of base and 0.1 g of KSCN	γ in presence of 0.2 g of base and 0.2 g of KSCN
230—240	130	0.11	41	15	34
240—260	165	0.9	47	27	47
260—280	190	0.8	49	33	46
280—300	168	0.9	39	28	35
300—320	150	0.1	52	39	50
320—330	165	0.9	47	39	44
330—345	180	0.85	47	44	62
345—360	187	0.8	48	47	46

There are two possible mechanisms of the action of the complex in the dissolution of iron. 1) The complex is formed on the metal surface. At first the positive surface adsorbs negative SCN' ions, forming compounds with surface iron atoms, and onium ions of the bases or SCN·RṄH complexes are added to these. 2) Complex formation occurs in solution, and the large neutral molecules of the complex are adsorbed on the metal surface by the action of specific-adsorption forces. Such a mechanism is possible because the surface charge is very low and is in the range where molecular adsorption predominates. Additional experiments are necessary in this connection.

Excess of SCN' ions also lowers the inhibitory effect somewhat. These ions may displace the neutral complexes from the metal surface, and since their own activity is lower, this leads to a decrease of the inhibitory effect.

SUMMARY

1. It is shown that the inhibitory activity of coal-tar nitrogeneous bases is greatly increased in presence of SCN', I', and Br' ions. Other anions: CN', Cl', $Fe(CN)_6^{-3}$, $Fe(CN)_6^{-4}$ increase the inhibitory effect only slightly.

2. It is shown that, in acid media, nitrogeneous heterocyclic bases combine with bivalent iron and SCN' ions to form complex compounds of the type $Fe(SCN)_6(RṄH)_4$, and with I' and Br' ions, compounds of the type RṄHI and RṄHBr.

LITERATURE CITED

[1] S. D. Beskov, Sci. Mem. Dept. Gen. Anal; Chem. Lenin Pedagogic Institute, Moscow 63, 4, 129 (1951).

[2] Z. A. Iofa, E. I. Lyakhovetskaya and K. Shafirov, Proc. Acad. Sci. USSR 84, 3, 543 (1952).

[3] E. O. Ayazyan, Proc. Acad. Sci. USSR 100, 3, 473 (1955).

THE COMPOSITION OF THE RESIN ACIDS OF TALLOIL

N. F. Komshilov and M. N. Letonmyaki

Laboratory of Wood Chemistry, Karelian Branch of the Academy of Sciences USSR

In a study of the composition of resin acids obtained by distillation of talloil from Pinus silvestris, Aschan and Virtanen [1] found a resin acid with m.p. 182°, $[\alpha] - 30.7°$, which they named pinabietic acid.

Subsequently Krestinsky, Persiantseva, and Novak [2], who used a similar material and the same methods of extraction, obtained an acid with m.p. 186-188° $[\alpha]_D^{20} - 17.36°$ (in alcohol), which they named high-melting abietic acid.

The resin acids of crude talloil were also studied by Harris [3], who found the following acids in the resin fraction of talloil (in %): (low-melting) abietic 30-40, neoabietic 10-20, dihydroabietic 14, tetrahydroabietic 14, dehydroabietic 5, dextrapimaric 8, isodextrapimaric 8, and levopimaric 1.

The opinion has been expressed [4] that high-melting abietic acid is either one of the dihydroabietic acids, or a mixture of acids formed by disproportionation of hydrogen in resin acids at high temperatures.

According to Harris, crude talloil contains a mixture of disproportionation products; this suggested to us that if high-melting abietic acid is a mixture, it can be isolated from crude as well as from distilled talloil.

We separated the resin acids of crude (undistilled) talloil by crystallization, and were not able to find high-melting abietic acid. On separation of the resin acids of crude talloil through the diacetonamine salts [5], we found that the main fraction of the mixture of resin acids contained low-melting abietic acid with m.p. 174° $[\alpha]_D^{20} - 105.93°$ (in alcohol). Only the first acid fraction had m.p. 173° $[\alpha]_D^{20} - 64.29°$, while the last (sixth) fraction had m.p. 170° $[\alpha]_D^{20} - 9.57°$. Subsequent experiments showed that in the last fraction there was an admixture of dextrapimaric acid with the low-melting abietic acid.

As Aschan and Virtanen [1] obtained high-melting abietic acid only after distillation of talloil, we also used the distillation method. The oil was distilled at 3 mm Hg residual pressure. The yield was 10% of crystalline resin acids. These acids were crystallized from alcohol and purified by the diacetonamine method [5]. As a result, the following acids were obtained: high melting abietic, m.p. 186-188° $[\alpha]_D^{21} + 15.45°$ (in alcohol); low-melting abietic, m.p. 173-174° $[\alpha]_D^{20} - 104.01$ (in alcohol); dextrapimaric, m.p. 210-211° $[\alpha]_D^{20} + 72.45°$ (in alcohol); neoabietic (incompletely purified), m.p. 164-165° $[\alpha]_D^{20} + 84.49°$ (in alcohol). High-melting abietic acid was present in the largest quantity. Less low-melting abietic acid was found. There was little dextrapimaric acid, and very little neoabietic. The last acid could not be adequately purified.

Our previous communication [6] contained certain evidence of the individuality of high-melting abietic acid. It was shown, for example, that high-melting abietic acid is obtained only from low-melting abietic acid, that additional purification through the diacetonamine salt gives high-melting abietic acid with m.p. 186° $[\alpha]_D^{18} + 30.2$ (in alcohol), that its composition exactly corresponds to the formula $C_{20}H_{30}O_2$, and that determination of the iodine number by the Kaufmann method shows the presence of two double bonds in the molecule.

In the present investigation the determinations of iodine number wee supplemented by determinations of the thiocyanate number. For a compound with two double bonds in the molecule, the ratio of the thiocyanate to the iodine number should be 0.5. Our experimental results gave values fairly close to the theoretical; the ratio of the thiocyanate to the iodine number was 0.41-0.42. The reason for this ratio is that thiocyanate is added selectively at only one of the two pairs of double bonds, while iodine is added at both.

Physical Constants of Resin Acid Fractions from Distilled Tall Oil

Original fractions after crystallization	Fractions obtained by separation as the diacetonamine salts									
	1		2		3		4		5	
	melting point (°C)	$[\alpha]_D^{21}$	melting point (°C)	$[\alpha]_D^{21}$	melting point (°C)	$[\alpha]_D^{21}$	melting point (°C)	$[\alpha]_D^{21}$	melting point (°C)	$[\alpha]_D^{21}$
I	180—183	−49.61	185—186	−40.87	185—187	− 9.95	186—188	+15.45	—	—
II	171—173	−57.58	171—173	−46.46	171—173	−23.10	172—175	+ 8.09	—	—
III	173—174	−53.73	170—173	−27.30	170—172	+21.93	168—170	+43.75	164—165	+48.49
IV	170—172	−76.41	168—170	−67.68	182—186	+39.91	183—187	+48.76	—	—

These facts show that high-melting abietic acid is not one of the dihydroabietic acids.

EXPERIMENTAL METHODS

Separation of the resin acids of crude talloil by crystallization. Crystallized talloil was pressed out on a Buchner funnel; the crystals of resin acids were washed with a little acetone, recrystallized from acetone, and separated as the diacetonamine salts [5]. Six salt fractions were obtained. The acids obtained after decomposition of the salts had the following constants:

Fraction I 0.2062 g substance, m.p. 173° at (α_D^{20} − 1.26, and l = 1.9009, c = 1.031), $[\alpha]_D^{20}$ − 64.29° (in alcohol);

Fraction IV 0.2046 g substance, m.p. 174° at (α_{20}^{D} − 2.06, and l = 1.9009, c = 1.023), $[\alpha]_D^{20}$ − 105.93° (in alcohol);

Fraction VI 0.1318 g substance, m.p. 170° at (α_D^{20} − 0.12 and l = 1.9009, c = 0.659), $[\alpha]_D^{20}$ − 9.57° (in alcohol).

These results provide some evidence that the principal component of the resin acids in crude talloil is low-melting abietic acid.

Vacuum fractionation of talloil and subsequent separation of the resin acids so obtained. The talloil taken for analysis (1040.7 g) was dried and then fractionated under 3 mm Hg residual pressure. Up to 205° fatty acids were distilled off, while between 205° and 213° a fraction of pure resin acids was obtained. The yield was 104.2 g of 10%. These acids were subjected to fractional crystallization from ethyl alcohol. After tenfold crystallization the work was interrupted and the crystals of resin acids were left in the crystallizing dishes for 6 months. At the end of this period the recrystallization was resumed. Large amounts of oxidation products were formed; these were removed by two additional recrystallizations. Crystal portions I, II, III, and IV were obtained. Each was purified through the diacetonamine salts [5]. In each case, salt fractions 1, 2, 3, and 4 were obtained, and decomposition of the latter gave the same number of acid fractions (a total of 17 fractions was obtained).

The melting points and specific rotations of these fractions of resins acids are given in the Table.

It is seen that acid Fraction I-4 had m.p. 186-188° $[\alpha]_D^{21}$ + 15.45° (in alcohol). We assumed that this was the pure high-melting acid. Fraction II-1 (heavy type in Table) with m.p. 171-173° $[\alpha]_D^{21}$ −57.58° (in alcohol) was repurified through the diacetonamine salt, from

which was obtained low-melting abietic acid, m.p. 173-174° (α_D^{20} −2.0°, c = 1.0115, l − 1.9009), $[\alpha]_D^{20}$ − 104.01° (in alcohol). The III-5 acid fraction, m.p. 164-165° $[\alpha]_D^{21}$ + 84.49° (in alcohol) was not purified further as very little was available. From Fraction IV-4, m.p. 181-187° $[\alpha]_D^{21}$ + 48.76° (in alcohol) simple crystallization gave dextrapimaric acid, m.p. 209-211° (α_D^{20} + 1.15, c = 0.835, l − 1.9009), $[\alpha]_D^{20}$ + 72.45° (in alcohol).

The equivalent, Kaufmann iodine number, and thiocyanate number of the high-melting abietic acid, m.p.186-188° $[\alpha]_D^{21}$ + 15.45° (in alcohol) were determined.

Determination of Equivalent

0.0514 g substance: 17.07 ml 0.01 N KOH, equivalent 301.11.
0.0560 g substance: 18.52 ml 0.01 N KOH, equivalent 302.37.

Determination of iodine number (Kaufmann) and number of double bonds

0.0920 g substance: 12.78 ml 0.1 N thiosulfate, iodine number 176.28.
0.0749 g substance: 10.22 ml 0.1 N thiosulfate, iodine number 173.15.

Determination of thiocyanate number

0.0852 g substance; 4.90 ml 0.1 N thiosulfate, thiocyanate number 72.98.
0.0720 g substance; 4.09 ml 0.1 N thiosulfate, thiocyanate number 72.09.

Ratio of thiocyanate/thiosulfate numbers = 0.41-0.42.

SUMMARY

1. It is shown that before vacuum distillation the resin acids of talloil chiefly consist of low-melting abietic acid, m.p. 174° $[\alpha]_D^{20}$ −105.93° (in alcohol) and dextrapimaric acid; after distillation they consist mainly of high-melting abietic acid, m.p. 186-188° $[\alpha]_D^{20}$ + 15.45° (in alcohol), dextrapimaric acid, m.p. 210-211° $[\alpha]_D^{20}$ + 72.45°, low-melting abietic acid, and probably neoabietic acid.

2. Evidence is provided for the view that high-melting abietic acid cannot be classified as a dihydro-abietic acid. The thiocyanate/iodine number is 0.41-0.42, indicating the presence of two double bonds.

LITERATURE CITED

[1] O. Aschan and A. Virtanen, Lieb. Ann. 424, 150 (1920).

[2] V. N. Krestinsky, N. I. Persiantseva and A. A. Novak, J. Appl. Chem. 12, 1407 (1939).

[3] G. C. Harris, Tappi Monograph, 6, 174 (1948); S. K. Kahila, Suomen Kemistilenti, 9, 175 (1951).

[4] J. Simonsen, The Terpenes, III, 417 (1952).

[5] E. V. Roginskaya, J. Appl. Chem. 22, 564 (1947).

[6] N. F. Komshilov, J. Appl. Chem. 30, 7, 1111 (1957).*

*Original Russian pagination. See C.B. Translation.

ERRATA

Journal of Applied Chemistry Vol. 30, No. 5, 1957

Page	Line	Reads	Should read
707,ff	Throughout text and tables	ag (subscript)	aq
718	22 and 23 from bottom	η_g	η_1
761	beneath Fig. 10	omission	A) Number of pores per 1 cm^2, B) concentration of sodium fluoride (in moles/liter). Sodium fluoride was added to the electrolyte instead of magnesium sulfate.
775	first two footnotes	*Electrolyte No. 1: Rp 735 D_C = 18 amp/dm^2; t = 90°. **Electrolyte No. 2; Rp 735 glycerol 80 g/liter; D_C = 20 amp/dm^2; t = 90°.	*Electrolyte No. 1: $FeCl_2$ • • $4H_2O$ = 500 g/liter; NaCl = = 100 g/liter; HCl = 2.2 g/ liter; D_C = 18 amp/dm^2; t = = 90°. **Electrolyte No. 2: $FeCl_2$ • • $4H_2O$ = 500 g/liter; NaCl = = 100 g/liter; HCl = 2.0 g/ liter; glycerol 80 g/liter; D_C = 20 amp/ dm^2; t = 90°.
811	Table heading beneath Analytical Data	omission	Elementary composition (in %)
828	4 from top	for hours.	for 8 hours.

All issues of the Journal of Applied Chemistry since 1950 are available in C.B. translation.